

ลักษณะเฉพาะและการปรับปรุงคุณภาพของโอปอมีค่าจากประเทศเอธิโอเปีย  
และโอปอไฟจากประเทศมาดากัสการ์



นางสาวสุพรรณษา โตอารีย์

จุฬาลงกรณ์มหาวิทยาลัย

CHULALONGKORN UNIVERSITY

บทคัดย่อและแฟ้มข้อมูลฉบับเต็มของวิทยานิพนธ์ตั้งแต่ปีการศึกษา 2554 ที่ให้บริการในคลังปัญญาจุฬาฯ (CUIR)  
เป็นแฟ้มข้อมูลของนิสิตเจ้าของวิทยานิพนธ์ ที่ส่งผ่านทางบัณฑิตวิทยาลัย

The abstract and full text of theses from the academic year 2011 in Chulalongkorn University Intellectual Repository (CUIR)  
are the thesis authors' files submitted through the University Graduate School.

วิทยานิพนธ์นี้เป็นส่วนหนึ่งของการศึกษาตามหลักสูตรปริญญาวิทยาศาสตรมหาบัณฑิต

สาขาวิชาโลกศาสตร์ ภาควิชาธรณีวิทยา

คณะวิทยาศาสตร์ จุฬาลงกรณ์มหาวิทยาลัย

ปีการศึกษา 2557

ลิขสิทธิ์ของจุฬาลงกรณ์มหาวิทยาลัย

CHARACTERISTICS AND QUALITY ENHANCEMENT OF PRECIOUS OPAL  
FROM ETHIOPIA AND FIRE OPAL FROM MADAGASCAR



A Thesis Submitted in Partial Fulfillment of the Requirements  
for the Degree of Master of Science Program in Earth Sciences

Department of Geology

Faculty of Science

Chulalongkorn University

Academic Year 2014

Copyright of Chulalongkorn University

Thesis Title	CHARACTERISTICS AND QUALITY ENHANCEMENT OF PRECIOUS OPAL FROM ETHIOPIA AND FIRE OPAL FROM MADAGASCAR
By	Miss Supansa Toaree
Field of Study	Earth Sciences
Thesis Advisor	Associate Professor Chakkaphan Sutthirat, Ph.D.
Thesis Co-Advisor	Bhuwadol Wanthanachaisaeng, Dr.rer.nat.

---

Accepted by the Faculty of Science, Chulalongkorn University in Partial  
Fulfillment of the Requirements for the Master's Degree

.....Dean of the Faculty of Science  
(Professor Supot Hannongbua, Dr.rer.nat.)

THESIS COMMITTEE

.....Chairman  
(Assistant Professor Sombat Yumuang, Ph.D.)

.....Thesis Advisor  
(Associate Professor Chakkaphan Sutthirat, Ph.D.)

.....Thesis Co-Advisor  
(Bhuwadol Wanthanachaisaeng, Dr.rer.nat.)

.....Examiner  
(Assistant Professor Pitsanupong Kanjanapayont, Dr.rer.nat.)

.....External Examiner  
(Somruedee Satitkune, Dr.rer.nat.)



# # 5572150123 : MAJOR EARTH SCIENCES

KEYWORDS: PRECIOUS OPAL / FIRE OPAL / ENHANCEMENT / HYDRATED SILICA SPHERES

SUPANSA TOAREE: CHARACTERISTICS AND QUALITY ENHANCEMENT OF PRECIOUS OPAL FROM ETHIOPIA AND FIRE OPAL FROM MADAGASCAR.  
ADVISOR: ASSOC. PROF. CHAKKAPHAN SUTTHIRAT, Ph.D., CO-ADVISOR: BHUWADOL WANTHANACHAISAEANG, Dr.rer.nat., 166 pp.

Precious opal from Ethiopia and fire opal from Madagascar were collected and analyzed for properties and characteristics prior to experimental enhancement. The main aims of this study are to search for the proper method of opal enhancement and to recognize the specific characteristics yielding gemological feature. Raman spectrometer indicates that the Ethiopian precious opals are typical opal-CT whereas Malagasy fire opals is opal-C. Microstructures of Ethiopian precious opals reveal bigger hydrated silica sphere (about 50-200 nm in diameter) with imperfect stacking which may lead to its weak play of color phenomenon compared to those found in Australian precious opals. On the other hand, Malagasy fire opal presents tiny hydrated silica spheres (about 10-100 nm in diameter).

After enhancements with various methods such as heating, water boiling and oil boiling at 100°C, all groups of opal appear to have been changed, differently. The Ethiopian precious opals may have more intense in play of color phenomena after heating and water boiling, properly. Malagasy fire opals appear to have no change after all enhancement techniques. The hydrated silica spheres of Ethiopian precious opals have turned to more perfect form. In conclusion, heating is quite effective enhancement for the Ethiopian precious opals due to property of hydrophane. Malagasy fire opal should have no potential for enhancement. The best enhancement of precious opal in this study is heating and boiling because it can improve play of color phenomena.

Department: Geology

Student's Signature .....

Field of Study: Earth Sciences

Advisor's Signature .....

Academic Year: 2014

Co-Advisor's Signature .....

## ACKNOWLEDGEMENTS

The author would like to acknowledge her thesis advisors, Associate Professor Dr. Chakkaphan Sutthirat and Dr. Bhuwadol Wanthanachaisaeng for their suggestion and supervision throughout the completion of this thesis.

Appriciation is also extended to Dr. Somruedee Satitkhun for being the external committee; her comments are very helpful.

The author sincerely appreciates the Department of Geology, Faculty of Science, Chulalongkorn University for sample preparation and other facilities. The Gem and Jewelry Institute of Thailand (Public Organization) provided analytical analyses.

Finally, the author would like express her special thank to family members and all friends at Earth Sciences Programs at Chulalongkorn University for their help, support and encouragement throughout this study.



## CONTENTS

	Page
THAI ABSTRACT .....	iv
ENGLISH ABSTRACT .....	v
ACKNOWLEDGEMENTS .....	vi
CONTENTS .....	vii
LIST OF TABLES .....	x
LIST OF FIGURES .....	xi
CHAPTER I INTRODUCTION.....	1
1.1 General Statement.....	1
1.2 Objectives .....	3
1.3 Methodology.....	3
1.4 Analytical Instruments.....	7
CHAPTER II LITERATURE REVIEWS .....	13
2.1 Opal.....	13
2.1.1 Precious Opal.....	15
2.1.2 Fire Opal .....	16
2.1.3 Common Opal.....	17
2.2 Opaline Characteristics.....	18
2.3 World Opal Deposit .....	21
2.4 Opal Deposit in Ethiopia .....	16
2.5 Opal Deposit in Madagascar.....	19
CHAPTER III SAMPLE COLLECTION AND CHARACTERISTICS .....	23
3.1 Introduction.....	23

	Page
3.2 Sample Collection .....	23
3.3 Physical and Gemological Properties.....	24
3.4 Internal Features .....	26
3.5 Microstructure .....	27
3.6 Fourier Transform Infrared Spectrometry (FTIR) .....	30
3.7 UV-Vis-NIR Spectrometry.....	33
3.8 Raman Spectrometry.....	35
3.9 Quantitative EPMA Analyses .....	39
CHAPTER IV EXPERIMENTAL ENHANCEMENTS.....	42
4.1 Introduction.....	42
4.2 Heating Experiment.....	43
4.2.1 Physical Properties.....	45
4.2.2 Field Emission Scanning Electron Microscope (FESEM).....	53
4.3 Boiling Experiment .....	55
4.3.1 Physical Properties.....	57
4.3.2 Field Emission Scanning Electron Microscope (FESEM).....	65
4.4 Oiling Experiment .....	67
4.4.1 Physical Properties.....	69
4.4.2 Field Emission Scanning Electron Microscope (FESEM).....	77
CHAPTER V DISCUSSIONS CONCLUSIONS AND RECOMMENDATIONS .....	80
5.1 Opal Characterization.....	80
5.1.1 Ethiopian Precious Opal .....	80
5.1.2 Malagasy Fire Opal.....	84



	Page
5.2 Opal Enhancements .....	88
5.2.1 Ethiopian Precious Opal .....	88
5.2.1 Malagasy Fire Opal.....	93
5.3 Conclusions .....	95
5.4 Recommendations .....	97
REFERENCES .....	98
APPENDIX.....	101
VITA.....	166



## LIST OF TABLES

Table 3.1 Summary of physical properties of representative opal samples in each group under this study. ....	26
Table 3.2 Various types of bonding of the Si-O system in opals. ....	39
Table 3.3 EPMA analyses of representative opal samples. ....	40
Table 4.1 Summary of gemological properties observed from Ethiopian precious opal, Malagasy white and orange fire opals before and after heating. ....	45
Table 4.2 Summary of the gemological properties of Ethiopian precious opal, Malagasy white and orange fire opals before and after boiling. ....	58
Table 4.3 Summary of gemological properties of Ethiopian precious opal, Malagasy white and orange fire opals before and after oiling. ....	70
Table 5.1 Summary of characteristics observed in Ethiopian precious opal and Malagasy fire opal. ....	88

## LIST OF FIGURES

Figure 1.1. Schematic diagram showing cause of play of color phenomena in opal (Ward, 2003).....	1
Figure 1.2 Flow-chart diagram showing methodology of this study.....	6
Figure 1.3 Gemological instruments including: (A) hydrostatic balance; (B) refractometer at Burapha Gemological Laborarory (BGL; (C) ultraviolet lamps (long wave short wave); (D) gemological microscope at The Gem and Jewelry Institute of Thailand (GIT). .....	7
Figure 1.4 PerkinElmer UV-Vis-NIR Spectrophotometers, the same model LAMBDA 950 based at the Burapha Gemological Laborarory (BGL) (A) and at the Gem and Jewelry Institute of Thailand (GIT) (B). .....	8
Figure 1.5 Thermo Scientific FTIR spectrometer, model Nicolet 6700, based at The Gem and Jewelry Institute of Thailand (GIT). .....	8
Figure 1.6 Renishaw Raman Spectroscope based at The Gem and Jewelry Institute of Thailand (GIT).....	9
Figure 1.7 Electron Probe Micro-Analyzer (EPMA) model JEOL JXA 8100 based at Department of Geology, Chulalongkorn University.....	10
Figure 1.8 Field Emission Scanning Electron Microscope (FESEM) model JSM-7001F based at Thailand Center of Excellence in Physics (ThEP), Department of physics, Chulalongkorn University.....	11
Figure 1.9 (A) Memmert electric furnace for heating experiment and (B) boiling and oiling facilities at the Department of Geology, Chulalongkorn University.....	12
Figure 2.1 precious opal (Ralph, 2008).....	14
Figure 2.2 SEM image showing well ordering of hydrated silica sphere with equal voids of Australian precious opal, width of view is 350. ....	14

Figure 2.3 Disordered hydrated silica spheres (80 nanometers in diameter) of fire opal from Slovakia (Gaillou et al., 2008). .....	15
Figure 2.4 Different types of precious opal: (A) black opal; (B) crystal opal; (C) white opal (Asnachinda, 2006). .....	16
Figure 2.5 Fire opals showing color shades of lemon opal (A) and cherry opal (B) (Asnachinda, 2006). .....	17
Figure 2.6 Varieties of common opals containing: (A) agate opal; (B) wood opal; (C) milk opal; (D) prase opal; (E) moss opal; (F) opalized bone; (G) hyalite (Asnachinda, 2006). .....	18
Figure 2.7 X-ray diffraction patterns showing peaks of all three opaline materials including opal-A, opal-CT and opal-C (Elzea and Rice, 1996). .....	19
Figure 2.8 Raman spectra in the 1200-200 $\text{cm}^{-1}$ range of the four Malagasy opals tested are compared to those of standard cristobalite and tridymite minerals from the RRUFF database (rruff.info) (Simoni et al., 2010) .....	20
Figure 2.9 Sedimentary and other opal deposits in the world (modified after Horton, 2004). .....	14
Figure 2.10 Geological map of Ethiopia (modified after Merla et al., 1973 and Schlüter, 2006). .....	17
Figure 2.11 The opal deposit is located in north-central Ethiopia, There are Mezezo province (Johnson et al., 1996) and Wegel Tena province (Rondeau et al., 2010). .....	19
Figure 2.12 Geologic map of Madagascar (modified after Besaire, 1964 and Schlüter, 2006). .....	21
Figure 2.13 Volcanic opal deposit near Bemia, in south-eastern Madagascar, is a relatively new source of gem-quality opal (Simoni et al., 2010). .....	22
Figure 3.1 Ethiopian precious opal and Malagasy fire opal were separated into three groups composed of: Group A, Ethiopian precious opals; Group B, Malagasy white fire opals; Group C, Malagasy orange fire opals. ....	24

Figure 3.2 Six representatives of Ethiopian precious opal with slightly show play of color phenomena (Group A). .....	24
Figure 3.3 Six representatives of Malagasy white fire opal (Group B). .....	25
Figure 3.4 Six representatives of Malagasy orange fire opal (Group C). .....	25
Figure 3.6 Clay minerals in Ethiopian precious opal (sample A3). .....	26
Figure 3.6 Finger print in Ethiopian precious opal (sample A2). .....	26
Figure 3.7 Minute particles in Ethiopian precious opal (samples A14). .....	27
Figure 3.8 Minute particles in Malagasy orange fire opal (sample C9). .....	27
Figure 3.9 Finger print in Malagasy orange fire opal (sample C8). .....	27
Figure 3.10 FESEM images (50,000x) of Ethiopian precious opals with low quality play-of-color. (A) and (B) show well order arrangement of larger hydrated silica spheres (about 222 nanometers in diameters) (samples A9 and A27, respectively). (C) tiny granular hydrated spheres (less than hundred nanometers in diameters) (sample A20). .....	28
Figure 3.11 FESEM images (50,000x) of Malagasy white fire opals (samples B10 (A), B20 (B) and B30 (C)) showing tiny irregular hydrated silica grains (smaller than hundred nanometers in diameters) with random arrangement. ....	29
Figure 3.12 FESEM images (50,000x) of Malagasy orange fire opal samples showing tiny irregular hydrated silica grains (less than hundred nanometers in diameters) with random orientation structure (samples C10, C20 and C30 in figures (A), (B) and (C), respectively). .....	30
Figure 3.13 Representative FTIR spectra of Ethiopian precious opals (Group A). .....	31
Figure 3.14 Representative FTIR spectra of Malagasy white fire opals (Group B). .....	32
Figure 3.15 Representative FTIR spectra of Malagasy orange fire opals (Group C). .....	32
Figure 3.16 Representative UV-Vis-NIR spectra of Ethiopian precious opal (Group A). .....	34

Figure 3.17 Representative UV-Vis-NIR spectra of Malagasy white fire opal (Group B)...	34
Figure 3.18 Representative UV-Vis-NIR spectra of Malagasy orange fire opal (Group C).....	35
Figure 3.19 Representative Raman spectra within 200-3500 $\text{cm}^{-1}$ region of Ethiopian precious opal.....	36
Figure 3.20 Raman spectra within 0-4000 $\text{cm}^{-1}$ region of Ethiopian precious opal (Rondeau et al., 2010). .....	37
Figure 3.21 Representative Raman spectra in 200-3500 $\text{cm}^{-1}$ region of Malagasy white fire opal. ....	37
Figure 3.22 Representative Raman spectra in 200-3500 $\text{cm}^{-1}$ region of Malagasy orange fire opal.....	38
Figure 3.23 Standard Raman pattern of cristobalite and tridymite from RRUFF database (ruff info.) derived from (Simoni et al., 2010). .....	38
Figure 3.24 Variation diagram of $\text{SiO}_2$ versus minor elements of Ethiopian precious opal, Malagasy white fire opal and Malagasy orange fire opal.....	41
Figure 4.1 Ethiopian precious opals (samples A1 and A2) show improvement of play of color phenomena after heating at 100°C under atmospheric condition.....	43
Figure 4.2 Malagasy white fire opals (samples B3 and B4) appear to have turbidity after heating at 100°C under atmospheric condition.....	44
Figure 4.3 Malagasy orange fire opals (samples C4 and C7) appear to have turbidity after heating at 100°C under atmospheric condition. ....	44
Figure 4.4 Plots of specific gravity versus refractive index before and after heating of Ethiopian precious opal, Malagasy white and orange fire opals.....	46
Figure 4.5 UV-Vis-NIR spectra of an Ethiopian precious opal (sample A4 of Group A) before and after heating. ....	47
Figure 4.6 UV-Vis-NIR spectra of a Malagasy white opal (sample B1 of Group B) before and after heating. ....	47

Figure 4.7 UV-Vis-NIR spectra of a Malagasy orange fire opal (sample C9 of Group C) before and after heating. ....	48
Figure 4.8 FTIR spectra of Ethiopian precious opal (sample A2) before and after heating. ....	49
Figure 4.9 FTIR spectra of Malagasy white fire opal (sample B3) before and after heating. ....	49
Figure 4.10 FTIR spectra of Malagasy orange fire opal (sample C7) before and after heating. ....	50
Figure 4.11 Raman spectra of Ethiopian opal (sample A2) before and after heating. .	51
Figure 4.12 Raman spectra of Malagasy white fire opal (sample B7) before and after heating.....	52
Figure 4.13 Raman spectra of Malagasy orange fire opal (sample C4) before and after heating.....	52
Figure 4.14 Representative FESEM images of Ethiopian precious opals with slightly show play of color phenomena before and after heating (sample A9). ....	54
Figure 4.15 Representative FESEM images of Malagasy white fire opal before and after heating (sample B10).....	54
Figure 4.16 Representative FESEM images of Malagasy orange fire opal before and after heating (sample C10).....	55
Figure 4.17 Ethiopian precious opals (samples A14 and A18) show improvement of play of color phenomena after boiling at 100°C in water. ....	56
Figure 4.18 Malagasy white fire opals (samples B17 and B20) appear to have no change after boiling at 100°C in water. ....	56
Figure 4.19 Malagasy orange fire opals (samples C16 and C17) did not change after boiling at 100°C in water. ....	57
Figure 4.20 Plots of specific gravity versus refractive index before and after boiling of Ethiopian precious opal, Malagasy white and orange fire opals.....	58

Figure 4.21 UV-Vis-NIR spectra of Ethiopian precious opal with slightly show play of color phenomena (group A) before and after boiling (sample A13). .....	59
Figure 4.22 UV-Vis-NIR spectra of Malagasy white opal (group B) before and after boiling (sample B18).....	60
Figure 4.23 UV-Vis-NIR spectra of Malagasy orange opal (group C) before and after boiling (sample C16). .....	60
Figure 4.24 FTIR spectra of Ethiopian precious opal (sample A16) before and after boiling.....	61
Figure 4.25 Similar FTIR spectra of Malagasy white fire opal (sample B15) before and after boiling.....	62
Figure 4.26 Similar FTIR spectra of Malagasy orange fire opal (group C) before and after boiling (sample C11).....	62
Figure 4.27 Raman spectra of Ethiopian opal (sample A17) before and after boiling.....	63
Figure 4.28 Raman spectra of Malagasy white fire opal (sample B16) before and after boiling.....	64
Figure 4.29 Raman spectra of Malagasy orange fire opal (sample C16) before and after boiling.....	64
Figure 4.30 Representative FESEM micrographs of Ethiopian precious opals with slightly show play of color phenomena before and after boiling (sample A20). .....	66
Figure 4.31 Representative FESEM micrographs of Malagasy white fire before and after boiling (sample B20).....	66
Figure 4.32 Representative FESEM micrographs of Malagasy orange fire opal before and after boiling (sample C20). .....	67
Figure 4.33 Ethiopian precious opals (samples A24 and A26) show improvement of play of color phenomena after oiling at 100°C.....	68



Figure 4.34 Malagasy white fire opals (samples B23 and B24) were not changed after oiling at 100°C.....	68
Figure 4.35 Malagasy orange fire opals (samples C25 and C26) were not changed after oiling at 100°C.....	69
Figure 4.36 Plots of specific gravity versus refractive index before and after oiling of Ethiopian precious opal, Malagasy white and orange fire opals.....	70
Figure 4.37 UV-Vis-NIR spectra of Ethiopian precious opal (sample A30 of Group A) before and after oiling.....	71
Figure 4.38 UV-Vis-NIR spectra of Malagasy white fire opal (sample B24 of Group B) before and after oiling.....	72
Figure 4.39 UV-Vis-NIR spectra of Malagasy orange fire opal (sample C29 of Group C) before and after oiling.....	72
Figure 4.40 FTIR spectra of Ethiopian precious opal (sample A21) before and after oiling.....	73
Figure 4.41 FTIR spectra of Malagasy white fire opal (sample B21) before and after oiling.....	74
Figure 4.42 FTIR spectra of Malagasy orange fire opal (sample C24) before and after oiling.....	74
Figure 4.43 Raman spectra of Ethiopian precious opal (Group A) before and after oiling (sample A24).....	76
Figure 4.44 Raman spectra of Malagasy white fire opal (Group B) before and after oiling (sample B29).....	76
Figure 4.45 Raman spectra of Malagasy orange fire opal (group C) before and after oiling (sample C27).....	77
Figure 4.46 Representative FESEM micrographs of Ethiopian precious opal losing play of color phenomena after oiling (sample A27).....	78

Figure 4.47 Representative FESEM micrographs of Malagasy white fire opal before and after oiling (sample B30). .....	78
Figure 4.48 Representative FESEM micrographs of Malagasy orange fire opal before and after oiling (sample C30). .....	79
Figure 5.1 Comparison between Raman spectra of opal-CT from Ethiopia under this study (A) and opal-CT from Wollo, Ethiopia (Rondeau et al., 2010) (B). .....	81
Figure 5.2 FTIR spectra of precious opals in the region of 4000-5500 $\text{cm}^{-1}$ : Ethiopian precious opal (A) and Australian precious opal (Filin and Puzynin, 2009) (B). .....	82
Figure 5.3 FESEM image of low quality Ethiopian precious opal (A) compared to SEM image of Australian precious opal (Smallwood et al., 2008) (B). .....	83
Figure 5.4 Comparison of Raman spectra of opal-C from Madagascar under this study (A), typical cristobalite (rruff.info) (B) and opal-C from Bemia, Madagascar (Simoni et al., 2010) (C). .....	85
Figure 5.5 FTIR spectra of fire opals showing significant absorptions in the region of 4000-6000 $\text{cm}^{-1}$ : Malagasy fire opal from this study (A) and Mexican fire opal from previous study (Choudhary and Bhandari, 2008) (B). .....	86
Figure 5.6 FESEM image of Malagasy fire opal (A) compared to SEM image of Mexican fire opal (Fritsch et al., 2006) (B). .....	87
Figure 5.7 Simplified structure of Ethiopian precious opal before and after heating. .	91
Figure 5. 8 TEM micrograph presenting porosity of hydrated silica sphere in Ethiopian precious opal (Chanmuang et al., 2015). .....	92
Figure 5.9 Simplified structure of Ethiopian precious opal before and after boiling....	92
Figure 5.10 Simplified structure of Ethiopian precious opal before and after oiling....	93
Figure 5.11 Simplified structure of Malagasy white and orange fire opals before and after heating.....	94

Figure 5.12 TEM images presenting no porosity in hydrated silica sphere of  
Malagasy fire opal (Chanmuang et al., 2015)..... 95



# CHAPTER I

## INTRODUCTION

### 1.1 General Statement

Opal ( $\text{SiO}_2 \cdot n\text{H}_2\text{O}$ ) is chemically characterized by silicon dioxide ( $\text{SiO}_2$ ) forming as hydrate silica spheres which are amorphous to poorly crystallized silica. Water also contains in the structure of opal. The most spectacular phenomena, called play of color, shows rainbow colors patches on the surface. There are many forms of water in the opal's structure that directly affect physical features and qualities. Play of color phenomena in opal is suspected to be caused by a regular three - dimensional stacking of hydrated silica spheres with voids between them leading to diffraction of visible light from the appropriate sphere diameter of about 150-300 nm (Jones et al., 1964, Ward, 2003).

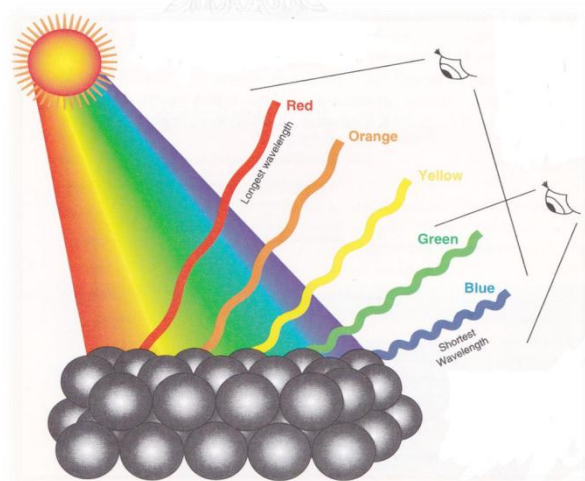


Figure 1.1. Schematic diagram showing cause of play of color phenomena in opal (Ward, 2003)

However, this ideal structure is rare in nature and not present in all opals. According to appearances, three varieties can be recognized as common opal, precious opal and fire opal. Common opal does not show play of color phenomena, while precious opal does. Fire opal is characterized by an orange body color. Opal can be found with high quantities in many localities around the world. The famous deposits of opal are in Australia, Mexico, Ethiopia, Madagascar etc. The water contained in opals from different origins are usually unequal due to environment of deposit. Opal can be found in two geologically distinct environments, generally defined as sedimentary deposit such as Australia and volcanic deposit such as Ethiopia (Smallwood et al., 2008).

Nowadays, gems and jewelry industries in Thailand have improved rapidly and made a lot of income to the country. Professional skill of gemstone enhancement in Thailand has led to the world color stone center. Opal is a famous gem which has potential to be enhanced to improve its gem quality. Therefore, many methods such as sugar treatment, composite, smoked treatment or heat treatment have been applied to these stones. However, there are a few studies focused on opal enhancement. This is because opal is easily cracked by heat which is the main problem of opal enhancement. In fact, physical properties of opal can be changed to yield better appearance of play of color, if appropriate heat is applied. Moreover, water contents in opal appear to be decreased after thermal enhancement (Zhuravlev, 2000, Thomas, 2008). Consequently, differences of geologic environments and chemical compositions would directly affect conditions of opal enhancement method (Toaree, 2011).

Duration of heating is one of the most important factor of opal enhancement. An appropriate temperature with a shorter time may not change appearance of opal. In the other hand, longer period at the same temperature may introduce cracks in

opal. Hence, proper temperatures and times are hardly combined for the best condition of opal enhancement.

This study was focused on enhancement of precious opal and fire opal from Ethiopia and Madagascar, respectively. Various methods such as heating, boiling and oiling then applied to both groups of opal samples. Gemological properties before and after enhancement were investigated using basic and advanced gemological instruments at Gem Testing Laboratory-Gem and Jewelry Institute of Thailand (GTL-GIT).

## 1.2 Objectives

The main objective of this research is to investigate gemological characteristics, particularly physical properties and internal features, of precious opal from Ethiopia and fire opal from Madagascar. Their characteristics were observed and analyzed before and after experimental enhancements. Comparison of appearances and other properties then made to suggest the best treatments of each opal group.

## 1.3 Methodology

Methods of the study project were designed to reach the targets. They can be summarized in Figure 1.2 and details were described below.

1. Literature Reviews: Geology of opal deposits, characteristics precious and fire opals and other related gemological researches were reviewed, initially. These information and basic knowledge actually led to research plan and experimental design throughout the project and critical discussions.

2. Sample Collection: All precious opal from Ethiopia and fire opal from Madagascar were bought directly from dealer in Thailand. These precious opal

samples slightly show play of color phenomena whereas fire opal samples have different color shades ranging from orange to yellow, white and colorless.

3. Sample Preparation: Precious opal samples were grouped by play of color quality while fire opal samples were grouped based on color and transparency. Subsequently, all sample were cut and polish to tablet shape which can be properly analyzed by basic and advanced gemological instruments.

4. Determination of Physical and Internal Features: All polished samples were weighted, photographed, given codes. Then physical and optical properties were observed and measured to confirm properties of opal. These basic properties include refractive index (RI) measured by refractometer and specific gravity (SG) using hydrostatic balance. Internal features were observed under a microscope before taking photos.

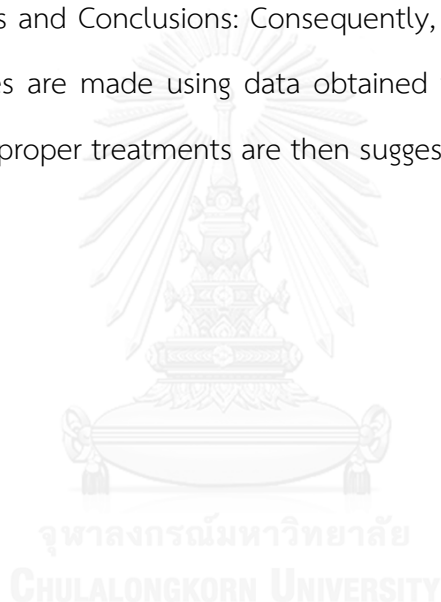
5. Absorption Spectroscopy: Absorption spectra were obtained from Ultraviolet-Visible-Near Infrared (UV-VIS-NIR) spectrophotometer. The UV-VIS-NIR absorption patterns can indicate causes of color in the gem samples before and after experimental treatments. Fourier Transform Infrared Spectrometer (FTIR) was used to study chemical bond especially water bonding before and after treatment. In addition, Raman Spectrometer was used to analyze crystallinity in each variety of opal sample both before and after treatment.

6. Internal Structure: of opal was investigated using Scanning Electron Microscope (SEM) to observe hydrated silica spheres that contain in the structure of opal. These hydrated silica spheres and their orientation should be related directly to physical properties and internal structure.

7. Chemical Composition: of opal samples were carried out using Electron Probe Micro-Analyzer (EPMA) which can analyze major composition (mostly SiO<sub>2</sub>) and some particular trace elements.

8. Experimental Treatments: was carried out into three different methods including heating, boiling and oiling. Interaction between different treatments and types of opal would be useful application for gems industry. The experiments were designed using optimum conditions that have been reported by previous researches.

10. Discussions and Conclusions: Consequently, discussions in crucial aspects to serve all objectives are made using data obtained from the research as well as literatures. The most proper treatments are then suggested to each type of opal.





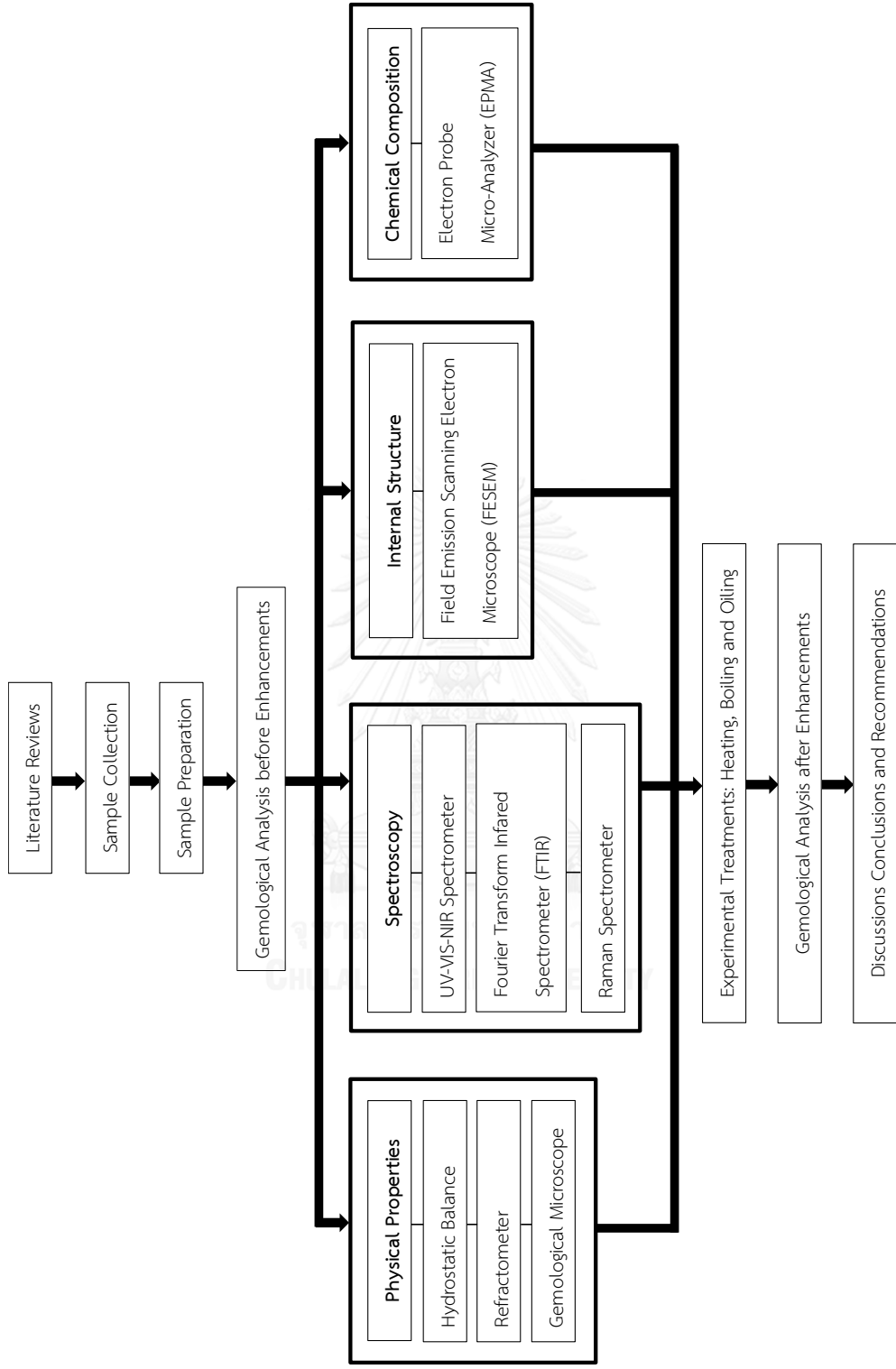


Figure 1.2 Flow-chart diagram showing methodology of this study

## 1.4 Analytical Instruments

1. Basic Gemological Instruments: Physical and optical properties of opal samples were collected using standard gemological instruments including hydrostatic balance, refractometer, ultraviolet lamps (long wave short wave) and gemological microscope. The first and second gemological instruments mentioned above are based at the Burapha Gemological Laboratory (BGL) and the rests belong to the Gems and Jewelry Institute of Thailand (GIT) (Figure 1.3).

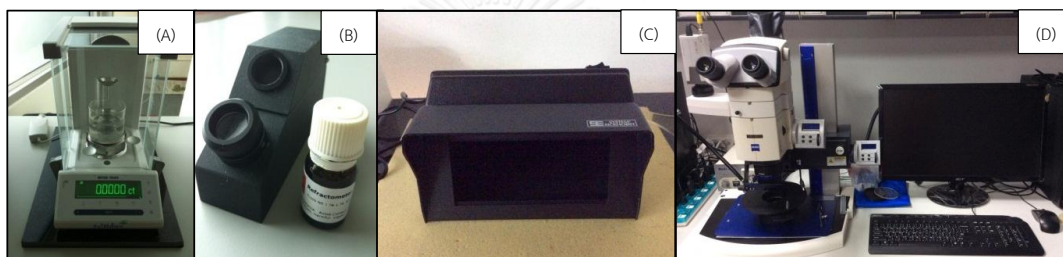


Figure 1.3 Gemological instruments including: (A) hydrostatic balance; (B) refractometer at Burapha Gemological Laboratory (BGL); (C) ultraviolet lamps (long wave short wave); (D) gemological microscope at The Gem and Jewelry Institute of Thailand (GIT).

2. UV-VIS-NIR Spectrophotometer: provided absorption spectra of all samples under this study which may be related to their body colors. The most crucial absorption spectra of opal and other gemstones are usually investigated within wavelength range between 200-2,000 nanometers. Two UV-VIS-NIR Spectrophotometers, the same model LAMBDA 950, based at the Gem and Jewelry Institute of Thailand (GIT) and the Burapha Gemological Laboratory (BGL) were used throughout the study (Figure 1.4).

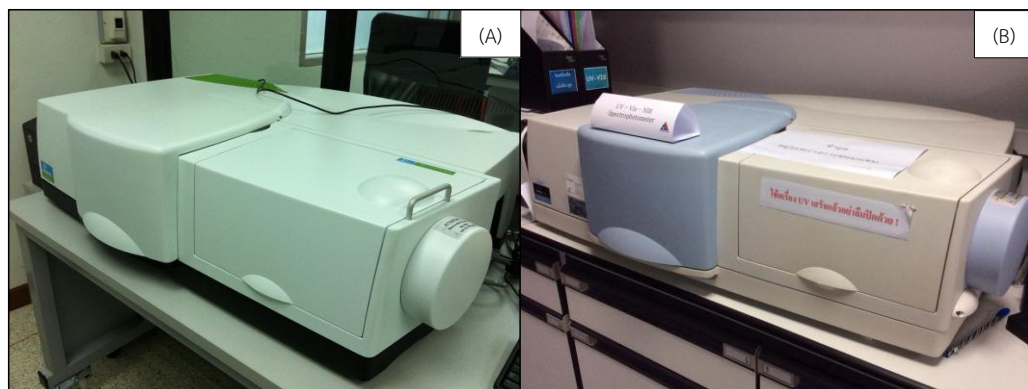


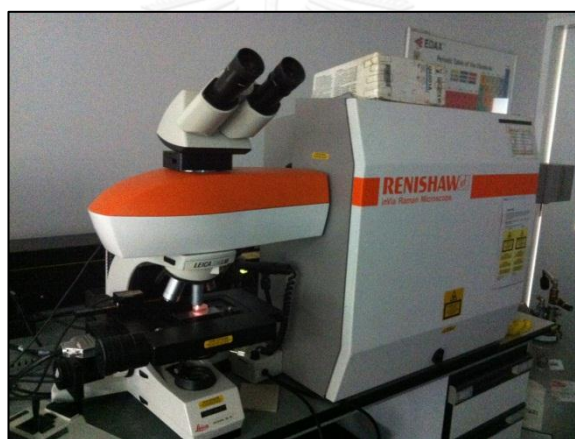
Figure 1.4 PerkinElmer UV-Vis-NIR Spectrophotometers, the same model LAMBDA 950 based at the Burapha Gemological Laboratory (BGL) (A) and at the Gem and Jewelry Institute of Thailand (GIT) (B).

3. Fourier Transform Infrared Spectrometer (FTIR): Infrared absorption spectra of all opal samples were obtained using a Thermo Scientific FTIR spectrometer, model Nicolet 6700, based at The Gems and Jewelry Institute of Thailand (GIT). The measurement was set up within mid Infrared range 200-9,000 wavenumber which may be related to structures and specific bonding of O-H stretching and bending (Figure 1.5).



Figure 1.5 Thermo Scientific FTIR spectrometer, model Nicolet 6700, based at The Gem and Jewelry Institute of Thailand (GIT).

4. Raman Spectrometer: All opal samples were analyzed by Renishaw Raman Spectrometer (Figure 1.6) based at the Gems and Jewelry Institute of Thailand (GIT). Raman spectrometer is a result of vibrational phenomena of molecular structure activated by light energy. The principal of vibrational spectroscopy is interaction between electrical field associated with photon changes induced by vibrational movements in electronic charges distribution within the substance. This advanced instrument yields Raman peaks that are characteristic of mineral structure including opal structure. Based on Raman spectrum, opal can be characterized into three categories, i.e., opal-A, opal-CT and opal-C.



CHULALONGKORN UNIVERSITY

Figure 1.6 Renishaw Raman Spectroscopy based at The Gem and Jewelry Institute of Thailand (GIT).

5. Electron Probe Micro-Analyzer (EPMA): is a non-destructive chemical analysis for solid samples. It is a quantitatively analytical method which is able to analyze within a certain tiny surface area (micrometers scale). All of opal samples were analyzed using an Electron Probe Micro-Analyzer (EPMA), JEOL model JXA 8100 equipped with WDXRF system, (Figure 1.7) based at Department of Geology, Chulalongkorn University. Chemical compositions of these opals may lead to

differentiation of their origins and appearances. Analytical conditions were set at 15 kV and  $2.51 \times 10^{-8}$  A with different counting times for each element. The beam spot probe diameter <1 micron. The measurement time using 30 seconds/peak count and background time 10 seconds/peak count. Standards used for calibration included Al, Si, Mn, Fe, Ca, Na and K for analyzed chemical composition of opal in each varieties.



Figure 1.7 Electron Probe Micro-Analyzer (EPMA) model JEOL JXA 8100 based at Department of Geology, Chulalongkorn University.

6. Field Emission Scanning Electron Microscope (FESEM) produces images of sample's surface by scanning a focused electron beam. The electrons interact with atoms in the sample producing various signals that can be detected and analyzed for sample's surface topography and composition. The electron beam is generally scanned in a raster scan pattern, and the beam's position is combined with the detected signal to produce an image. SEM can achieve resolution better than 1 nanometer. For this research, the selected samples were investigated with this advanced instrument, Model JSM-7001F (Figure 1.8), based at Thailand Center of Excellence in Physics (ThEP), Department of physics, Chulalongkorn University. High

resolution from 1.2 nm operated at 30 kV with high magnification until 100,000x were set for observation of hydrated silica sphere in opal's structure.



Figure 1.8 Field Emission Scanning Electron Microscope (FESEM) model JSM-7001F based at Thailand Center of Excellence in Physics (ThEP), Department of physics, Chulalongkorn University.

7. Experimental Facilities for Treatment: Three treatment techniques, heating, boiling and oiling, were designed for this study. Ten samples from each opal group were selected for individual experiments. The experiment's condition of heating was set at 100°C. Twenty four hours for soaking time under atmosphere using Memmert electric furnace (Figure 1.9). This condition had been reported by the previous study (Johnson et al., 1996, Thomas, 2008). Boiling was set at 100°C and soaking for three hours using hotplate, beaker and thermometer (Figure 1.9). The last methods was oiling in coconut oil with 100°C and soaking for three hours. Hotplate, beaker and thermometer were used similar to the previous boiling. Facilities of all experiments were provided by the Department of Geology, Chulalongkorn University.

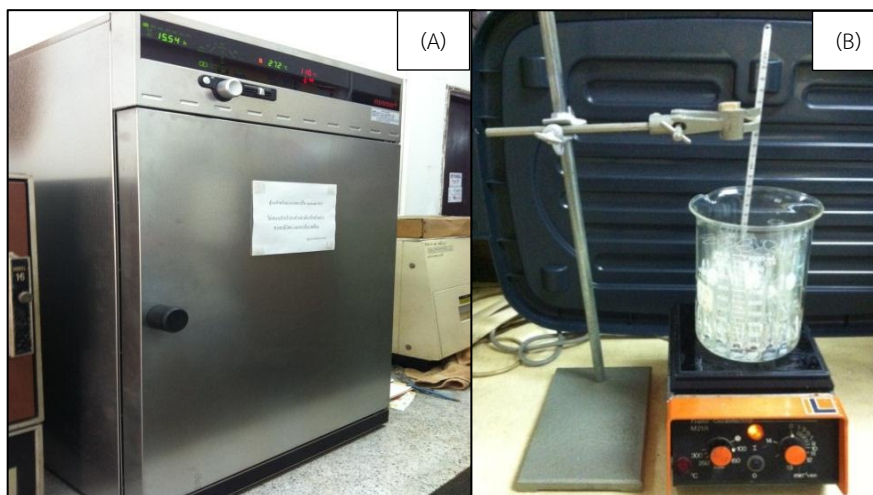
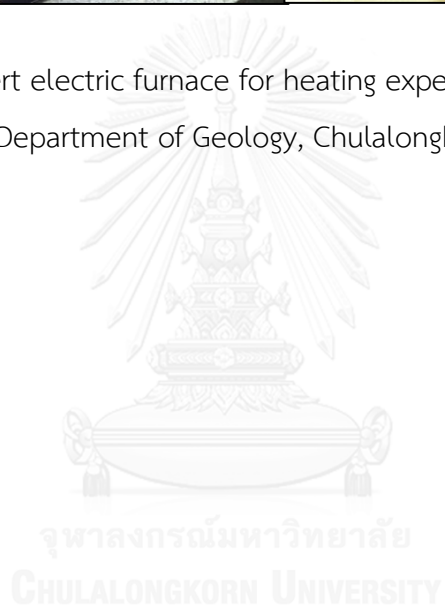


Figure 1.9 (A) Memmert electric furnace for heating experiment and (B) boiling and oiling facilities at the Department of Geology, Chulalongkorn University.



## CHAPTER II

### LITERATURE REVIEWS

#### 2.1 Opal

Opal is amorphous or poorly crystalline hydrated silica with the chemical formula  $\text{SiO}_2 \cdot n\text{H}_2\text{O}$ . Water content in opal is usually about 4-9% or up to 19%. Its specific gravity is averaged at 2.15 within range of 1.25 - 2.23 while refractive index is averaged at about 1.45 with range of 1.37 – 1.53. Opal is transparent to opaque. Fracture is normally developed as conchoidal feature. Body colors of opal have a variety ranging from colorless or white to orange, pink and others. These body colors are caused by trace elements (Fritsch et al., 2006). Opals with highly prizing would show light diffraction yielding play-of-color effect, usually called precious opal (Figure 2.1). The structure of opal with play-of-color effect should be controlled by well orderly regular three-dimensional stacking of hydrated silica spheres with voids between them. This morphology leads to the diffraction of visible light. The appropriate sizes of sphere may range about 150-300 nm in diameter (Jones et al., 1964). However, play of color phenomena in opal depends on several factors such as size, uniformity and alignment of silica spheres as well as orientation towards light source (Fritsch et al., 2006). A previous study using scanning electron microscope for opal imaging in 2008 revealed that the structure of Australian precious opal show ordered arrangement of voids and hydrated silica spheres with equal size of about 350 nm (Figure 2.2). This ordered structure causes play of color phenomena (Smallwood et al., 2008).





Figure 2.1 precious opal (Ralph, 2008)

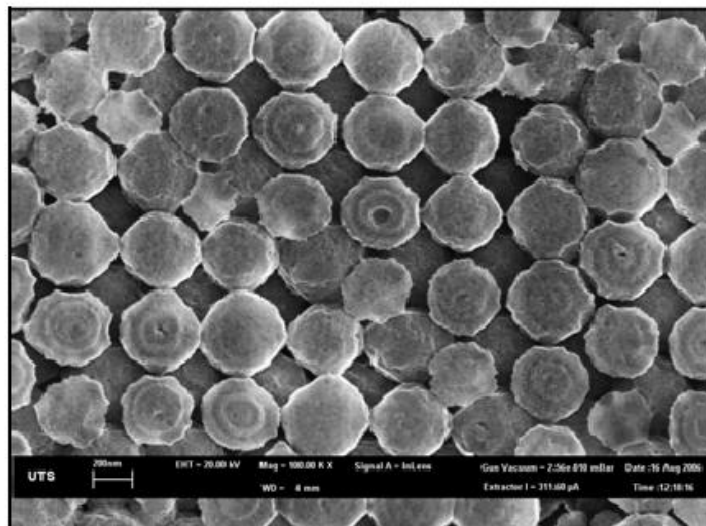


Figure 2.2 SEM image showing well ordering of hydrated silica sphere with equal voids of Australian precious opal, width of view is 350.

Opals without play-of-color phenomena and have a white body color may be called as common opal or potch opal. On the other hand opals have orange body color with or without play-of-color are grouped as fire opal (Simoni et al., 2010). The fire opal is also a variety of attractive and commercial gems in the world gem markets. Both opal varieties do not show the typical structure of play-of-color opal but they are usually composed of random aggregates of hydrated silica grains (smaller than 150 nm in diameters) (Fritsch et al., 2006, Gaillou et al., 2008). These

tiny sizes of hydrated silica spheres cannot diffract the visible light for color interference to yield play-of-color phenomena (Ward, 2003). Scanning electron image revealed the structure of fire opal from Slovakia consisting of disordered hydrated silica spheres with size of about 80 nanometers (Figure 2.3) which they are not big enough to exhibit play-of-color phenomena (Gaillou et al., 2008).

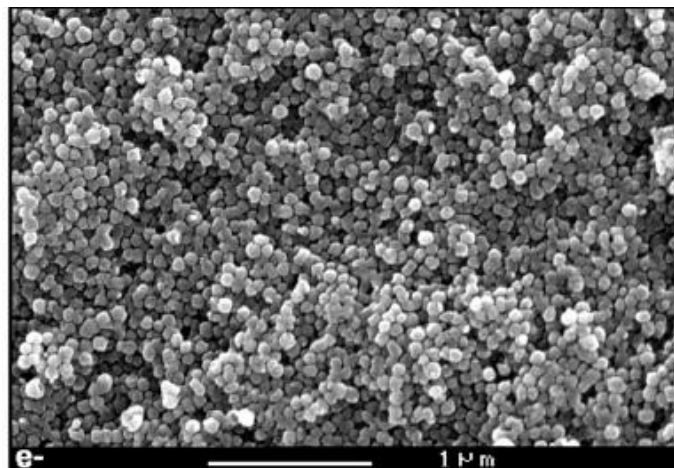


Figure 2.3 Disordered hydrated silica spheres (80 nanometers in diameter) of fire opal from Slovakia (Gaillou et al., 2008).

Many varieties of opal are characterized by body color and play-of-color phenomena as followed (Asnachinda, 2006).

#### 2.1.1 Precious Opal

Opal exhibits play-of-color phenomena because hydrated silica spheres align in good order. This variety can be divided into 5 categories depending on color body and transparency.

**Black opal:** includes precious opal with dark body color such as black, green, blue etc. (see Figure 2.4A). Their transparency are usually transparent to opaque. This characteristic is the most expensive opal variety.

**Crystal opal:** is typically transparent to semi-transparent with pale

play-of-color phenomena (Figure 2.4B).

White opal: is commonly found with milky white color and obvious play-of-color phenomena (Figure 2.4C).

Hydrophane opal: is characterized by specific structure available for water losing and resorption. Consequently, its transparency turns into opaque without play-of-color phenomena after water losing. After immersion into the water, water resorption can be taken place and yield more transparency and play-of-color phenomena.

Water jelly opal: appears similarly to jelly; hence, it is typically named as *jelly opal*. This opal is transparent to semi-transparent and sometimes shows play-of-color.

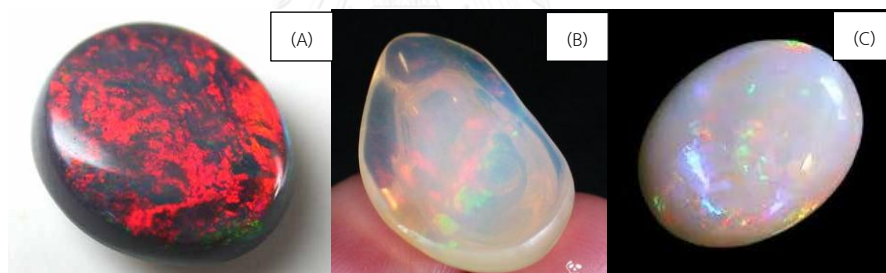


Figure 2.4 Different types of precious opal: (A) black opal; (B) crystal opal; (C) white opal (Asnachinda, 2006).

### 2.1.2 Fire Opal

This variety of opal may or may not exhibit play-of-color phenomena. Transparency to semi-transparency can be observed with orange body color shading from yellow in lemon opal to red in cherry opal etc. (Figure 2.5).

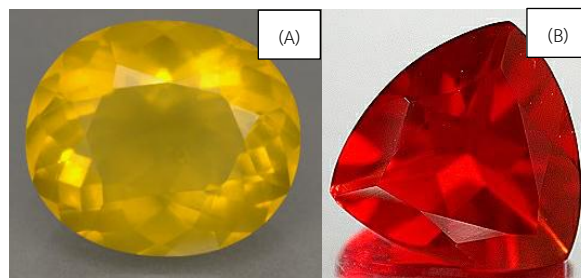


Figure 2.5 Fire opals showing color shades of lemon opal (A) and cherry opal (B) (Asnachinda, 2006).

### 2.1.3 Common Opal

Common opal has low gemological properties and no value. Turbid body color opaque and the value of this opal varieties is less than both opals varieties above. And in this varieties can divided in to 10 categories below.

Agate opal: is a special characteristic of agate which contains some opal in its texture (Figure 2.6A).

Wood opal or petrified wood: occurred in petrified wood (Figure 2.6B).

Milk opal: is translucent opal with pearly luster (Figure 2.6C).

Porcelain opal: is opaque texture with sparkling white similar to porcelain tile

Prase opal: is an opaque apple green opal (Figure 2.6D).

Wax opal: has yellow or brown body color sparkling like a candle.

Moss opal: contains manganese inclusion similar to moss (Figure 2.6E).

Opalized bone: is found in ancient partly replaced by silica solution (Figure 2.6F).

Opalized shell: is also found in ancient shell partly replaced by silica solution. It usually shows semi-transparency with yellowish white pearly luster.

Hyalite: is transparent and has no body color with vitreous luster (glass-like luster) (Figure 2.6G).

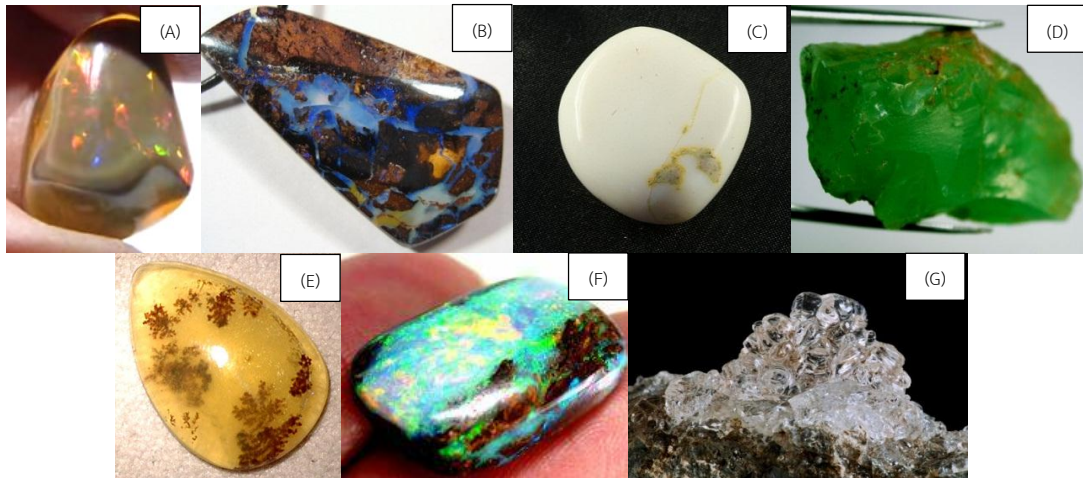


Figure 2.6 Varieties of common opals containing: (A) agate opal; (B) wood opal; (C) milk opal; (D) prase opal; (E) moss opal; (F) opalized bone; (G) hyalite (Asnachinda, 2006).

## 2.2 Opaline Characteristics

Opaline silica, a natural hydrous silica with the general formula  $\text{SiO}_2 \cdot n\text{H}_2\text{O}$ , has been found to occur with a range of morphologies depending on the environment in which the opal was formed. Based on x-ray diffraction (XRD) analyses, Jones and Segnite (Smallwood et al., 2008) originally divided opaline silica into three categories including Opal-A, Opal-CT and Opal-C.

Opal-A: is a highly disordered, near amorphous, structure showing only amorphous material. This opal is formed by solution process with slow concentration of the silica and then precipitation of colloidal particles, respectively. This opal structure is derived from sedimentary environments may also belong to opal-A.

Opal-CT: is a combination between cristobalite and tridymite formed within a disordered structure. This opal structure is derived from volcanic environments may also belong to opal-CT.

Opal-C: is well ordered cristobalite structure as clearly observed in XRD pattern. This opal is commonly found associated with lava flows.

In 1996, Elzea and Rice studied all 3 types of opaline characteristics using X-ray diffraction. The XRD pattern of opal-A is detected by a single diffused peak centered at approximately 4.1 Å. It is indicated as a highly disordered to almost amorphous material which is similar to glass that may show tiny peak of quartz. Opal-CT should show higher peak than opal-A because of crystallizations of cristobalite and tridymite in the structure. The highest peak is actually observed in opal-C and also shows narrow peak base. This characteristic indicates high crystallinity of opal. Therefore, it can be concluded that opal-C and opal-CT had higher crystalline than opal-A (see Figure 2.7).

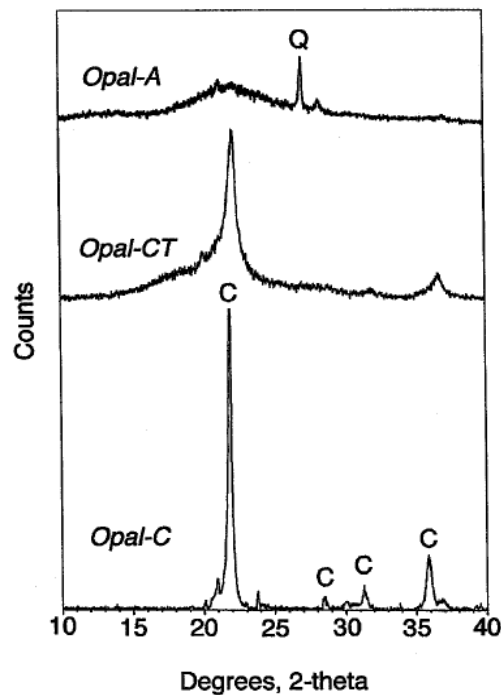


Figure 2.7 X-ray diffraction patterns showing peaks of all three opaline materials including opal-A, opal-CT and opal-C (Elzea and Rice, 1996).

In addition, Raman spectrometer can also be used to characterize all opaline types. In 2010, a new opal deposit was discovered near the city of Bemia, Madagascar 70 km from the coast. These opals occurred in Cretaceous rhyodacite volcanics rocks. They are typical fire opal with various colors without play-of-color phenomena. They are characterized by opal-CT and opal-C, revealing a peaks of cristobalite and tridymite dominated in the structure (Figure 2.8). The Raman spectra show a broad band peak centered at  $\sim 350\text{ cm}^{-1}$  which is typical opal-CT; on the other hand, some samples are identified as opal-C that exhibit Raman scattering at 412 and  $226\text{ cm}^{-1}$  which are main character peaks of cristobalite (see Figure 2.8) (Simoni et al., 2010)

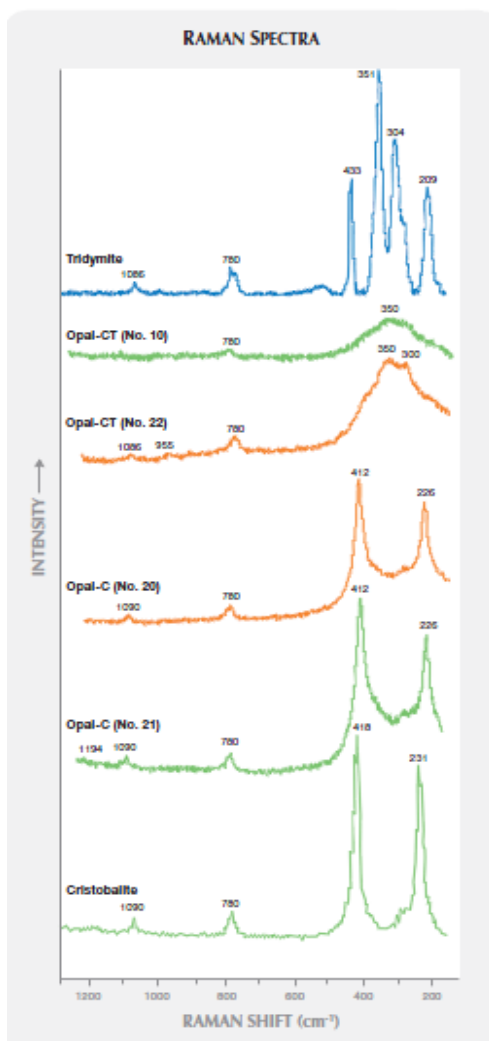


Figure 2.8 Raman spectra in the  $1200\text{-}200\text{ cm}^{-1}$  range of the four Malagasy opals tested are compared to those of standard cristobalite and tridymite minerals from the RRUFF database (ruff.info) (Simoni et al., 2010)

### 2.3 World Opal Deposit

The world major source of opal is in Australia Continent which is the main source of sedimentary opal. The most crucial deposit is in the Great Artesian District in which is dry weather region in the central Australia. Australia has been currently producing approximately 95 percent of the world's precious opal (Smallwood et al., 2008). On the other hand, opal from other continents are mostly from volcanic opal deposits that usually provide fire opal, common opal and occasionally precious opal. The significant producers are Mexico and Brazil; although, opal deposits in Slovakia and Czech Republic have provided the world's bulk production for over 2,000 years. Opal deposits in the other countries have been reported in Canada, USA, Tanzania, Kazakhstan, Turkey, Ethiopia and Madagascar. Ethiopia and Madagascar was the last two new opal mines which discovered in 2010 (Rondeau et al., 2010, Simoni et al., 2010). Distribution of the world opal deposits are present in Figure 2.9 (Horton, 2004). Fire opal is mainly from Mexico deposits whereas others locations have been found in Kazakhstan, Turkey, Ethiopia and USA. In USA, there are many volcanic opals which is located on the west such as Nevada, Kansas, Colorado, Texas, Utah, Nebraska, Idaho, Oregon, South Dakota and California. Canada is a precious opal source of the world; there are both volcanic and sedimentary opal deposits. Most deposits are in British Columbia State, west of Central America Continent. In the South America, volcanic opals have been discovered in Mexico, Honduras and Brazil. In Africa, opal were reported from Ethiopia and Madagascar. However, there are just a few opal deposits that are valuably and commercially operated in Europe and Asia. Moreover, common opal deposits have been found in Greenland Island, Denmark and Slovakia in central of Europe as well as in Java Island, Indonesia in Asia. In Thailand, a few opal deposits were reported to have associated with agate and chalcedony deposit in Tertiary volcanic terrane in Lam Narai, Lopburi Province. Nakhorn Ratchasima is another opal deposit in association with petrified wood.



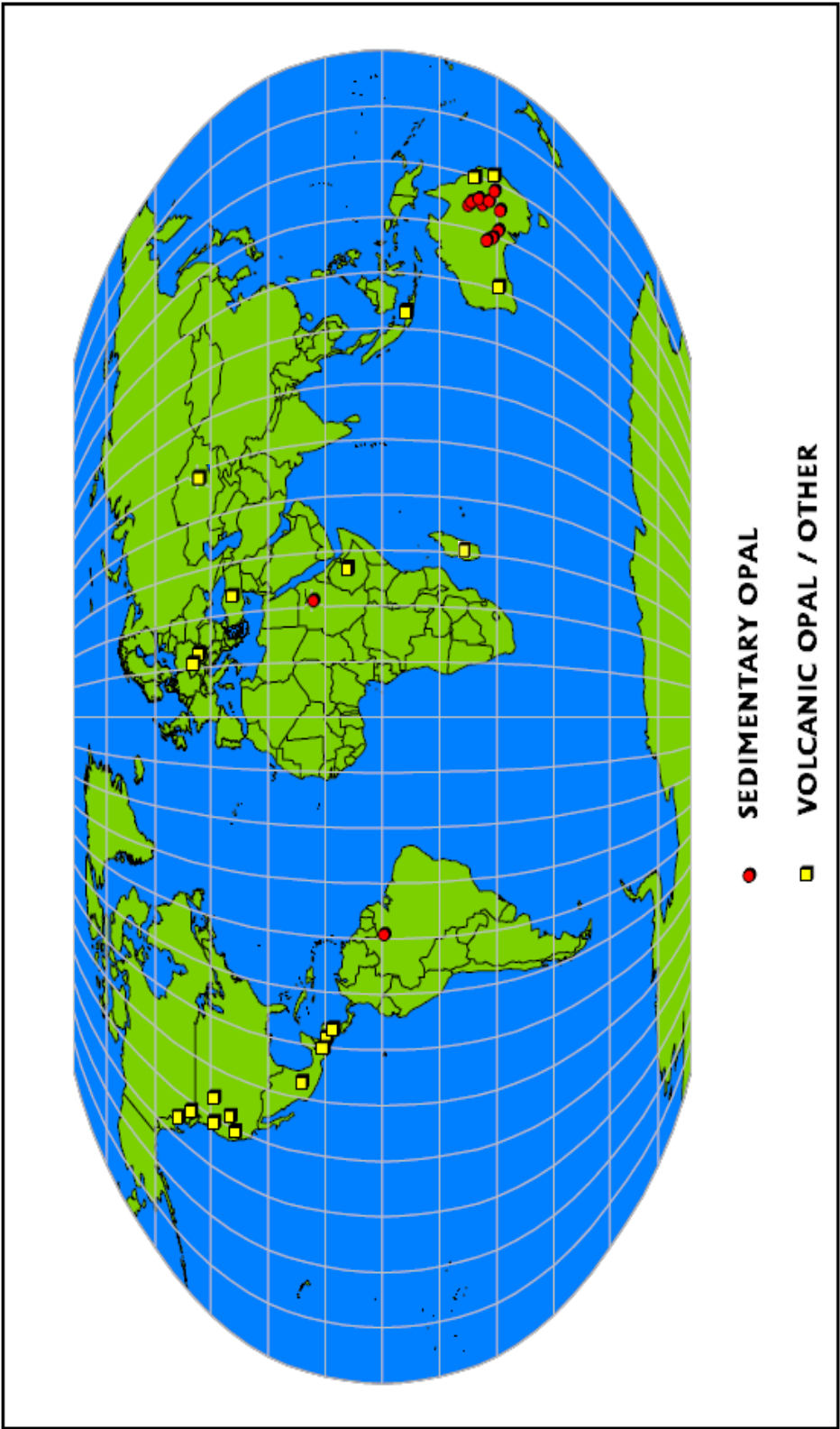


Figure 2.9 Sedimentary and other opal deposits in the world (modified after Horton, 2004).

The main geological environments of opal deposits are sedimentation and volcanism as reported above. Both types of deposit are normally associated with the weathered host rocks such as sandstone and rhyolite prior to precipitation of  $\text{SiO}_2$ -enriched liquid in cavities. Opal is not pure silica but it contains water as a main component. Moreover, some impurities including trace elements may also be contained its structure. The most common impurity is aluminum which substitutes silicon (Gaillou et al., 2008).

Most of sedimentary opal is associated with weathered sandstone in desert. Dry weather, precipitation and groundwater level are main factors of opal deposit.  $\text{SiO}_2$  colloidal liquid may be formed by highly weathering process of sandstone due to dry and heavy rainfall in desert and subsequently enriched by changing of groundwater level. Then opal deposit, opalization, may take place in the weathered host rocks or nearby rocks. This low temperature process usually yields opal-A. In Australia, the commercial production of precious opal occurs mainly in the sedimentary environments producing 90% of total world precious opal (Smallwood et al., 2008).

Occurrences of volcanic opal have also scattered around the world. They may associate with the weather vesicular basalt, rhyolite and andesite (Coenraads and Zenil, 2006, Rondeau et al., 2010). Volcanic flow, hydrothermal solution and dry weather are the main factor of the volcanic opal deposit. Silica solution from lava flows may be dissolved by hydrothermal solution; subsequently, this  $\text{SiO}_2$ -enriched liquid will deposit into the cavities of the host volcanic rocks. Opal-CT and opal-C is typically formed by this high temperature process, based on occurrences of cristobalite and tridymite which may actually formed during the volcanism prior to opalization. The most famous locality for volcanic opal, has been producing fine material for more than 100 years, is Mexico. Brazil, Slovakia, Czech Republic, Canada, USA, Tanzania, Kazakhstan and Turkey. Moreover, Ethiopia have also been producing

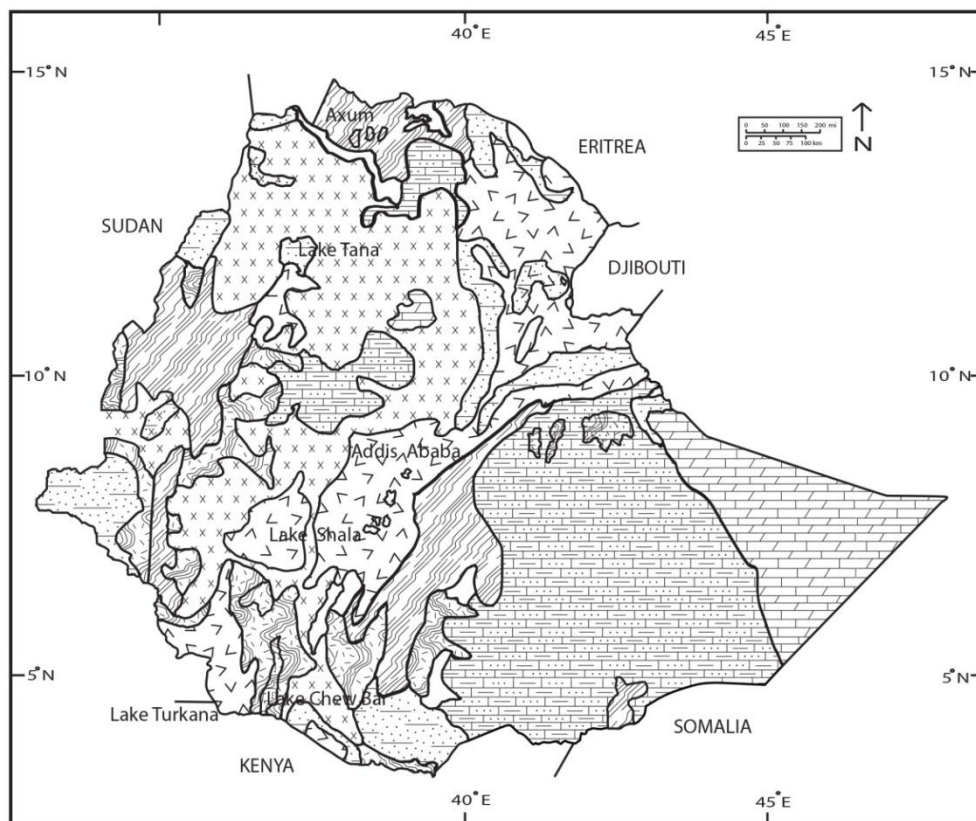
fire opal and precious deposits since 1996 (Johnson et al., 1996) and the latest opal mine deposit in Wollo since 2010 (Rondeau et al., 2010). In addition, volcanic opal have been discovered fire opal in Madagascar since 2010 (Simoni et al., 2010).

## 2.4 Opal Deposit in Ethiopia

Ethiopia is a country located in the Horn of Africa. It is bordered by Eritrea to the north and northeast, Djibouti and Somalia to the east, Sudan and South Sudan to the west, and Kenya to the south. With about 92,000,000 inhabitants, Ethiopia is the most populous landlocked country in the world, as well as the second-most populated nation on the Ethiopian continent. It occupies a total area of 1,100,000 square kilometers (420,000 square meters). Its capital and largest city is Addis Ababa.





Geology of Ethiopia contains a wide variety of sedimentary, volcanic and intrusive rocks which have been metamorphosed with various degrees. The basement rocks are in the south and west of the country where predominate granitic and gneissic rocks have been higher metamorphosed than the Precambrian sequences in the north.

Volcanism has taken place until the present time in Afar region. Lavas range from basalt to siliceous rocks. The youngest sediments are of Quaternary age. These include conglomerate, sand clay and reef limestone which accumulated in the Afar depression basin and the northern end of the main Rift Valley. Sediments which accumulated in the ancient lakes occur in the south end of the Afar, in the main Rift Valley, and in the Omo valley. Undifferentiated Quaternary sediments and superficial deposits occurred intermittently along the Sudanese and Kenyan borders (Merla et al., 1973, Schlüter, 2006) (Figure 2.10). The satellite image of Ethiopia shows volcanoes in both opal fields (Nasa, 2015).



## Ethiopia

### CENOZOIC

-  Alluvials, lacustrine/Volcano-lacustrine and swamp deposits
-  Rhyolitic and basaltic lavas, ignimbrites lacustrine and swamp deposit
-  Limestones, evaporites, clays
-  Highland Volcanics (basaltic rocks, tuffs, rhyolites)

### MESOZOIC

-  Sandstones, evaporites, limestones, marls

### PALEOZOIC

-  Sandstones, dolerites (Karoo Supergroup equivalents)

### PROTEROZOIC



-  Low-grade metamorphic rocks (slates, phyllites, chloritic and sericitic schists)
-  High-grade metamorphic rocks (gneisses, granulites, amphibolites, quartzites)

Figure 2.10 Geological map of Ethiopia (modified after Merla et al., 1973 and Schlüter, 2006).

Ethiopia has potentials of various mineral resources including lead, zinc, silver, ores and varieties of gemstones. The first report of gem opals in Ethiopia appeared in the February 1994 ICA Gazette (Barot, 1994). According to the report, Ethiopian opals were firstly seen in the Nairobi gem market in mid-1993. Some of these opals (obtained from Nairobi and sold as Ethiopian origin but with unconfirmed locality) were subsequently examined and reported in the Spring 1994 Gem News section (Koivula et al., 1994a). In Summer 1995, Gem News section published a short report describing opals from the Yita Ridge area of Shewa Province (Kammerling et al., 1996). Opal deposits in Ethiopia are found closely with volcanic rocks. Johnson et al. (1996) reported that opal Shewa province are near-colorless to white, yellow, orange, ray, or brown body occurred as nodules in volcanic rocks found in opal locality in Menz Gische District of Shewa Province, Ethiopia. Opals colors; some stones show face-up play-of-color and many stones have contra play-of-color phenomena. Preliminary stability tests indicate that these materials absorb water and some crazes may develop when expose to light and heat. The opal nodules occur in a continuous layer of welded tuff about 3 m thick between weathered rhyolite layers. Their specific gravity ranges between 1.35 and 2.03 and refractive indices are between 1.40 and 1.45.

Subsequently, Rondeau et al. (2010) reported a new occurrence of precious opal in Ethiopia that was discovered in 2008 near the village of Wegel Tena in Wollo Province (Figure 2.11). Unlike previous Ethiopian opals, these opal materials are mostly white with play-of-color often very vivid. However, its properties are consistent with those of opal-CT and most volcanic opals. The characteristics of these opal origins are hydrophane and prone to breakage. Specific gravity ranges from 1.74 to 1.89 and RI values are between 1.42 and 1.44 but some samples may be low as 1.36 to 1.38. UV luminescence of Ethiopian opal is quite variable, ranging

from bluish white to greenish white, yellow, and green. TEM micrograph of this opal origin reveals a microstructure consisting of spheres ~170 nm in diameter.



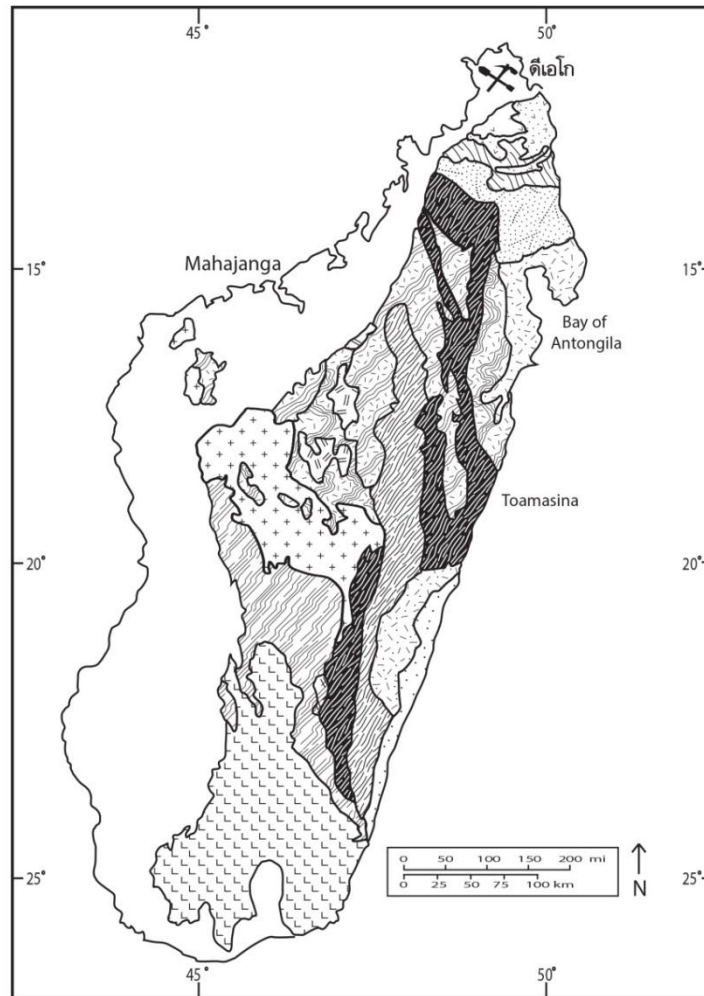
Figure 2.11 The opal deposit is located in north-central Ethiopia, There are Mezezo province (Johnson et al., 1996) and Wegel Tena province (Rondeau et al., 2010).

## 2.5 Opal Deposit in Madagascar

Madagascar is an island in the Indian Ocean apart from the eastern coast of Mozambique. It is the world's fourth largest island which appears to have drifted about 400 kilometers eastward from the mainland of Ethiopia and in to the Indian Ocean. It covers an area about 587,040 square kilometers. Madagascar's climate is tropical along coast, temperate inland, and arid in the south. The island has a narrow coastal plain with a high plateau and mountains in the center. Its lowest elevation is the Indian Ocean at 0 msl and below whereas the highest elevation is Maromokotro 2,876 m above msl.

Geologically, Madagascar is mainly composed of Precambrian rocks, which occupy two thirds of the island, particularly in the east, and sedimentary basins in the western part. In the west and northwest of Madagascar, Cretaceous volcanism of basalt and rare rhyolite erupted in the area. Tertiary-Quaternary basalts are found in the region of Antananarivo province, central Madagascar and in the district of Diego province in the north. In the east and the central of the country, high temperatures and high pressure metamorphic rocks such as gneisses, schists, migmatite and quartzite with very old age (around 2,600 Ma) of Archean have been mapped (Besaire, 1964, Schlüter, 2006) (Figure 2.12).





**Madagascar**

Paleozoic and younger rocks

**Bemarivo Block**

Neoproterozoic migmatite

Daraina-Milanoa Group (Neoproterozoic calc-alkaline volcanics and sediment)

Andriba Group (Neoproterozoic calc-alkaline intrusive)

Sambirano Group (Mesoproterozoic high-grade clastic rocks)

**Bekily Block**

Vohibory, Graphite and Androyan Sequences, Gneulite, Charnockite, marble and undifferentiated granulite and amphibolite facies rocks

**Antananarivo Block**

Amboropotsy Group, quartzite, schist, carbonate, mafic gneiss

Late Archean green stone belts, biotite gneiss, amphibolite, gabbro

Angavo-Nondiana belt, high-grade late Archean and Neoproterozoic rocks

Early Neoproterozoic (790-640 Ma) arc-related granitoids

Late Archean gneiss and migmatite

Late Neoproterozoic granitoids

**Antongi Block**

Late Archean biotite granite and granodiorite, orthogneiss and migmatite

Middle-Archean paragneiss and migmatite gneiss

Figure 2.12 Geologic map of Madagascar (modified after Besaire, 1964 and Schlüter, 2006).



Opals from a volcanic deposit located near Bemia, in southeastern Madagascar was reported in 2010 (Simoni et al., 2010) (Figure 2.13). Fire opal is also known from various regions in Madagascar, particularly deposit near the capital city of Antananarivo (Lacroix, 1992). Recently, common and fire opals are found near the city of Bemia, 70 km from the coast. These opals occurred in Cretaceous rhyodacite volcanic rocks. They formed as nodules with size up to several centimeters in diameter or in veins up to 20-30 cm long, with large variation in quality and color (Simoni et al., 2010).

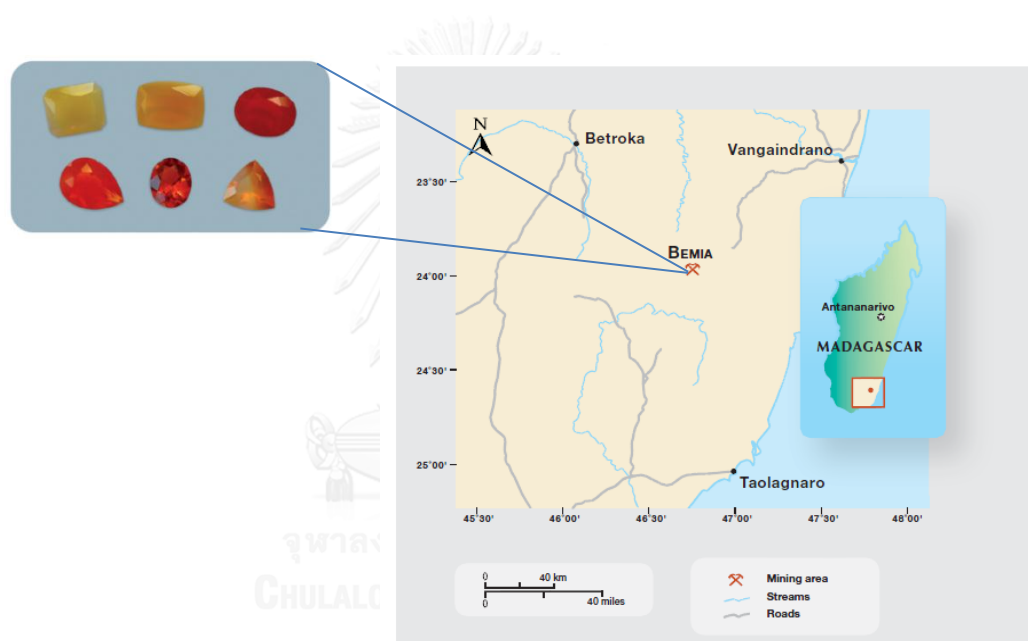


Figure 2.13 Volcanic opal deposit near Bemia, in south-eastern Madagascar, is a relatively new source of gem-quality opal (Simoni et al., 2010).

## CHAPTER III

### SAMPLE COLLECTION AND CHARACTERISTICS

#### 3.1 Introduction

All ninety samples were selected to represent the whole sample batch (more than 200 stones) which were provided by Thai and African traders. The selection was usually based on varieties, color and quality. Subsequently, they were cut and polished as flat tablets before observation and analyses of physical and gemological properties. These properties include specific gravity, refractive index, luminescence and internal features. For advanced instruments and detailed investigation, their results are reported in the next chapters. General gemological properties are described below.

#### 3.2 Sample Collection

All together 90 samples were selected from Ethiopian precious opals and Malagasy fire opals and subsequently separated into three groups. Precious opals from Ethiopia were grouped based on their quality of play-of-color phenomena whereas the second and third groups of Malagasy fire opals were classified based on their color and transparency. The first group, Ethiopian precious opals, has white body color with low quality of play-of-color phenomena (samples A1 to A30). The second group from Madagascar are white fire opals (samples B1 to B30) and the third group is Malagasy orange fire opals (samples C1 to C30) (see Figure 3.2). Observation of color appearance was carried out under standard daylight 6500 K.



Figure 3.1 Ethiopian precious opal and Malagasy fire opal were separated into three groups composed of: Group A, Ethiopian precious opals; Group B, Malagasy white fire opals; Group C, Malagasy orange fire opals.

### 3.3 Physical and Gemological Properties

Most opal samples are rectangular shape less than 2.5 carats in weight after cutting and polishing (Figures 3.2 to 3.4). Their gemological properties are collected in Appendix A and summarized in Table 3.1

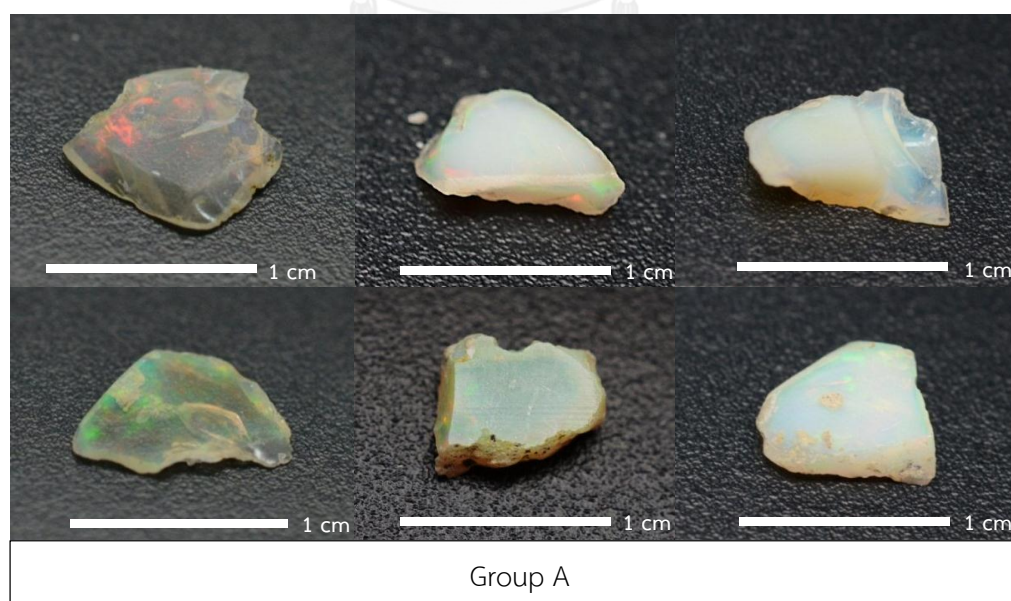


Figure 3.2 Six representatives of Ethiopian precious opal with slightly show play of color phenomena (Group A).

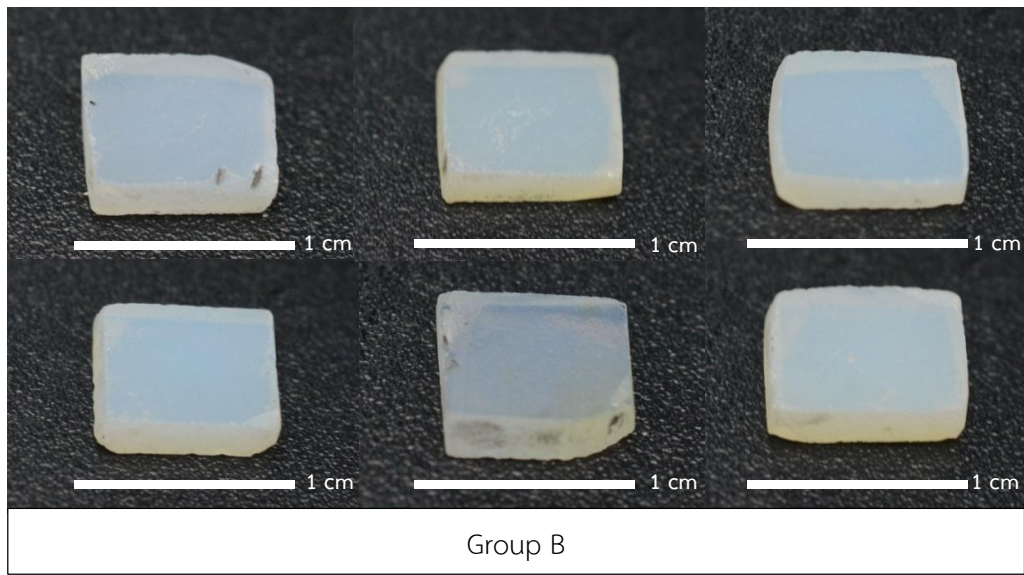


Figure 3.3 Six representatives of Malagasy white fire opal (Group B).

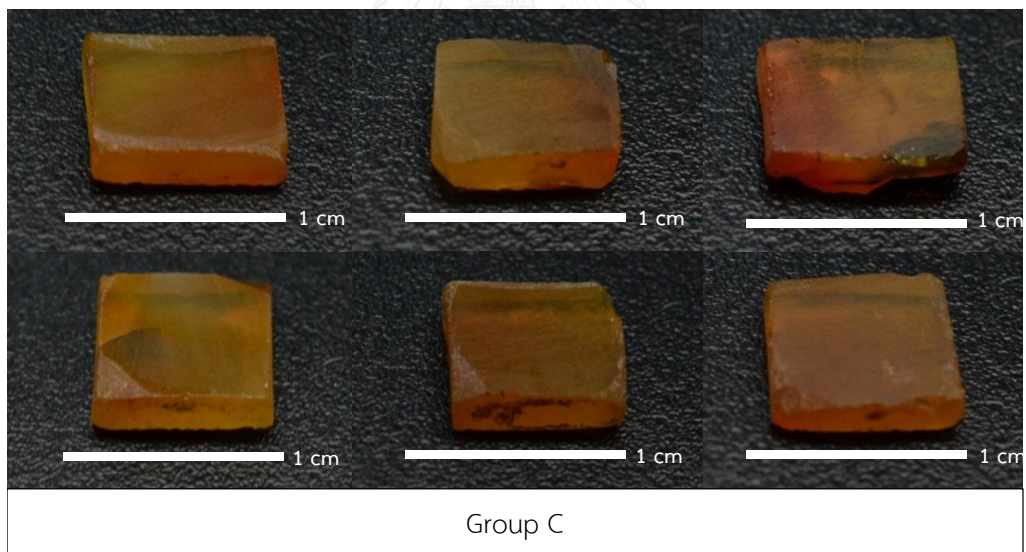


Figure 3.4 Six representatives of Malagasy orange fire opal (Group C).

Table 3.1 Summary of physical properties of representative opal samples in each group under this study.

Groups	Samples	SG.	RI.	Luminescence (UV light)	
				LW	SW
A	Ethiopian precious opal	1.85 - 1.97 (av. 1.91)	1.41 - 1.46	inert	inert
B	Malagasy white fire opal	2.02 - 2.19 (av. 2.11)	1.42 - 1.45	inert	inert
C	Malagasy orange fire opal	2.08 - 2.18 (av. 2.13)	1.43 - 1.47	inert	inert

### 3.4 Internal Features

Internal features observed under microscope in Ethiopian precious opals (group A) are generally characterized by clay minerals, fingerprint and minute inclusions (Figures 3.5-3.7).

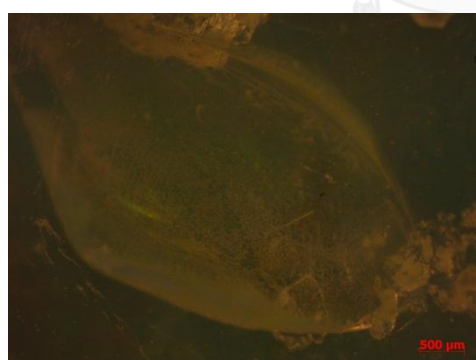


Figure 3.6 Finger print in Ethiopian precious opal (sample A2).



Figure 3.6 Clay minerals in Ethiopian precious opal (sample A3).

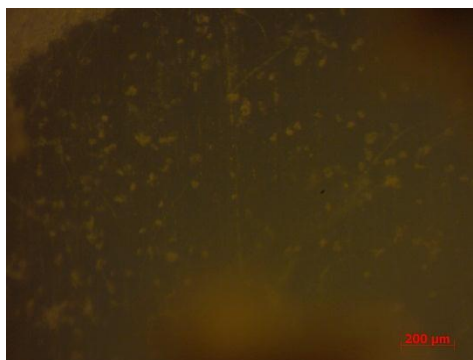


Figure 3.7 Minute particles in Ethiopian precious opal (samples A14).

Malagasy fire opals (Groups B and C) generally show fingerprint and minute inclusions (Figures 3.8 and 3.9) without clay minerals inclusion.



Figure 3.9 Finger print in Malagasy orange fire opal (sample C8).

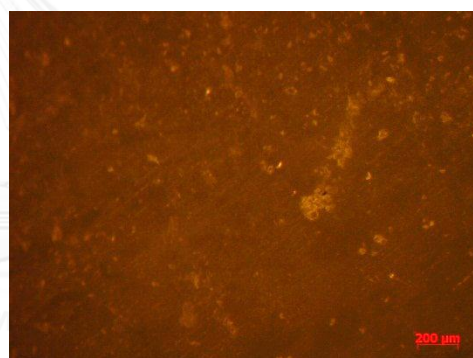


Figure 3.8 Minute particles in Malagasy orange fire opal (sample C9).

### 3.5 Microstructure

Nine opal samples representing all three groups were taken for observation of microstructure. Three Ethiopian precious opal samples (Group A), three Malagasy white fire opal (Group B) and three Malagasy orange fire opal (Group C) were investigated using Field Emission Scanning Electron Microscopy (FESEM) JSM-7001F based at Department of Physics, Faculty of Science, Chulalongkorn University.

Secondary Electron Image (SEI) with magnifications up to 100,000x can be operated. The cleaned fractured surface was prepared by etching in 10% hydrofluoric acid (HF) for 30 seconds. Subsequently, these samples were coated by about 20 nm thin film gold.

FESEM image of Ethiopian precious opal samples generally show tiny granular hydrated silica spheres with size smaller than hundred nanometers in diameters in most part of the structure (see Figure 3.10B). However, a few areas show well order arrangement of hydrated silica sphere with larger size of about 222 nanometers in diameters (Figures 3.10A and C) which may cause slightly play of color phenomena.

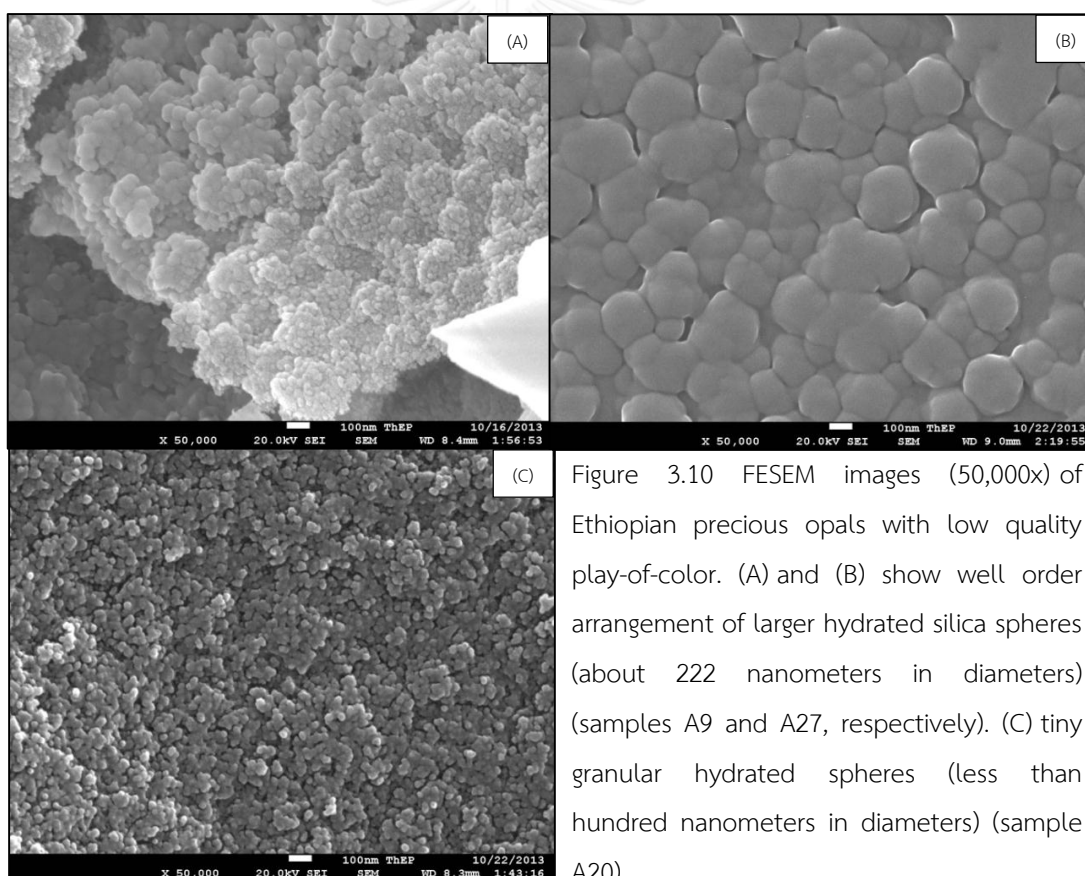


Figure 3.10 FESEM images (50,000x) of Ethiopian precious opals with low quality play-of-color. (A) and (B) show well order arrangement of larger hydrated silica spheres (about 222 nanometers in diameters) (samples A9 and A27, respectively). (C) tiny granular hydrated spheres (less than hundred nanometers in diameters) (sample A20).

Three representatives of Malagasy white fire opals (Group B) appear to have random orientation of irregular shaped silica hydrated grains varying from 10-100 nanometers in diameters (Figure 3.11).

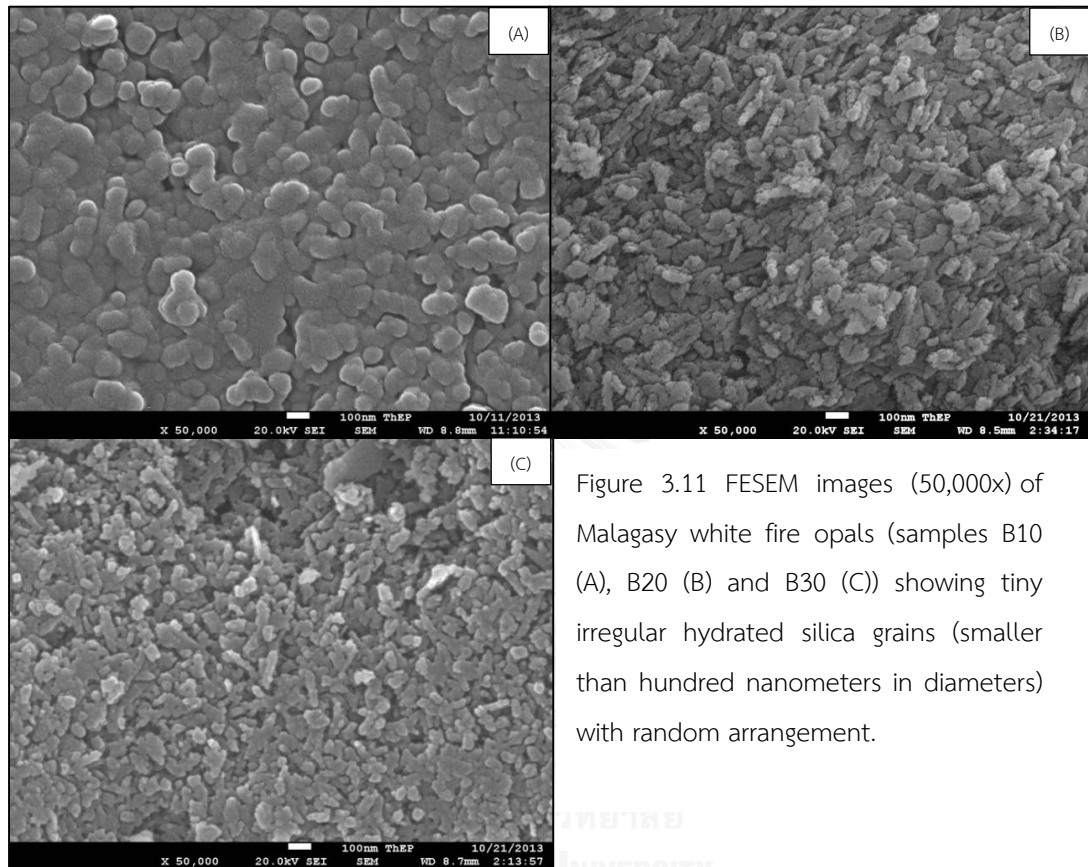


Figure 3.11 FESEM images (50,000x) of Malagasy white fire opals (samples B10 (A), B20 (B) and B30 (C)) showing tiny irregular hydrated silica grains (smaller than hundred nanometers in diameters) with random arrangement.

Malagasy orange fire opals show similar microstructure of the former group which consists of tiny irregular shaped hydrated silica grains (smaller than hundred nanometers in diameter arranging randomly in the structure (Figure 3.12).



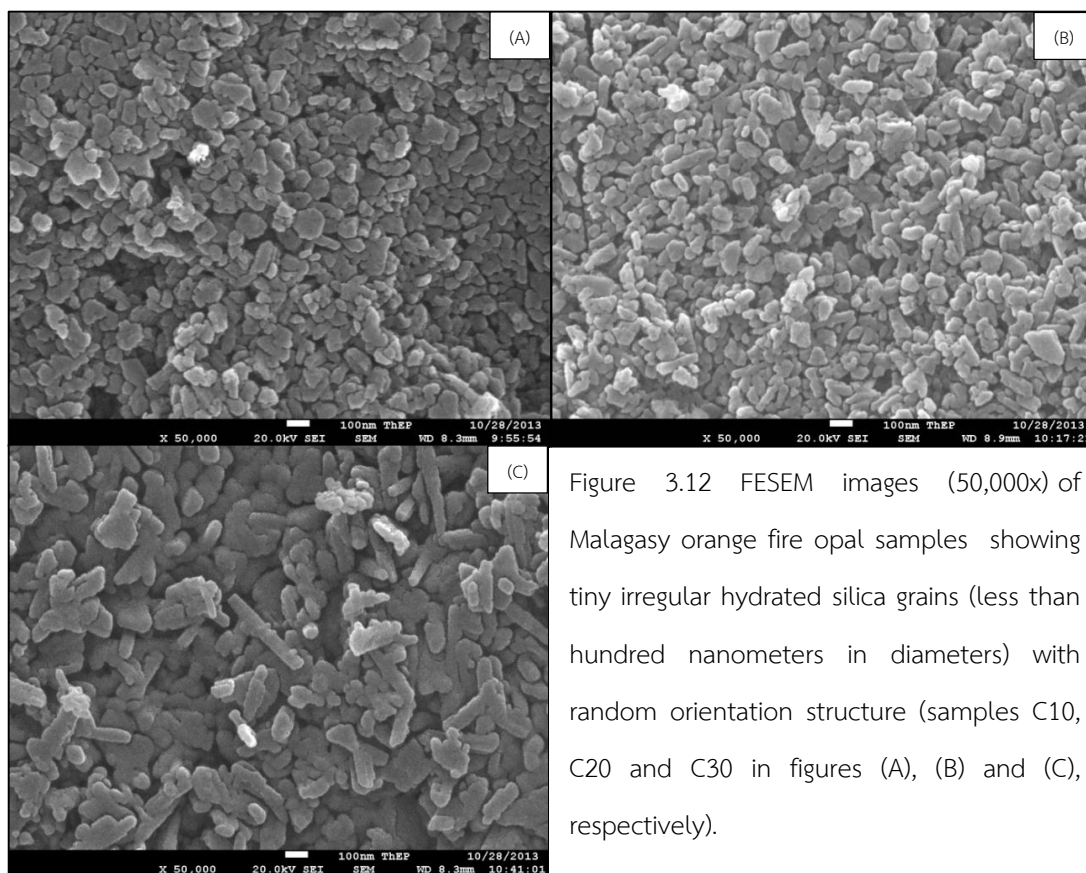


Figure 3.12 FESEM images (50,000x) of Malagasy orange fire opal samples showing tiny irregular hydrated silica grains (less than hundred nanometers in diameters) with random orientation structure (samples C10, C20 and C30 in figures (A), (B) and (C), respectively).

### 3.6 Fourier Transform Infrared Spectrometry (FTIR)

FTIR spectrum may give information on some structural and bonding of molecules which may reflect characteristics of material. In this research, the FTIR spectra were measured with absorption mode within the range of 200-9,000  $\text{cm}^{-1}$  using a Nicolet FTIR spectrophotometer (model NEXUS 670) based at the Gems and Jewelry Institute of Thailand (GIT). Absorption features relating to the structural O-H and Si-O stretching and bending for opal are usually present within this range. Three representative FTIR spectra of Ethiopian precious opal (group A) are displayed in Figure 3.13. Their absorption spectra exhibited similar features, particularly an absorption band in the range 5000-5400  $\text{cm}^{-1}$  with some sharp peaks caused by  $\text{H}_2\text{O}$

stretching and bending and a hump of SiOH stretching and bending in the range 4300-4600  $\text{cm}^{-1}$ .

Three representative FTIR spectra of Malagasy white fire opal (Group B) and three representative of Malagasy orange fire opal (Group C) appear to have the same pattern of Ethiopian precious opal (Group A). The main peak of H<sub>2</sub>O stretching and bending in the range of 5000-5400  $\text{cm}^{-1}$  are significantly present; however, hump of SiOH stretching and bending in the range of 4300-4600  $\text{cm}^{-1}$  are unclearly present (Figures 3.14 and 3.15).

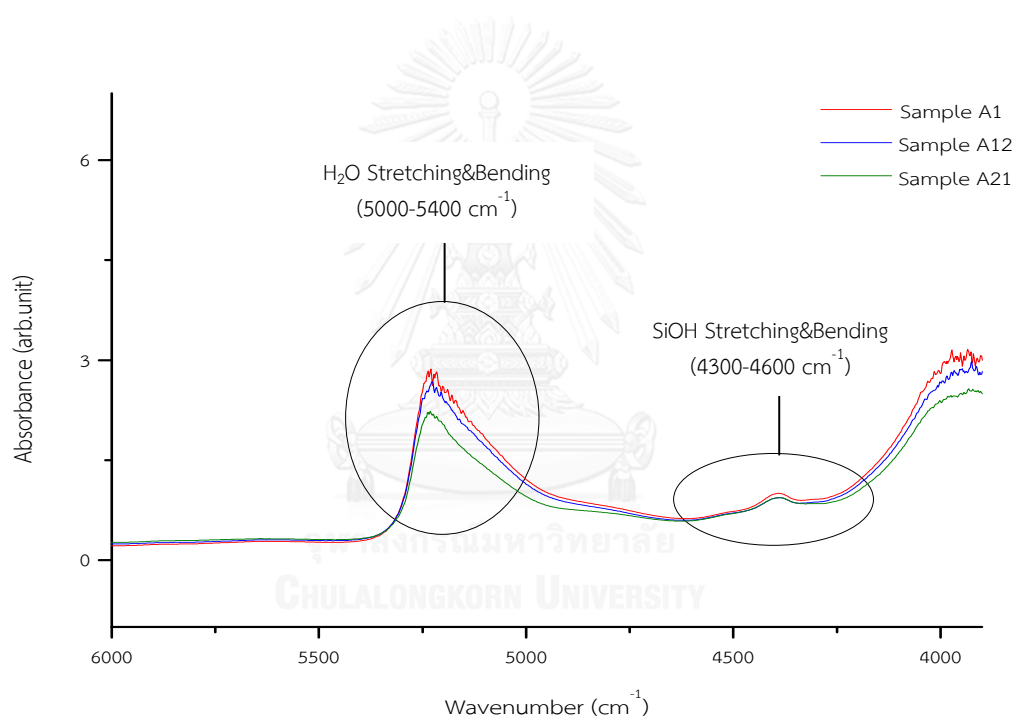


Figure 3.13 Representative FTIR spectra of Ethiopian precious opals (Group A).

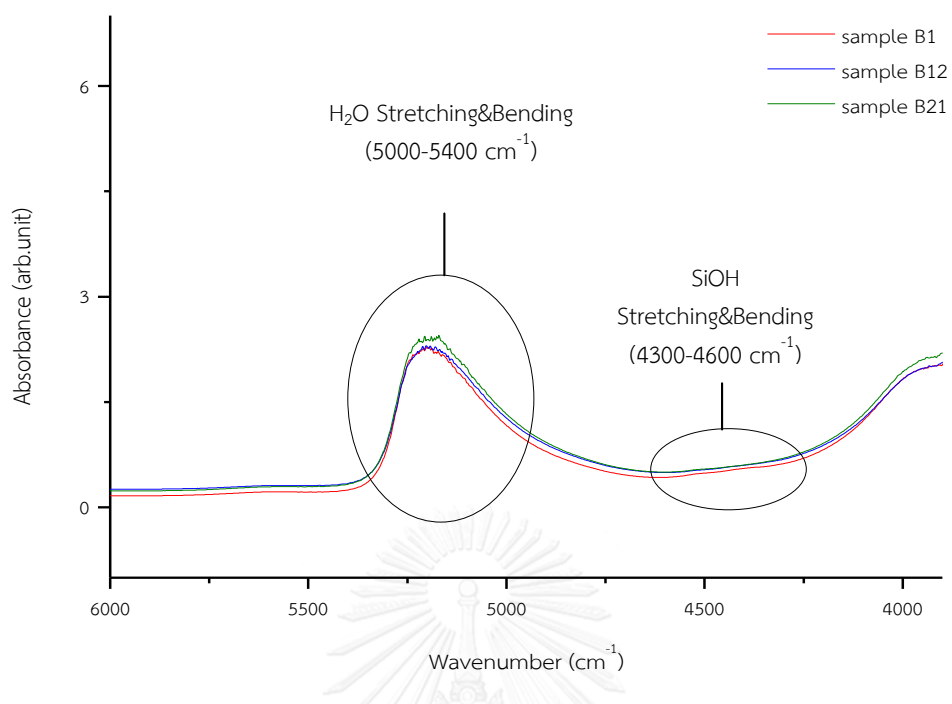


Figure 3.14 Representative FTIR spectra of Malagasy white fire opals (Group B).

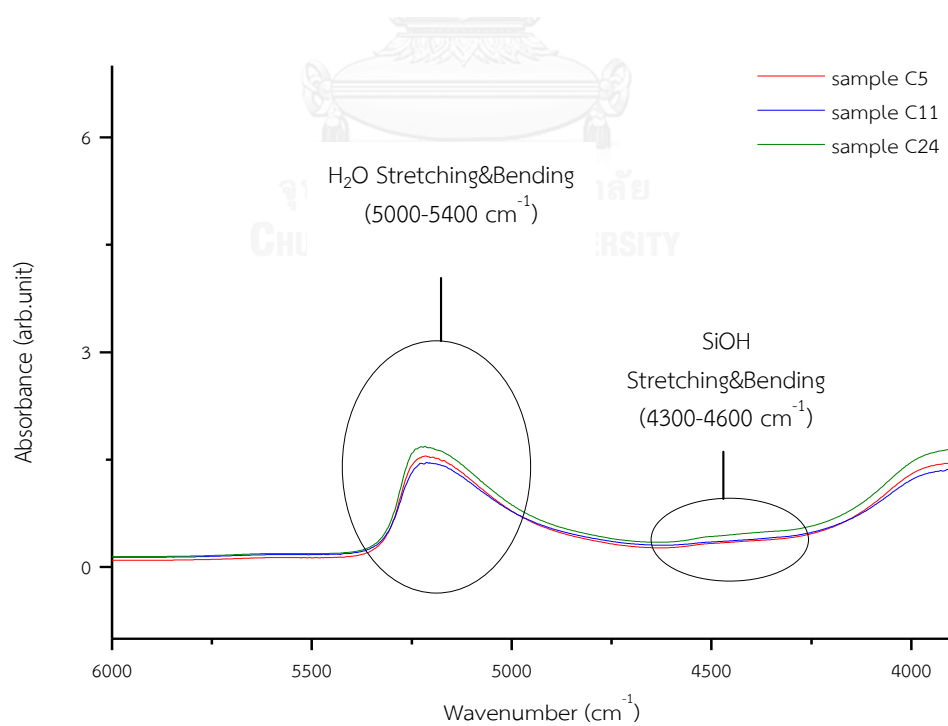


Figure 3.15 Representative FTIR spectra of Malagasy orange fire opals (Group C).

### 3.7 UV-Vis-NIR Spectrometry

In this research, the UV-Vis-NIR spectra of opals from Ethiopia and Madagascar were analyzed with absorption mode in the range of 200-2000 nm using Thermo Scientific FTIR spectrometer model Nicolet 6700 based at The Gem and Jewelry Institute of Thailand (GIT). This absorption range relates to body color. The body color of opal is mainly caused by trace elements such as Fe that is generally found in orange body color. The representative UV-Vis-NIR spectra of Ethiopian precious opals (Group A) are displayed in Figure 3.16. They generally show similar pattern without any significant absorption in this range due to their white or colorless body color (samples A4, A13 and A23).

Representative of UV-Vis-NIR spectra of Malagasy white fire opal (Group B), also show the same flat pattern without any significant absorption within this visible range due to its white body color (samples B5, B15 and B25) (see Figure 3.17). On the other hand, representative UV-Vis-NIR spectra of Malagasy orange fire opal (Group C) show a high absorption in the region of violet and ultraviolet (below 550 nm) which is actually cause of its orange body color (samples C9, C20 and C28) (Figure 3.18).

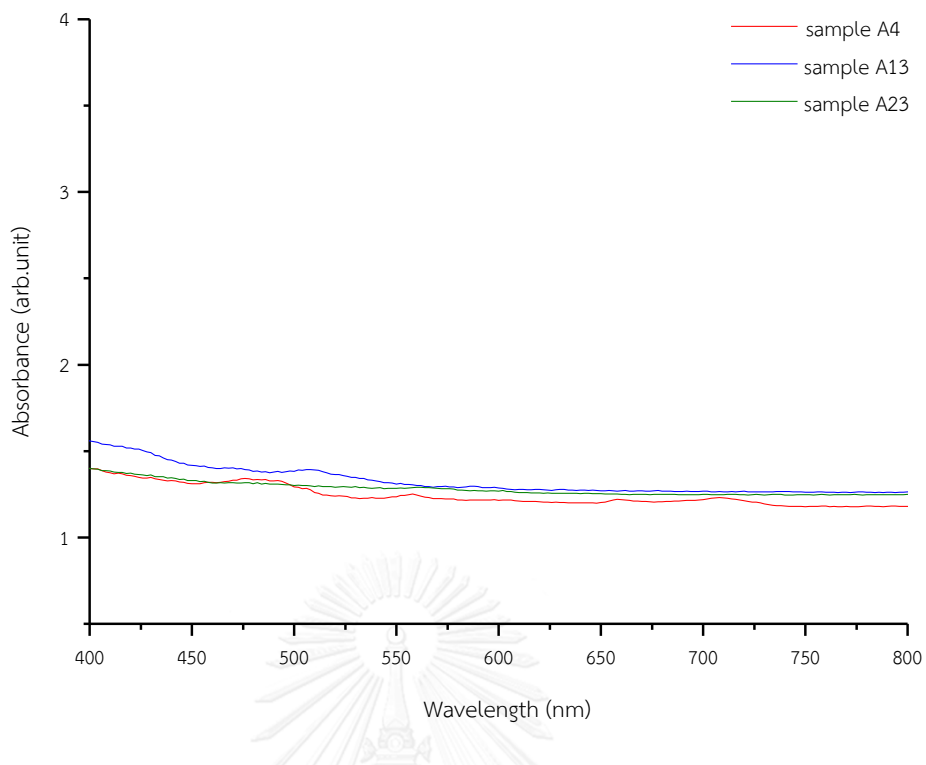


Figure 3.16 Representative UV-Vis-NIR spectra of Ethiopian precious opal (Group A).

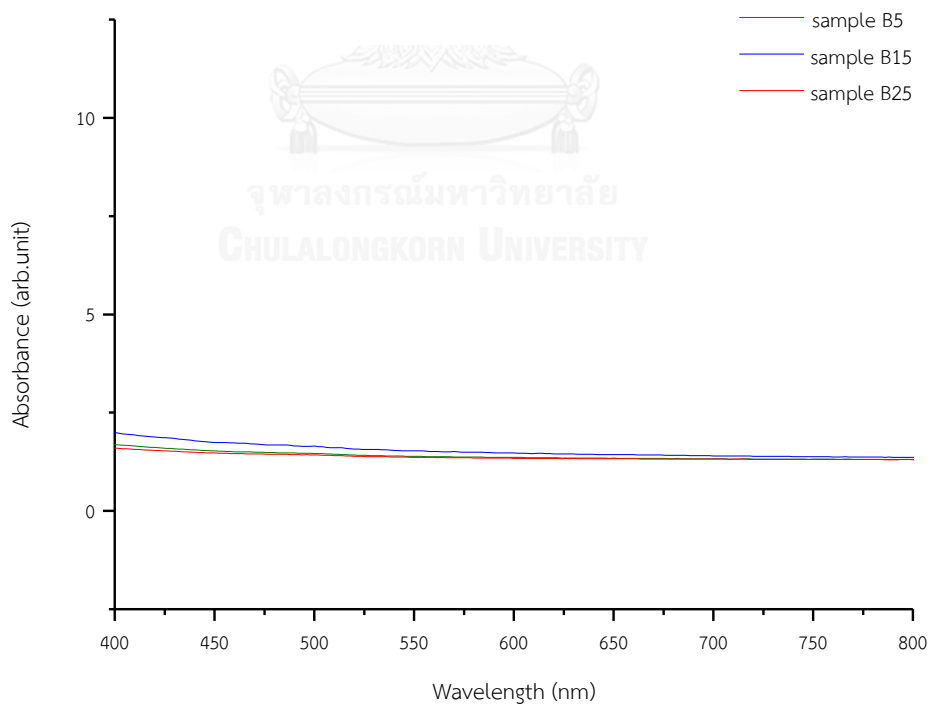


Figure 3.17 Reprtentative UV-Vis-NIR spectra of Malagasy white fire opal (Group B).

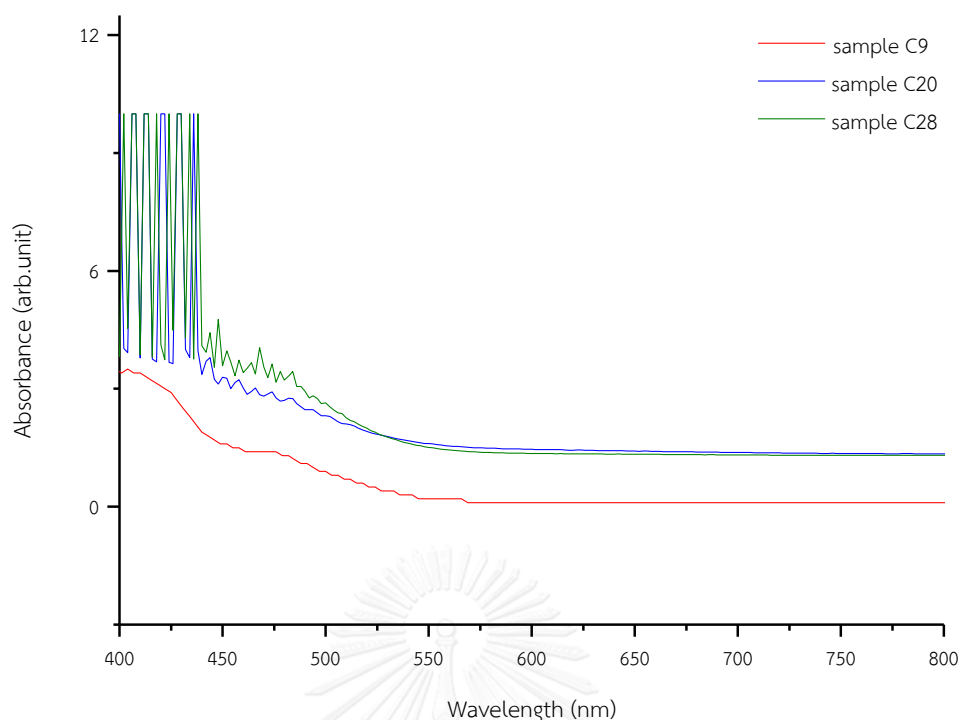


Figure 3.18 Representative UV-Vis-NIR spectra of Malagasy orange fire opal (Group C).

### 3.8 Raman Spectrometry

Raman spectrometry is vibrational phenomena of molecular structure activated by light energy which is characteristic of material. Therefore, crystalline morphology of opal may be recognized by the Raman spectra. Vibration spectra of silica polymorphs are used to identify opals (Smallwood et al., 1997). The Raman spectra within the range of  $200\text{-}3500\text{ cm}^{-1}$  using Renishaw Raman Spectrometer based at the Gems and Jewelry Institute of Thailand (GIT) were collected from opal samples in this study. This range is particularly useful for classification of crystalline structure, opaline mineral. They are different forms of silica occurred from different degrees of crystallinity. Three opal groups have been recognized based on these opaline materials. Opal-A is completely amorphous; opal-CT is semi-crystalline including cristobalite and tridymite; opal-C is a well ordered form of cristobalite.

Several peaks in the  $200\text{-}3500\text{ cm}^{-1}$  region usually present due to different stretching and bending vibration modes of the Si-O system. However, the most intense Raman peaks located in the  $300\text{-}350\text{ cm}^{-1}$  range are typical features of

tridymite and cristobalite (Simoni et al., 2010). Representative Raman spectra of Ethiopian precious opal (Group A) are displayed in Figure 3.19. They present similar pattern including particularly broad band centered at  $345\text{ cm}^{-1}$  with shift left indicating typical opal-CT as suggested by Rondeau et al., (2010) (Figure 3.20). The other peaks show different stretching and bending vibration modes of the Si-O system able to be observed are listed in Table 3.2.

Malagasy white fire opal (Group B) and Malagasy orange fire opal (Group C) show the same pattern of Raman peaks as displayed in Figures 3.21 and 3.22, representatively. The main peaks present at around  $230\text{ cm}^{-1}$  and  $416\text{ cm}^{-1}$  indicating character of cristobalite which may occupy in the opal structure. This is comparable to the study of Simoni et al. (2010) (Figure 3.23). Consequently, these opals are identified as opal-C.

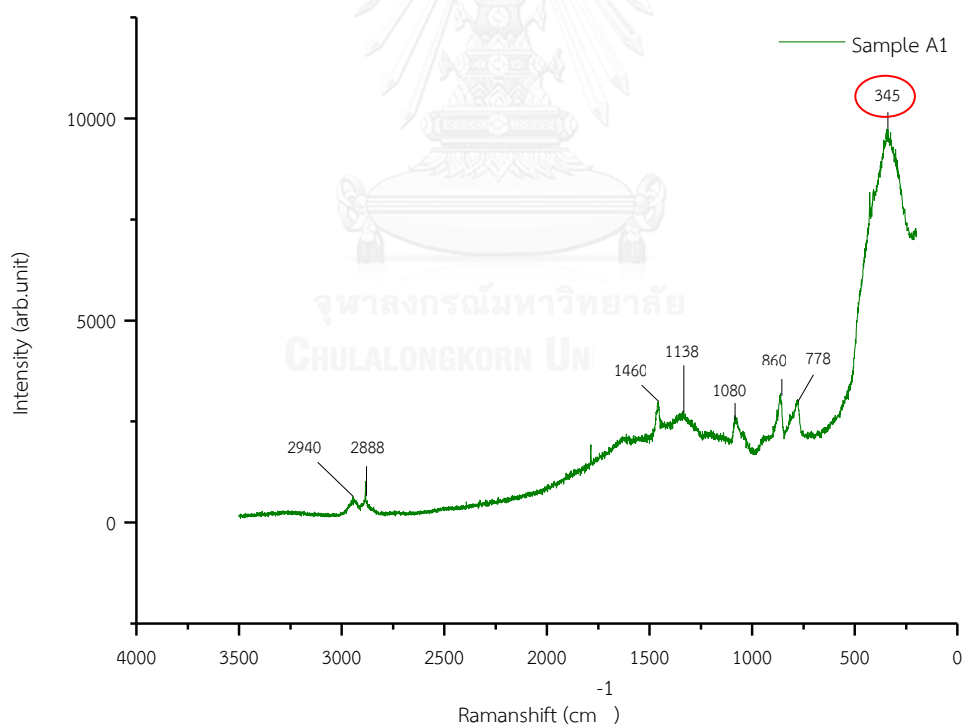


Figure 3.19 Representative Raman spectra within  $200\text{-}3500\text{ cm}^{-1}$  region of Ethiopian precious opal.

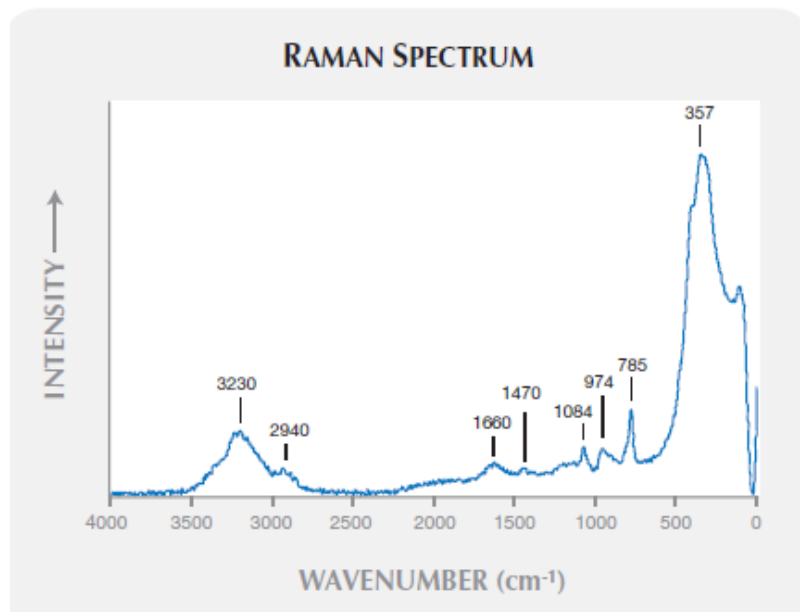


Figure 3.20 Raman spectra within 0-4000 cm<sup>-1</sup> region of Ethiopian precious opal (Rondeau et al., 2010).

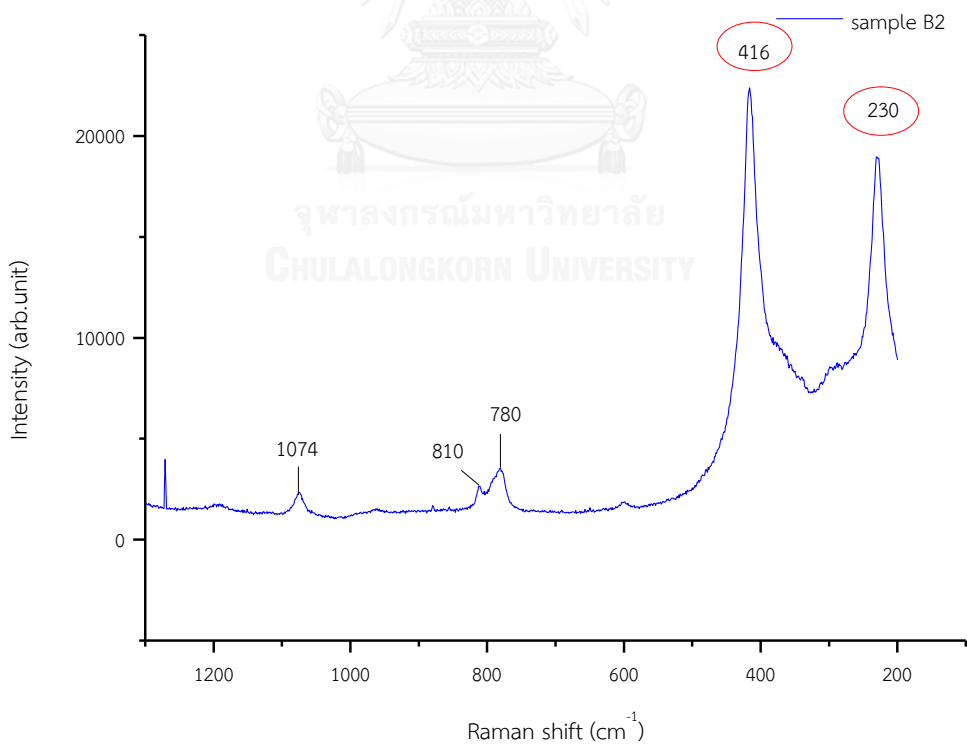


Figure 3.21 Representative Raman spectra in 200-3500 cm<sup>-1</sup> region of Malagasy white fire opal.



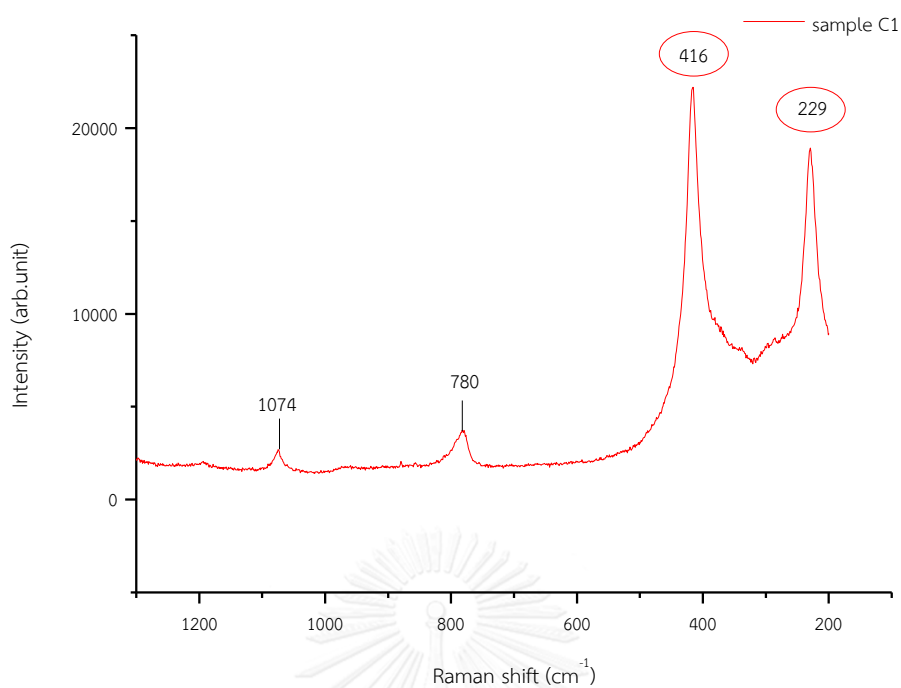


Figure 3.22 Representative Raman spectra in  $200\text{-}3500\text{ cm}^{-1}$  region of Malagasy orange fire opal.

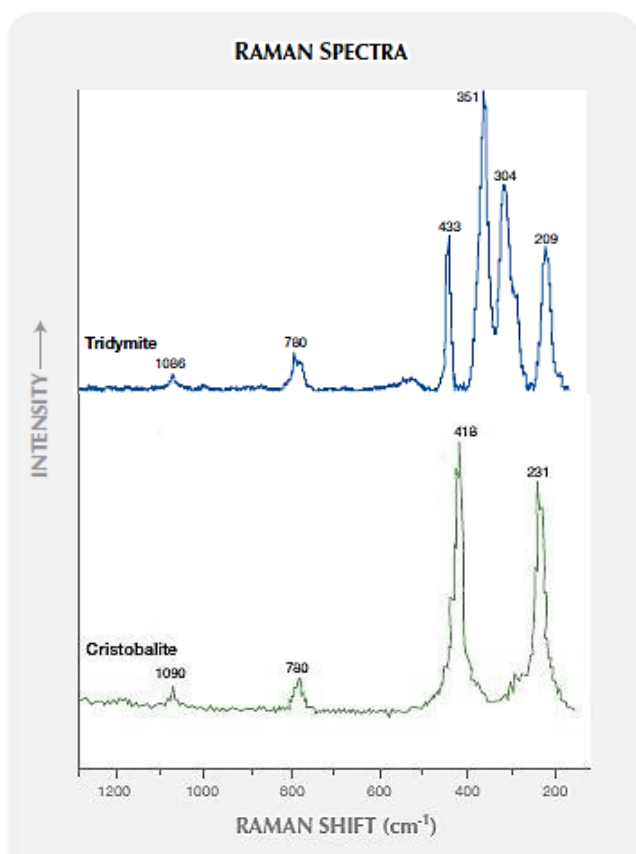


Figure 3.23 Standard Raman pattern of cristobalite and tridymite from RRUFF database (rruff info.) derived from (Simoni et al., 2010).

Table 3.2 Various types of bonding of the Si-O system in opals.

Assignment based on the spectra of crystalline and amorphous silica	Origins		
	(Volcanic)	(Volcanic)	(Volcanic)
	Ethiopian precious opal	Malagasy white fire opal	Malagasy orange fire opal
O-Si-O deformation (silicates)	338	230	229
Si-O-Si bending		416	415
Si-O-Si symmetric stretch for	778	780	779
Three and four memberd rings	860	810	
Si-O stretch (silicates)		960	960
Si-O-Si asymmetric stretch	1080	1074	1074
	1138	1190	1194
Unknow	1460	1451	1346
	2888	2946	1453
	2940		

### 3.9 Quantitative EPMA Analyses

Twenty seven samples of precious opal, white fire opal and orange fire opal were analyzed using the a JEOL Electron Probe Micro-Analyzer (EPMA) model JXA 8100 based at Department of Geology, Faculty of Science, Chulalongkorn University. Quantitative major and trace compositions, i.e., SiO<sub>2</sub>, Al<sub>2</sub>O<sub>3</sub>, CaO, MnO, FeO, Na<sub>2</sub>O, and K<sub>2</sub>O, were analyzed.

EPMA analyses of the same sample groups are quite consistent and different from the other groups. Lower SiO<sub>2</sub> and higher Al<sub>2</sub>O<sub>3</sub> contents of Ethiopian precious opal compare to those of Malagasy white and orange fire opals. CaO contents of Malagasy white and orange fire opal are likely lower than those of Ethiopian precious opal. In addition, Na<sub>2</sub>O and K<sub>2</sub>O contents of Malagasy white and orange fire opals are quite lower than those of Ethiopian precious opal. MnO and FeO contents of all groups are very low and negligible. As a result, Ethiopian precious opals contain with low SiO<sub>2</sub>, Therefore, impurities of Ethiopian precious opal are much higher than those of Malagasy fire opal groups. Representative EPMA analyses of these opal groups are shown in Table 3.3 and variation diagrams are shown in Figure 3.24 which they clearly differentiate all three groups from each other.

Table 3.3 EPMA analyses of representative opal samples.

Groups	Samples	Concentration (weight %)							Total
		SiO <sub>2</sub>	Al <sub>2</sub> O <sub>3</sub>	CaO	MnO	FeO	Na <sub>2</sub> O	K <sub>2</sub> O	
Group A (Ethiopian precious opal with slightly play of color phenomena)	A1	92.19	3.51	1.08	0.01	0.00	0.96	1.94	99.71
	A2	92.52	3.51	1.08	0.01	0.00	0.46	1.52	99.12
	A3	92.67	3.30	1.07	0.00	0.01	0.54	1.47	99.09
	A11	92.50	3.92	1.45	0.01	0.00	0.04	0.74	98.68
	A12	92.79	3.54	1.21	0.01	0.00	0.24	1.02	98.84
	A13	92.17	3.98	1.21	0.02	0.00	0.32	1.52	99.24
	A21	92.49	3.50	1.15	0.01	0.00	0.26	0.97	98.41
	A22	92.53	4.28	1.19	0.06	0.01	0.15	0.94	99.18
	A23	92.10	3.70	1.32	0.03	0.00	0.37	1.20	98.75
Group B (Malagasy white fire opal)	B1	98.49	0.20	0.15	0.00	0.02	0.28	0.04	99.21
	B2	98.97	0.43	0.16	0.00	0.00	0.14	0.04	99.77
	B3	98.12	0.34	0.14	0.00	0.01	0.03	0.02	98.68
	B11	98.44	0.32	0.08	0.04	0.00	0.11	0.08	99.10
	B12	98.92	0.27	0.08	0.01	0.03	0.06	0.14	99.54
	B13	98.70	0.31	0.07	0.01	0.01	0.06	0.11	99.28
	B21	97.49	0.24	0.09	0.00	0.03	0.05	0.17	98.10
	B22	97.66	0.23	0.06	0.00	0.00	0.13	0.15	98.26
	B23	97.78	0.08	0.06	0.00	0.02	0.06	0.17	98.18
Group C (Malagasy orange fire opal)	C1	97.74	0.39	0.12	0.02	0.01	0.06	0.03	98.39
	C2	97.89	0.42	0.09	0.03	0.03	0.06	0.07	98.63
	C3	97.95	0.42	0.15	0.00	0.00	0.06	0.07	98.67
	C11	98.29	0.35	0.07	0.00	0.00	0.07	0.06	98.87
	C12	97.22	0.38	0.12	0.02	0.04	0.16	0.05	98.01
	C13	98.57	0.29	0.15	0.05	0.00	0.02	0.03	99.14
	C21	98.70	0.42	0.11	0.03	0.01	0.10	0.05	99.44
	C22	97.39	0.43	0.14	0.02	0.00	0.10	0.03	98.14
	C23	98.27	0.40	0.11	0.00	0.02	0.10	0.04	98.96

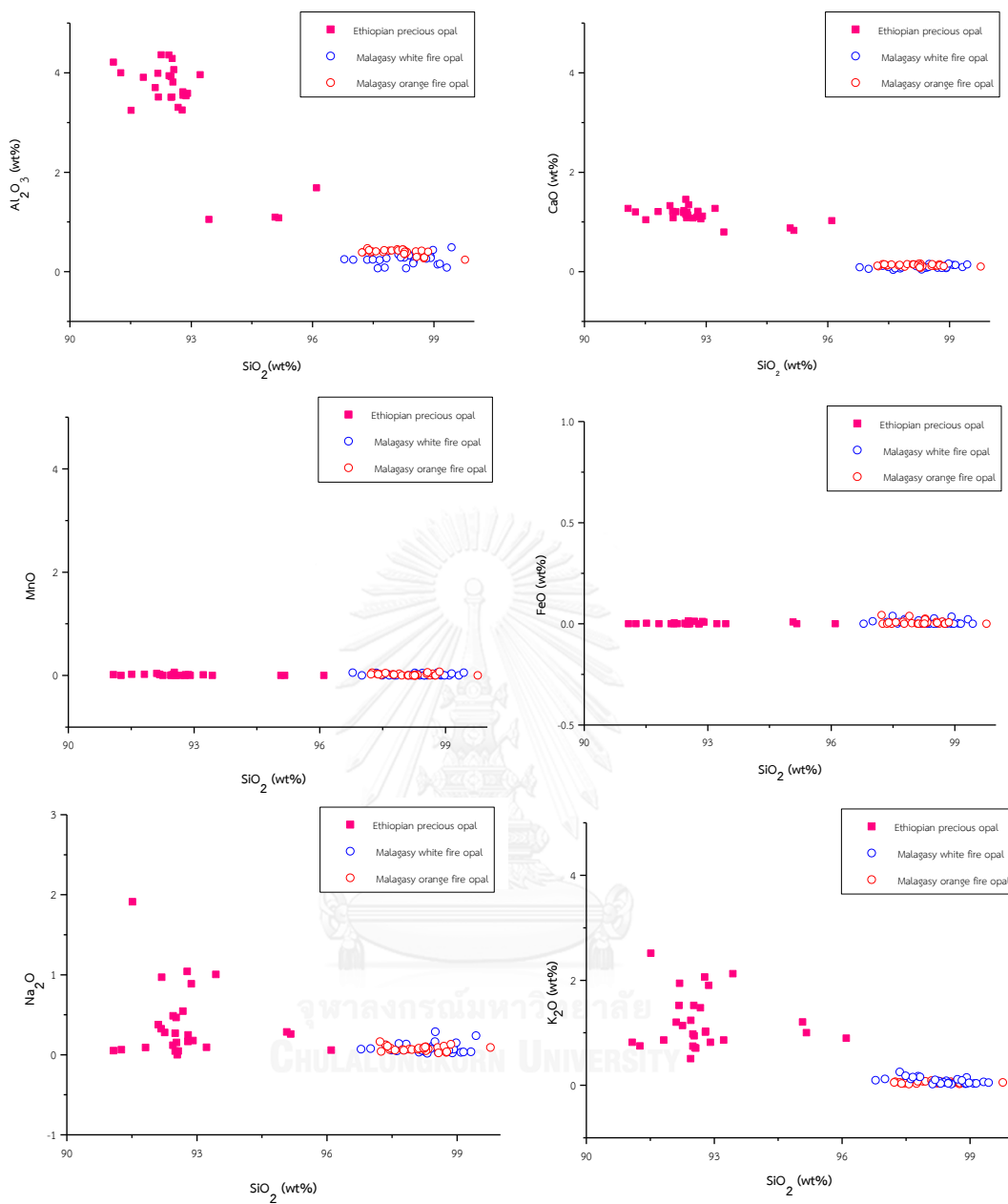


Figure 3.24 Variation diagram of SiO<sub>2</sub> versus minor elements of Ethiopian precious opal, Malagasy white fire opal and Malagasy orange fire opal.

## CHAPTER IV

### EXPERIMENTAL ENHANCEMENTS

#### 4.1 Introduction

Gemstone enhancements have existed for hundreds of years; these processes have provided large amount of beautiful gemstones supplying into the world markets. Color, clarity and special phenomena of gemstone are the most important properties gained from enhancement which can make stone more valuable. There are many methods applied to improve play of color phenomena in opal such as heat treatment, boiling, sugar treatment etc. For this research, three groups of opal sample including Ethiopian precious opal, Malagasy white fire opal and Malagasy orange fire opal were designed for experimental enhancements. Appropriate and potential opal enhancements such as heating, boiling and oiling may produce more intense play of color phenomena.

Three experiments including heating, boiling and oiling were designed to ten samples of each group. The first experiment (heating) was carried out using Memmert electrical furnace belonging to Department of Geology, Faculty of Science, Chulalongkorn University. According to experimental results reported by Johnson et al. (1996), Thomas (2008) and Toaree (2011), the most proper heating condition was set at 100°C with 24 hours soaking time under atmospheric condition which was designed for this experiment. The second experiment (boiling) was carried out using hotplate and beaker. Boiling condition was set at 100°C with 3 hours soaking time. The last experiments (oiling) was carried out using coconut oil, hotplate and beaker set at 100°C with 3 hours soaking time.

## 4.2 Heating Experiment

After heating experiment, Ethiopian precious opal samples (Group A, samples A1-A10) appear to have more intense play of color phenomena and their body colors turn to light yellowish white with a few cracks (see Figure 4.1). Heating may reduce size and rearrange hydrated silica sphere in well ordering structure leading to better scattering of visible light which causes play of color phenomena. On the other hand, Malagasy white fire opal samples B1-B10 (Group B) and orange fire opal samples C1-C10 (Group C) show more turbidity after heating (see Figures 4.2 and 4.3).

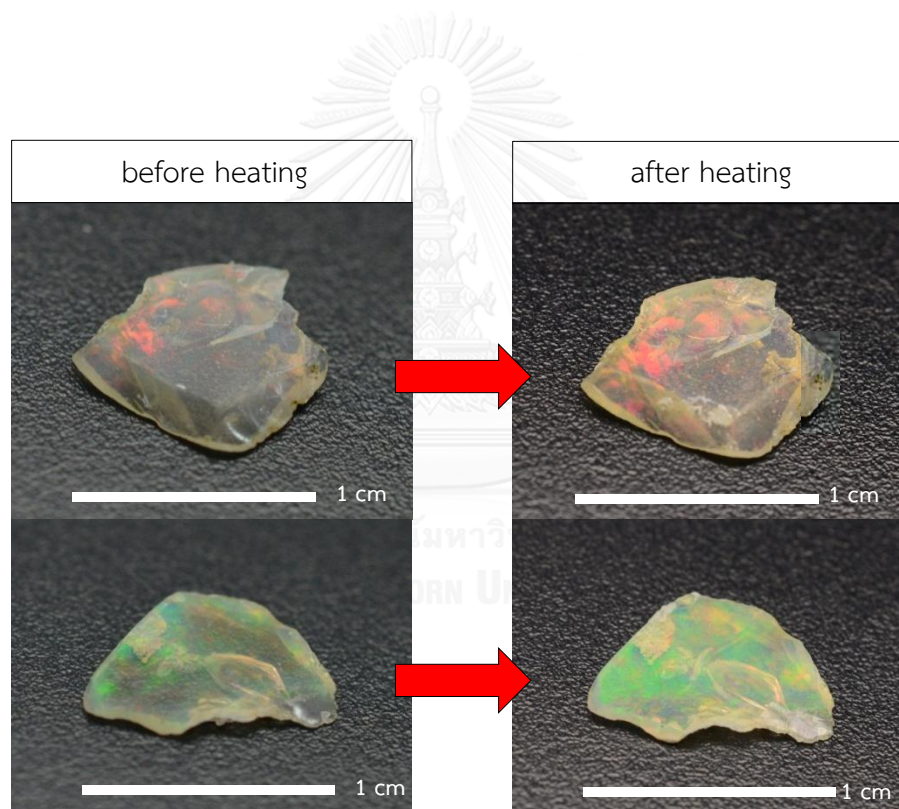


Figure 4.1 Ethiopian precious opals (samples A1 and A2) show improvement of play of color phenomena after heating at 100°C under atmospheric condition.

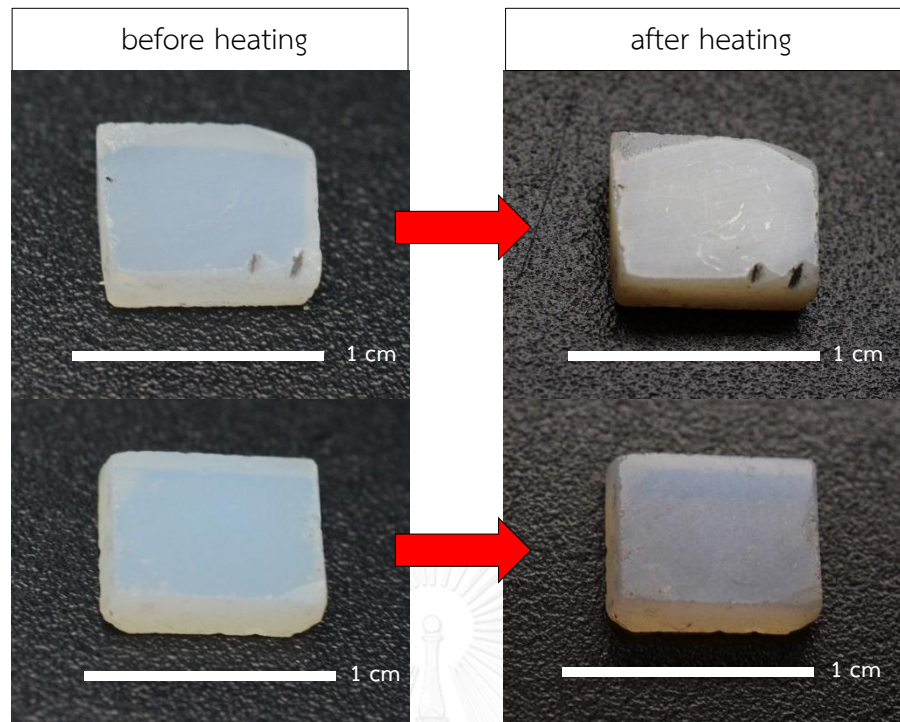


Figure 4.2 Malagasy white fire opals (samples B3 and B4) appear to have turbidity after heating at 100°C under atmospheric condition.

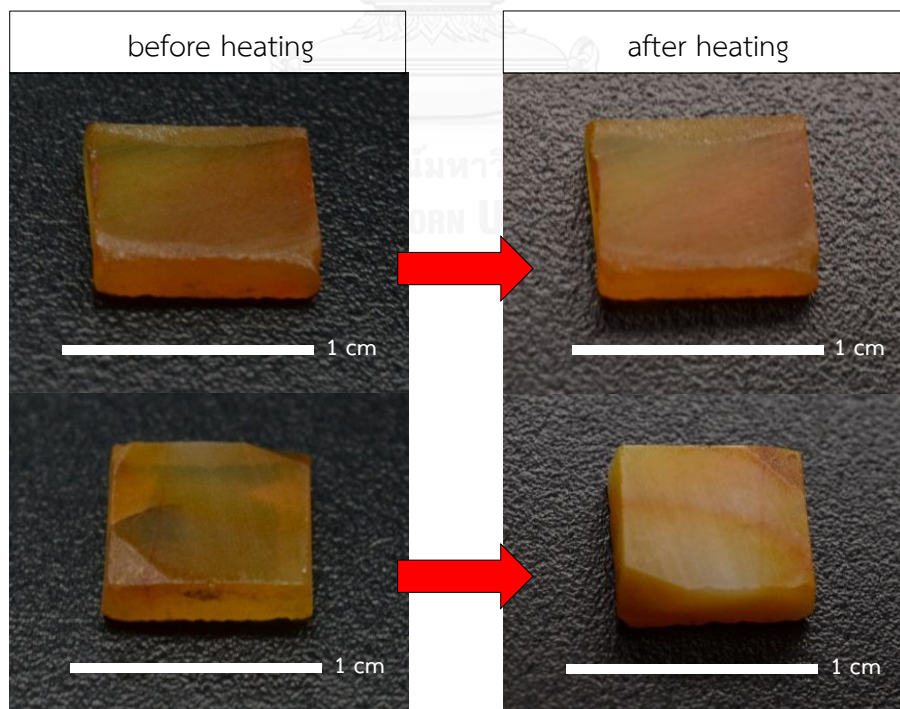


Figure 4.3 Malagasy orange fire opals (samples C4 and C7) appear to have turbidity after heating at 100°C under atmospheric condition.

#### 4.2.1 Physical Properties

Physical properties of opal samples were also observed and measured again after heating experiment for comparison with the untreated properties; these data are summarized in Table 4.1. Refractive index (R.I.) and specific gravity (S.G.) of Ethiopian precious opals fall within narrow ranges of 1.42-1.46 and 1.91-1.90. After heating experiment, these properties appear to be decreased to 1.39-1.43 and 1.72-1.87, respectively. As well as Malagasy white and orange fire opals (Groups B and C), they were decreased in refractive index and specific gravity after heating; R.I. ranges of 1.43-1.45 (Group B) and 1.44-1.46 (Group C) decreased to 1.41-1.45 and 1.42-1.44 whereas S.G. ranges of 2.03-2.19 (Group B) and 2.09-2.20 (Group C) reduced to 1.91-2.18 and 2.01-2.19, respectively. Plots of S.G. against R.I. (Figure 4.4) show graphical correlation as reported above.

During heating, water is loosing in hydrated silica spheres and spaces between spheres, so called hydrophane character (Asnachinda, 2006).

Table 4.1 Summary of gemological properties observed from Ethiopian precious opal, Malagasy white and orange fire opals before and after heating.

Samples	Experiment method	Before heating		After heating	
		S.G.	R.I	S.G.	R.I
Ethiopian precious opal (A)	heating	1.91 - 1.97 (av. 1.94)	1.42-1.46	1.72-1.87 (av. 1.79)	1.39-1.43
Malagasy white fire opal (B)	heating	2.03-2.19 (av. 2.11)	1.43-1.45	1.91-2.18 (av. 2.04)	1.41-1.45
Malagasy orange fire opal (C)	heating	2.09-2.20 (av. 2.14)	1.44-1.46	2.01-2.19 (av. 2.10)	1.42-1.44



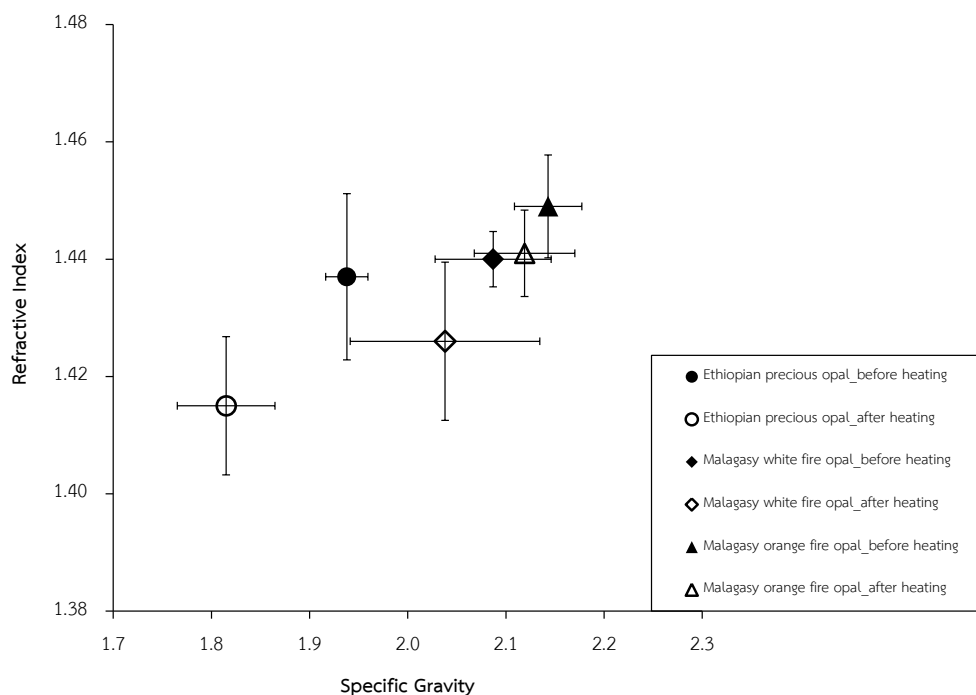


Figure 4.4 Plots of specific gravity versus refractive index before and after heating of Ethiopian precious opal, Malagasy white and orange fire opals.

The UV-Vis-NIR spectra within wavelength between 400-800 nanometers of representative samples are displayed in Figures 4.5 to 4.7 and all samples spectra are collected in Appendix B. UV-Vis-NIR spectra of Ethiopian precious opals (Group A) before heating (Figure 4.5) do not show any absorption due its white body color. After heating, opals in this group present absorption range from 400-600 nanometers that is related to yellowish white body color developed during heating.

All of the UV-Vis-NIR spectra of Malagasy white fire opals (Group B) mostly show similar pattern without absorption both before and after heating; this is clearly due to white body color unchanged after heating. On the other hand, absorption spectra of Malagasy orange fire opal show absorption peaks at 475 and 550 nanometers which is clearly due to orange body color before heating. After heating, more absorption peaks at 401, 415 and 424 nanometers are clearly observed (see Figure 4.7) that may be caused by more intense yellow occurred after heating.

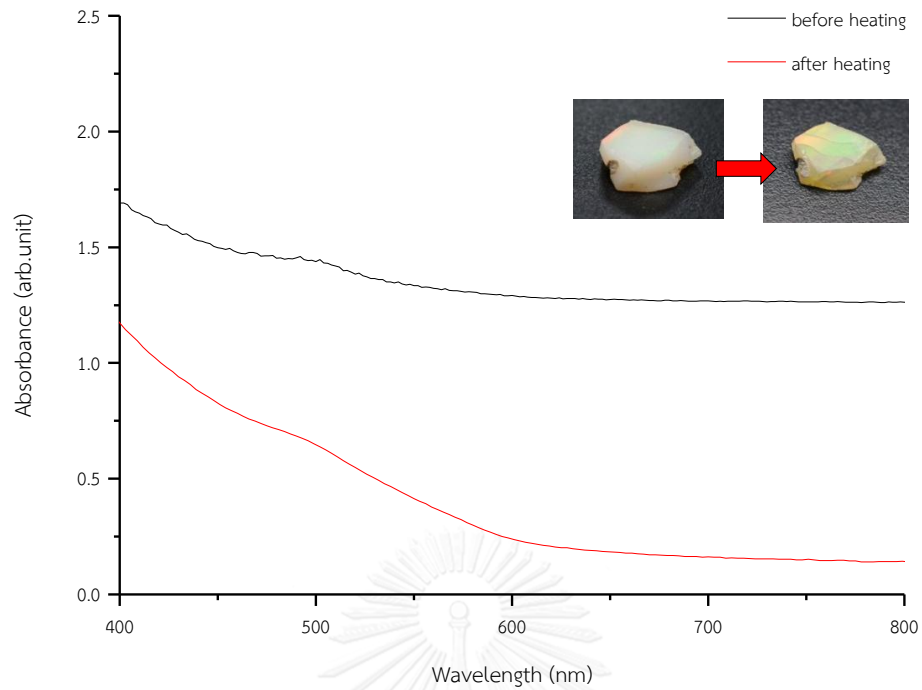


Figure 4.5 UV-Vis-NIR spectra of an Ethiopian precious opal (sample A4 of Group A) before and after heating.

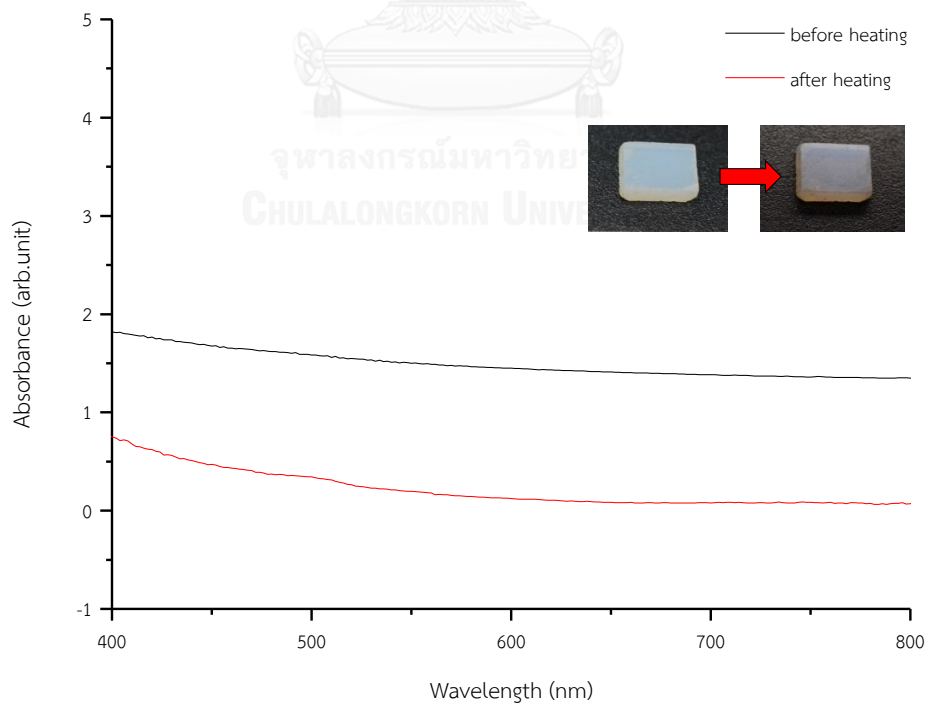


Figure 4.6 UV-Vis-NIR spectra of a Malagasy white opal (sample B1 of Group B) before and after heating.

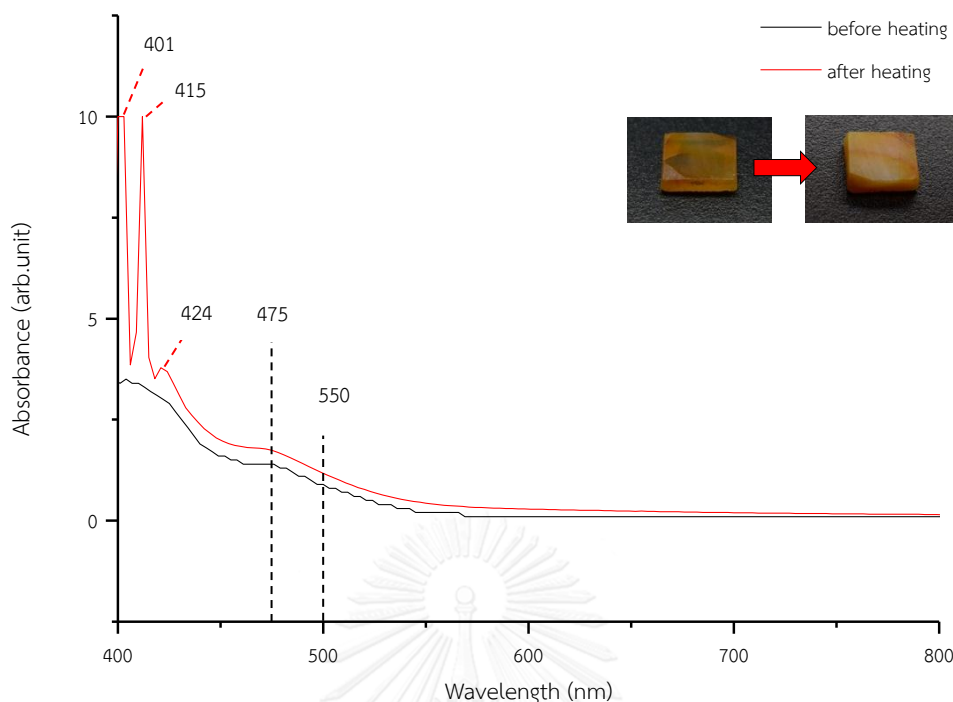


Figure 4.7 UV-Vis-NIR spectra of a Malagasy orange fire opal (sample C9 of Group C) before and after heating.

Representative Fourier Transform Infrared Spectra of Ethiopian precious opals (Group A) before and after heating are displayed in Figure 4.8. Moreover, all FTIR spectra are collected in Appendix C. As shown in the figure, H<sub>2</sub>O stretching and bending absorption peaks at 5000-5400 cm<sup>-1</sup> and SiOH stretching and bending absorption peaks at 4300-4600 cm<sup>-1</sup> are decreased probably due to losing of water after heating.

Malagasy fire opals both Groups B and C show FTIR spectra similar to those of Ethiopian precious opal; however, they have unclear absorption band at 4300-4600 cm<sup>-1</sup> caused by SiOH stretching and bending. After heating, most samples of both groups show decreasing of H<sub>2</sub>O stretching and bending absorption peaks at 5000-5400 cm<sup>-1</sup> probably due to losing of water (see Figures 4.9 and 4.10).

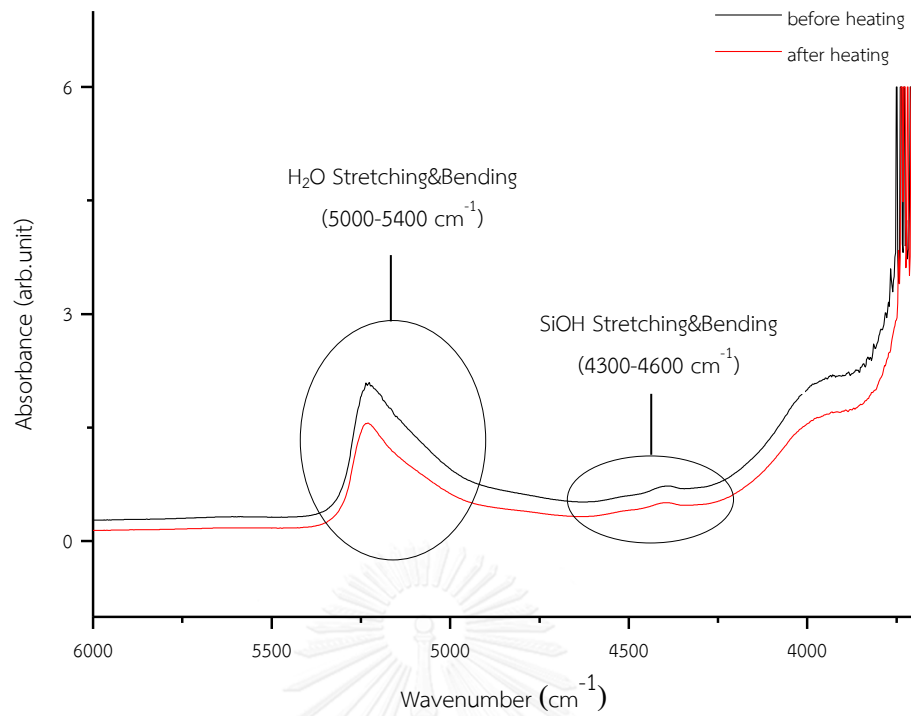


Figure 4.8 FTIR spectra of Ethiopian precious opal (sample A2) before and after heating.

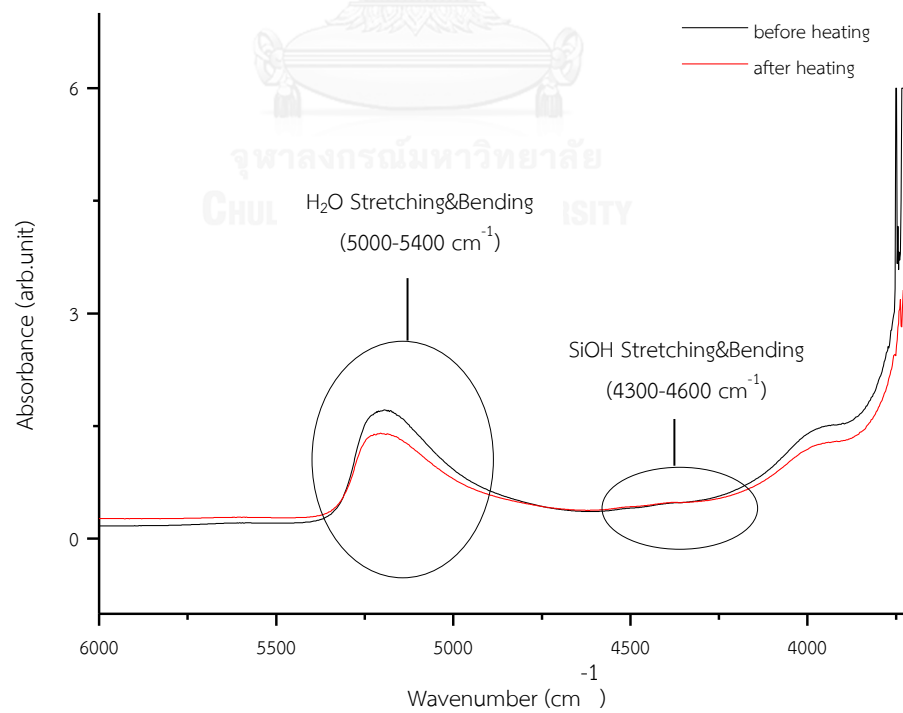


Figure 4.9 FTIR spectra of Malagasy white fire opal (sample B3) before and after heating.

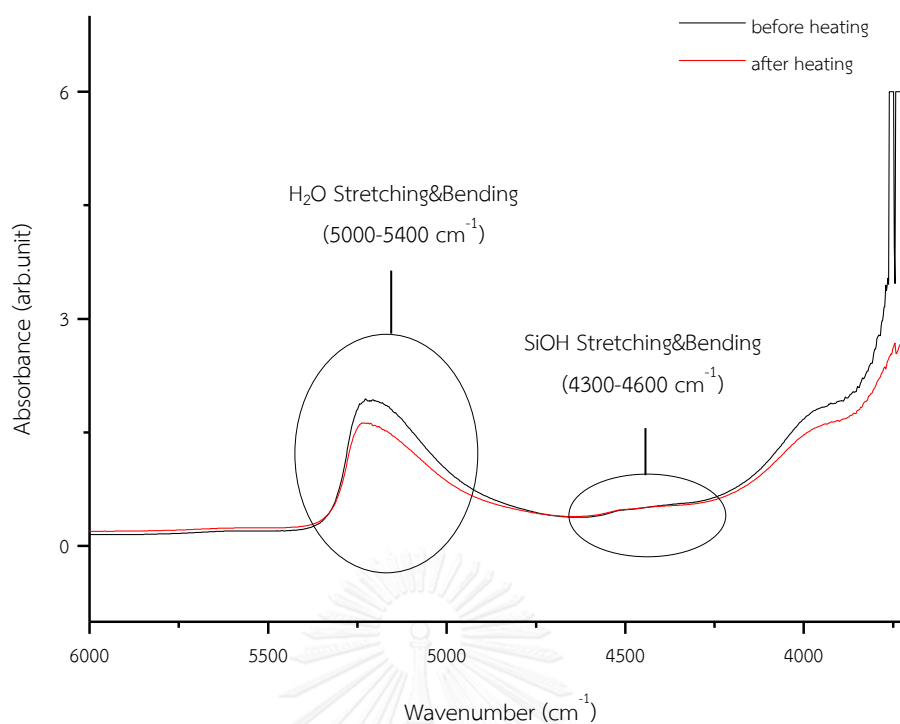


Figure 4.10 FTIR spectra of Malagasy orange fire opal (sample C7) before and after heating.

The Raman spectra of all Ethiopian precious opal samples (Group A) have a same pattern that reveals a band at  $\sim 345\text{ cm}^{-1}$  with left shifting close to  $350\text{ cm}^{-1}$  peak of volcanic opal with cristobalite and tridymite components (opal-CT). This peak is not sharp indicating crystalline phase as suggested by (Smallwood et al., 1997, Rondeau et al., 2010). In addition, appearances of peak in the  $750\text{--}850\text{ cm}^{-1}$  region are associated with symmetric Si-O-Si stretching. The peak presents at  $1079\text{ cm}^{-1}$  is of Si-O-Si asymmetric stretch. After heating, the absorption peaks appear in the same positions without significant changing (Figure 4.11).

The Raman spectra of Malagasy white fire opal (Group B) and Malagasy orange fire opal (Group C) have a same pattern of spectrum which may be cause by the same formation. They exhibit essential peaks at  $230$  and  $418\text{ cm}^{-1}$  revealing cristobalite components. This characteristic is typical opal-C in volcanic environment (Ilieva et al., 2007). In addition, the spectra also present small features at  $782$  and

1075  $\text{cm}^{-1}$  which is a poor Raman scattering. After heating, the absorption peaks appear at the same positions without significant changing. Raman spectra of both opal groups are displayed in Figures 4.12 and 4.13, respectively.

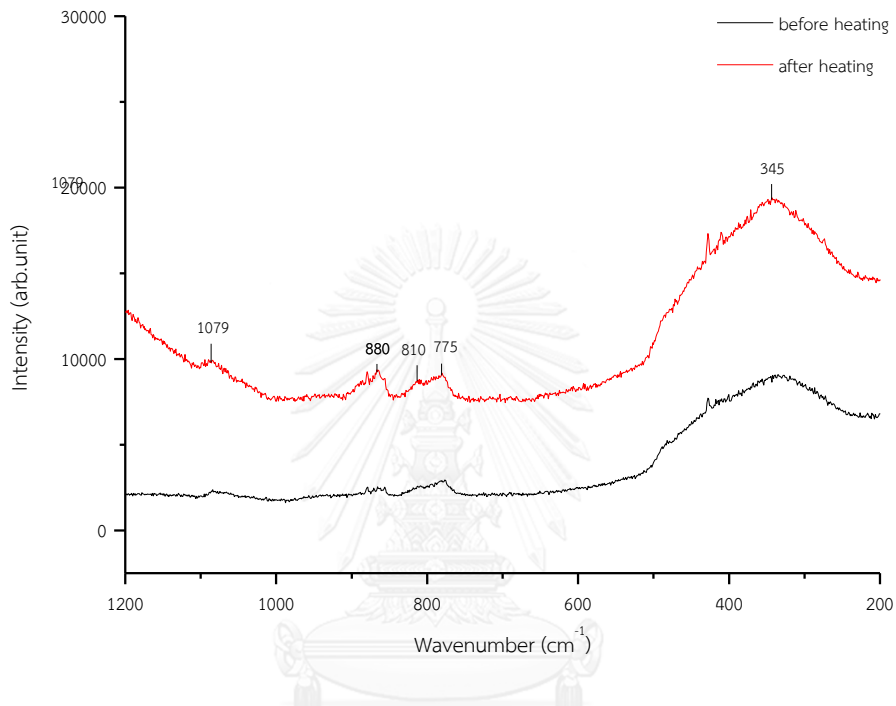


Figure 4.11 Raman spectra of Ethiopian opal (sample A2) before and after heating.

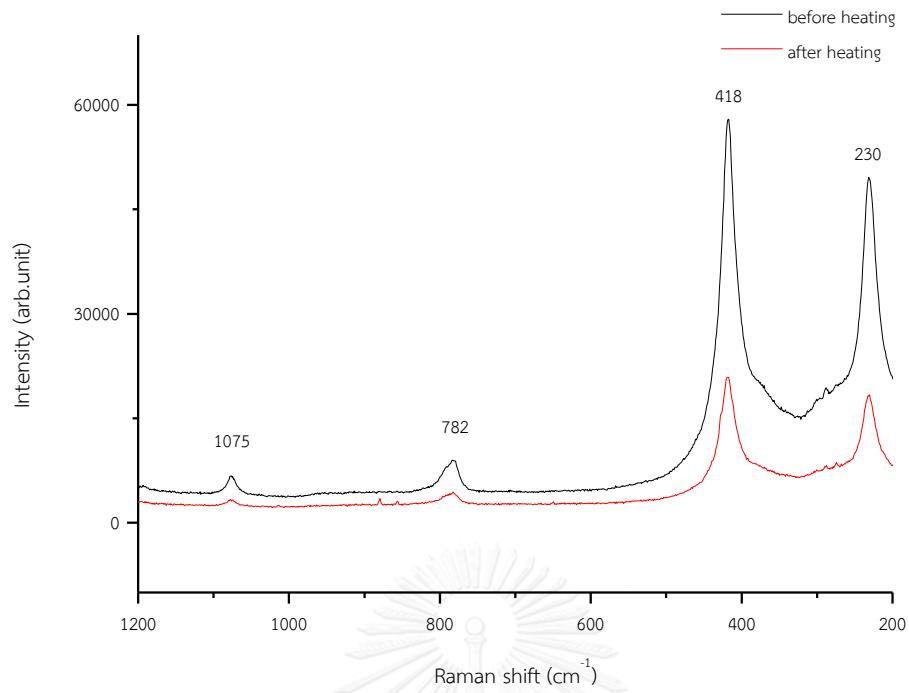


Figure 4.12 Raman spectra of Malagasy white fire opal (sample B7) before and after heating.

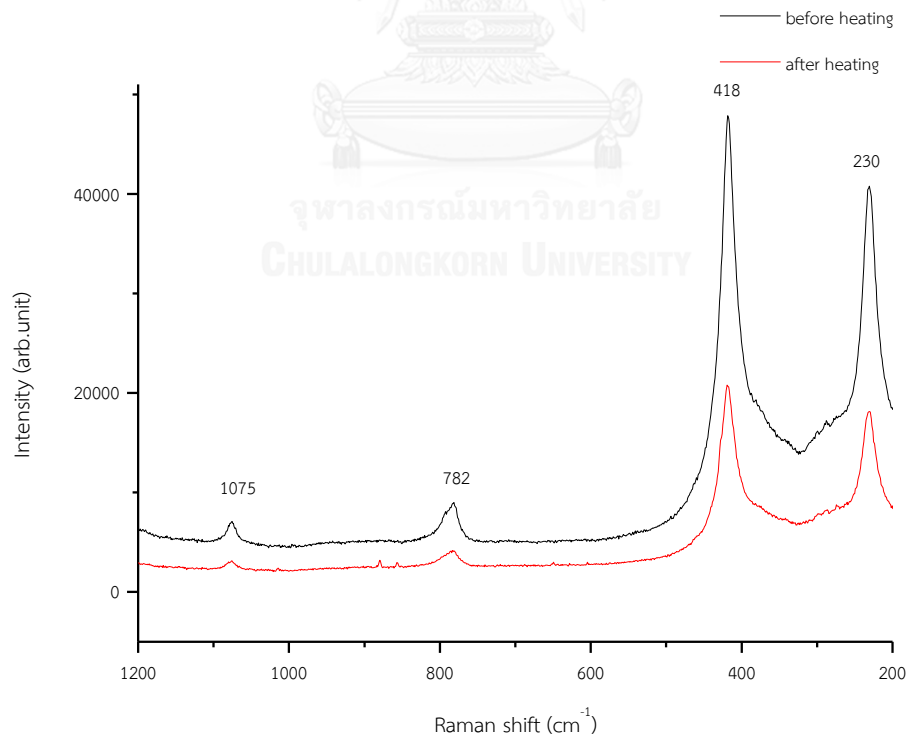


Figure 4.13 Raman spectra of Malagasy orange fire opal (sample C4) before and after heating.

#### 4.2.2 Field Emission Scanning Electron Microscope (FESEM)

Field Emission Scanning Electron Microscope (FESEM) revealed the arrangement of hydrated silica sphere in the structure of opal, and these are related to play of color phenomena that show on its surface. However, if hydrated silica spheres exhibit a range of sizes, imperfectly shaped, too large or too small leading to unordered arrangement. Therefore, the visible light cannot diffracted properly then play of color phenomena should not appear (Gaillou et al., 2008).

Field Emission Scanning Electron Microscopic (FESEM) images taken from Ethiopian precious opal show that hydrated silica spheres are imperfect sphere shape with diameters of about 222 nm. After heating, hydrate silica spheres are nearly perfect 3D stacking, and have more spherical distribution. Their spheres are actually reduced to about 200 nm. Consequently, hydrated silica spheres appear to have more perfect form and well ordering arrangement in the opal structure after heating, this relates to clearer play of color phenomena (Figure 4.14).

The second group, Malagasy white fire opals appears to have nanoparticles much less than hundred nm without space between these particles. After heating, hydrated silica spheres are even smaller and randomly stacking (Figure 4.15). The third group, Malagasy orange fire opal show irregular shape of hydrated silica spheres smaller than hundred nm without space between these particles. After heating, hydrated silica spheres are even smaller and randomly arranged (Figure 4.16).



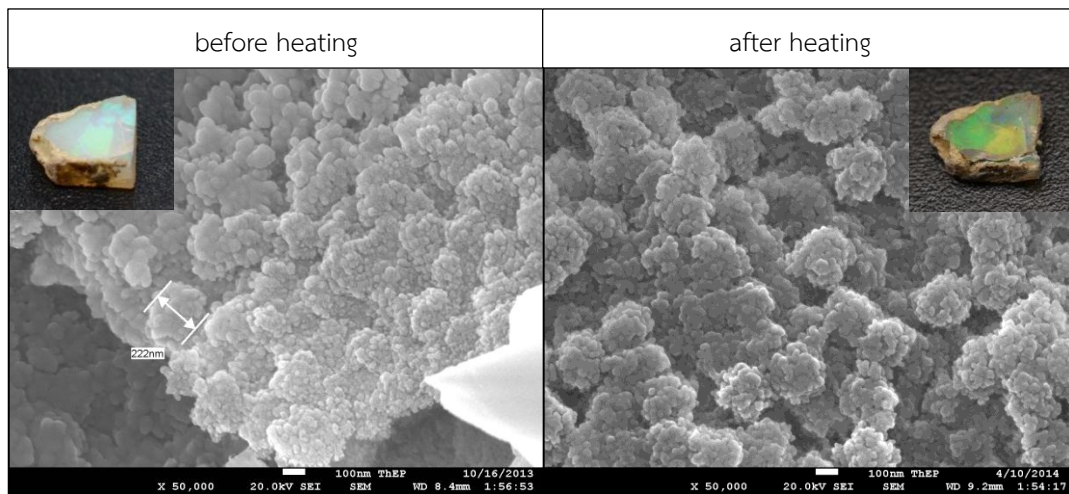


Figure 4.14 Representative FESEM images of Ethiopian precious opals with slightly show play of color phenomena before and after heating (sample A9).

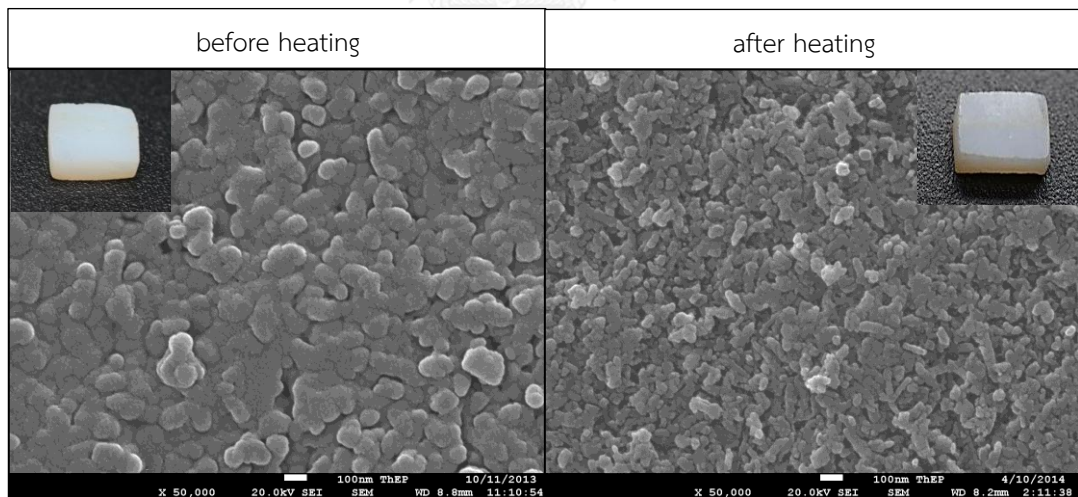


Figure 4.15 Representative FESEM images of Malagasy white fire opal before and after heating (sample B10).

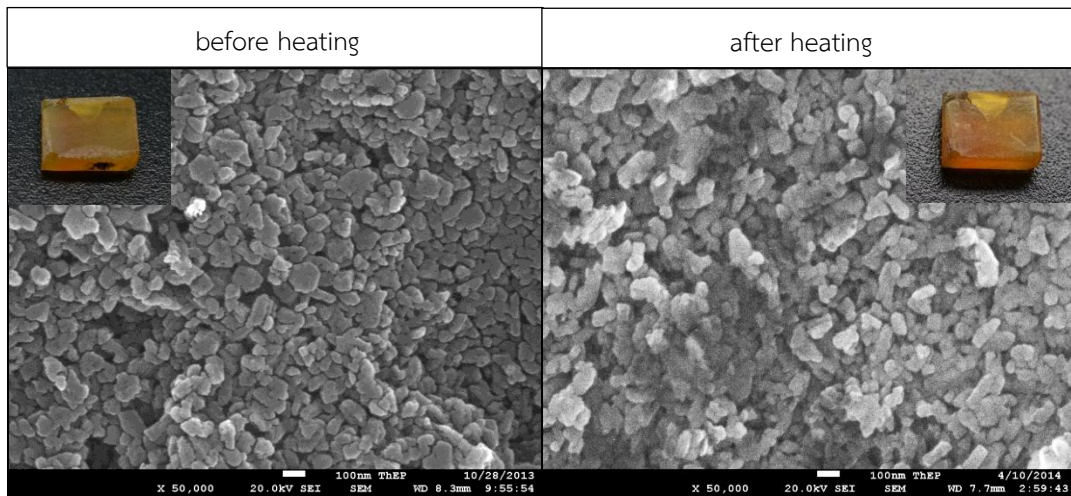


Figure 4.16 Representative FESEM images of Malagasy orange fire opal before and after heating (sample C10).

### 4.3 Boiling Experiment

After boiling experiment, Ethiopian precious opal samples (Group A, samples A11-A20) appear to have more intense play of color phenomena but their body colors were not changed (see Figure 4.17). Boiling may rearrange hydrated silica sphere in the well ordering structure leading to better scattering of visible light which causes play of color phenomena. On the other hand, Malagasy white fire opal samples B11-B20 (Group B) and orange fire opal samples C11-C20 (Group C) did not change after boiling experiment (see Figure 4.18 and 4.19).

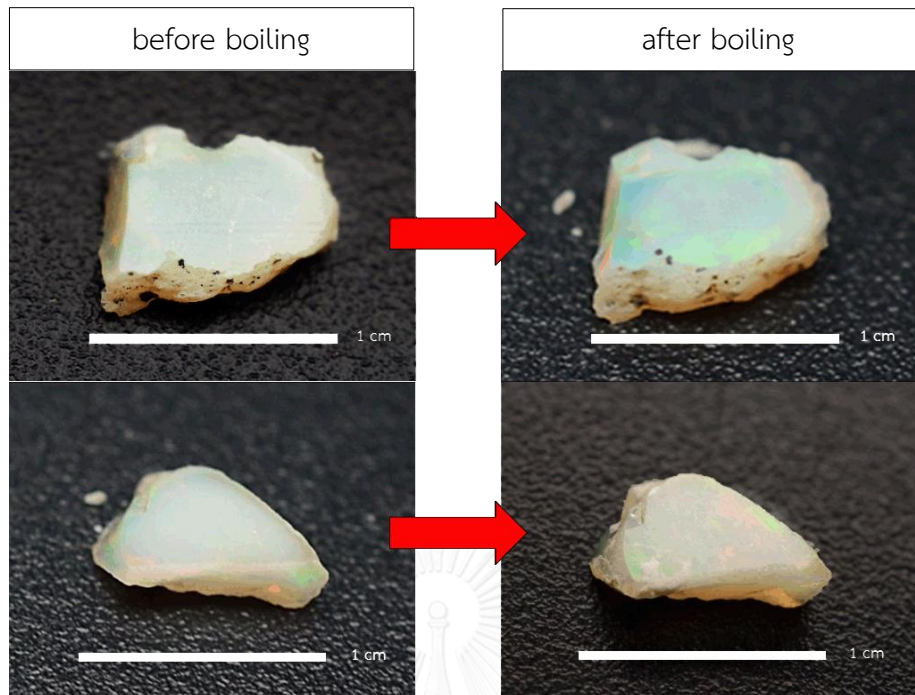


Figure 4.17 Ethiopian precious opals (samples A14 and A18) show improvement of play of color phenomena after boiling at 100°C in water.

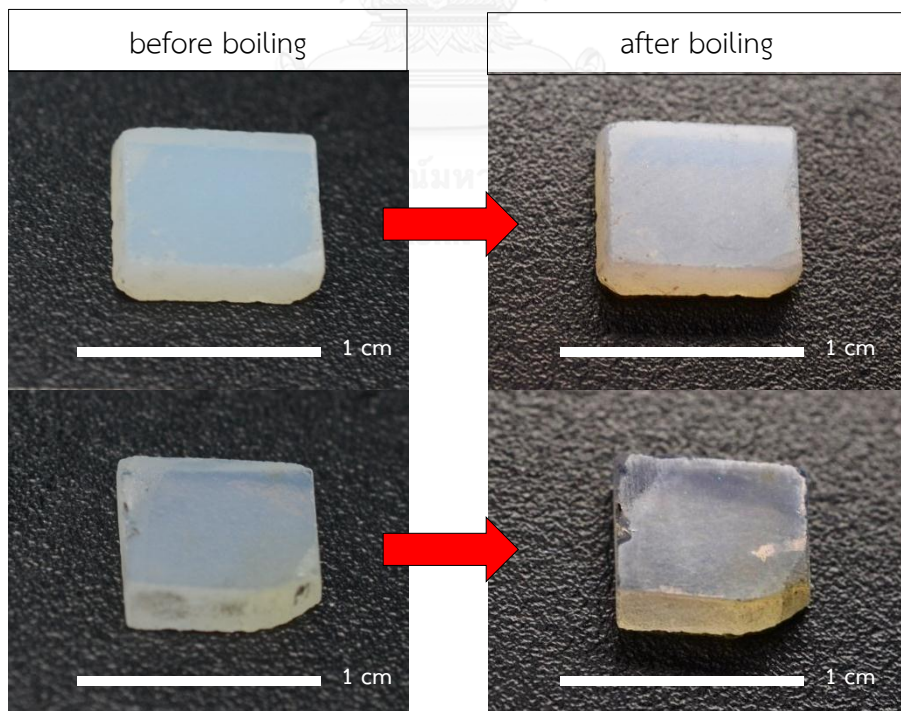


Figure 4.18 Malagasy white fire opals (samples B17 and B20) appear to have no change after boiling at 100°C in water.

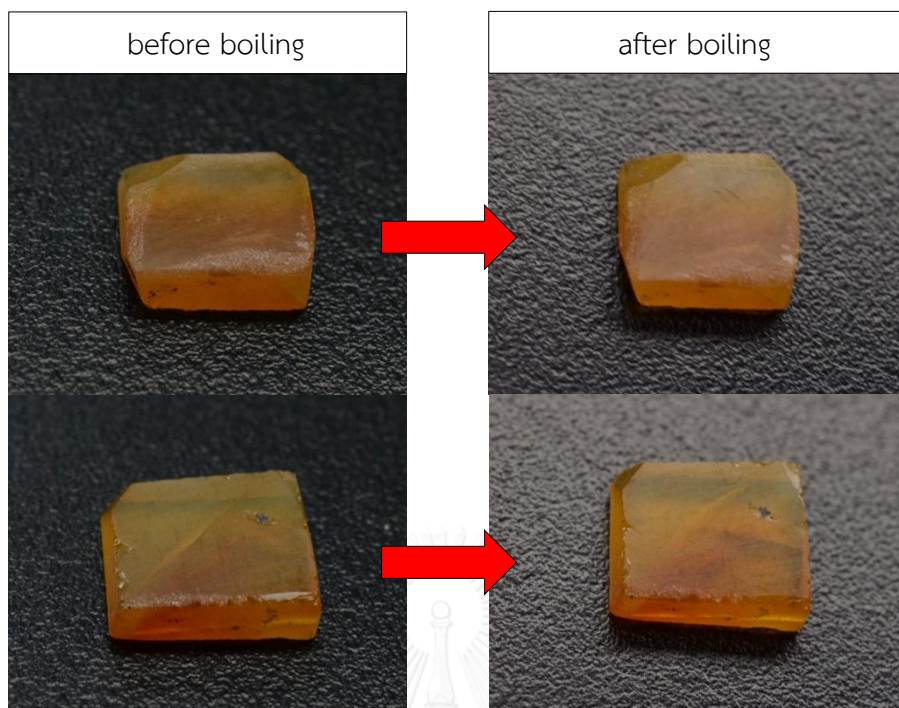


Figure 4.19 Malagasy orange fire opals (samples C16 and C17) did not change after boiling at 100°C in water.

#### 4.3.1 Physical Properties

Physical properties of opal samples were also observed and measured again after boiling experiment for comparison with the untreated properties; these data are summarized in Table 4.2. Refractive index (R.I.) and specific gravity (S.G.) of Ethiopian precious opals fall within narrow ranges of 1.42-1.45 and 1.85-1.97, respectively. After boiling experiment, these properties appear to be decreased to 1.39-1.43 and 1.72-1.94. On the other hand, Malagasy white and orange fire opals (Groups B and C) appear to have no change of refractive index and specific gravity after boiling: R.I. ranges of 1.43-1.45 (Group B) and 1.43-1.45 (Group C) still remained at 1.43-1.46 and 1.42-1.44 as same as S.G. ranges of 2.03-2.18 (Group B) and 2.02-2.18 (Group C) remained at 1.91-2.18 and 2.01-2.19, respectively. Plots of S.G. against R.I. (Figure 4.20) show graphical correlation as reported above.

During boiling, water may be absorbed into hydrated silica spheres and spaces of opal's structure, so called hydrophane character (Asnachinda, 2006). It is recognized in Ethiopian precious opals (Group A).

Table 4.2 Summary of the gemological properties of Ethiopian precious opal, Malagasy white and orange fire opals before and after boiling.

Samples	Experiment method	Before boiling		After boiling	
		S.G.	R.I	S.G.	R.I
Ethiopian precious opal (A)	boiling	1.85 - 1.97 (av. 1.91)	1.42-1.45	1.72-1.94 (av. 1.83)	1.39-1.43
Malagasy white fire opal (B)	boiling	2.03-2.17 (av. 2.10)	1.43-1.45	2.03-2.18 (av. 2.10)	1.43-1.46
Malagasy orange fire opal (C)	boiling	2.08-2.20 (av. 2.14)	1.43-1.45	2.02-2.18 (av. 2.10)	1.43-1.46

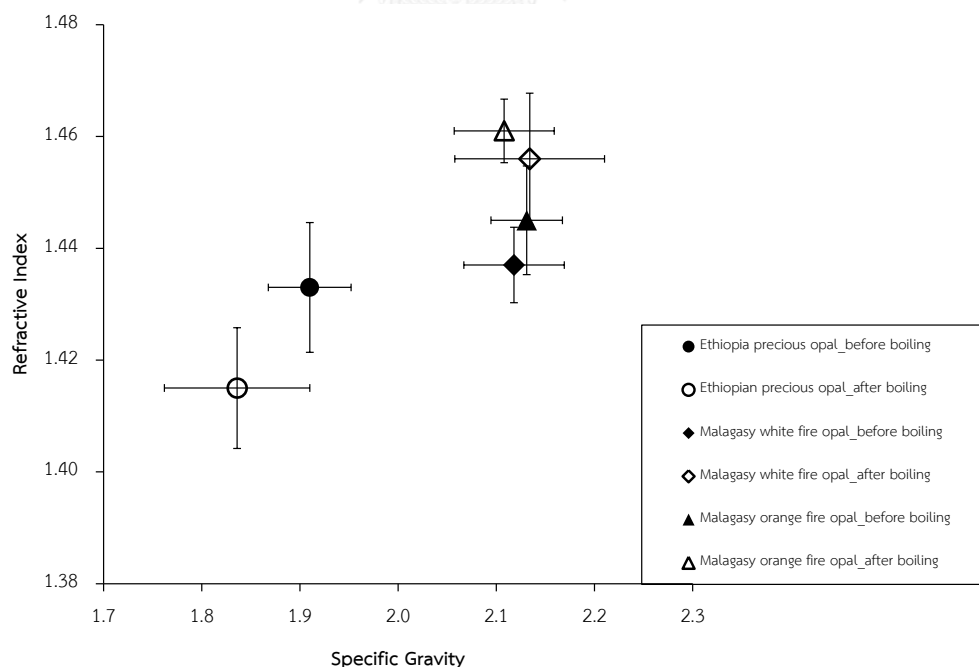


Figure 4.20 Plots of specific gravity versus refractive index before and after boiling of Ethiopian precious opal, Malagasy white and orange fire opals.

The UV-Vis-NIR spectra within wavelength range of 400-800 nanometers of representative samples are displayed in Figures 4.21 to 4.23 and all samples' spectra are collected in Appendix B. UV-Vis-NIR spectra of Ethiopian precious opals (Group A) before boiling (Figure 4.21) do not show any absorption leading to white body color. After boiling, they still show similar pattern without absorption.

All of the UV-Vis-NIR spectra of Malagasy white fire opals (Group B) mostly show similar pattern without absorption both before and after boiling; this clearly leads to white body color (see Figure 4.22). On the other hand, absorption spectra of Malagasy orange fire opal show absorption peaks at 405, 415 and 475 nm which clearly lead to orange body color before boiling. After boiling, similar pattern also still present (see Figure 4.23).

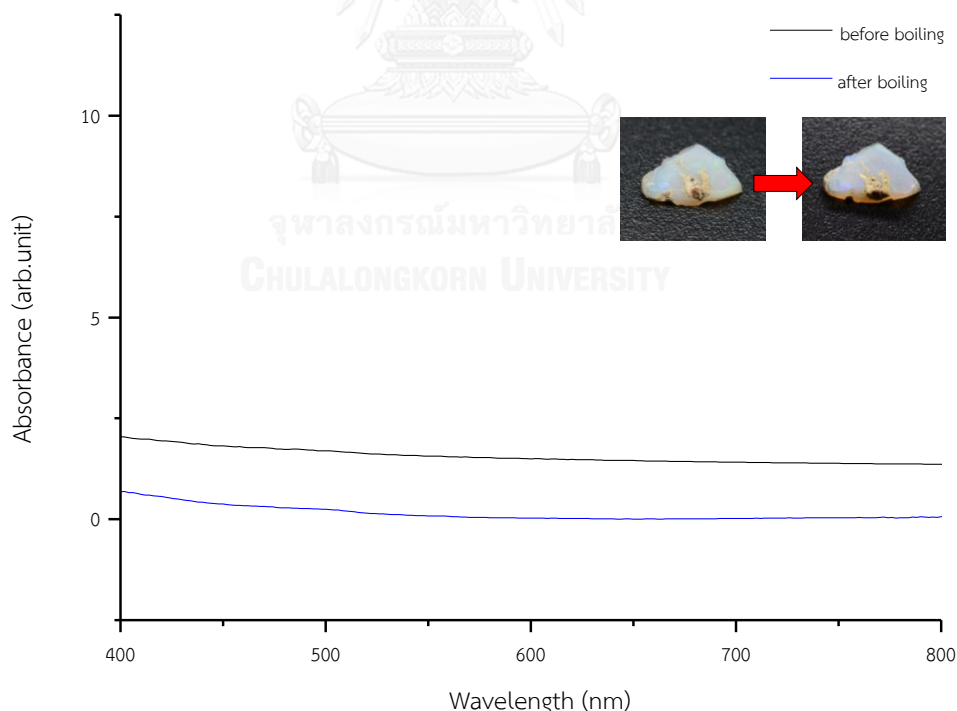


Figure 4.21 UV-Vis-NIR spectra of Ethiopian precious opal with slightly show play of color phenomena (group A) before and after boiling (sample A13).

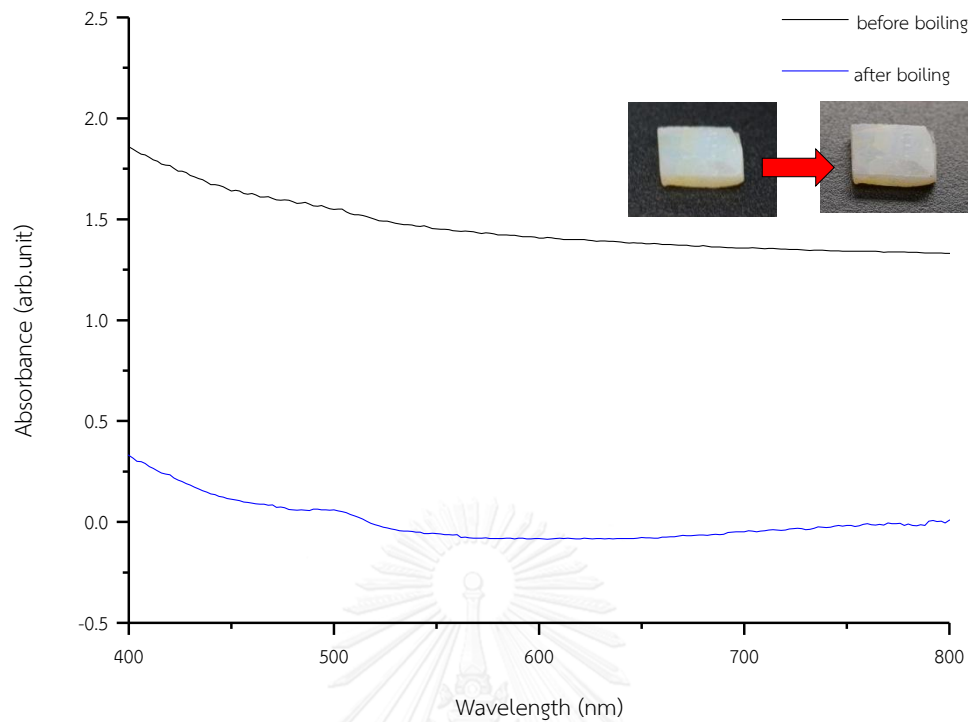


Figure 4.22 UV-Vis-NIR spectra of Malagasy white opal (group B) before and after boiling (sample B18).

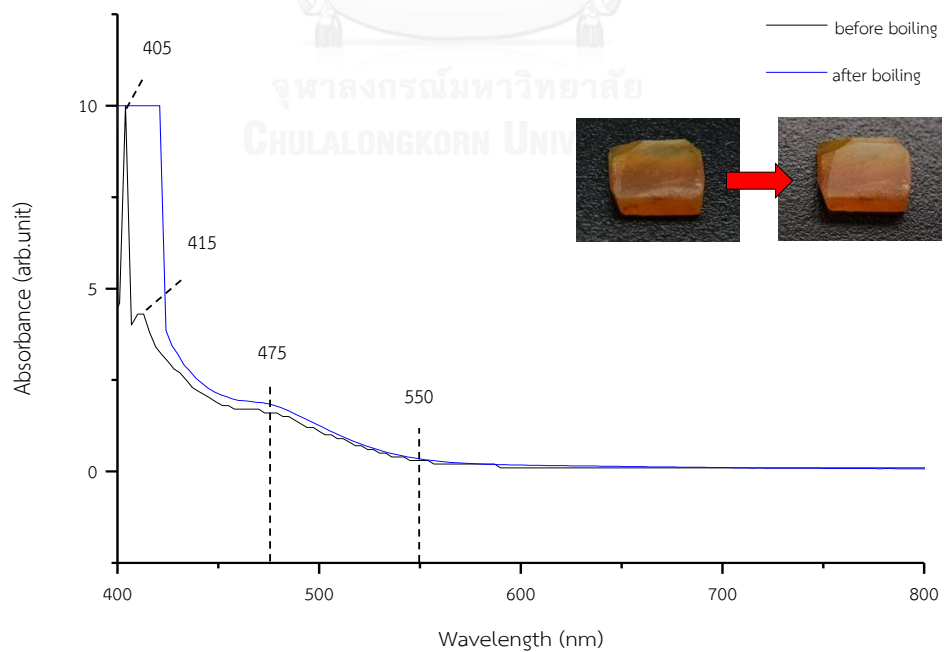


Figure 4.23 UV-Vis-NIR spectra of Malagasy orange opal (group C) before and after boiling (sample C16).

Representative Fourier Transform Infrared Spectra of Ethiopian precious opals (Group A) before and after boiling are displayed in Figure 4.24. Moreover, all FTIR spectra are collected in Appendix C. As shown in the figure, H<sub>2</sub>O stretching and bending absorption peaks at 5000-5400 cm<sup>-1</sup> and SiOH stretching and bending absorption peaks at 4300-4600 cm<sup>-1</sup> are increased probably due to increasing of water in the structure after boiling.

Malagasy fire opals both Groups B and C show FTIR spectra similar to those of Ethiopian precious opal; however, they have unclear absorption band at 4300-4600 cm<sup>-1</sup> region probably caused by SiOH stretching and bending. After boiling, most samples show unchanged pattern of H<sub>2</sub>O stretching and bending absorption peaks at 5000-5400 cm<sup>-1</sup> probably due to their microstructure arrangement (see Figures 4.25 and 4.26).

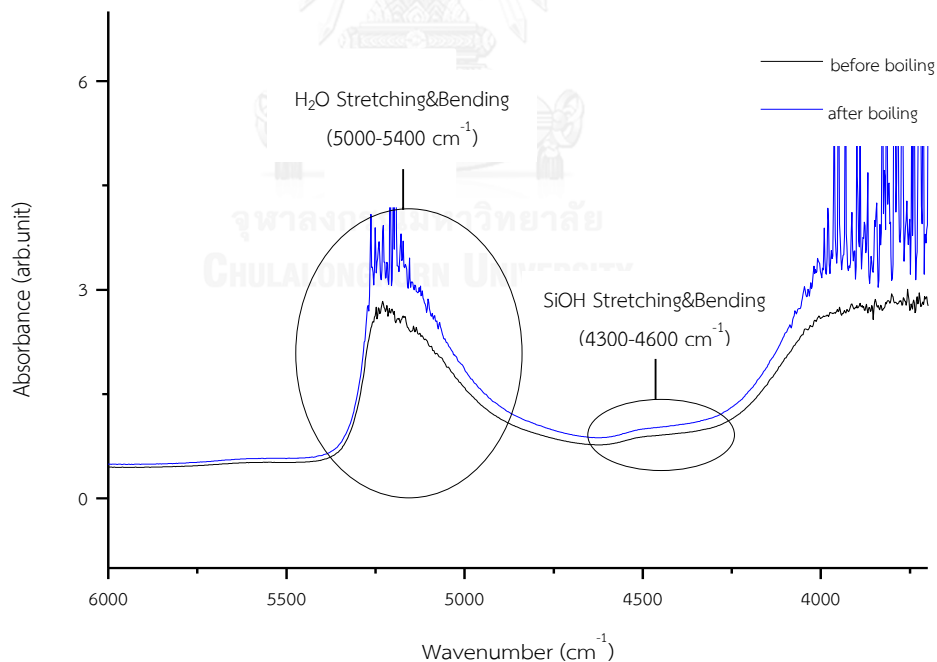


Figure 4.24 FTIR spectra of Ethiopian precious opal (sample A16) before and after boiling.



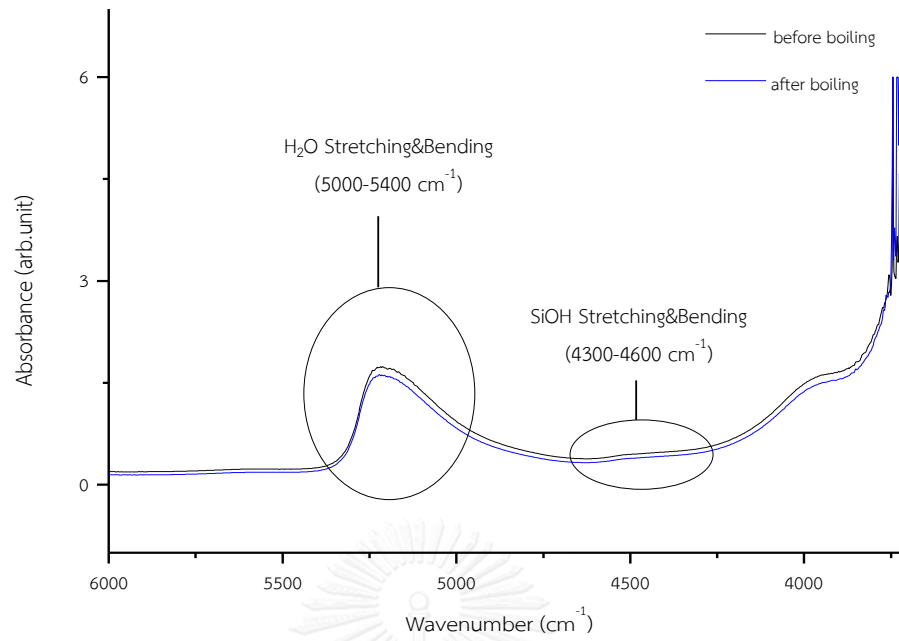


Figure 4.25 Similar FTIR spectra of Malagasy white fire opal (sample B15) before and after boiling.

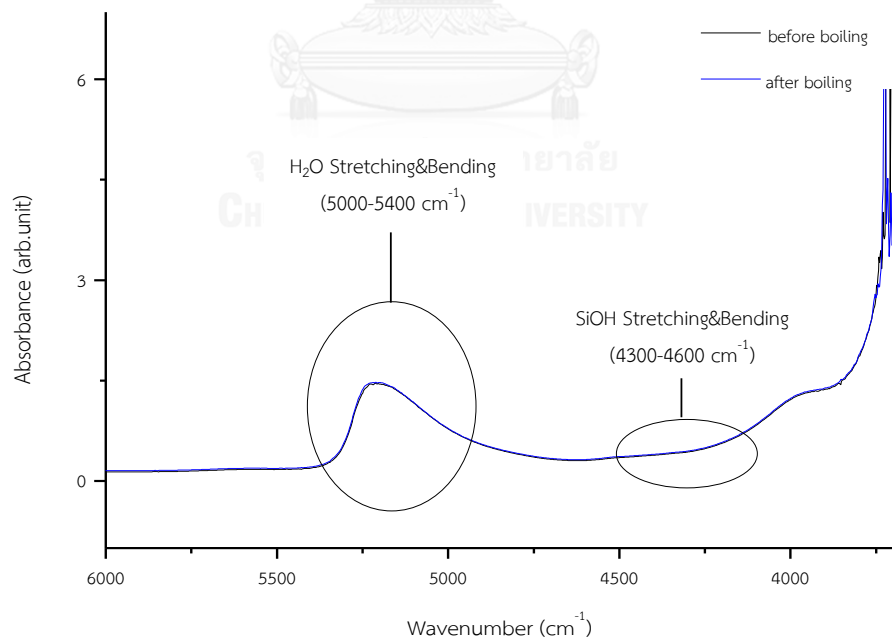


Figure 4.26 Similar FTIR spectra of Malagasy orange fire opal (group C) before and after boiling (sample C11).

Raman spectra of all Ethiopian precious opal samples (Group A) have a same pattern that reveal a band  $\sim 337\text{ cm}^{-1}$  with left shifting close to the  $350\text{ cm}^{-1}$  peak of typical volcanic opal related to cristobalite and tridymite components (opal-CT). This peak is not sharp indicating crystalline phase as suggested by Smallwood et al. (1997) and Rondeau et al. (2010). In addition, appearance of peaks in the  $750\text{-}850\text{ cm}^{-1}$  region is associated with symmetric Si-O-Si stretching. Peak presents at  $1078\text{ cm}^{-1}$  is of Si-O-Si asymmetric stretch. After boiling the absorption peaks appear in the same positions without significant changing (Figure 4.27).

Raman spectra of Malagasy white fire opal (Group B) and Malagasy orange fire opal (Group C) have a same pattern of spectra which may relate to the same formation. They exhibit essential peaks at  $231$  and  $418\text{ cm}^{-1}$  revealing cristobalite components. This characteristic is typical opal-C in volcanic environment (Ilieva et al., 2007). In addition, the spectra also present small features at  $781$  and  $1075\text{ cm}^{-1}$  which is a poor Raman scattering. After boiling, the absorption peaks appear at the same positions without significant changing. Raman spectra of both opal groups are displayed in Figures 4.28 and 4.29, respectively.

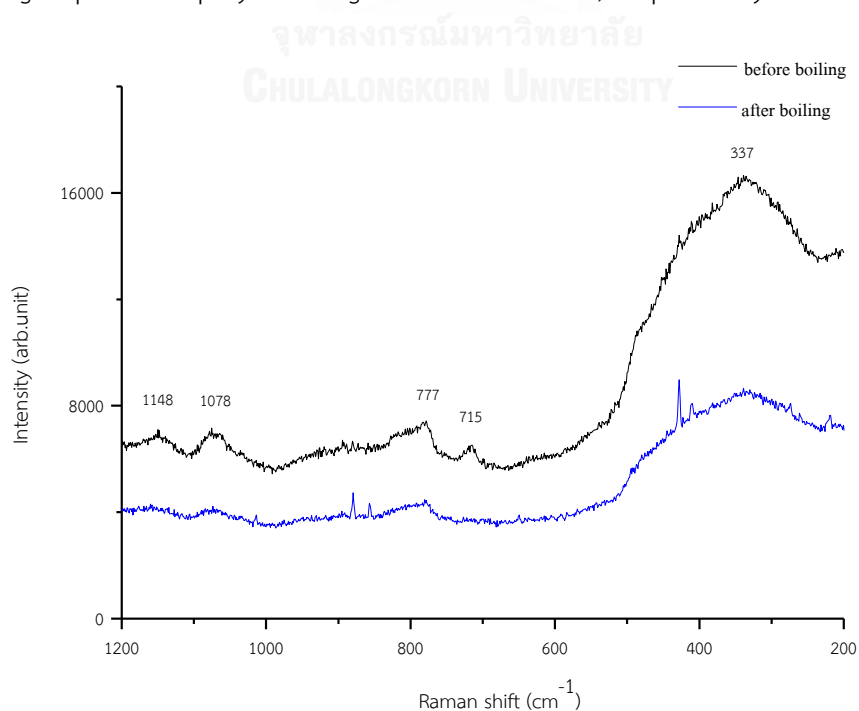


Figure 4.27 Raman spectra of Ethiopian opal (sample A17) before and after boiling.

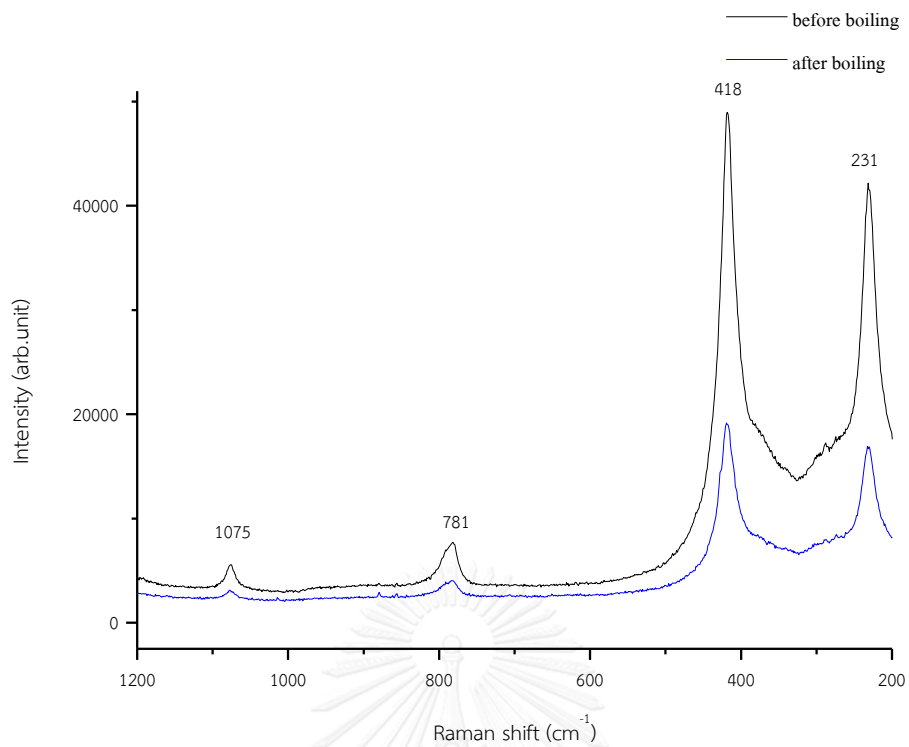


Figure 4.28 Raman spectra of Malagasy white fire opal (sample B16) before and after boiling.

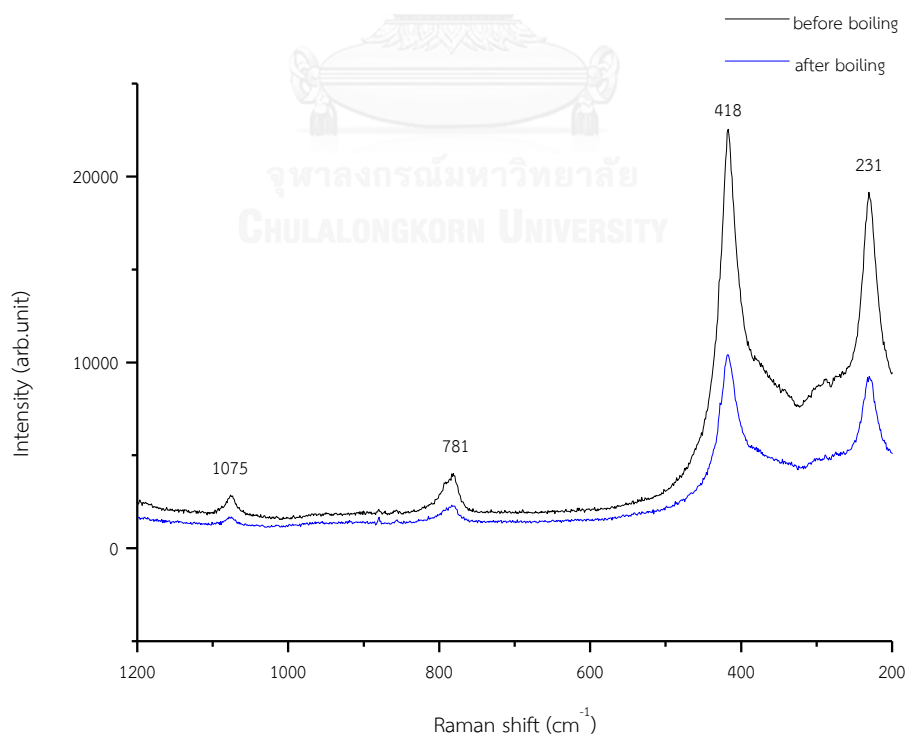


Figure 4.29 Raman spectra of Malagasy orange fire opal (sample C16) before and after boiling.

#### 4.3.2 Field Emission Scanning Electron Microscope (FESEM)

Field Emission Scanning Electron Microscope (FESEM) revealed the arrangement of hydrated silica sphere in the structure of opal, and these are related to play of color phenomena shown on the surface. However, if hydrated silica spheres exhibit improper size with various sizes, imperfect shape, or unordered arrangement, the visible light will not diffract properly then play of color phenomena cannot appear (Gaillou et al., 2008).

Field Emission Scanning Electron Microscopic (FESEM) images taken from Ethiopian precious opal show that hydrated silica spheres are imperfect sphere shape with diameters less than hundred nanometers in diameters in most part of the structure. After boiling, hydrate silica spheres are reformed to nearly perfect 3D stacking. Their spheres are actually about 100-150 nm. Consequently, hydrated silica spheres appear to have more perfect form and well ordering arrangement in the opal structure with enlarged size of hydrated silica sphere after boiling, this relates to clearer play of color phenomena (Figure 4.30).

The second group, Malagasy white fire opal appears to have nanoparticles much less than hundred nanometers without space between these particles. After heating, hydrated silica spheres are even smaller and randomly stacking (Figure 4.31). The third group, Malagasy orange fire opal, shows irregular shape of hydrated silica spheres smaller than hundred nanometers without space between these particles. After boiling, hydrated silica spheres are even smaller and randomly arranged (Figure 4.32).

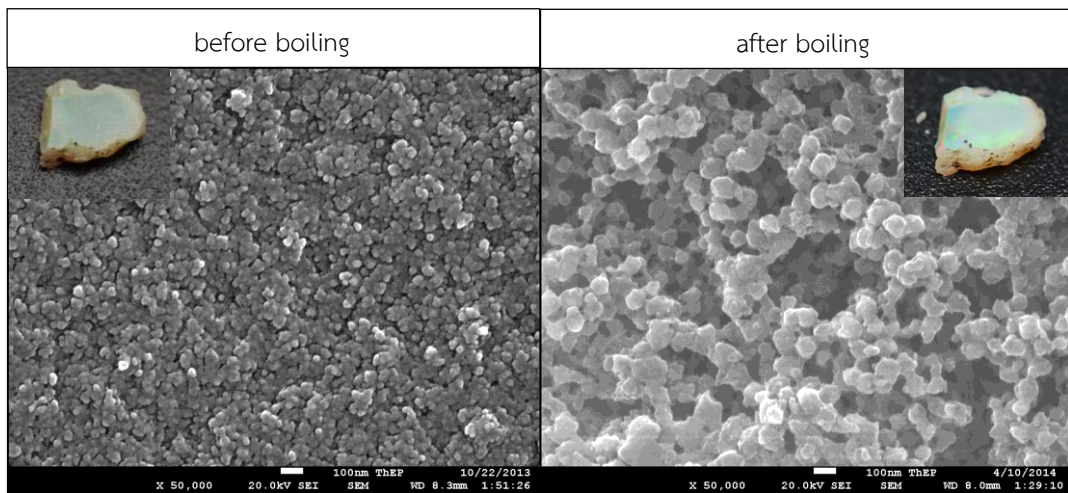


Figure 4.30 Representative FESEM micrographs of Ethiopian precious opals with slightly show play of color phenomena before and after boiling (sample A20).

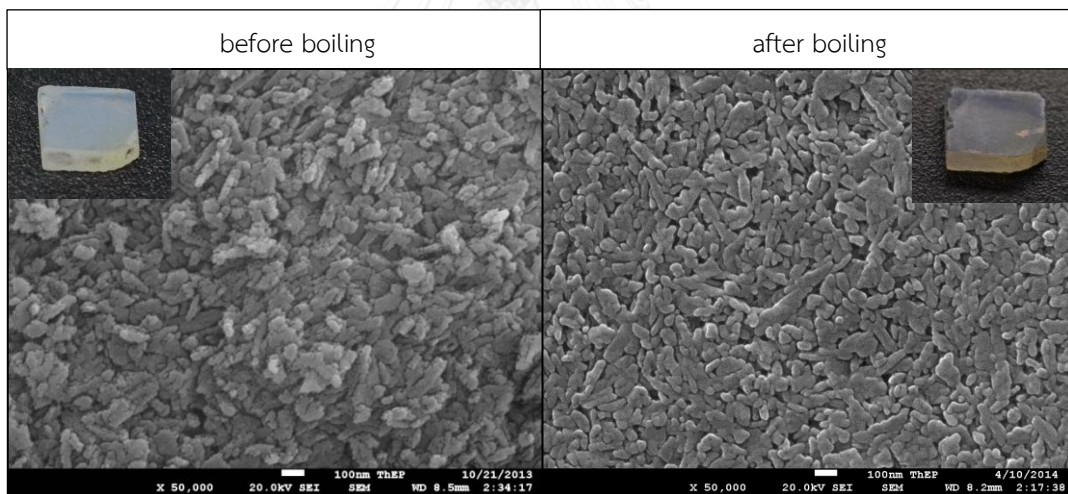


Figure 4.31 Representative FESEM micrographs of Malagasy white fire before and after boiling (sample B20).

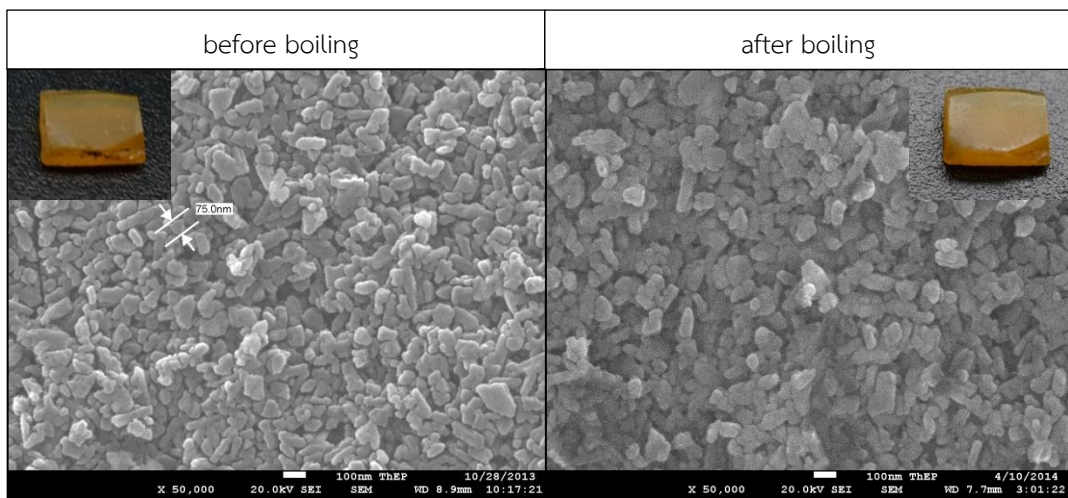


Figure 4.32 Representative FESEM micrographs of Malagasy orange fire opal before and after boiling (sample C20).

#### 4.4 Oiling Experiment

After oiling experiment, Ethiopian precious opal samples (Group A, samples A21-A30) appear to have very slightly play of color phenomena and their body colors turn to yellow (see Figure 4.33). Oiling may rearrange hydrated silica spheres to random orientation and reform irregular shaped silica particles leading to poor scattering of visible light. On the other hand, Malagasy white fire opal samples B21-B30 (Group B) and orange fire opal samples C21-C30 (Group C) were not changed after oiling experiment (see Figures 4.34 and 4.35).



Figure 4.33 Ethiopian precious opals (samples A24 and A26) show improvement of play of color phenomena after oiling at 100°C.

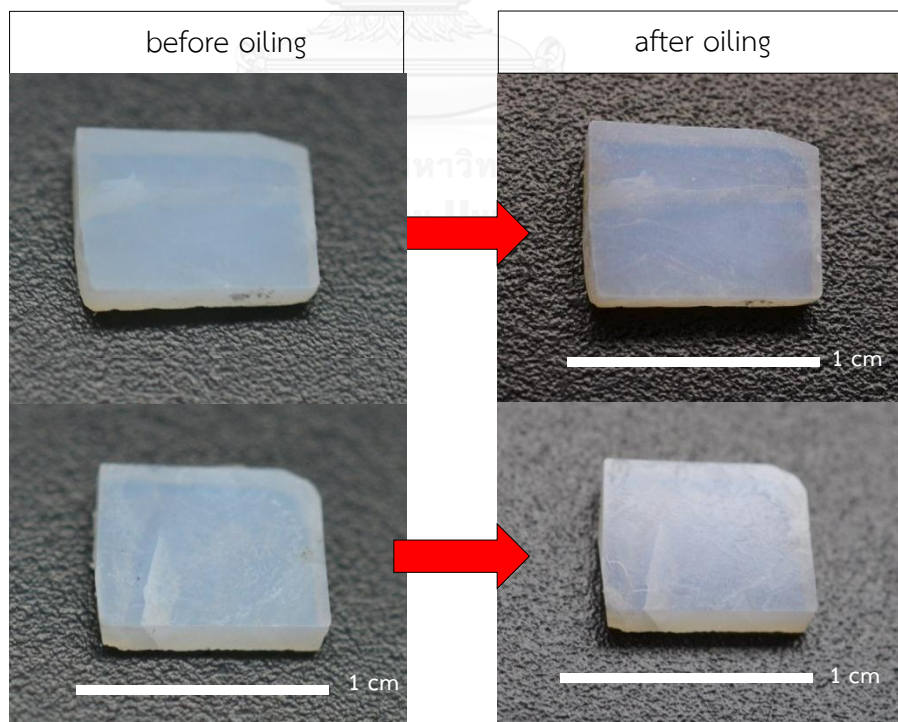


Figure 4.34 Malagasy white fire opals (samples B23 and B24) were not changed after oiling at 100°C.

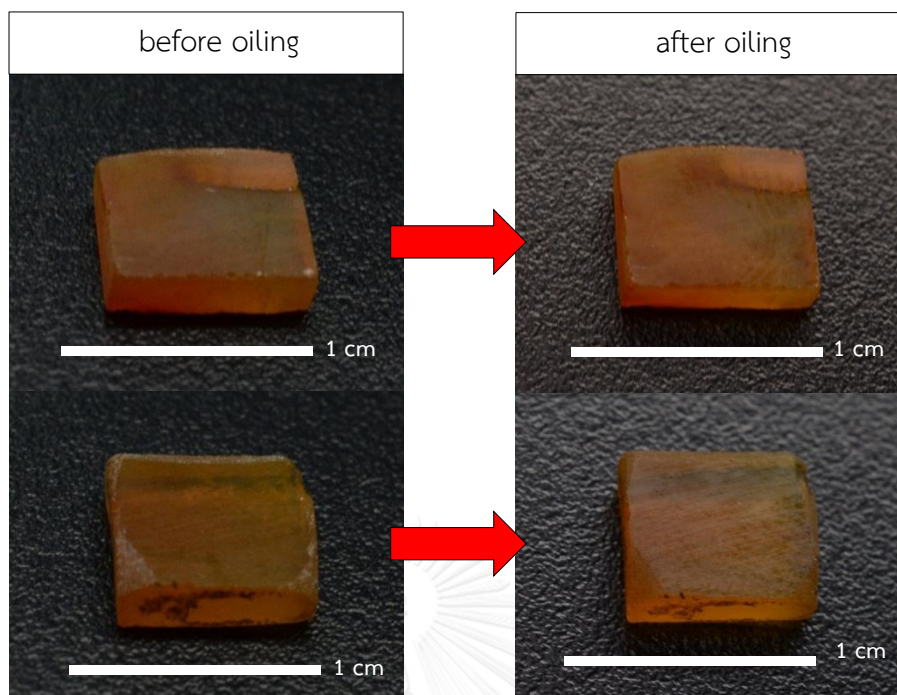


Figure 4.35 Malagasy orange fire opals (samples C25 and C26) were not changed after oiling at 100°C.

#### 4.4.1 Physical Properties

Physical properties of opal samples were analyzed and summarized in Table 4.3. Refractive index (R.I.) and specific gravity (S.G.) of Ethiopian precious opals fall within narrow ranges of 1.41-1.45 and 1.86-1.96, respectively. After oiling experiment, refractive index was increased to 1.46-1.47 while specific gravity was decreased to 1.80-1.93. On the other hand, Malagasy white and orange fire opals (Groups B and C) were not changed in refractive index and specific gravity: R.I. ranges of 1.42-1.45 (Group B) and 1.43-1.47 (Group C) remained at 1.43-1.45 and 1.43-1.44 as well as S.G. ranges of 2.02-2.18 (Group B) and 2.10-2.17 (Group C) still remained at 2.03-2.16 and 2.07-2.18, respectively. Plots of S.G. against R.I. (Figure 4.36) show graphical correlation as reported above.



Table 4.3 Summary of gemological properties of Ethiopian precious opal, Malagasy white and orange fire opals before and after oiling.

Samples	Experiment method	Before oiling		After oiling	
		S.G.	R.I	S.G.	R.I
Ethiopian precious opal (A)	oiling	1.86 - 1.96 (av. 1.91)	1.41-1.45	1.80-1.93 (av. 1.86)	1.46-1.47
Malagasy white fire opal (B)	oiling	2.02-2.18 (av. 2.10)	1.42-1.45	2.03-2.16 (av. 2.09)	1.43-1.45
Malagasy orange fire opal (C)	oiling	2.10-2.17 (av. 2.13)	1.43-1.47	2.07-2.18 (av. 2.10)	1.43-1.44

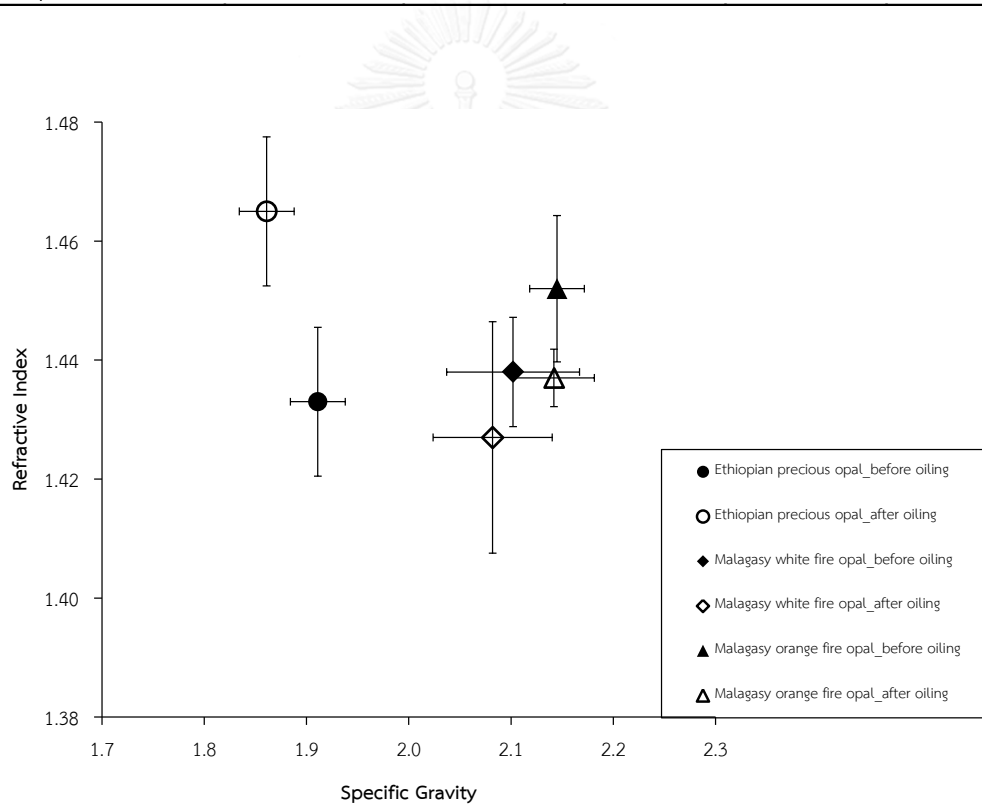


Figure 4.36 Plots of specific gravity versus refractive index before and after oiling of Ethiopian precious opal, Malagasy white and orange fire opals.

UV-Vis-NIR spectra within wavelength range of 400-800 nanometers of representative samples are displayed in Figures 4.37 to 4.39 and all samples spectra are collected in Appendix B. UV-Vis-NIR spectra of Ethiopian precious opals (Group A) before oiling (Figure 4.37) do not show any absorption leading to white body color. After oiling, opals in this group present absorption range of 400-550 nanometers related to yellow body color developed during oiling.

All of the UV-Vis-NIR spectra of Malagasy white fire opals (Group B) mostly show similar pattern without absorption both before and after oiling; this clearly leads to white body color (see Figure 4.38). On the other hand, absorption spectra of Malagasy orange fire opal show absorption peak at 475 nanometers which leads to orange body. After oiling, more absorption peaks at 414 and 424 nanometers are clearly observed (see Figure 4.39) but they were not significant changed.

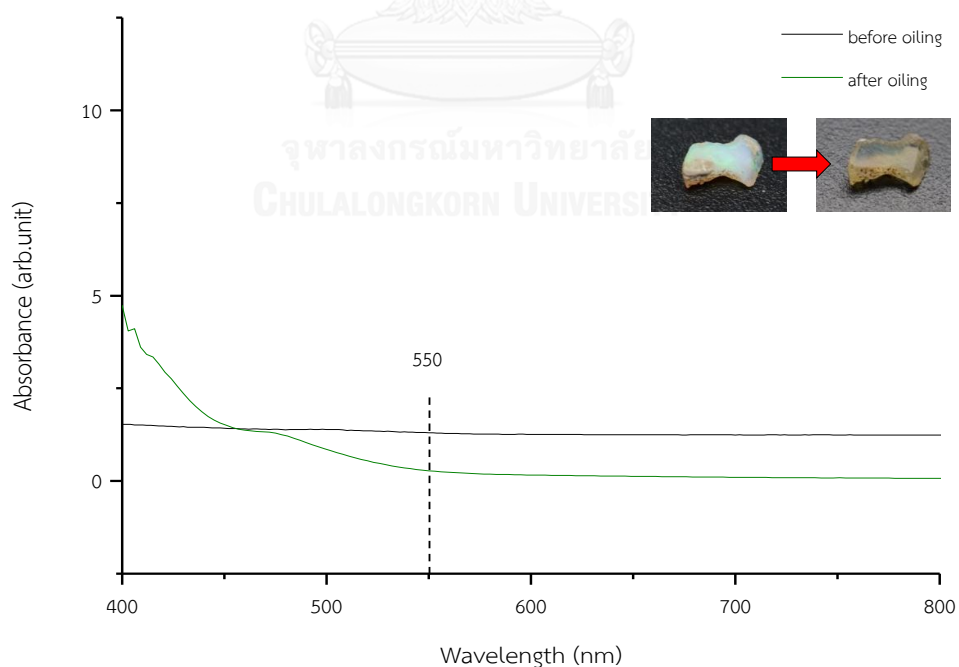


Figure 4.37 UV-Vis-NIR spectra of Ethiopian precious opal (sample A30 of Group A) before and after oiling.

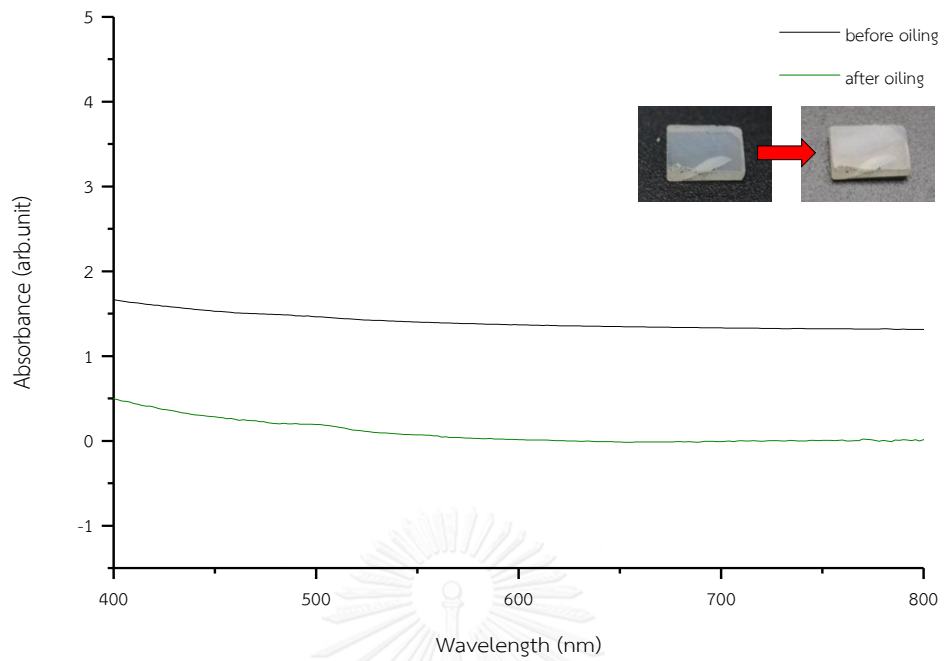


Figure 4.38 UV-Vis-NIR spectra of Malagasy white fire opal (sample B24 of Group B) before and after oiling.

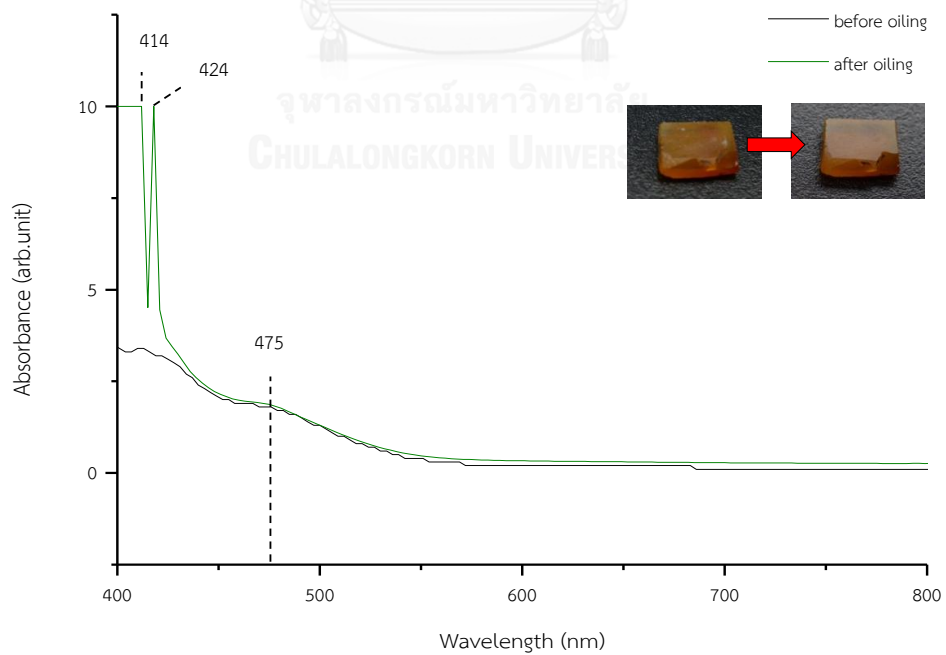


Figure 4.39 UV-Vis-NIR spectra of Malagasy orange fire opal (sample C29 of Group C) before and after oiling.

Representative Fourier Transform Infrared Spectra of Ethiopian precious opals (Group A) before and after oiling are displayed in Figure 4.40. Moreover, all FTIR spectra are collected in Appendix C. As shown in the figure, H<sub>2</sub>O stretching and bending absorption peaks at 5000-5400 cm<sup>-1</sup> is decreased probably due to losing of water after oiling. On the other hand, absorption peaks appear at ~4,250-4,300 cm<sup>-1</sup> near SiOH stretching and bending (4300-4600 cm<sup>-1</sup>).

Malagasy fire opals both Groups B and C show FTIR spectra similar to those of Ethiopian precious opal; however, they have unclear absorption band at 4300-4600 cm<sup>-1</sup> caused by SiOH stretching and bending. After oiling, most samples show unchanged pattern of H<sub>2</sub>O stretching and bending absorption peaks at 5000-5400 cm<sup>-1</sup> (see Figures 4.41 and 4.42).

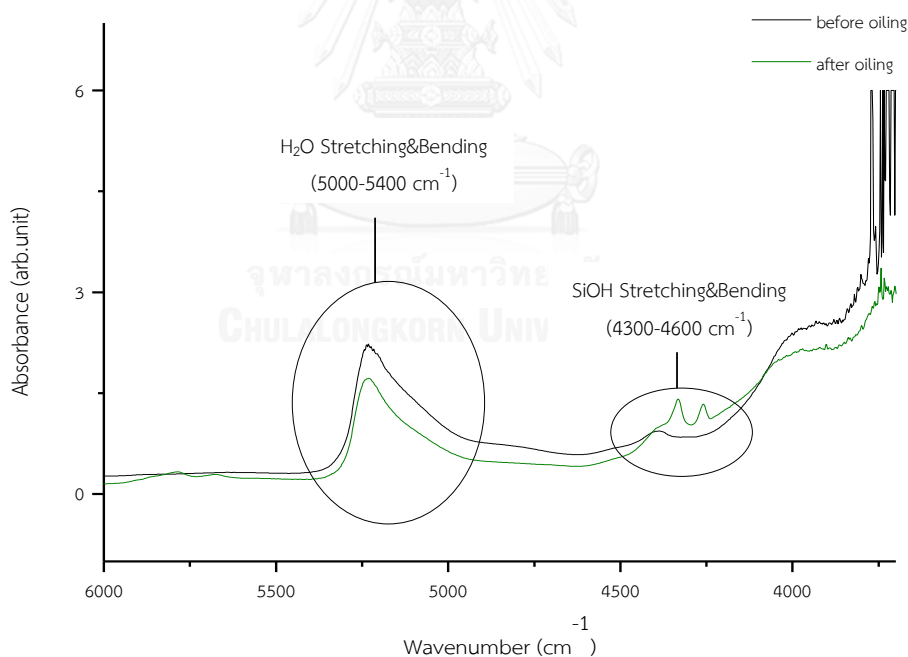


Figure 4.40 FTIR spectra of Ethiopian precious opal (sample A21) before and after oiling.

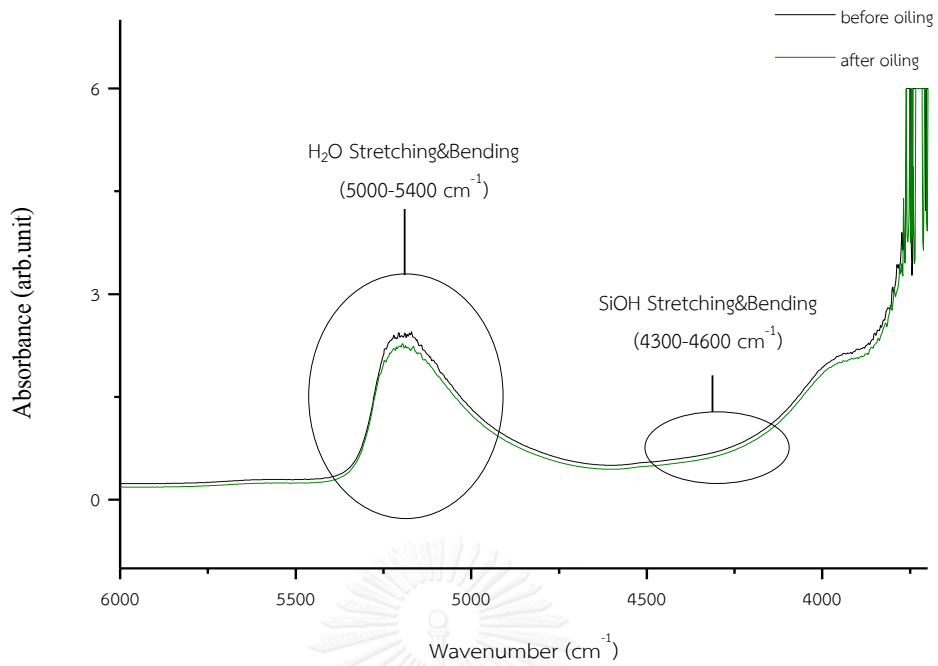


Figure 4.41 FTIR spectra of Malagasy white fire opal (sample B21) before and after oiling.

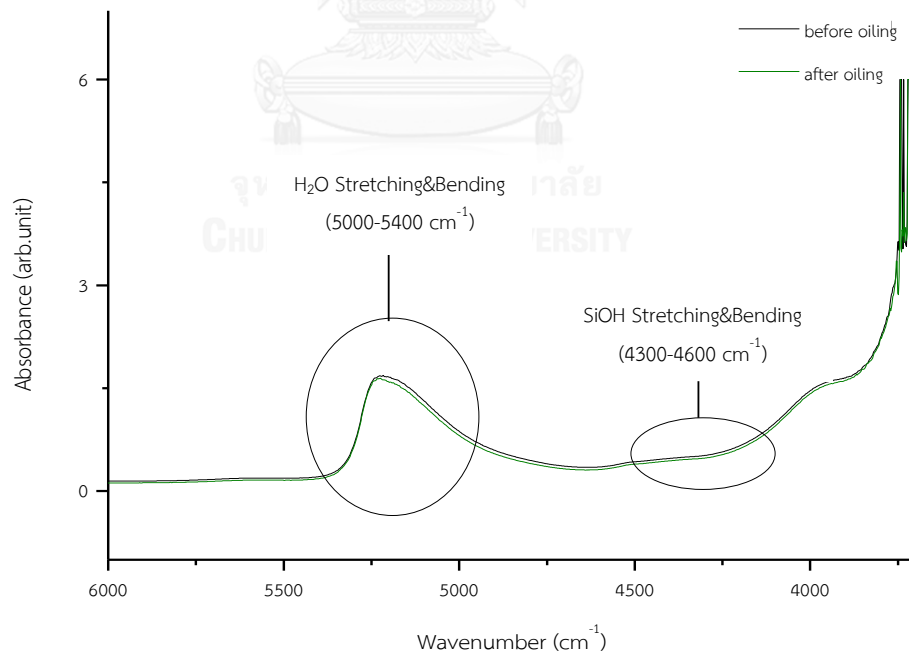


Figure 4.42 FTIR spectra of Malagasy orange fire opal (sample C24) before and after oiling.

Raman spectra of all Ethiopian precious opal samples (Group A) have the same pattern that reveals a broad band centered at  $\sim 333\text{ cm}^{-1}$  with left shifting close to the  $350\text{ cm}^{-1}$  peak of volcanic opal related to cristobalite and tridymite components (opal-CT). This peak is not sharp but can indicate crystalline phase as suggested by Smallwood et al. (1997) and Rondeau et al. (2010). In addition, appearance of peaks in the  $750\text{-}850\text{ cm}^{-1}$  region is associated with symmetric Si-O-Si stretching. The peak presents at  $1072\text{ cm}^{-1}$  is of Si-O-Si asymmetric stretch. After oiling the absorption peaks appear at the same positions without significant changing (Figure 4.43).

Raman spectra of Malagasy white fire opal (Group B) and Malagasy orange fire opal (Group C) have the same spectra this may be caused by the same formation. They exhibit essential peaks at  $230$  and  $418\text{ cm}^{-1}$  revealing cristobalite components. This characteristic is typical opal-C in volcanic environment (Ilieva et al., 2007). In addition, the spectra also present small features at  $783$  and  $1076\text{ cm}^{-1}$  which is a poor Raman scattering. After oiling, the absorption peaks appear at the same positions without significant changing. Raman spectra of both opal groups are displayed in Figures 4.44 and 4.45, respectively.

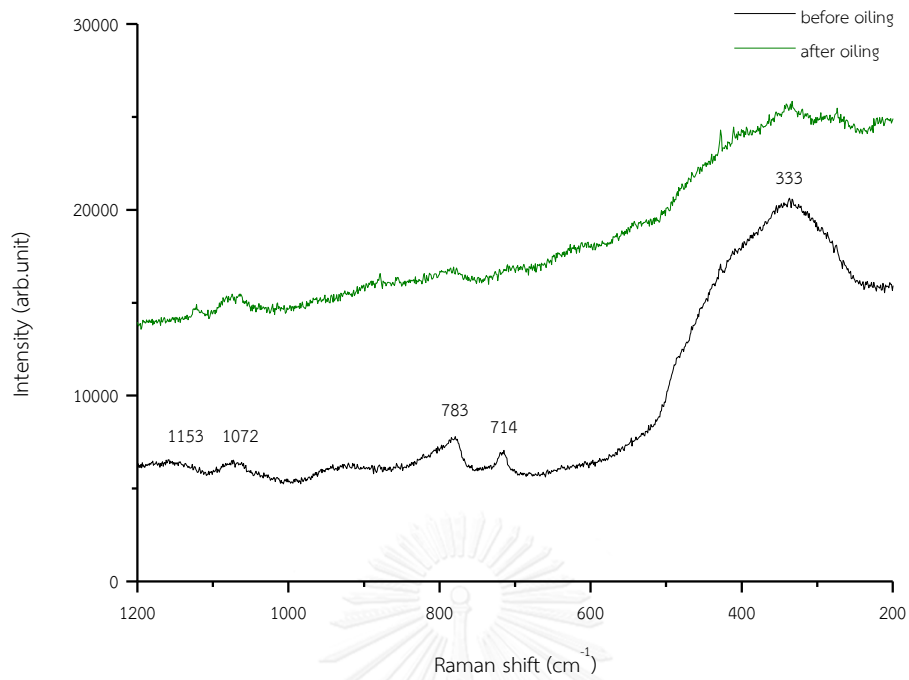


Figure 4.43 Raman spectra of Ethiopian precious opal (Group A) before and after oiling (sample A24).

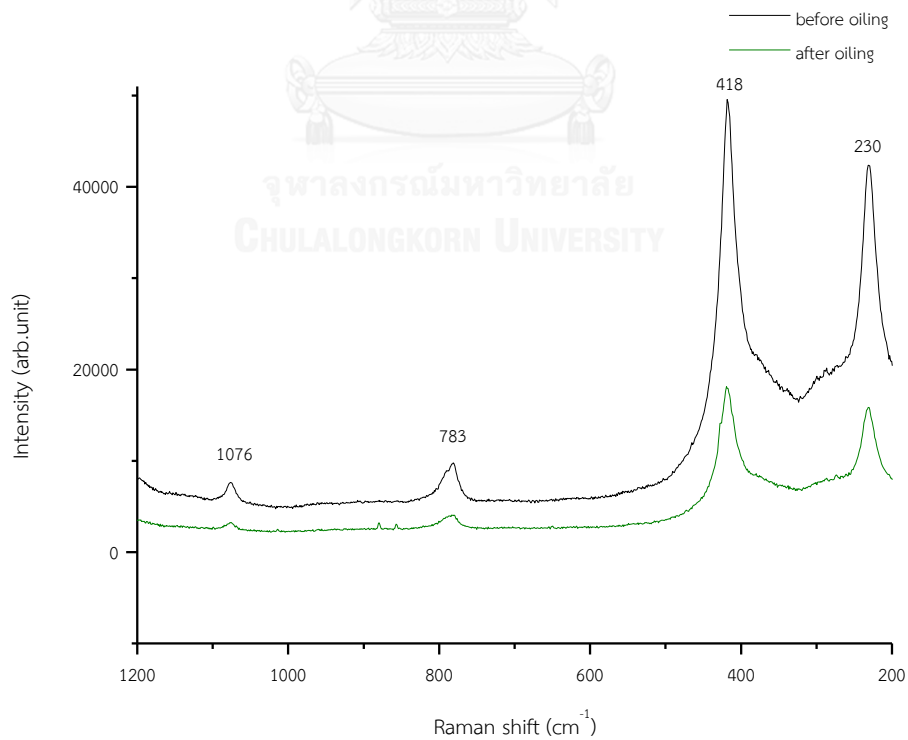


Figure 4.44 Raman spectra of Malagasy white fire opal (Group B) before and after oiling (sample B29).

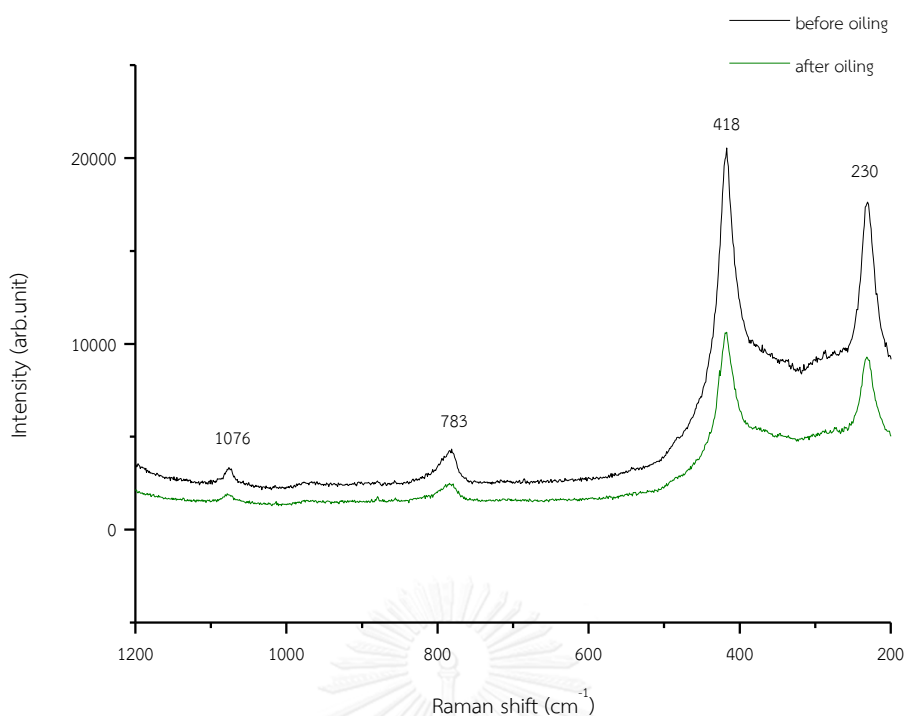


Figure 4.45 Raman spectra of Malagasy orange fire opal (group C) before and after oiling (sample C27).

#### 4.4.2 Field Emission Scanning Electron Microscope (FESEM)

Field Emission Scanning Electron Microscopic (FESEM) images taken from Ethiopian precious opal show that hydrate silica spheres are nearly perfect 3D stacking sphere shape with diameters of about 50 to 200 nm. After oiling, hydrate silica spheres are rearrange to imperfect sphere shape with smaller than hundred nm and without space. Consequently, hydrate silica spheres appear to have imperfect form and poorly ordering arrangement in the structure after oiling, this relates to very slightly play of color phenomena (Figure 4.46).

The second group, Malagasy white fire opal appears to have nanoparticles much less than hundred nm without space between these particles. After oiling, hydrated silica spheres are even smaller and randomly stacking (Figure 4.47). The third group, Malagasy orange fire opal show irregular shape of hydrated



silica spheres smaller than hundred nm without space between these particles. After oiling, hydrated silica spheres are even smaller and randomly arranged (Figure 4.48).

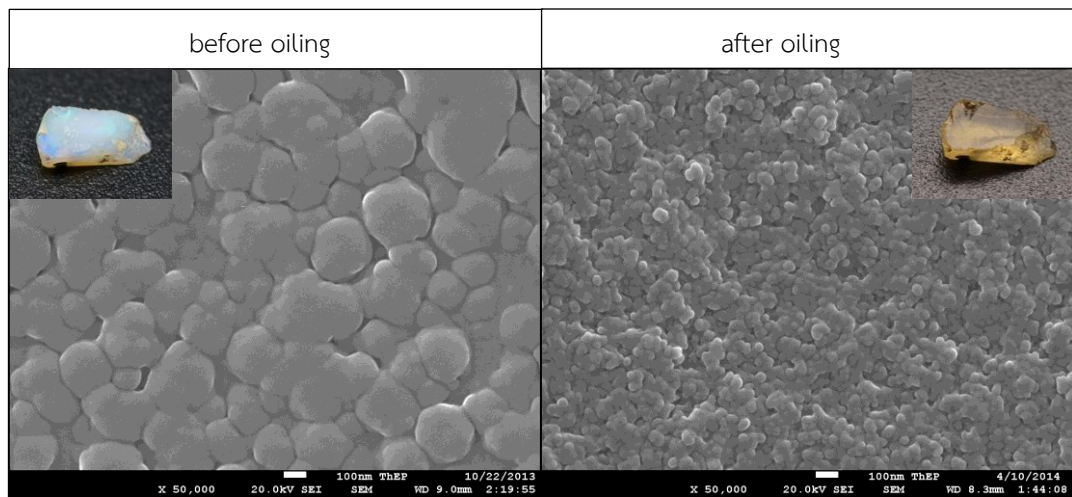


Figure 4.46 Representative FESEM micrographs of Ethiopian precious opal losing play of color phenomena after oiling (sample A27).

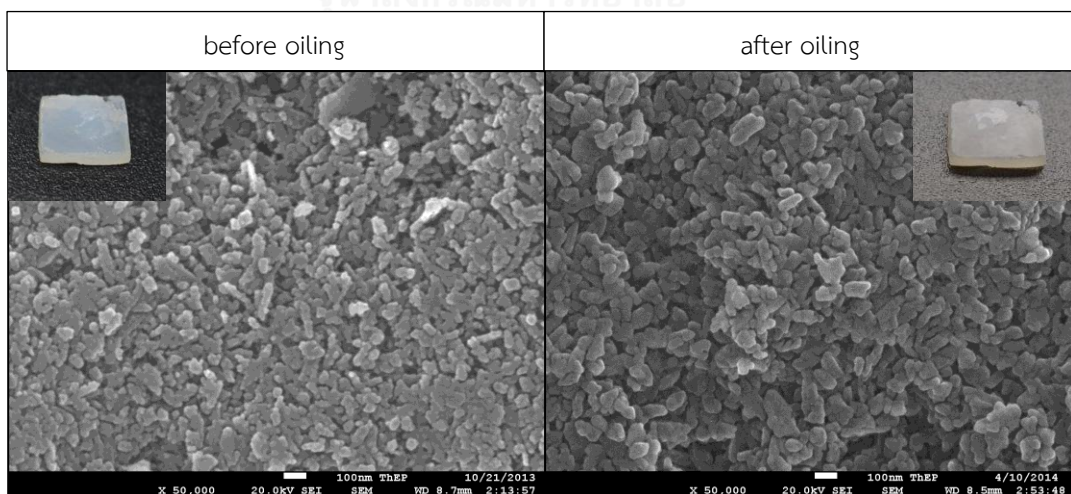


Figure 4.47 Representative FESEM micrographs of Malagasy white fire opal before and after oiling (sample B30).

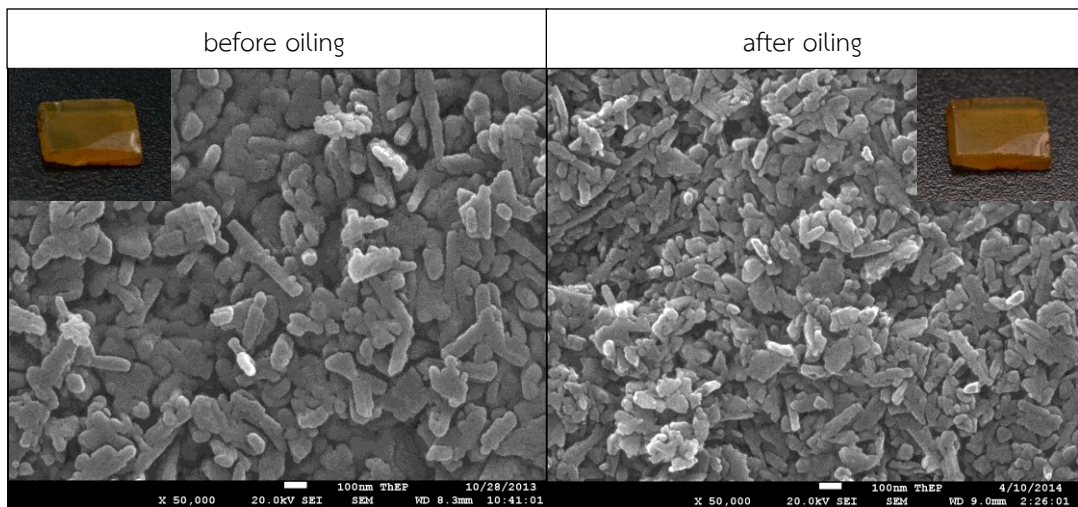


Figure 4.48 Representative FESEM micrographs of Malagasy orange fire opal before and after oiling (sample C30).

## CHAPTER V

### DISCUSSIONS CONCLUSIONS AND RECOMMENDATIONS

#### 5.1 Opal Characterization

##### 5.1.1 Ethiopian Precious Opal

Ethiopian precious opals with slightly play of color phenomena were investigated for physical properties. Their refractive index (RI) falls within a narrow range of 1.41 to 1.46 whereas their low specific gravity ranges from 1.85 to 1.97. The low specific gravity should relate to porosity and arrangement of microstructures as suggested by (Rondeau et al., 2010). Johnson et al. (1996) reported that precious opals from Shewa, Ethiopian are from volcanic environment; they also present low specific gravity within range of 1.83-2.03 indicating porosity in the structure. Similar narrow range of refractive index (1.40 to 1.45) was also reported. Subsequently, Rondeau et al. (2010) reported that precious opals from Wollo, Ethiopian have low specific gravity within range of 1.74-1.89 and wider range of refractive index from 1.37 to 1.45; however, most of samples were difficult to read. These low specific gravity values are overlapping to the results of this study. On the other hand, Australian precious opal present higher specific gravity  $\sim 2.00$  with similar R.I. range of 1.40-1.42 (Smallwood et al., 2008).

Ethiopian precious opals show Raman peak with left shifting at  $347\text{ cm}^{-1}$  with other small features at 780, 956, 1086, 1361 and  $2949\text{ cm}^{-1}$  which are typical characters of opal-CT as suggested by Rondeau et al. (2010) (see Figure 5.1). Moreover, the Raman peak of cristobalite can also be confirmed by the study of Ilieva et al. (2007) which they discussed on Raman signals near  $230\text{ cm}^{-1}$  and  $415\text{ cm}^{-1}$  related to the cristobalite-like domains and peaks near  $300\text{ cm}^{-1}$  and  $350\text{ cm}^{-1}$  related to

the tridymite-like domains. Raman patterns of Ethiopian precious opal show essential peaks of cristobalite and tridymite with sharper peaks; this may indicate crystalline morphology polymorph of SiO<sub>2</sub> at high temperature (Smallwood et al., 1997).

From the previous studies, Ethiopian precious opals have been reported since 1996. Geography of Ethiopia is significantly occupied by volcanoes in which volcanic opals may be originated widely (Rondeau et al., 2010). Smallwood et al. (2008) suggested that most opal-CT is volcanic opal. Typical opal-CT from Ethiopia is indicated by crystalline phase which should be formed in the volcanic environment as suggested by Smallwood et al. (2008). They may be formed by silica solution from lava flows or may be dissolved by hydrothermal solution. Subsequently, this SiO<sub>2</sub>-enriched liquid would deposit into the cavities of the host volcanic rocks.

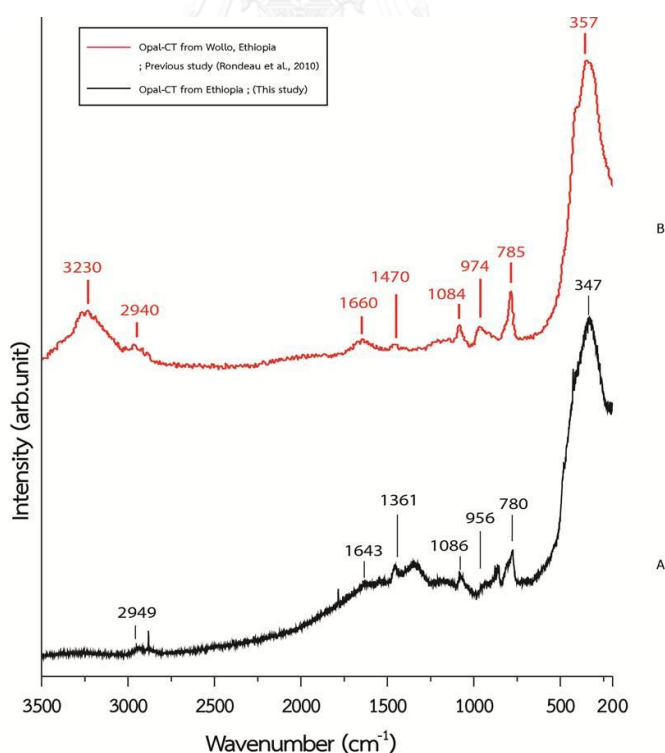


Figure 5.1 Comparison between Raman spectra of opal-CT from Ethiopia under this study (A) and opal-CT from Wollo, Ethiopia (Rondeau et al., 2010) (B).

The FTIR spectra of Ethiopian precious opal in this study show the same absorption pattern as precious opal from Australia (Day and Jones, 2008, Filin and Puzynin, 2009). These show absorption of water molecule consisting of a broad absorption band in the range of 5000-5400  $\text{cm}^{-1}$  and molecular SiOH groups in the range of 4300-4600  $\text{cm}^{-1}$  (Lee, 2007, Bobon et al., 2011). However, the absorption bands of SiOH groups in Ethiopian precious opal seem likely lower intensity than those from Australia. The absorption bands of SiOH are related to the water in hydrated silica sphere of the structure (Lee, 2007, Bobon et al., 2011). Therefore, this can conclude that the water in hydrated silica sphere of Ethiopian precious opal is less than Australian precious opal and may also contain smaller hydrated silica sphere because of the smaller SiOH Band (Figure 5.2).

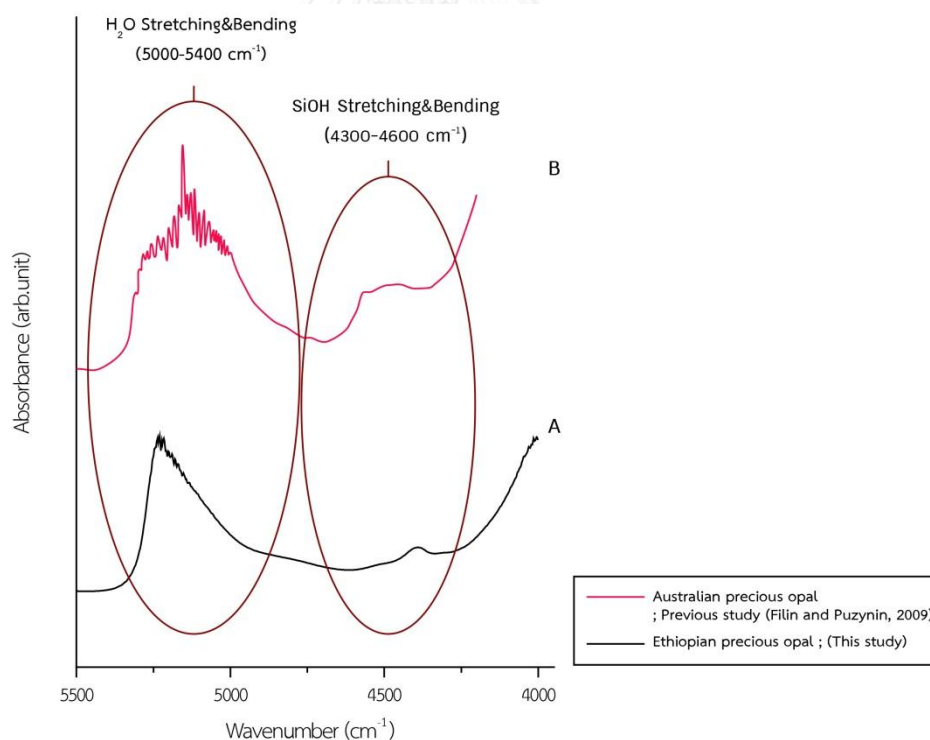


Figure 5.2 FTIR spectra of precious opals in the region of 4000-5500  $\text{cm}^{-1}$ : Ethiopian precious opal (A) and Australian precious opal (Filin and Puzynin, 2009) (B).

Field Emission Scanning Electron Microscopic (FESEM) images of Ethiopian precious opal show different arrangement patterns of hydrated silica spheres in their structures. Ethiopian precious opal with slightly show play of color phenomena commonly contains hydrated silica spheres (~50-200 nm in diameter) arranged with enough space for light diffraction; however, it is not regular pattern (Rondeau et al., 2010). Play of color phenomena should be appeared by arrangement of silica spheres with size ranging between 150 and 300 nm as suggested by (Jones et al., 1964). The FESEM image of Ethiopian precious opal is similar to SEM image of precious opal from Coober Pedy, Australia which has ordered stacking of hydrated silica spheres with about 350 nm in diameter (Smallwood et al., 2008). Similarity of these opals' structure is displayed in Figure 5.3. However, low quality opal from Ethiopia has relatively less irregular structure than those of the Australian precious opals.

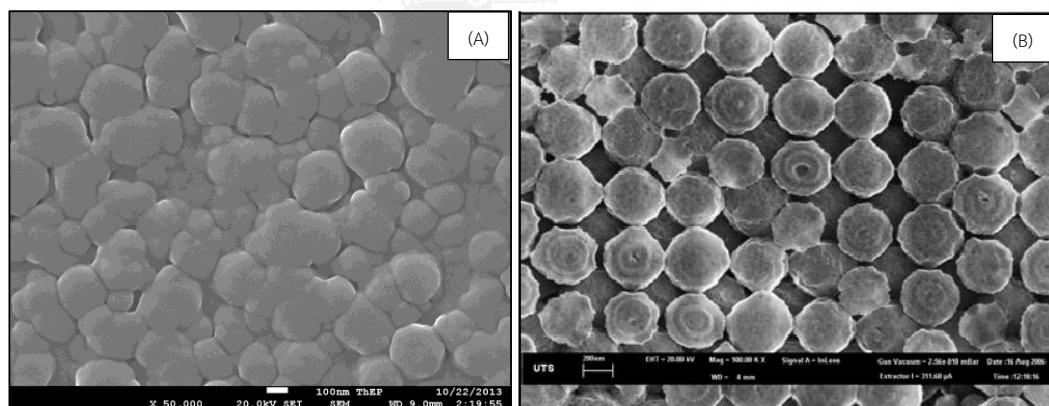


Figure 5.3 FESEM image of low quality Ethiopian precious opal (A) compared to SEM image of Australian precious opal (Smallwood et al., 2008) (B).

### 5.1.2 Malagasy Fire Opal

Malagasy fire opals both white and orange groups (sample groups B and C) have a narrow range of refractive index (RI) (1.42-1.47). These are agreeable to the findings of Simoni et al. (2010). This previous study reported data of Malagasy fire opal from Bemia, Madagascar. They presented that refractive index is slightly higher than those of other volcanic opals such as the famous opal from Querétaro, Mexico (1.42–1.43, rarely down to 1.37) as published by Koivula et al. (1983) and Gübelin (1986). Refractive indices of Malagasy fire opal in this study present slightly higher than those of Ethiopian precious opals which are from volcanic environment. Specific gravity (S.G.) of Malagasy fire opals ranges between 2.02 to 2.19. However, these S.G. values overlap with reading of Malagasy fire opal from Bemia deposit (Simoni et al., 2010).

Regarding to Figure 5.4, Malagasy fire opals (both Groups B and C) yield typical peaks of Opal-C with a number of cristobalite peaks at about 230 and 418  $\text{cm}^{-1}$  indicating crystalline morphology  $\text{SiO}_2$  polymorph likely cristobalite (Simoni et al., 2010). Malagasy fire opal should be formed in the volcanic environment. Silica solution of lava flows may be dissolved by hydrothermal solution; subsequently, this  $\text{SiO}_2$ -enriched liquid would deposit into the cavities of the host volcanic rocks as suggested by (Smallwood et al., 2008).

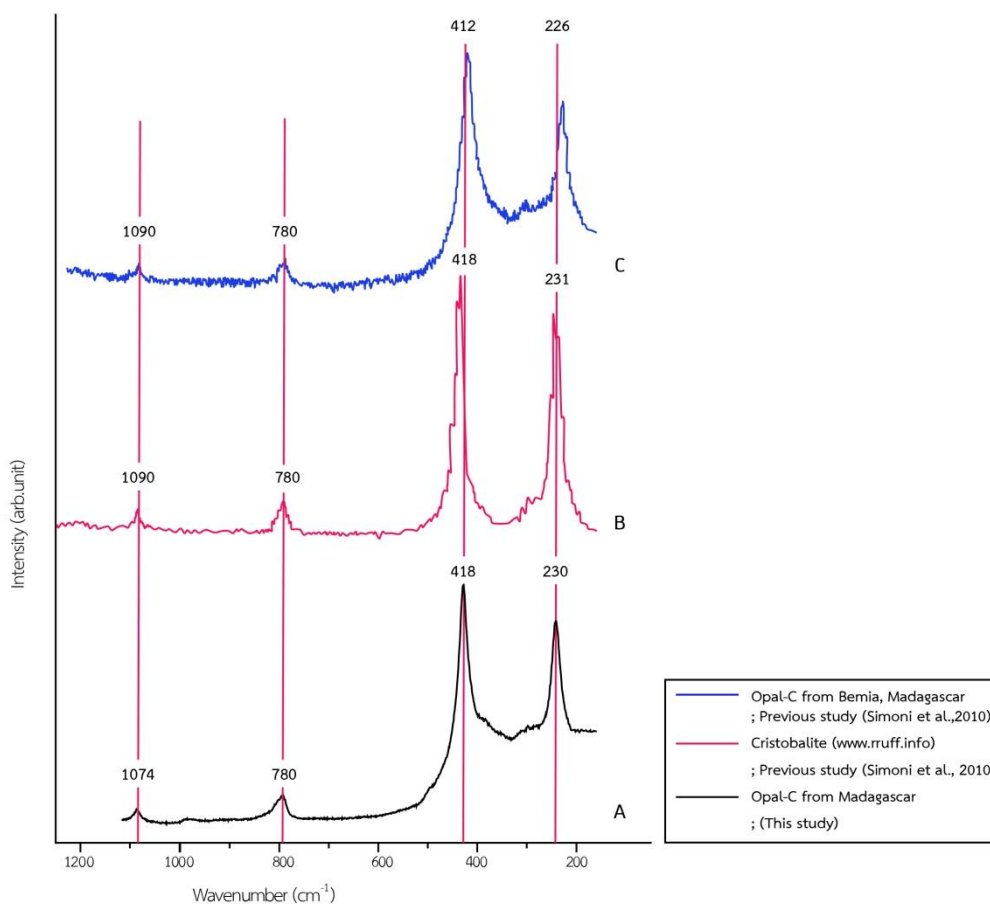


Figure 5.4 Comparison of Raman spectra of opal-C from Madagascar under this study (A), typical cristobalite (ruff.info) (B) and opal-C from Bemia, Madagascar (Simoni et al., 2010) (C).

The FTIR spectra of Malagasy fire opal in this study show similar absorption pattern of fire opal from other origins. Malagasy fire opal shows water absorptions consisting of a broad absorption band in the range of  $5000\text{--}5400\text{ cm}^{-1}$ ; moreover, molecular SiOH groups are found in the range of  $4300\text{--}4600\text{ cm}^{-1}$ . As a result, fire opals from Madagascar may have very low content of SiOH in the structure. On the other hand, Choudhary and Bhandari (2008) reported that Mexican fire opals show an absorptions of molecular water as a broad absorption band at



5000-5350  $\text{cm}^{-1}$  and hump of molecular water and SiOH between 4300-4600  $\text{cm}^{-1}$  which could not be observed in Malagasy fire opal (Figure 5.5).

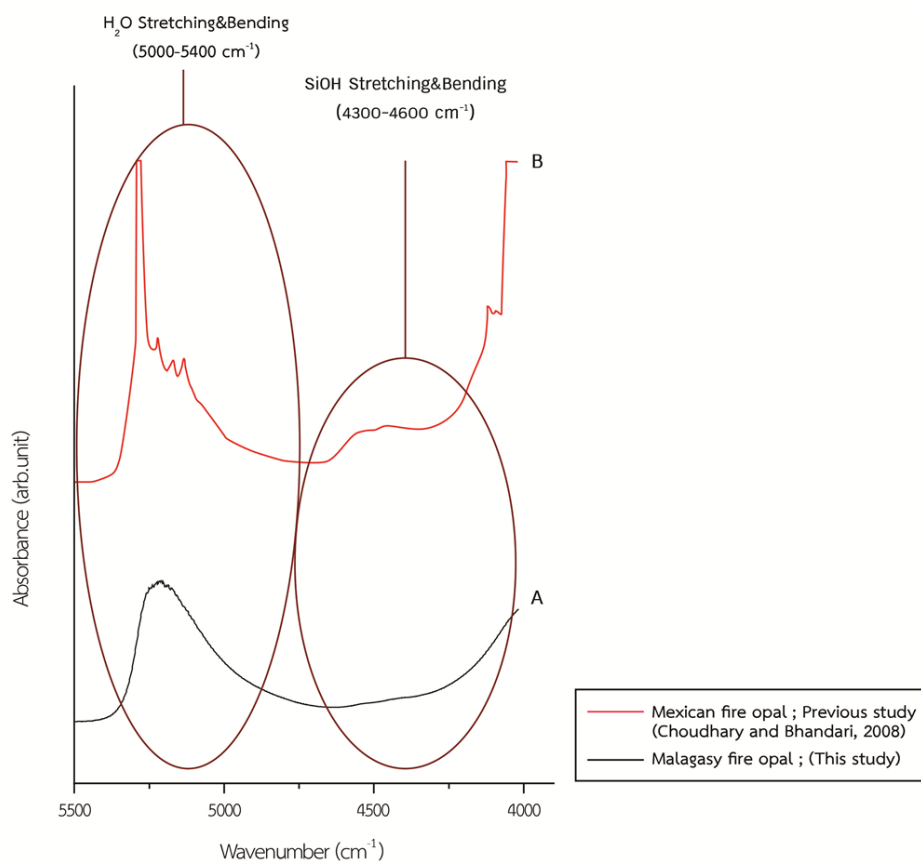


Figure 5.5 FTIR spectra of fire opals showing significant absorptions in the region of 4000-6000  $\text{cm}^{-1}$ : Malagasy fire opal from this study (A) and Mexican fire opal from previous study (Choudhary and Bhandari, 2008) (B).

Field Emission Scanning Electron Microscopic (FESEM) images of Malagasy fire opal show nanoparticles of the hydrated silica sphere less than hundred nm in diameter and poorly arrangement with lacking of regular space (Figure 5.6). As a result, light diffraction could not be occurred (Jones et al., 1964). This is comparable to the hydrated silica sphere of Mexican fire opal (see also Figure 5.6) which contains silicate spheres with size of about 10-30 nm and lacks regular space.

These characters cannot allow light diffraction due to tight arrangement of hydrated spheres (Fritsch et al., 2006).

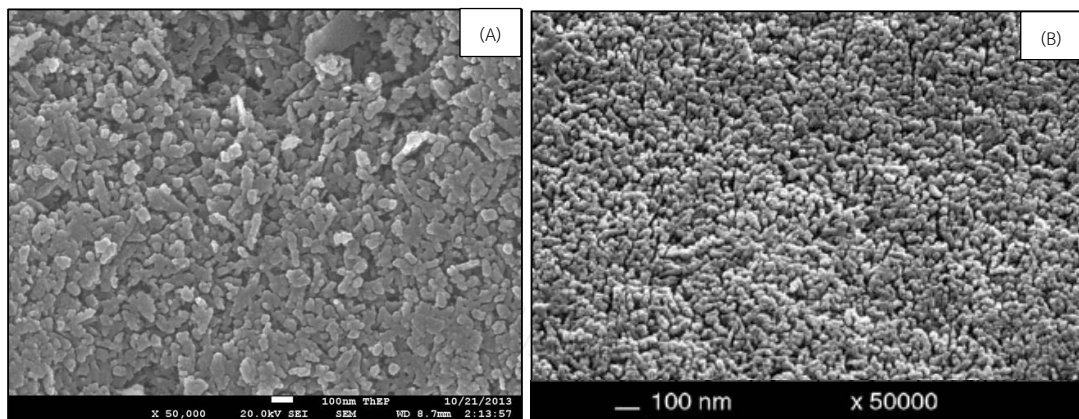


Figure 5.6 FESEM image of Malagasy fire opal (A) compared to SEM image of Mexican fire opal (Fritsch et al., 2006) (B).

As a result, The characteristics of Ethiopian precious opal with slightly play of color phenomena and Malagasy fire opal which investigated by basic instruments (hydrostatic balance and refractometer) and advance instruments (UV-Vis-NIR Spectrophotometer, Raman Spectrometer, Fourier Transform Infrared Spectrometer and Field Emission Scanning Electron Microscope) were shown in Table 5.1

Table 5.1 Summary of characteristics observed in Ethiopian precious opal and Malagasy fire opal.

Property	Ethiopian precious opal	Malagasy fire opal
Body color	White with slightly play of color	White and orange
Refractive Index (R.I.)	1.41 - 1.46	1.42 - 1.47
Specific Gravity (S.G.)	1.85 - 1.97	2.02 - 2.19
Raman Spectrometer	opal-CT	opal-C
Fourier Transform Infrared Spectrometer (FTIR)	absorption bands of water molecular ( $\sim 5,000-5,400\text{ cm}^{-1}$ ) and SiOH molecular ( $\sim 4,300-4,600\text{ cm}^{-1}$ )	absorption bands of water molecular ( $\sim 5,000-5,400\text{ cm}^{-1}$ ) and very low SiOH molecular ( $\sim 4,300-4,600\text{ cm}^{-1}$ )
Field Emission Scanning Electron Microscope (FESEM)	almost perfect stacking sphere shape with diameters of about 50 to 200 nm	imperfect form and poorly ordering arrangement of nanograin sizes $\sim 10-100\text{ nm}$

## 5.2 Opal Enhancements

### 5.2.1 Ethiopian Precious Opal

This study was concentrated to enhancement low quality precious opal from Ethiopia. Various methods such as heating, boiling and oiling then applied to these opal samples. After heating experiment, refractive index and the specific gravity appear to be decreased from 1.42-1.46 to 1.39-1.43 and 1.91-1.97 to 1.72-1.87, respectively. As a result, heating experiment may lead to water removal in opal, particularly shrinkage of hydrated silica spheres may take place leading to more space in the structure. After water removal, air should replace positions of water in, particularly space of the structure. This directly causes deduction of refractive index and specific gravity because air has lower R.I. and lighter than water. These results are comparable to the study of Tariaferro (1935). This previous study also suggested that water content of opal relates to refractive index and specific gravity after heating. Hydrated silica sphere of Ethiopian precious opal presented nearly perfect arrangement of imperfect silica spheres with various sizes that yields low quality play

of color phenomena. Because such structural should cause slightly light diffraction. In addition, Ethiopian precious opal samples appear to have more intense play of color phenomena and their white body color turn to light yellowish white with a few cracks. The hydrated silica spheres are nearly perfect 3D stacking and have more spherical distribution. Their spheres are actually reduced from 220 nm to about 200 nm as recognized in the FESEM image (see Figure 4.14). As a result, shrinkage of hydrated silica sphere may lead to reforming of better shape spheres with equal spacing. This proper arrangement would yield better light diffraction and appear to have more intense of play of color phenomena (Figure 5.7). This finding is also supported by previous studies. Arrangement of hydrated silica spheres with size ranging between 150 and 300 nm suggested by (Jones et al., 1964) usually produces play of color. Moreover, Thomas (2008) was heating precious opal from Australia with various temperatures. The most proper heating condition was lower than 200°C because the hydrated silica sphere still arranged in the perfect form. These can conclude that heating experiment can rearrange hydrated silica spheres which is agreeable to this study. Chanmuang et al., (2015) applied Transmission Electron Microscope (TEM) technique to investigate Ethiopian precious opal from the same sample batch under this study. TEM images of these Ethiopian precious opal show clearly porosity of the hydrated silica sphere (see Figure 5.8). This can support that Ethiopian precious opal has hydrophane character leading to dehydration or water resorption of structure. Fourier Transform Infrared Spectra also show decreasing of absorption band of H<sub>2</sub>O at 5000-5400 cm<sup>-1</sup> and SiOH at 4300-4600 cm<sup>-1</sup> after heating (Figure 4.8); These are comparable to the previous study (Segnite et al., 1965) suggesting that water content is probably losing because of pore after heating. Moreover, absorption band of H<sub>2</sub>O at 5000-5400 cm<sup>-1</sup> is easier decreased than absorption band of SiOH at 4300-4600 cm<sup>-1</sup>. Slowly decreasing of absorption of H<sub>2</sub>O

appear to be controlled by heating temperatures from 25°C to 1,200°C (Hannay, 1877, Zhuravlev, 2000).

After boiling experiment, refractive index and the specific gravity also appear to be decreased slightly from 1.42-1.45 to 1.39-1.43 and 1.85-1.97 to 1.72-1.94. As a result, the refractive index and specific gravity was deduction. Water should diffuse and access into the opal's structure as detected by FTIR spectra. However, slightly deduction of the refractive index and specific gravity may be uncertainty of measurement. Rondeau et al. (2010) was immersing Ethiopian precious opal by rehydration process for less than one hours and found weighted increased as much as 10.2% related to higher SG value similar to this study should be. Dehydration and rehydration of opal is so-called hydrophane character (Asnachinda, 2006). Moreover, Ethiopian precious opal samples also present clearer play of color phenomena. Hydrated silica spheres are nearly perfect 3D stacking. They reform to larger size, from less than hundred nm to about 100-150 nm as recognized by FESEM image (Figure 4.30). As a result, regular spaces between silica spheres should be caused by rearrangement of equal silica spheres leading to better light diffraction and clearer play of color phenomena, consequently (Figure 5.9). The absorption band of H<sub>2</sub>O and SiOH seem to be higher intensity (see Figure 4.24) due to increasing of water content in the structure similarly reported by Bobon et al. (2011). Bobon et al. (2011) studied state of water molecules in opal from Slovakia which was analyzed by near infrared spectroscopic. They concluded that high intensity and expansion of absorption band relate to more water content in the structure.

After oiling experiment, the refractive index was increased slightly from 1.41-1.45 to 1.46-1.47 whereas specific gravity was decreased from 1.86-1.96 to 1.80-1.93. During oiling, oil may diffuse and replace some positions of water, particularly space between hydrated silica spheres. This should cause increasing of

refractive index and decreasing of specific gravity because coconut oil has higher R.I. and lighter than water. Hydrated silica spheres in Ethiopian precious opals may reform to more random orientation of irregular shaped leading to poor scattering causing very slightly play of color after this treatment. After oiling experiment, Ethiopian precious opal samples appear to have very pale play of color phenomena and their body colors turn to yellow. Their spheres are actually reformed in nanograin size, from 50-200 nm to mostly less than hundred nm as recognized by FESEM image (Figure 4.46). As a result, these tiny hydrated silica spheres would have irregular shape and very less space between these silica grains. Also, the altered yellow body color is actually caused by oil diffusion. The imperfect structure of irregular arrangement should cause poor light diffraction and leading very pale play of color phenomena (Figure 5.10). The absorption band of  $\text{H}_2\text{O}$  at  $5000\text{-}5400\text{ cm}^{-1}$  seem to be lower the initial absorption probably due to water losing in the structure. This is because of oil diffusion to replace water, partly. On the other hand, absorption band at  $4300\text{-}4600\text{ cm}^{-1}$  of  $\text{SiOH}$  appear to have an addition peak nearly  $4,250, 4,300\text{ cm}^{-1}$  (see Figure 4.40); however, this peak has never been reported, previously.

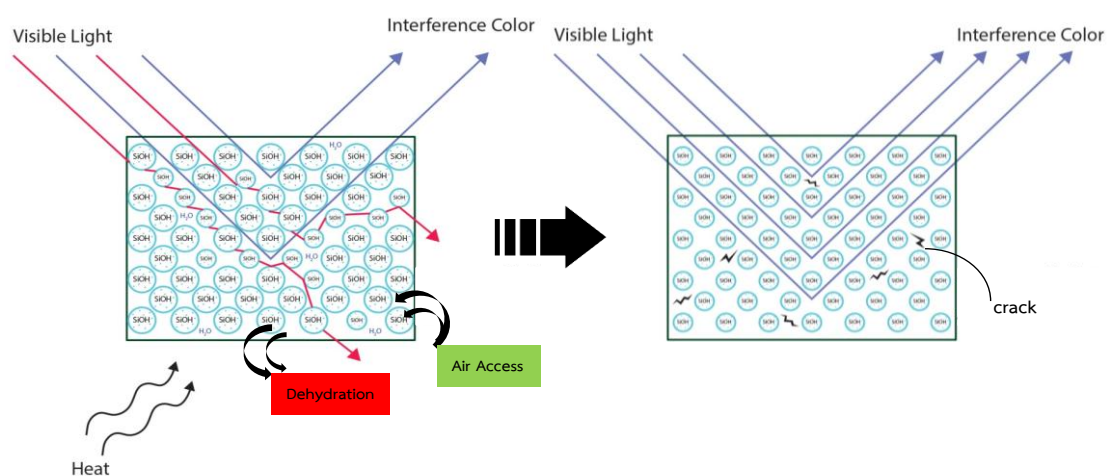


Figure 5.7 Simplified structure of Ethiopian precious opal before and after heating.

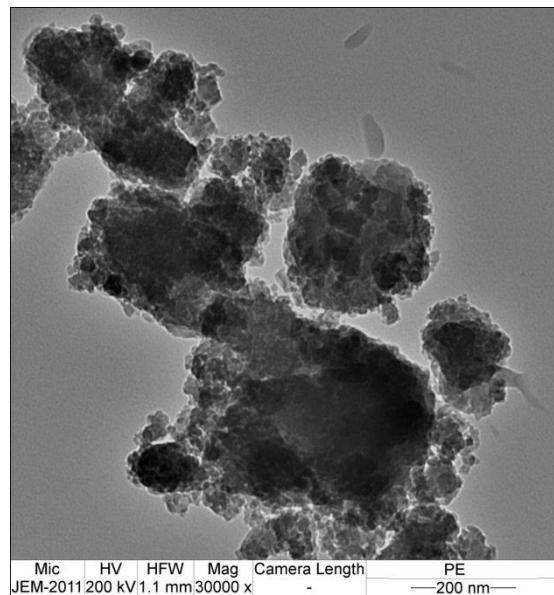


Figure 5. 8 TEM micrograph presenting porosity of hydrated silica sphere in Ethiopian precious opal (Chanmuang et al., 2015).

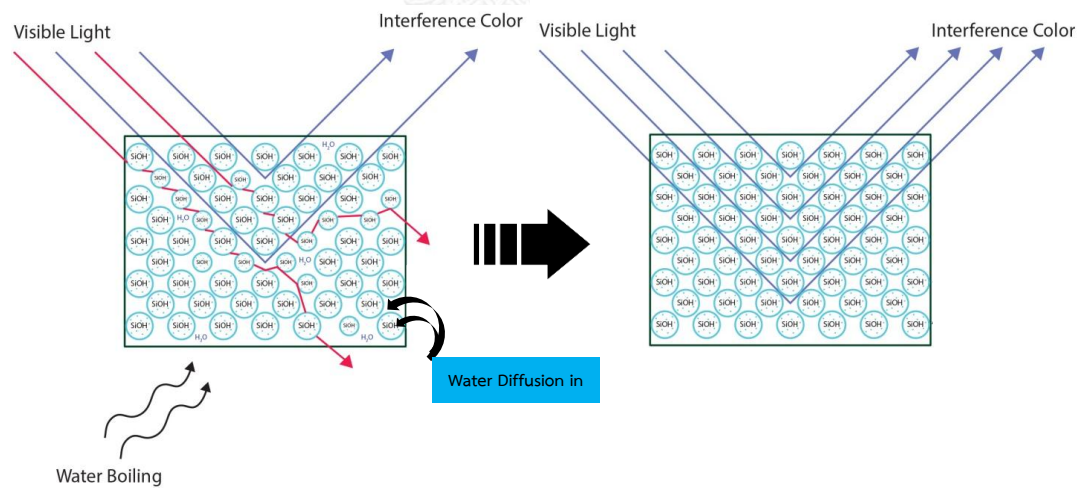


Figure 5.9 Simplified structure of Ethiopian precious opal before and after boiling.

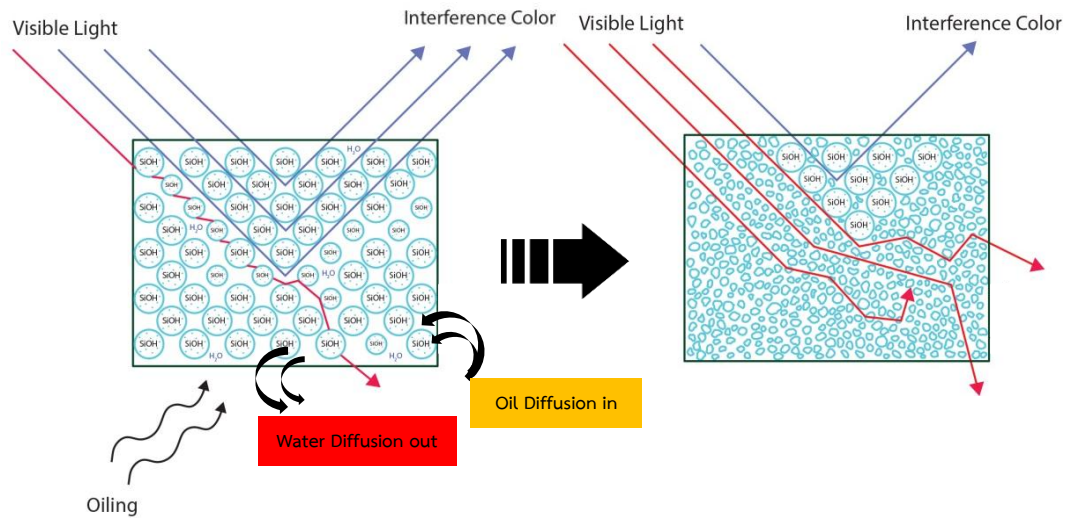


Figure 5.10 Simplified structure of Ethiopian precious opal before and after oiling.

### 5.2.1 Malagasy Fire Opal

Heating, boiling and oiling were designed enhancement of Malagasy white and orange fire opals. After all experiments, Malagasy white and orange fire opals appear to have been changed only by heating experiment. This is because dehydration should be taken place easier than it is happened in boiling and oiling processes. Malagasy white and orange fire opal turned to have turbidity that may be caused by micro-cracks formed during dehydration in the structure. This result is similar to the study of Johnson et al. (1996) that reported dehydrated opal after 24 hours heating experiment developed cracks inside the structure. This result is confirmed by FTIR spectra that shows decreasing of  $\text{H}_2\text{O}$  stretching and bending absorption peaks in the  $5000\text{-}5400\text{ cm}^{-1}$  region. This is probably due to losing of water as suggested by (Hannay, 1877, Zhuravlev, 2000). Therefore, light cannot pass through easily because there are many internal reflection related to micro-cracks (see Figure 5.11). The hydrated silica spheres are even smaller and randomly stacking compared to the initial structure. After water removal, air then replace position of



water in the structure. This should cause slightly deduction of refractive index and specific gravity; they have changed from 1.42-1.46 to 1.39-1.43 for R.I. and 1.91-1.90 to 1.72-1.87 for S.G. because air has lower R.I. and lighter than water. This result is also similar to the study of Tariaferro (1935).

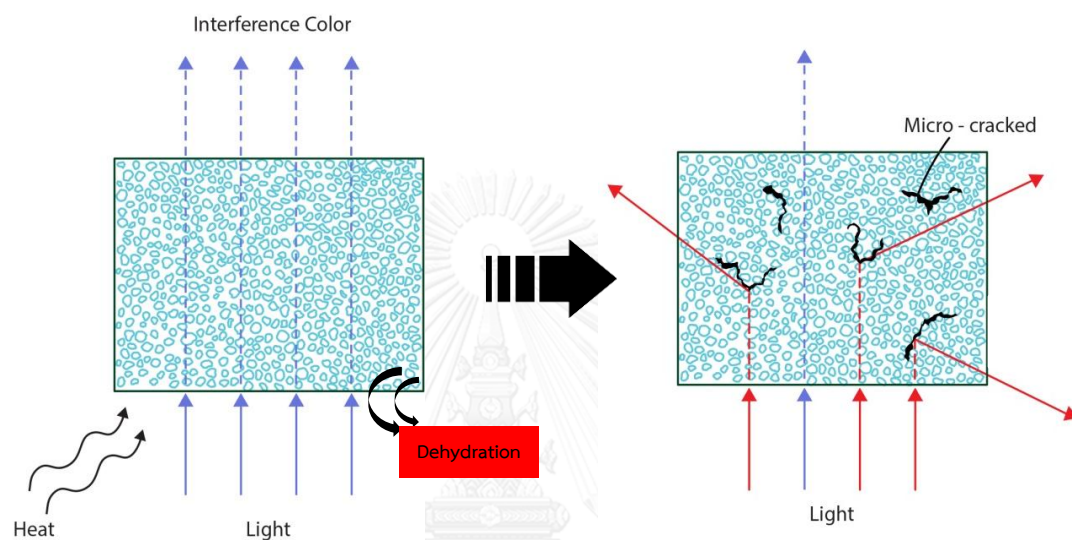


Figure 5.11 Simplified structure of Malagasy white and orange fire opals before and after heating.

Malagasy white and orange fire opals were not changed after boiling and oiling because of unsuitable sphere and lacking of space (Jones et al., 1964). Malagasy fire opal has less porosity and not hydrophane characteristics which are hardly to be changed its gem properties. This is similar to the previous studies (Tariaferro, 1935, Segnite et al., 1965). Segnite et al. (1965) found that changing of water content is controlled by porosity.

Chanmuang et al. (2015) used Transmission Electron Microscope (TEM) to investigate Malagasy fire opal samples from the same batch of this study. TEM images of Malagasy fire opals appear to have no porosity of the hydrated silica sphere (see Figure 5.12). This can confirm that Malagasy fire opal does not have hydrophane character. Fourier Transform Infrared Spectra as well as refractive index, specific gravity and FESEM image of these samples still have the same initial appearances as reported in the former chapter (see Figures 4.15, 4.16, 4.31, 4.32, 4.47 and 4.48).

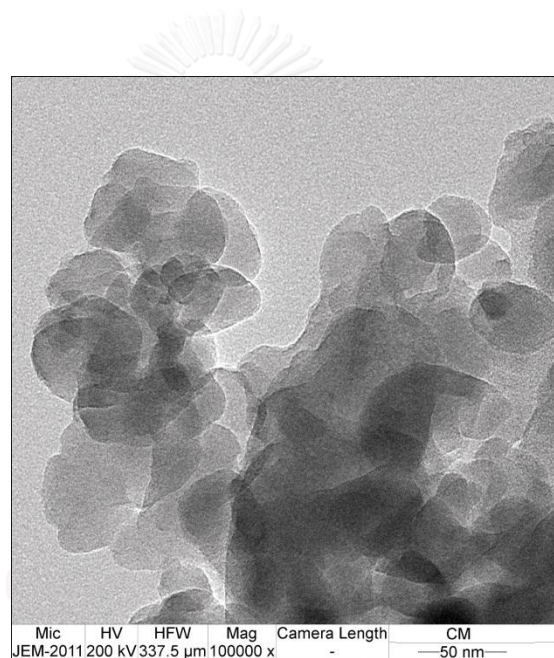


Figure 5.12 TEM images presenting no porosity in hydrated silica sphere of Malagasy fire opal (Chanmuang et al., 2015).

### 5.3 Conclusions

The main objective of this research is to characterize, particularly physical properties and internal features of precious opal from Ethiopia and fire opal from Madagascar before and after enhancement. Three different enhancement methods

(i.e., heating, boiling and oiling) were also carried out for these opal samples. All the results can be concluded below.

1. Specific gravity of Ethiopian precious opal is lower than Malagasy fire opal. These may be caused by hydrophane property.

2. Ethiopian precious opal is typical opal-CT from the crystalline phase while Malagasy white and orange fire opals are classified as opal-C because of dominant cristobalites. These results may lead to the assumption that geologic environments of both formations have derived from volcanism.

3. FESEM images of precious opal and fire opal show distinct differences of hydrated silica sphere in both types of opal. Ethiopian precious opal shows nearly ordered arrangement of hydrated silica sphere which may cause slightly play of color and its low density. On the other hand, Malagasy fire opals show random arrangement of nanograins of silica with irregular shape which could not generate play of color effect and have higher density.

4. Ethiopian precious opal has special characteristic, so-called hydrophane character. It can give a good result of potential enhancement because of its high porosity. The Malagasy white and orange fire opals could not be changed after all enhancement techniques because of tight arrangement of hydrated silica particles without hydrophane character.

5. Both heating and boiling experiments can enhance play of color phenomena of Ethiopian precious opal because they can change and rearrange size and position of silica sphere providing equal spacing which should lead to better light diffraction and then more intense play of color. On the other hand, oiling change imperfectly structural arrangement which causes very pale play of color. Therefore, oiling process should not be used in Ethiopian precious opal enhancement.

#### 5.4 Recommendations

1. Although, some experimental enhancements of this study are appropriate for particular precious opal; this preliminary study still need further investigation. For instant, coconut oil could not improve gemological properties of stone samples under this study. Therefore, more different types of oil are recommended for oiling experiment in the future.

2. The most significant property of opal for potential enhancement is hydrophane character. Because this character can lead to water absorption and dehydration of silica sphere which may lead to potential enhancement of proper shape and size for improvement of play of color phenomena. Therefore, it is practically applicable to commercial opal treatment.



## REFERENCES

- Asnachinda, P. (2006). Gemstone deposit. Department of Geology, Faculty of Science, Chiang Mai University.
- Barot, N. R. (1994). New precious opal found in Ethiopia. ICA Gazette(February): 2.
- Besaire, H. (1964). Carte Géologique de Madagascar.
- Bobon, M., Christy, A. A., Kluvanec, D. and Illánová, L. (2011). State of water molecules and silanol groups in opal minerals: a near infrared spectroscopic study of opals from Slovakia. Phys Chem Minerals(38): 809–818.
- Chanmuang, C., Singto, S. and Wanthanachaisaeng, B. (2015). An investigation of natural opal from Ethiopia, Madagascar and Australia. The 8<sup>th</sup> ASEAN Microscopy Conference & 32<sup>nd</sup> Microscopy Society of Thailand Annual Conference. Nakhon Pathom, Thailand.
- Choudhary, G. and Bhandari, R. (2008). A new type of synthetic fire opal: Mexifire. Gems & Gemology 44(3): 228 – 233.
- Coenraads, R. R. and Zenil, R. A. (2006). Leopard opal: play of color opal in vesicular basalt from Zimapan, Hidalgo State, Mexico. 236-246.
- Day, R. and Jones, B. (2008). Variations in water content in opal-A and opal-CT from Geyser discharge aprons. Journal of Sedimentary Research 78: 301-315.
- Elzea, M. and Rice, B. (1996). TEM and X – ray diffraction evidence for cristobalite and tridymite stacking sequences in opal. Clays and Clay Minerals 44(4): 492 – 500.
- Filin, S. V. and Puzynin, A. I. (2009). Prevention of cracking in Ethiopian opal. The Australian Gemmologist 23: 579-582.
- Fritsch, E., Gaillou, E., Rondeau, B., Barreau, A., Albertini, D. and Ostroumov, M. (2006). The nanostructure of fire opal. Journal of Non - Crystalline Solids 352: 3957-3960.
- Gaillou, E., Delaunay, A., Rondeau, B., Bouhnik-le-Coz, M., Fritsch, E., Cornen, G. and Monnier, C. (2008). The geochemistry of gem opals as evidence of their origin. Ore Geology Reviews 34(1–2): 113-126.

- Gaillou, E., Fritsch, E., Aguilar – Reyes, B., Rondeau, B., Post, J. and Barreau, A. (2008). Common gem opal : An investigation of micro to nano structure. American Mineralogist 93: 1865 - 1873.
- Hannay, J. B. (1877). Examination of the Hydrous Constituent in Minerals. Mineralogist Magazine 1: 106-109.
- Horton, D. (2004). Australian Sedimentary Opal-Why is Australia unique? Opal horizon limited.
- Ilieva, A., Mihailova, B., Tsintsov, Z. and Petrov, O. (2007). Structural state of microcrystalline opals: A Raman spectroscopic study. American Mineralogist 92: 1325-1333.
- Johnson, M. L., Kammerling, R. C., Deghionno, D. G. and Koivula, J. I. (1996). Opal from Shewa province. Gems & Gemology 32(2): 112-120.
- Jones, J. B., Sanders, J. V. and Segnite, E. R. (1964). The structure of opal. Nature 4962: 991.
- Kammerling, R. C., Koivula, J. I. and Fritsch, E. (1996). Gem news: Updated on opal from Ethiopia. Gems & Gemology 31(2): 132.
- Koivula, J. I., Kammerling, R. C. and Fritsch, E. (1994a). Gem News: Opal from Ethiopia. Gems & Gemology 30(1): 52-53.
- Lacroix, A. (1992). Minéralogie de Madagascar 1: 269-273.
- Lee, D. R. (2007). Characterisation and the diagenetic transformation of non and micro-crystalline silica minerals. Department of Earth and Ocean Sciences, University of Liverpool, 4 Brownlow Street, Liverpool L69 3GP, UK.
- Merla, G., Abbate, E., Canuti, P., Sagri, M. and Tacconi, P. (1973). Geological Map of Ethiopia and Somalia, 1:2,000,000., Consiglio Nazionale delle Ricerche Italy.
- Nasa. (2015). Geography of Sudan. from [http://en.wikipedia.org/wiki/Geography\\_of\\_Sudan](http://en.wikipedia.org/wiki/Geography_of_Sudan).
- Ralph, J. (2008). Yowah opal field, Paroo shire, Queensland, Australia. from <http://www.mindat.org/photo-196838.html>.
- Rondeau, B., Fritsch, E., Mazzero, F., Gauthier, J., Cenki-Tok, B., Bekele, E. and Gaillou, E. (2010). Play of color opal from Wegel Tena, Wollo Province, Ethiopia. Gems & Gemology 46(2): 90 – 105.

- Schlüter, T. (2006). Geological atlas of Africa. Kenya, UNESCO Nairobi Office.
- Segnite, E. R., Stevens, T. J. and Jones, J. B. (1965). The role of water in opal. Journal of the Geological Society of Australia: An International Geoscience Journal of the Geological Society of Australia.
- Simoni, M., Caucia, F., Adamo, I. and Galinetto, P. (2010). New occurrence of fire opal from Bemia, Madagascar. Gems & Gemology 46(2): 114-121.
- Smallwood, A. G., Thomas, P. S. and Ray, A. S. (1997). Characterisation of sedimentary opals by Fourier transform raman spectroscopy. Spectrochimica Acta Part A 53: 2341 - 2345.
- Smallwood, A. G., Thomas, P. S. and Ray, A. S. (2008). Comparative analysis of sedimentary and volcanic precious opals from Australia. Journal of Australian ceramic society 44(2): 17-22.
- Tariaferro, N. L. (1935). Some Properties of Opal. American Journal Science Series 5(30): 450-474.
- Thomas, P. S. (2008). The Colloidal Chemistry and Materials Properties of Opal. The Materials Chemistry of Opal: 1-26.
- Toaree, S. (2011). Characteristics of annealed opal from Brazil and Sudan. Bachelor Degree, Burapha University.
- Ward, F. (2003). Opals. Opalgraphics: 1.
- Zhuravlev, L. T. (2000). The surface chemistry of amorphous silica. Zhuravlev model. Colloids and surfaces(173): 1-38.



APPENDIX

จุฬาลงกรณ์มหาวิทยาลัย  
CHULALONGKORN UNIVERSITY



The logo of Chulalongkorn University is a large, faint watermark in the center of the page. It features a central figure, likely a royal emblem, surrounded by a sunburst or radiating lines. Below the figure, the university's name is written in Thai script and English.

## APPENDIX A

Table A.1 Showing the gemological properties of Ethiopian precious opal, Malagasy white fire opal and Malagasy orange fire opal before heating, boiling and oiling

Table A.2 Showing the gemological properties of Ethiopian precious opal, Malagasy white fire opal and Malagasy orange fire opal after heating, boiling and oiling

Table A.1 Showing the gemological properties of opal before heating, boiling and oiling.

Sample no.	Enhancement experiments	S.G.	R.I.	Fluorescence	
				SWUV	LWUV
Precious opal					
A1	heating	1.95	1.42	inert	inert
A2	heating	1.96	1.42	inert	inert
A3	heating	1.96	1.45	inert	inert
A4	heating	1.91	1.44	inert	inert
A5	heating	1.93	1.44	inert	inert
A6	heating	1.92	1.42	inert	inert
A7	heating	1.93	1.44	inert	inert
A8	heating	1.97	1.46	inert	inert
A9	heating	1.91	1.45	inert	inert
A10	heating	1.94	1.43	inert	inert
A11	boiling	1.88	1.43	inert	inert
A12	boiling	1.96	1.43	inert	inert
A13	boiling	1.88	1.42	inert	inert
A14	boiling	1.89	1.42	inert	inert
A15	boiling	1.97	1.45	inert	inert
A16	boiling	1.95	1.45	inert	inert
A17	boiling	1.85	1.44	inert	inert
A18	boiling	1.94	1.44	inert	inert
A19	boiling	1.91	1.43	inert	inert
A20	boiling	1.87	1.42	inert	inert
A21	oiling	1.89	1.42	inert	inert
A22	oiling	1.86	1.42	inert	inert
A23	oiling	1.91	1.44	inert	inert
A24	oiling	1.91	1.41	inert	inert
A25	oiling	1.91	1.44	inert	inert
A26	oiling	1.96	1.44	inert	inert
A27	oiling	1.92	1.44	inert	inert
A28	oiling	1.91	1.45	inert	inert
A29	oiling	1.90	1.43	inert	inert
A30	oiling	1.94	1.44	inert	inert

Table A.1 Showing the gemological properties of opal before heating, boiling and oiling (continued).

Sample no.	Enhancement experiments	S.G.	R.I.	Fluorescence	
				SWUV	LWUV
Fire opal (white)					
B1	heating	2.08	1.44	inert	inert
B2	heating	2.18	1.44	inert	inert
B3	heating	2.03	1.44	inert	inert
B4	heating	2.10	1.44	inert	inert
B5	heating	2.07	1.44	inert	inert
B6	heating	2.11	1.44	inert	inert
B7	heating	2.19	1.44	inert	inert
B8	heating	2.05	1.45	inert	inert
B9	heating	2.03	1.43	inert	inert
B10	heating	2.03	1.44	inert	inert
B11	boiling	2.10	1.43	inert	inert
B12	boiling	2.04	1.43	inert	inert
B13	boiling	2.03	1.43	inert	inert
B14	boiling	2.09	1.43	inert	inert
B15	boiling	2.17	1.44	inert	inert
B16	boiling	2.16	1.44	inert	inert
B17	boiling	2.16	1.45	inert	inert
B18	boiling	2.14	1.44	inert	inert
B19	boiling	2.13	1.44	inert	inert
B20	boiling	2.16	1.44	inert	inert
B21	oiling	2.04	1.43	inert	inert
B22	oiling	2.02	1.44	inert	inert
B23	oiling	2.04	1.43	inert	inert
B24	oiling	2.02	1.42	inert	inert
B25	oiling	2.12	1.44	inert	inert
B26	oiling	2.16	1.45	inert	inert
B27	oiling	2.18	1.45	inert	inert
B28	oiling	2.16	1.44	inert	inert
B29	oiling	2.16	1.44	inert	inert
B30	oiling	2.12	1.44	inert	inert

Table A.1 Showing the gemological properties of opal before heating, boiling and oiling (continued).

Sample no.	Enhancement experiments	S.G.	R.I.	Fluorescence	
				SWUV	LWUV
Fire opal (orange)					
C1	heating	2.14	1.46	inert	inert
C2	heating	2.10	1.44	inert	inert
C3	heating	2.13	1.46	inert	inert
C4	heating	2.20	1.45	inert	inert
C5	heating	2.17	1.45	inert	inert
C6	heating	2.17	1.44	inert	inert
C7	heating	2.13	1.45	inert	inert
C8	heating	2.13	1.44	inert	inert
C9	heating	2.17	1.46	inert	inert
C10	heating	2.09	1.44	inert	inert
C11	boiling	2.20	1.45	inert	inert
C12	boiling	2.12	1.45	inert	inert
C13	boiling	2.08	1.45	inert	inert
C14	boiling	2.10	1.45	inert	inert
C15	boiling	2.18	1.45	inert	inert
C16	boiling	2.13	1.46	inert	inert
C17	boiling	2.12	1.43	inert	inert
C18	boiling	2.15	1.44	inert	inert
C19	boiling	2.12	1.44	inert	inert
C20	boiling	2.11	1.43	inert	inert
C21	oiling	2.17	1.46	inert	inert
C22	oiling	2.17	1.46	inert	inert
C23	oiling	2.17	1.46	inert	inert
C24	oiling	2.12	1.45	inert	inert
C25	oiling	2.14	1.46	inert	inert
C26	oiling	2.15	1.47	inert	inert
C27	oiling	2.11	1.45	inert	inert
C28	oiling	2.17	1.44	inert	inert
C29	oiling	2.10	1.44	inert	inert
C30	oiling	2.15	1.43	inert	inert

Table A.2 Showing the gemological properties of opal after heating, boiling and oiling (continued).

Sample no.	Enhancement experiments	S.G.	R.I.	Fluorescence	
				SWUV	LWUV
Precious opal					
A1	heating	1.84	1.42	inert	inert
A2	heating	1.87	1.42	inert	inert
A3	heating	1.85	1.40	inert	inert
A4	heating	1.77	1.39	inert	inert
A5	heating	1.85	1.43	inert	inert
A6	heating	1.82	1.42	inert	inert
A7	heating	1.81	1.42	inert	inert
A8	heating	1.86	1.41	inert	inert
A9	heating	1.72	1.42	inert	inert
A10	heating	1.76	1.42	inert	inert
A11	boiling	1.77	1.42	inert	inert
A12	boiling	1.94	1.43	inert	inert
A13	boiling	1.83	1.41	inert	inert
A14	boiling	1.86	1.42	inert	inert
A15	boiling	1.90	1.42	inert	inert
A16	boiling	1.91	1.42	inert	inert
A17	boiling	1.80	1.42	inert	inert
A18	boiling	1.88	1.41	inert	inert
A19	boiling	1.72	1.41	inert	inert
A20	boiling	1.75	1.39	inert	inert
A21	oiling	1.85	1.46	inert	inert
A22	oiling	1.80	1.47	inert	inert
A23	oiling	1.87	1.47	inert	inert
A24	oiling	1.81	1.46	inert	inert
A25	oiling	1.86	1.47	inert	inert
A26	oiling	1.89	1.47	inert	inert
A27	oiling	1.90	1.46	inert	inert
A28	oiling	1.85	1.46	inert	inert
A29	oiling	1.85	1.47	inert	inert
A30	oiling	1.93	1.46	inert	inert

Table A.2 Showing the gemological properties of opal after heating, boiling and oiling (continued).

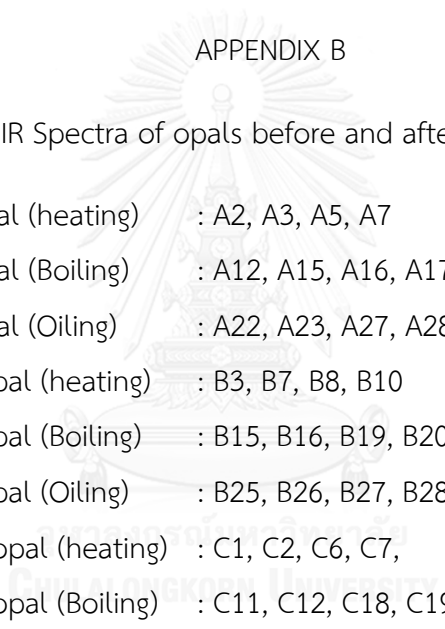
Sample no.	Enhancement experiments	S.G.	R.I.	Fluorescence	
				SWUV	LWUV
Fire opal (white)					
B1	heating	1.91	1.42	inert	inert
B2	heating	2.15	1.45	inert	inert
B3	heating	1.94	1.41	inert	inert
B4	heating	2.14	1.42	inert	inert
B5	heating	2.04	1.42	inert	inert
B6	heating	2.06	1.43	inert	inert
B7	heating	2.18	1.45	inert	inert
B8	heating	2.05	1.42	inert	inert
B9	heating	1.94	1.42	inert	inert
B10	heating	1.97	1.42	inert	inert
B11	boiling	2.16	1.47	inert	inert
B12	boiling	2.03	1.47	inert	inert
B13	boiling	2.01	1.43	inert	inert
B14	boiling	2.13	1.45	inert	inert
B15	boiling	2.18	1.45	inert	inert
B16	boiling	2.26	1.46	inert	inert
B17	boiling	2.18	1.46	inert	inert
B18	boiling	2.16	1.45	inert	inert
B19	boiling	2.07	1.46	inert	inert
B20	boiling	2.16	1.46	inert	inert
B21	oiling	2.03	1.44	inert	inert
B22	oiling	2.02	1.40	inert	inert
B23	oiling	2.03	1.41	inert	inert
B24	oiling	2.05	1.41	inert	inert
B25	oiling	2.11	1.44	inert	inert
B26	oiling	2.16	1.45	inert	inert
B27	oiling	2.03	1.40	inert	inert
B28	oiling	2.15	1.44	inert	inert
B29	oiling	2.16	1.44	inert	inert
B30	oiling	2.08	1.44	inert	inert

Table A.2 Showing the gemological properties of opal after heating, boiling and oiling (continued).

Sample no.	Enhancement experiments	S.G.	R.I.	Fluorescence	
				SWUV	LWUV
Fire opal (orange)					
C1	heating	2.18	1.44	inert	inert
C2	heating	2.12	1.43	inert	inert
C3	heating	2.08	1.44	inert	inert
C4	heating	2.13	1.45	inert	inert
C5	heating	2.10	1.45	inert	inert
C6	heating	2.19	1.44	inert	inert
C7	heating	2.12	1.44	inert	inert
C8	heating	2.01	1.44	inert	inert
C9	heating	2.15	1.45	inert	inert
C10	heating	2.11	1.43	inert	inert
C11	boiling	2.15	1.47	inert	inert
C12	boiling	2.18	1.46	inert	inert
C13	boiling	2.11	1.46	inert	inert
C14	boiling	2.10	1.46	inert	inert
C15	boiling	2.02	1.47	inert	inert
C16	boiling	2.14	1.46	inert	inert
C17	boiling	2.05	1.46	inert	inert
C18	boiling	2.10	1.46	inert	inert
C19	boiling	2.16	1.46	inert	inert
C20	boiling	2.07	1.45	inert	inert
C21	oiling	2.11	1.44	inert	inert
C22	oiling	2.13	1.44	inert	inert
C23	oiling	2.18	1.44	inert	inert
C24	oiling	2.13	1.44	inert	inert
C25	oiling	2.16	1.44	inert	inert
C26	oiling	2.15	1.44	inert	inert
C27	oiling	2.07	1.43	inert	inert
C28	oiling	2.19	1.44	inert	inert
C29	oiling	2.11	1.43	inert	inert
C30	oiling	2.19	1.43	inert	inert

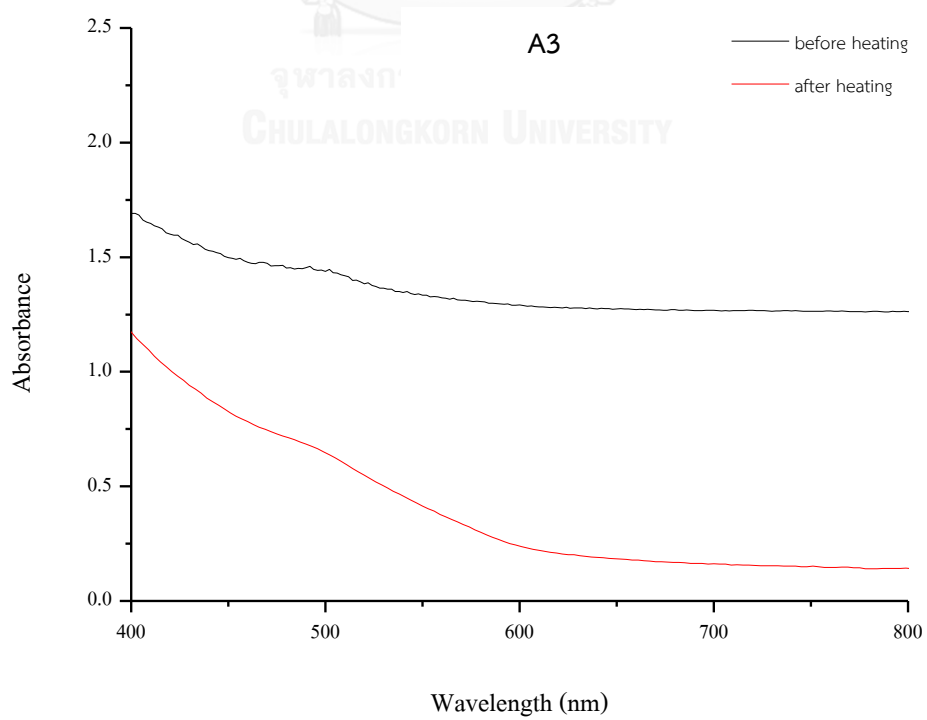
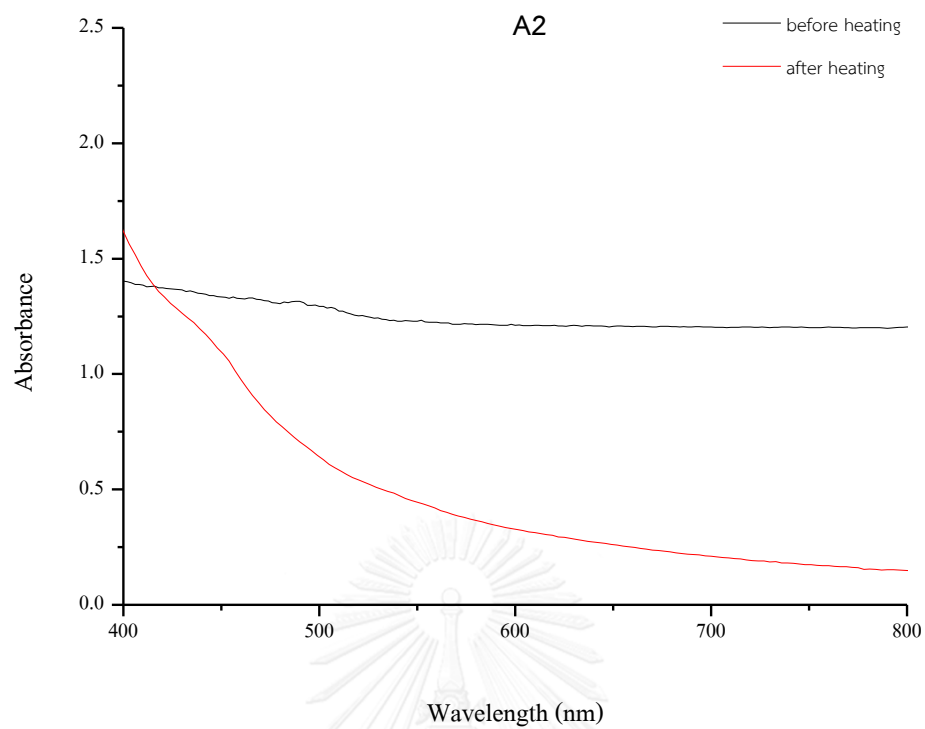
## APPENDIX B

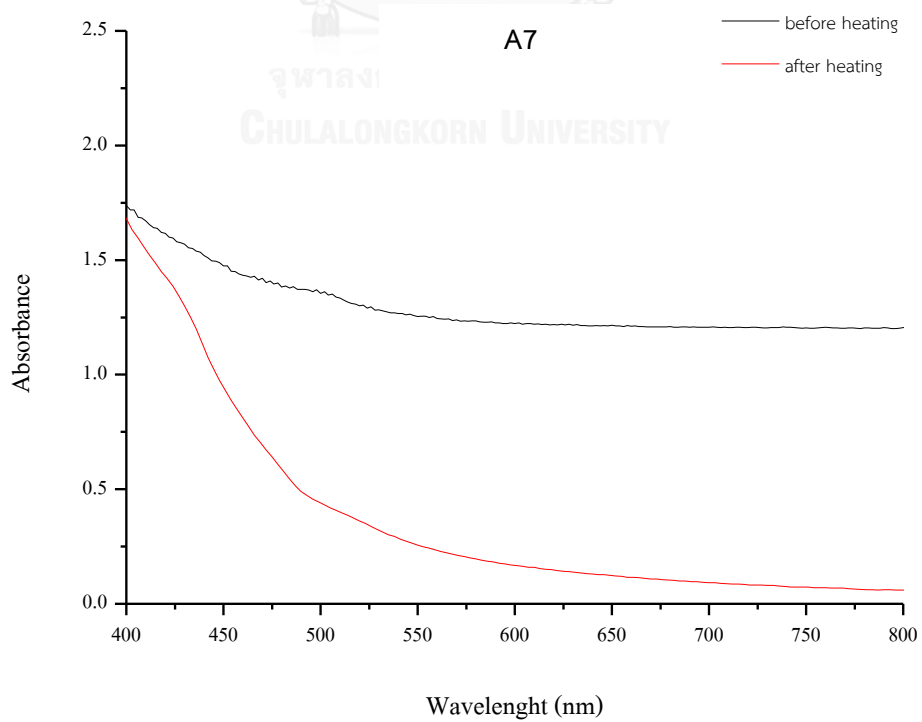
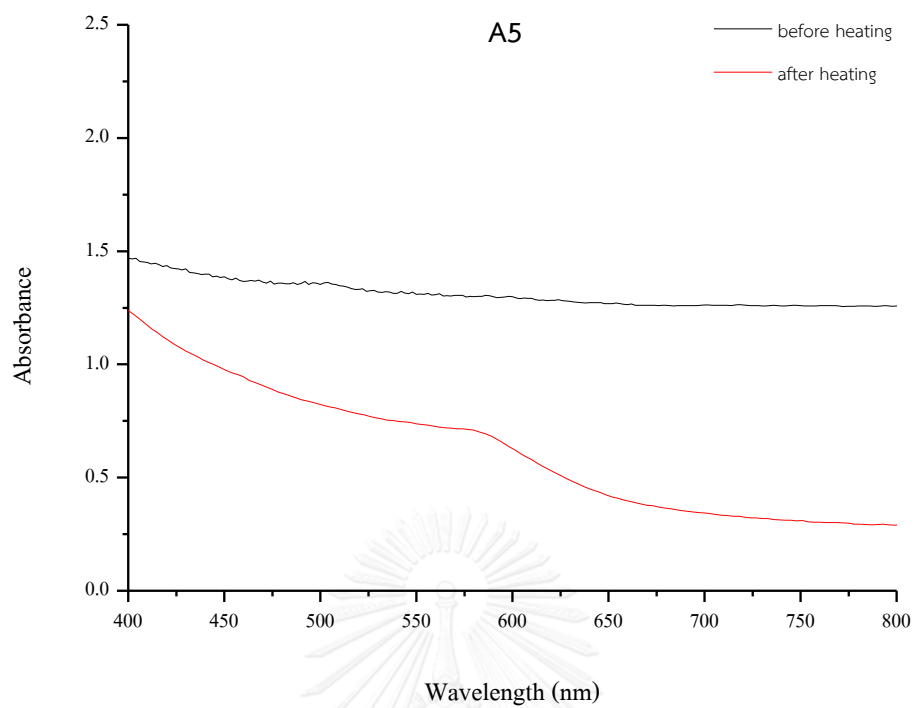
## UV-Vis-NIR Spectra of opals before and after enhancement

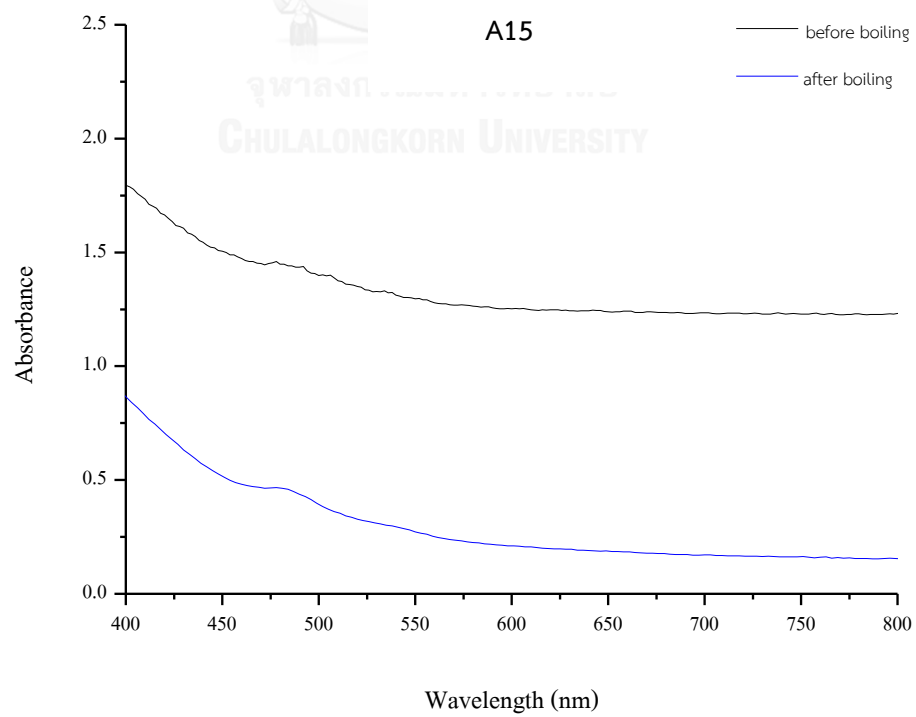
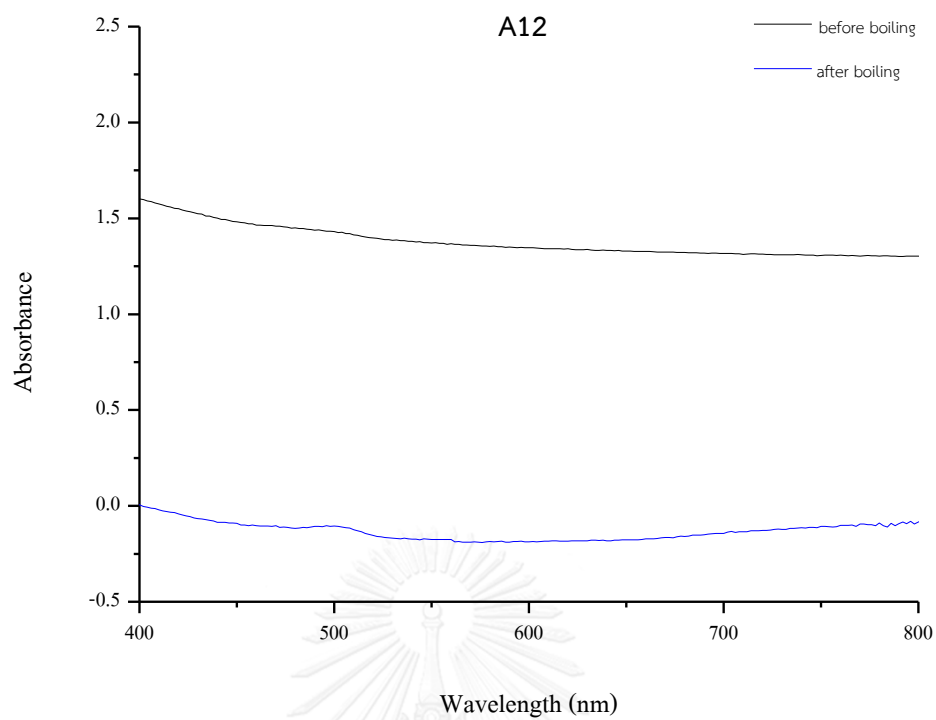


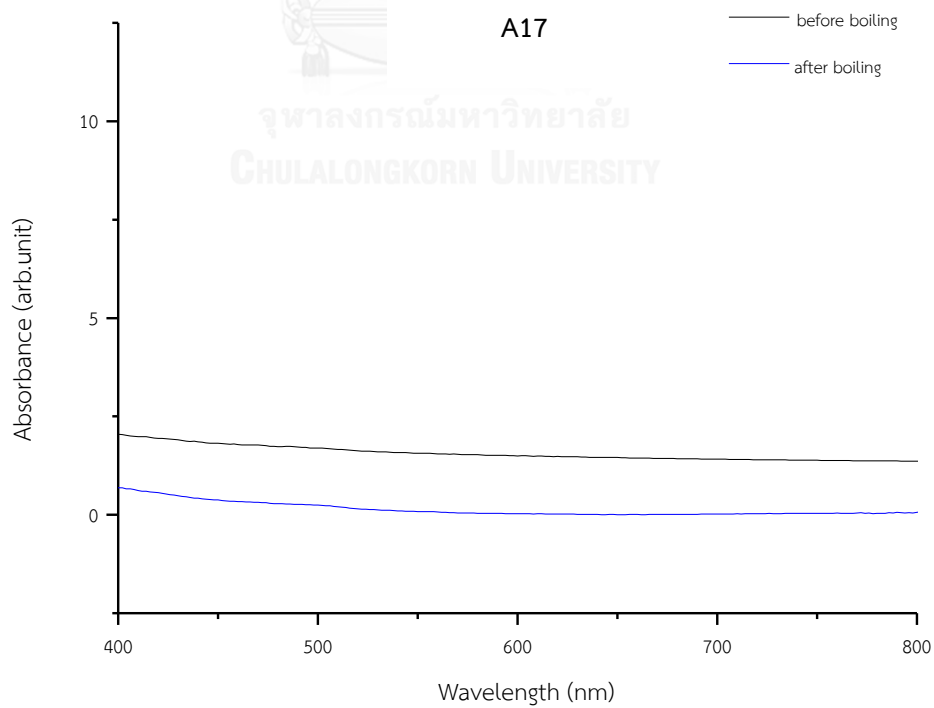
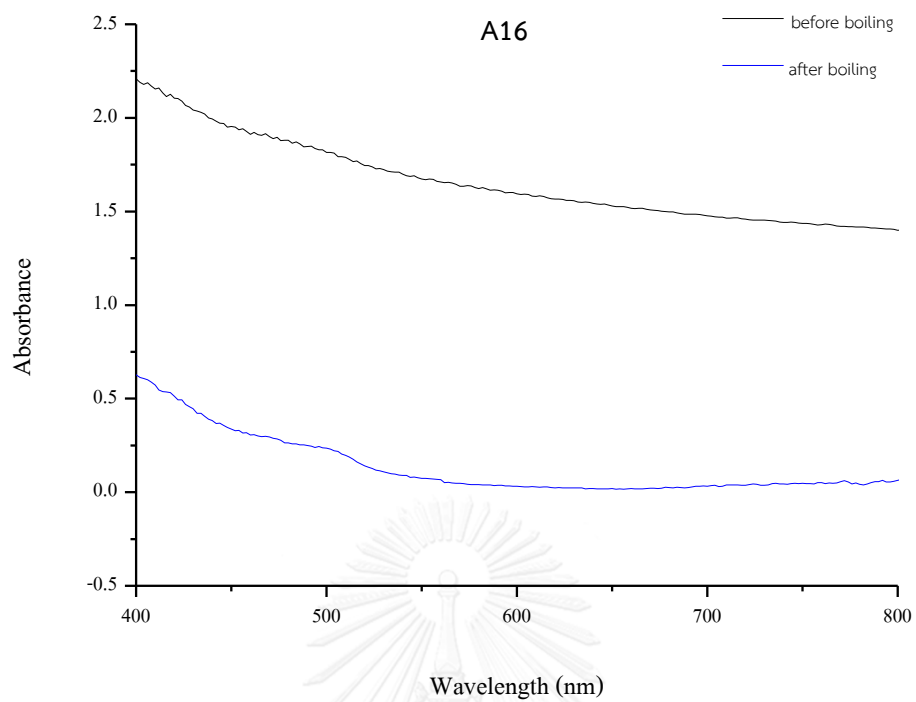
Ethiopian Precious opal (heating)	: A2, A3, A5, A7
Ethiopian Precious opal (Boiling)	: A12, A15, A16, A17
Ethiopian Precious opal (Oiling)	: A22, A23, A27, A28
Malagasy White fire opal (heating)	: B3, B7, B8, B10
Malagasy White fire opal (Boiling)	: B15, B16, B19, B20
Malagasy White fire opal (Oiling)	: B25, B26, B27, B28
Malagasy Orange fire opal (heating)	: C1, C2, C6, C7,
Malagasy Orange fire opal (Boiling)	: C11, C12, C18, C19
Malagasy Orange fire opal (Oiling)	: C21, C22, C23, C24

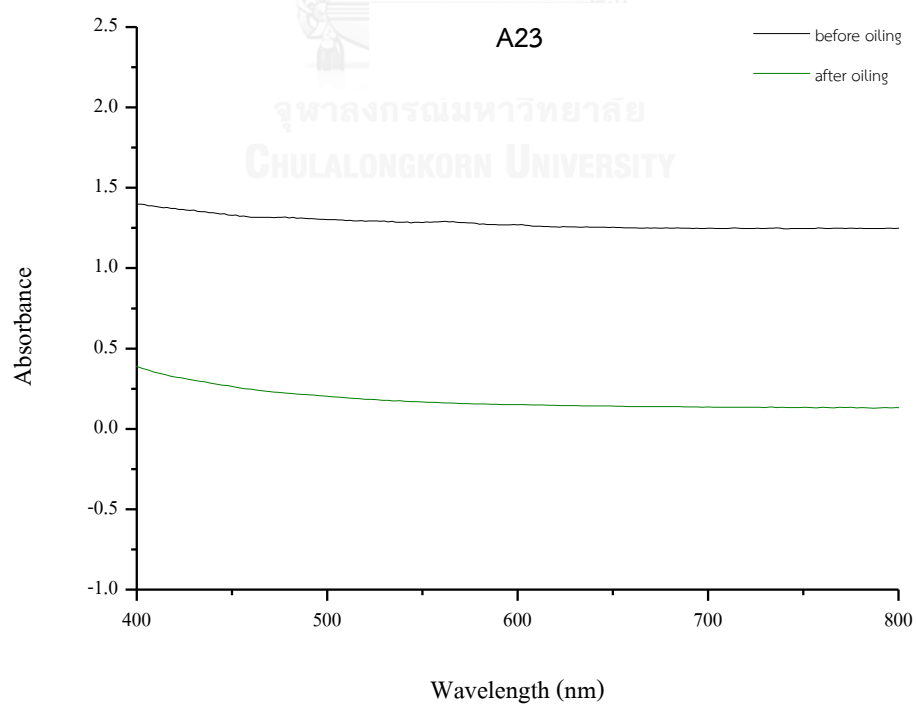
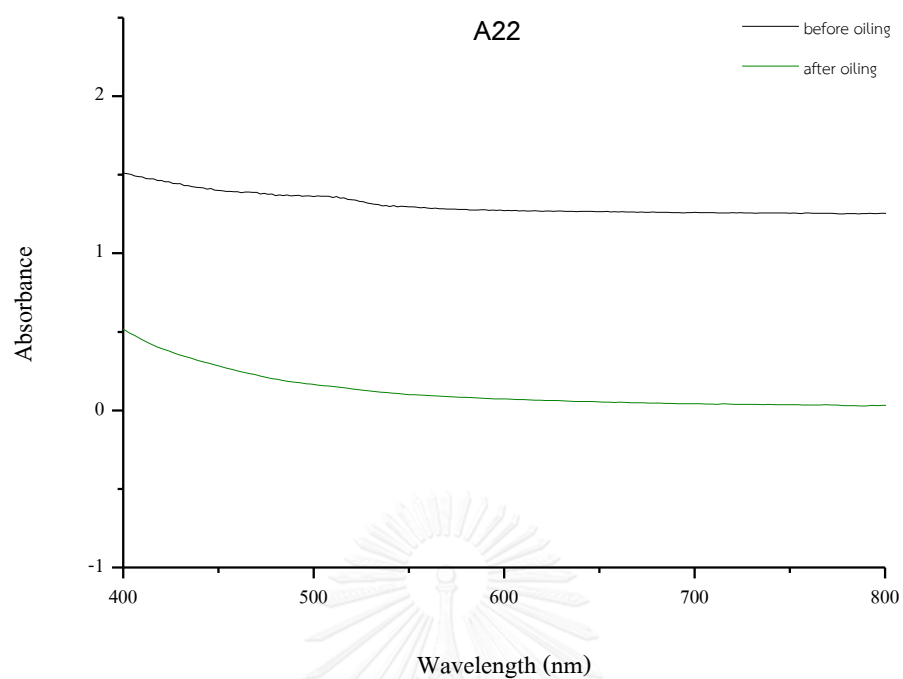


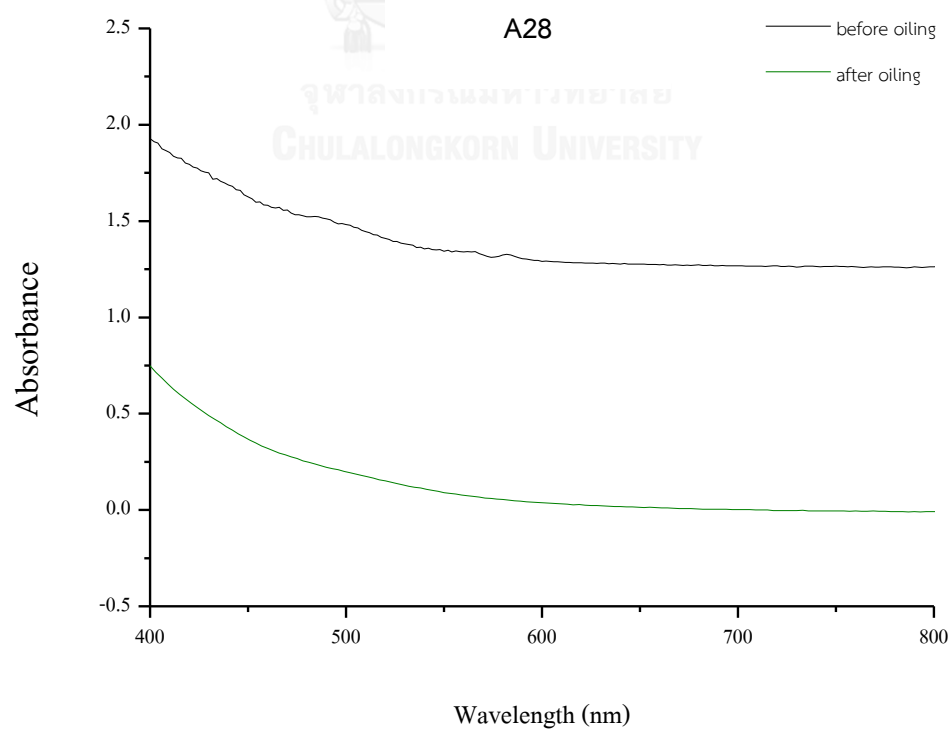
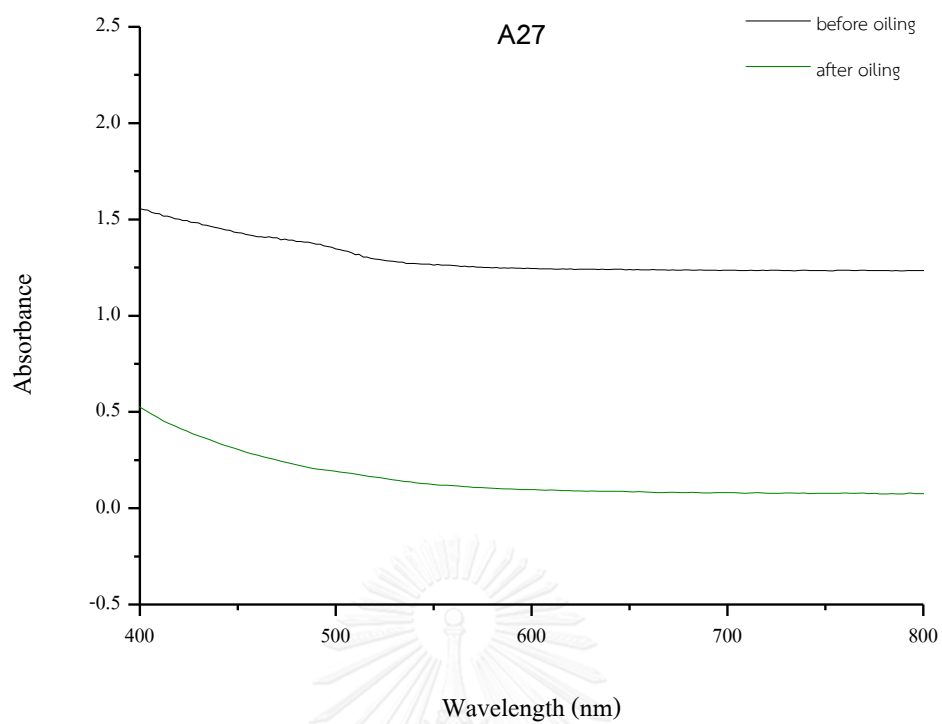


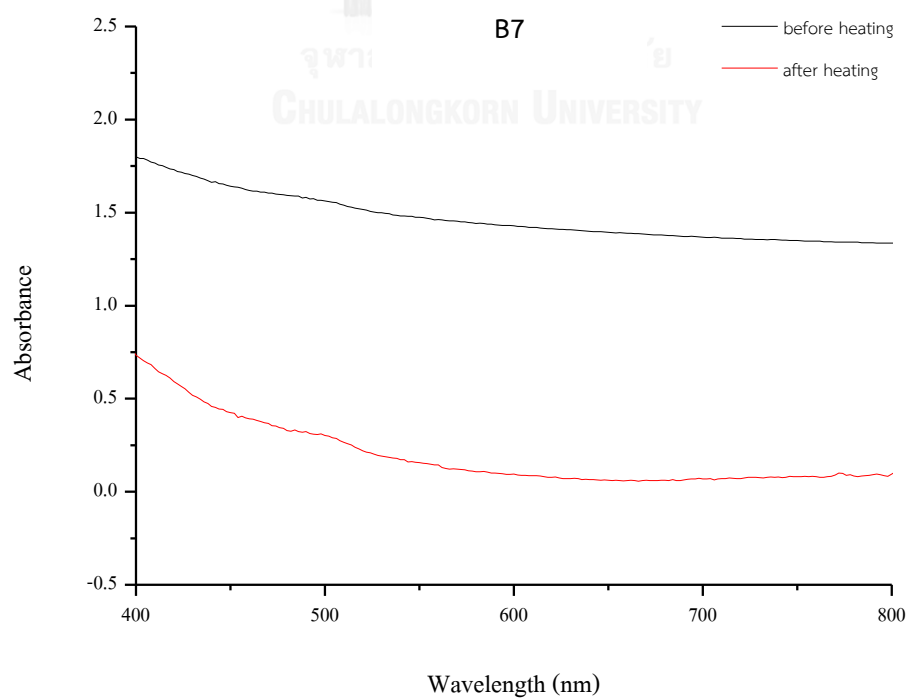
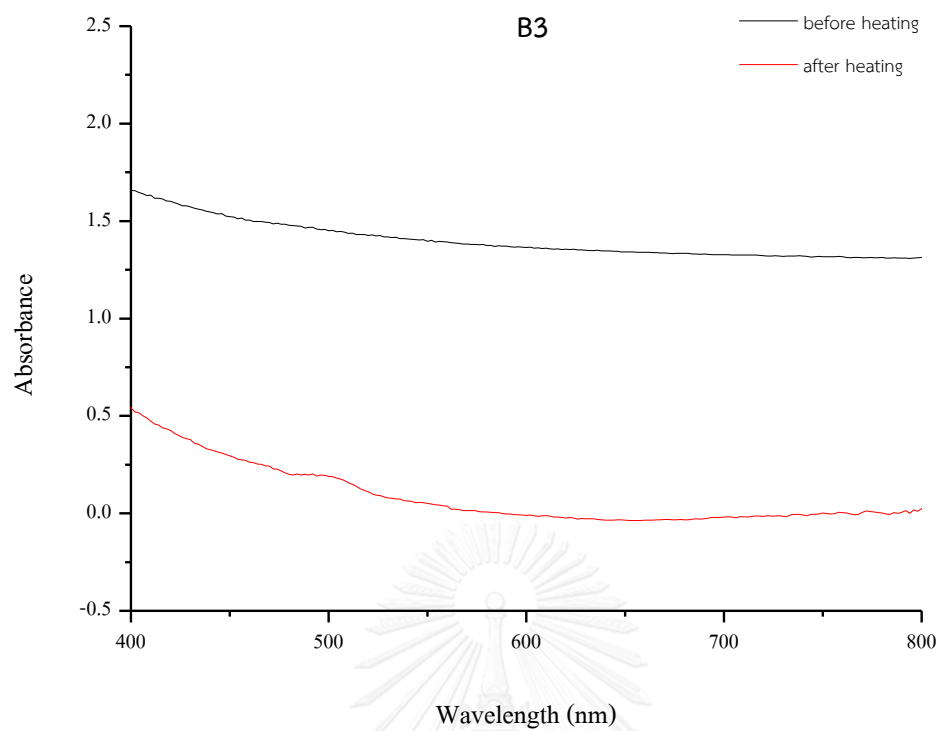


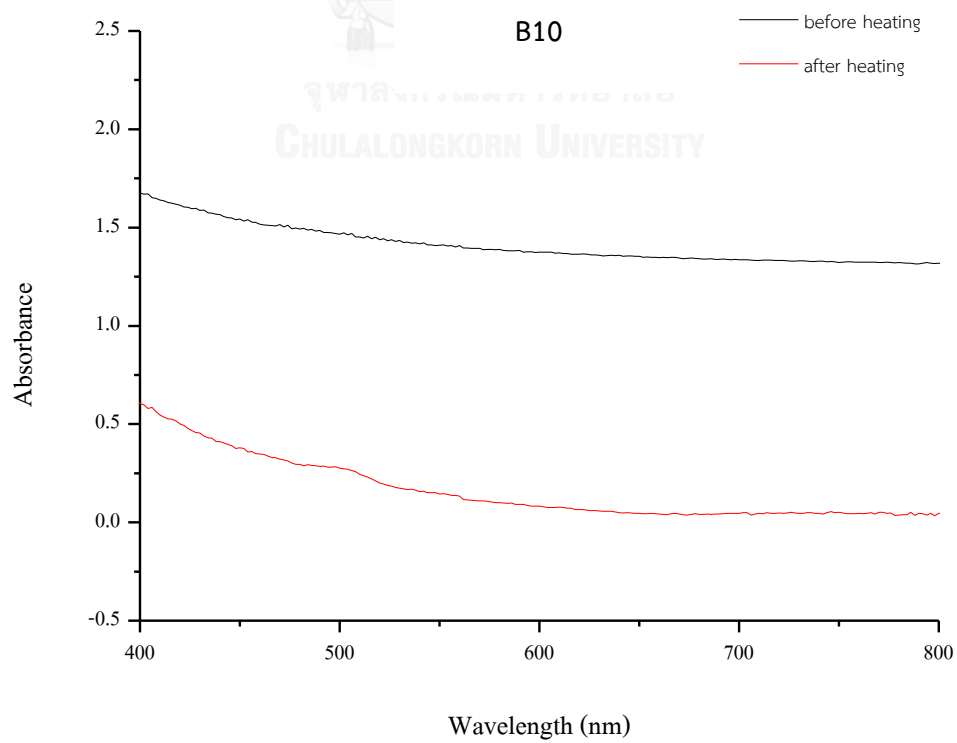
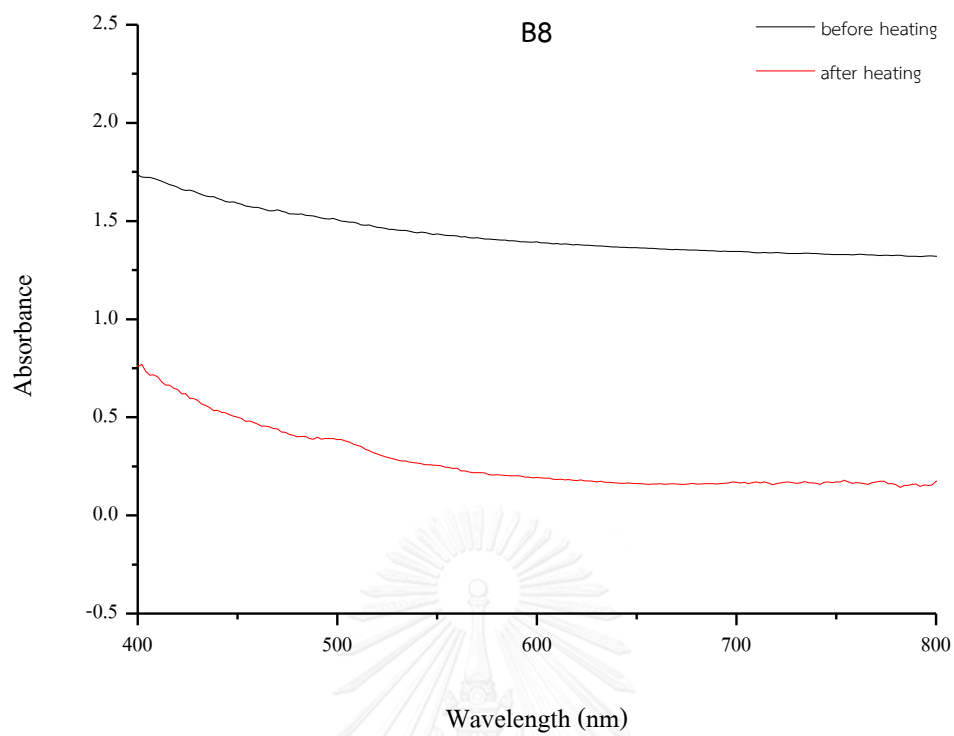




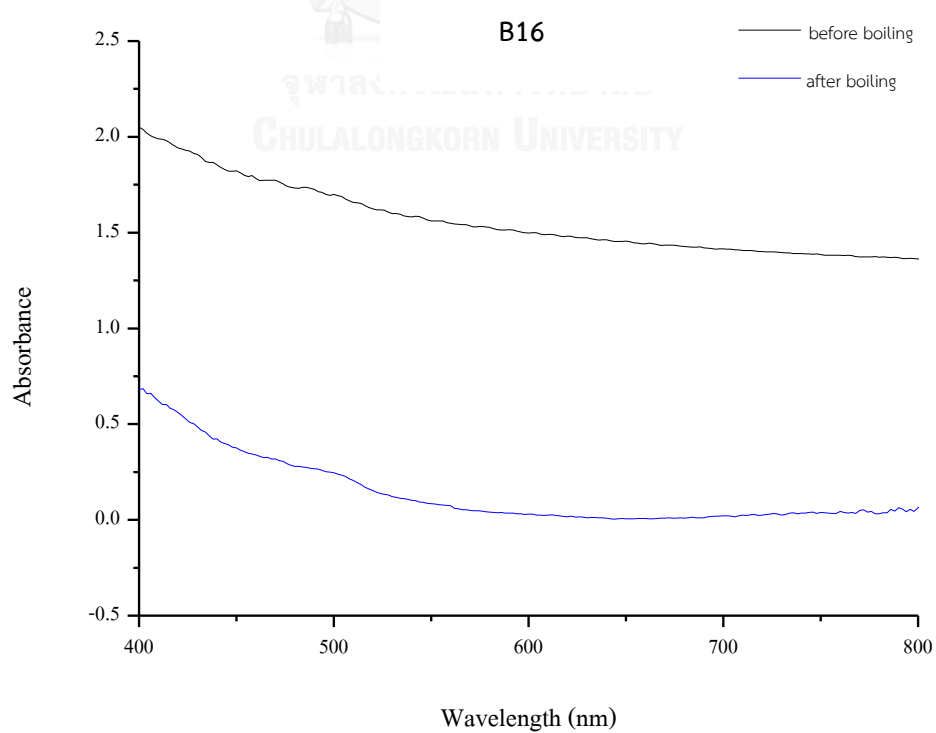
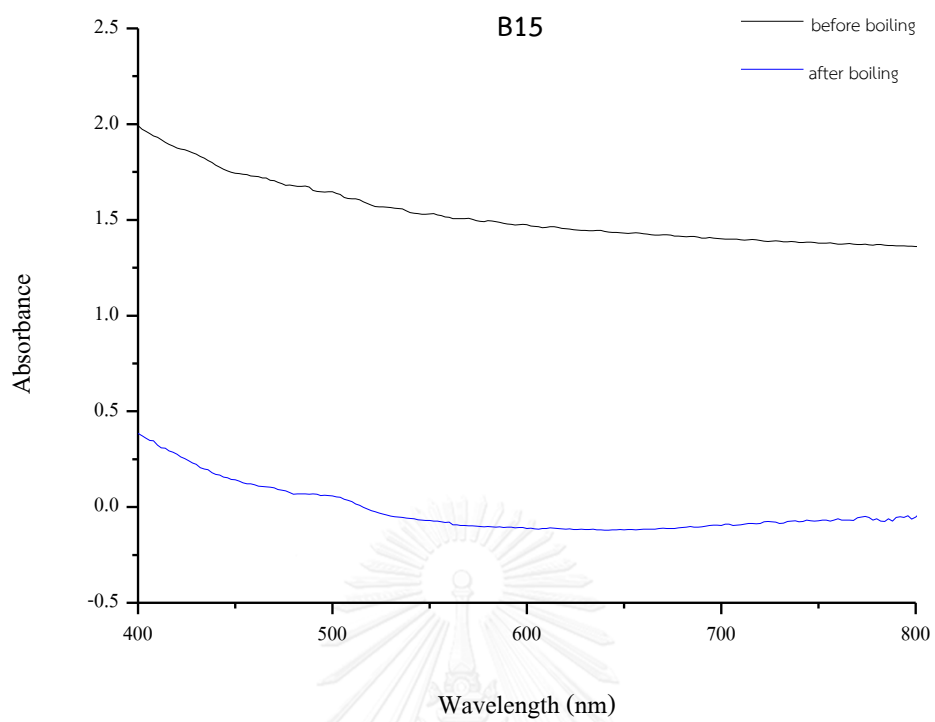


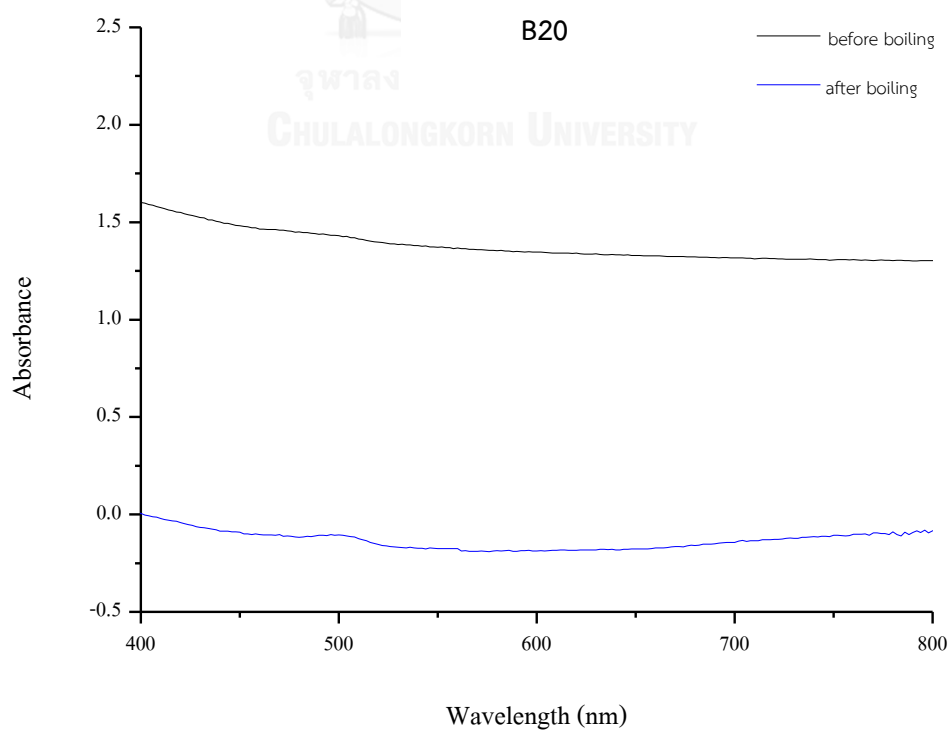
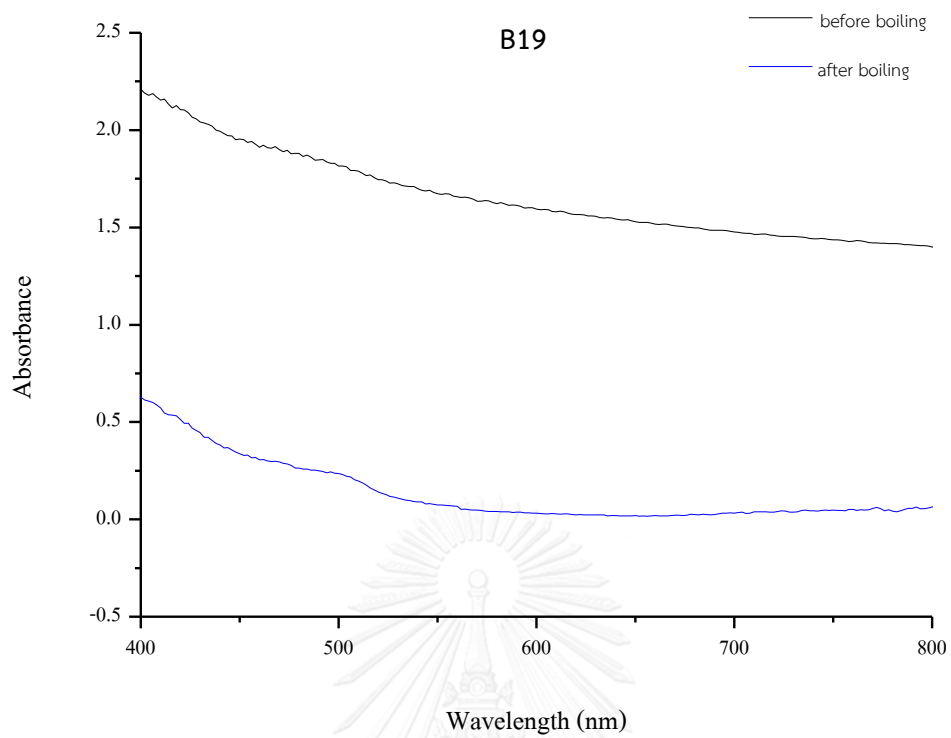


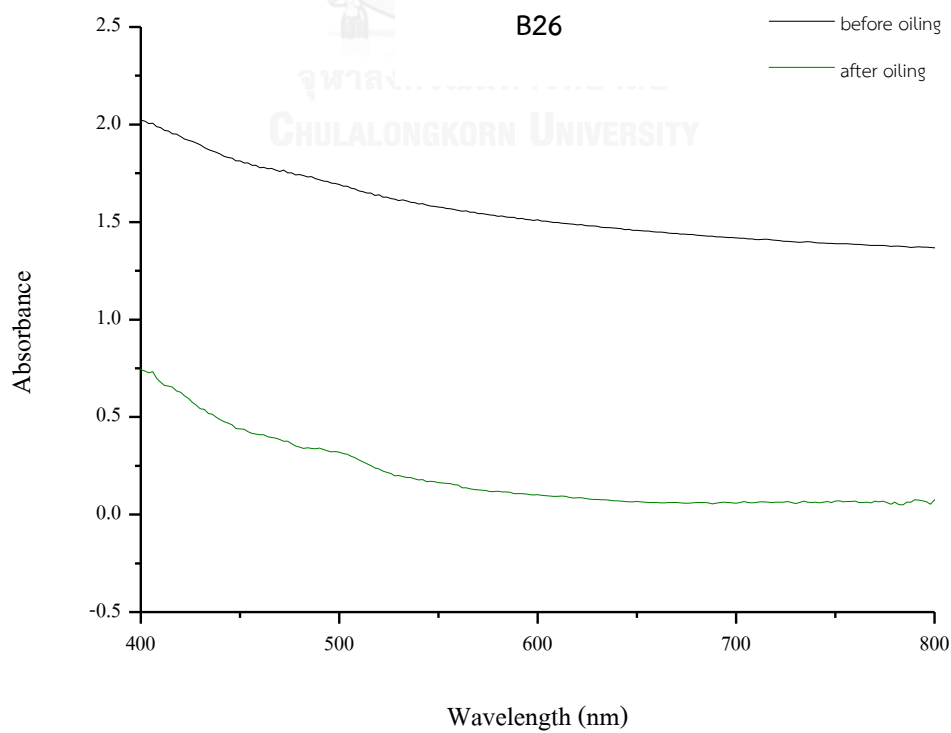
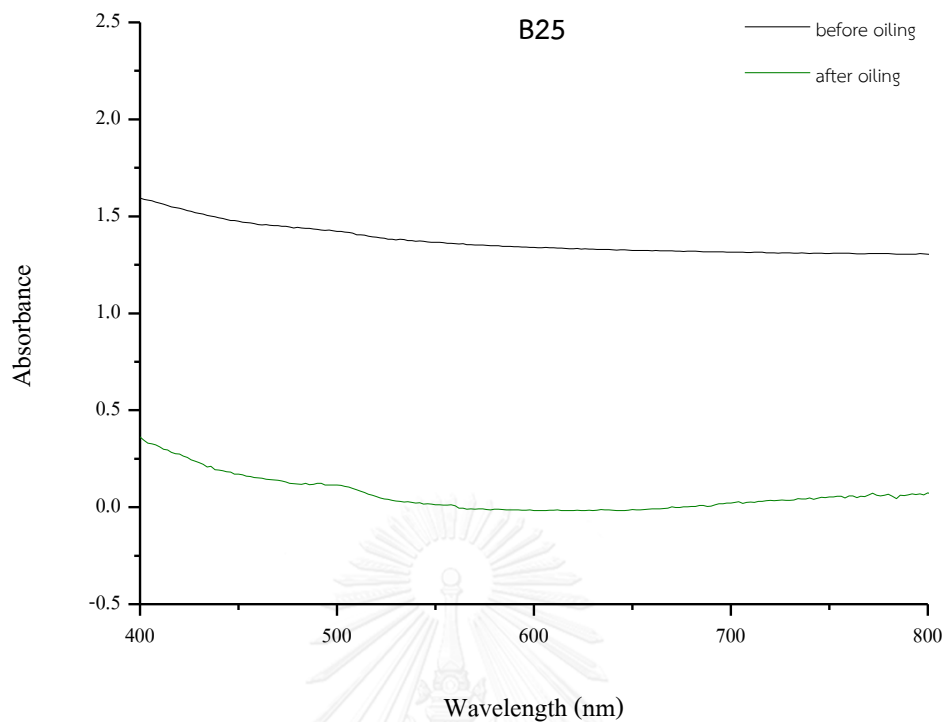


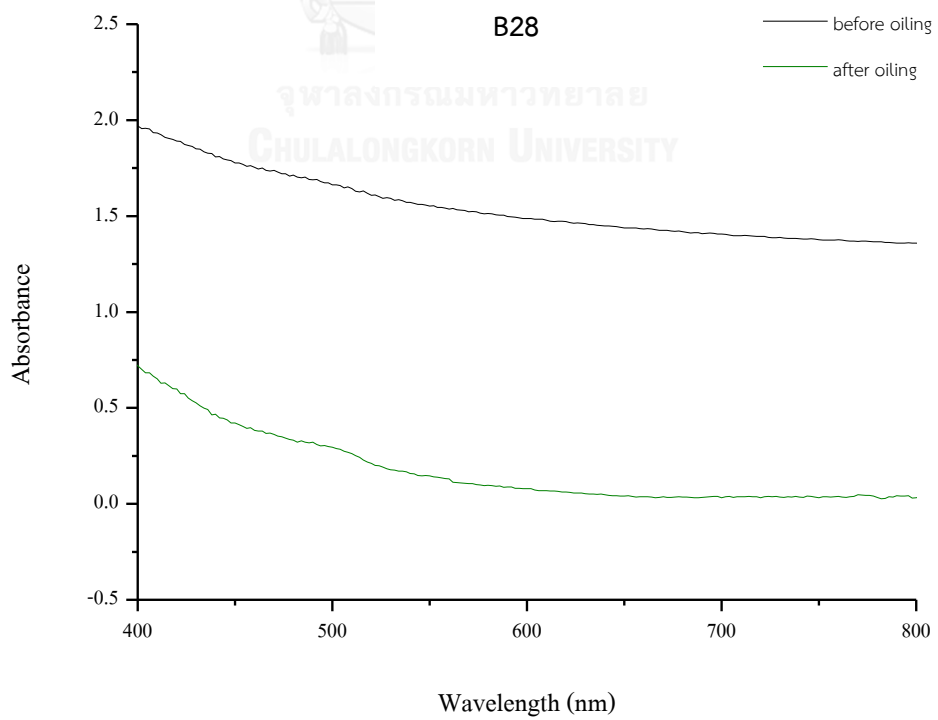
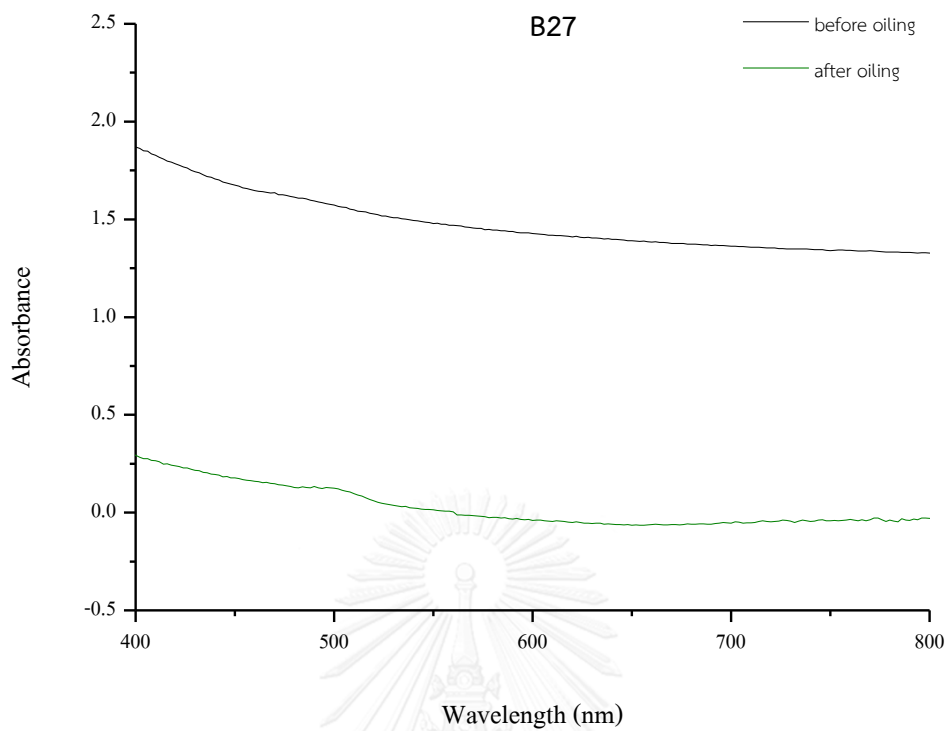


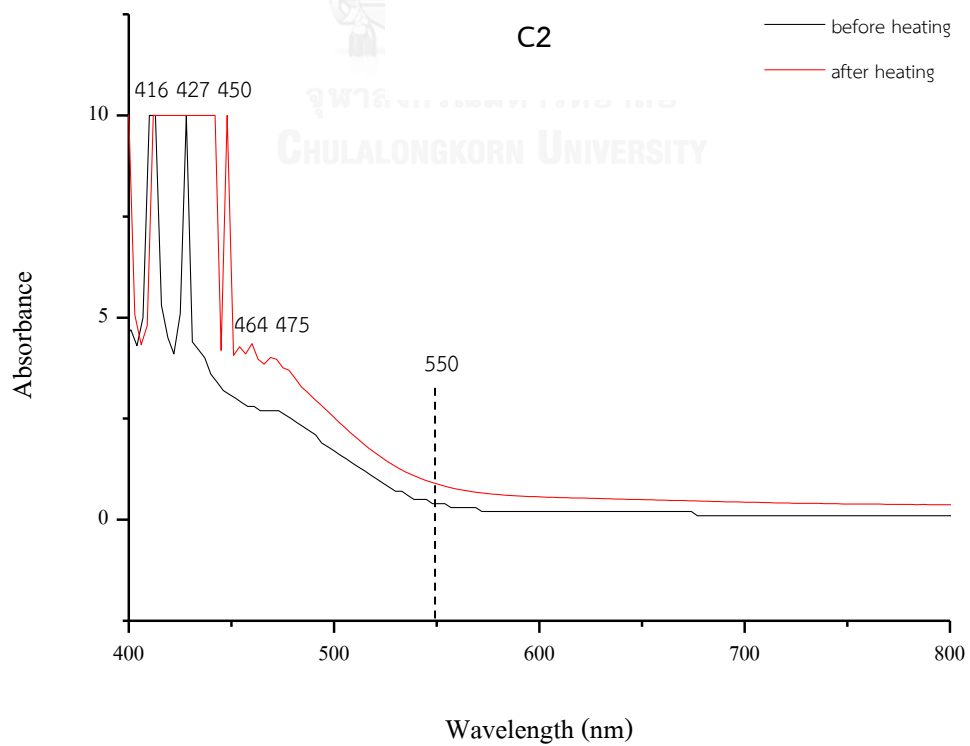
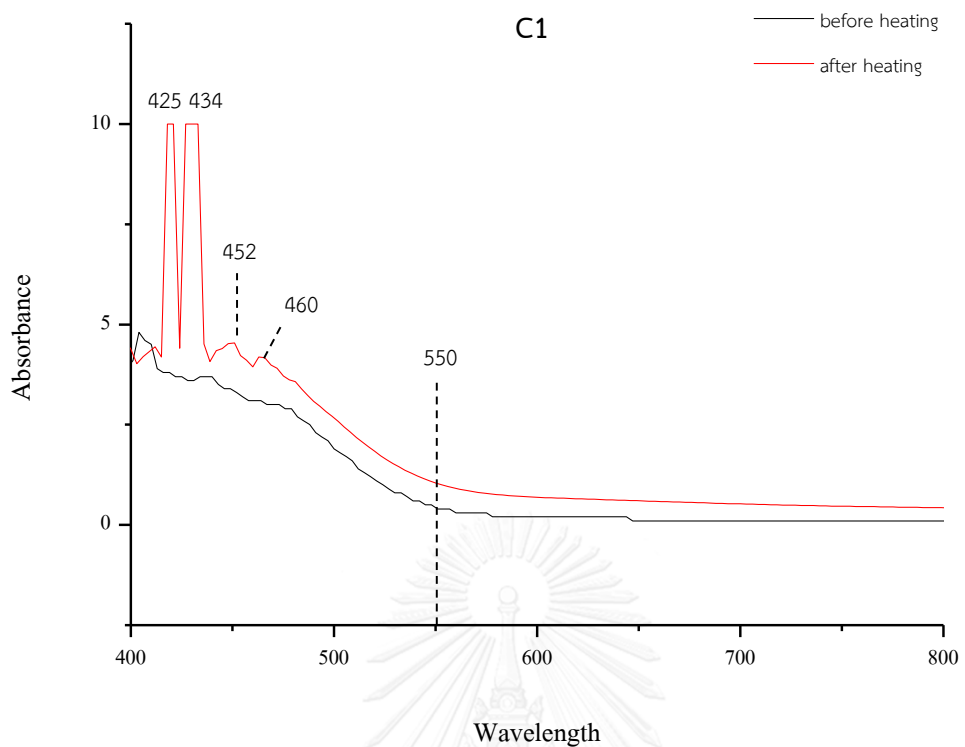


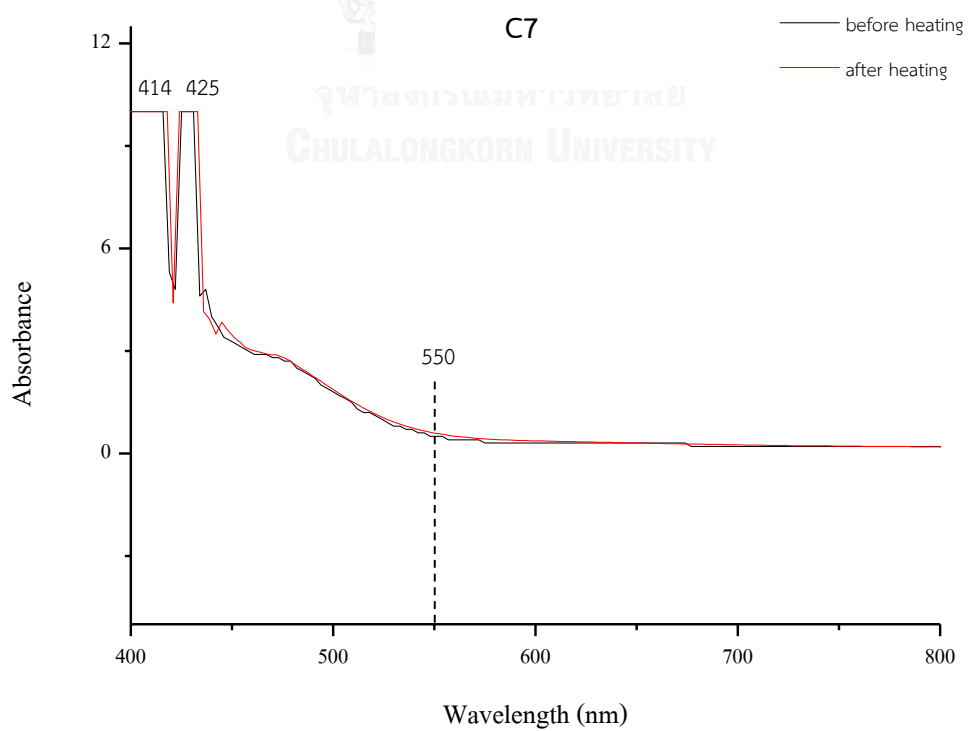
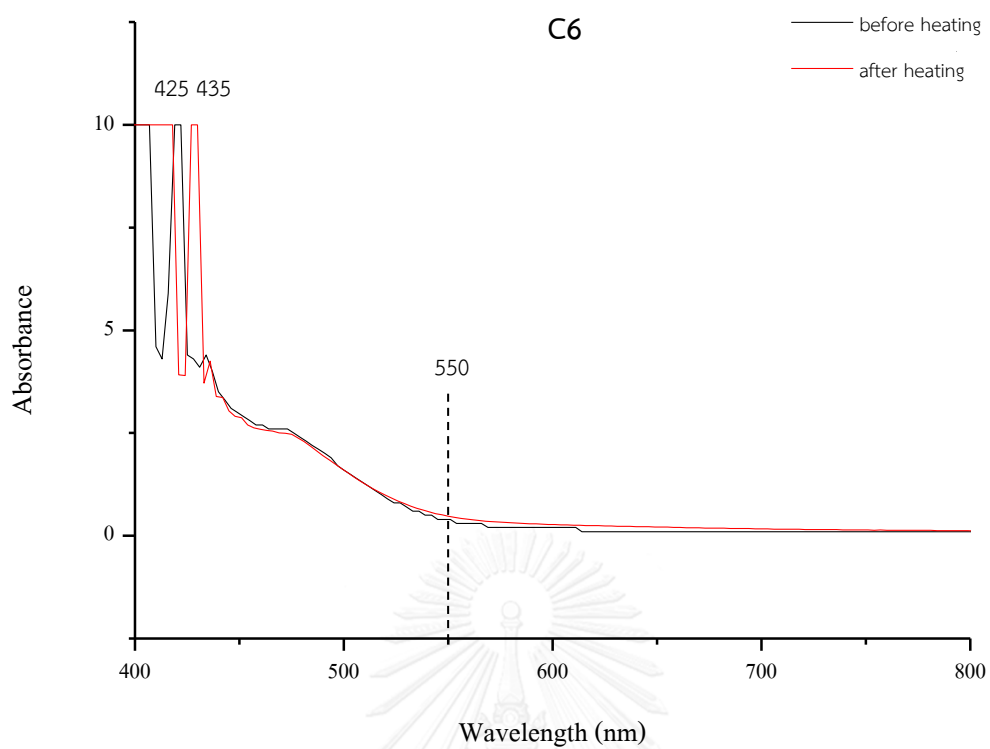


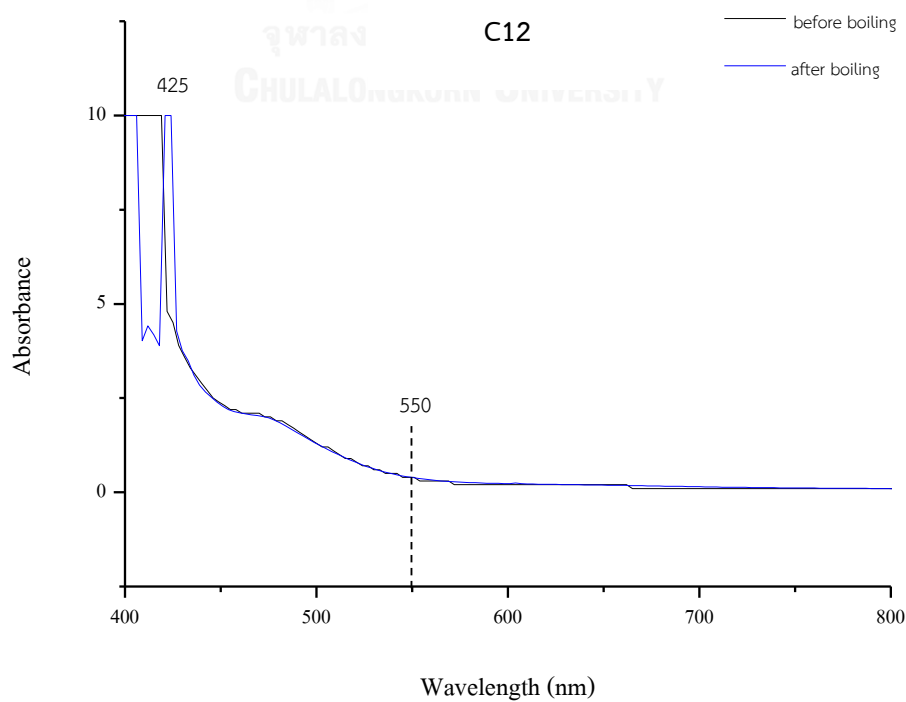
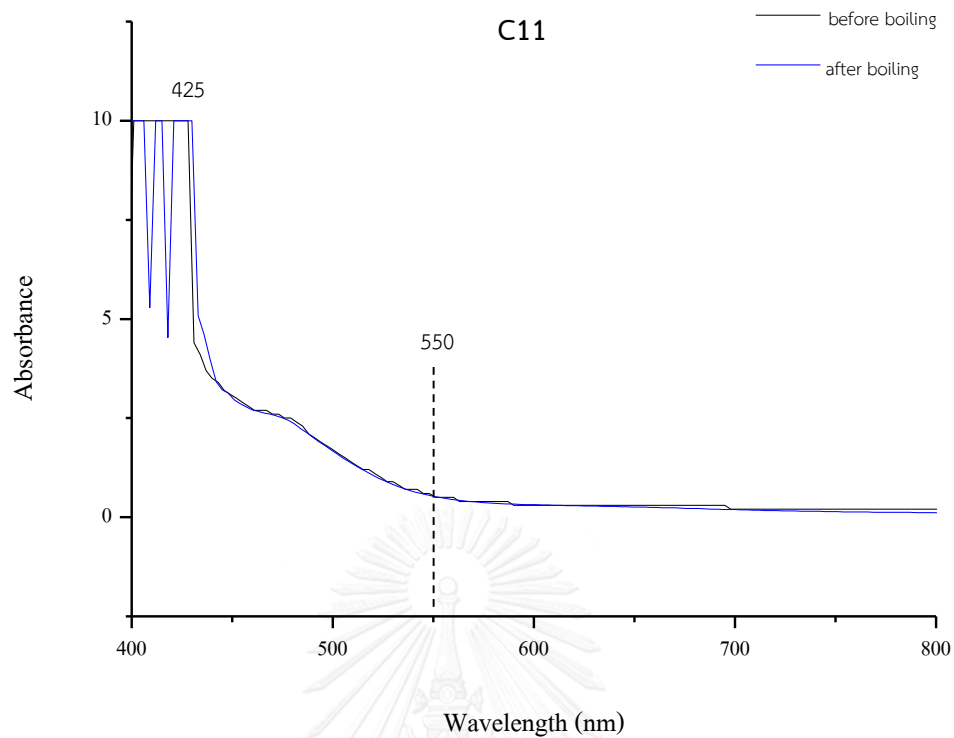


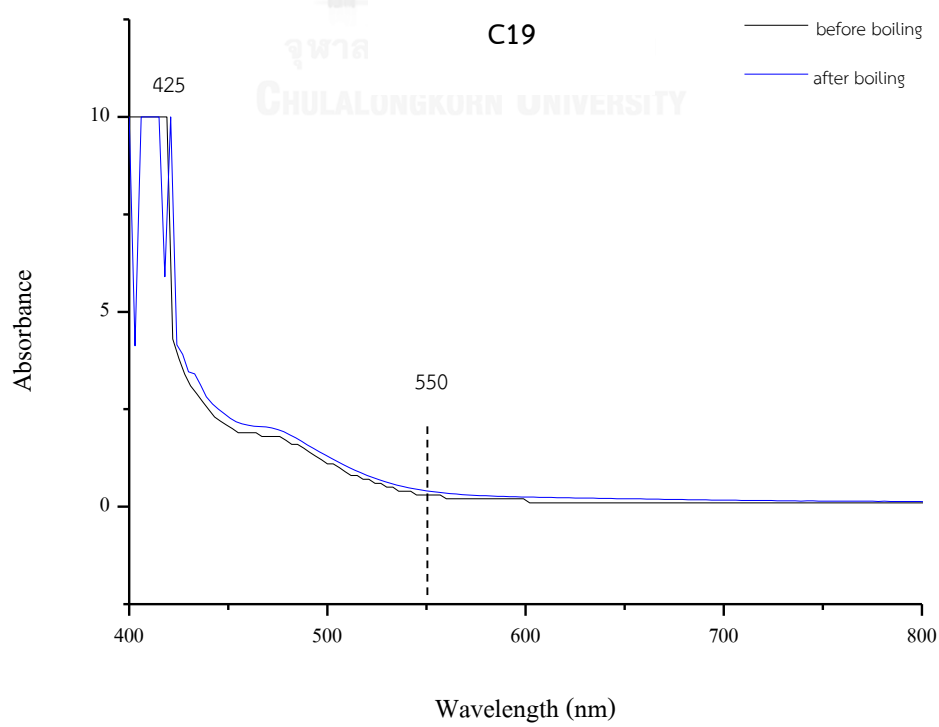
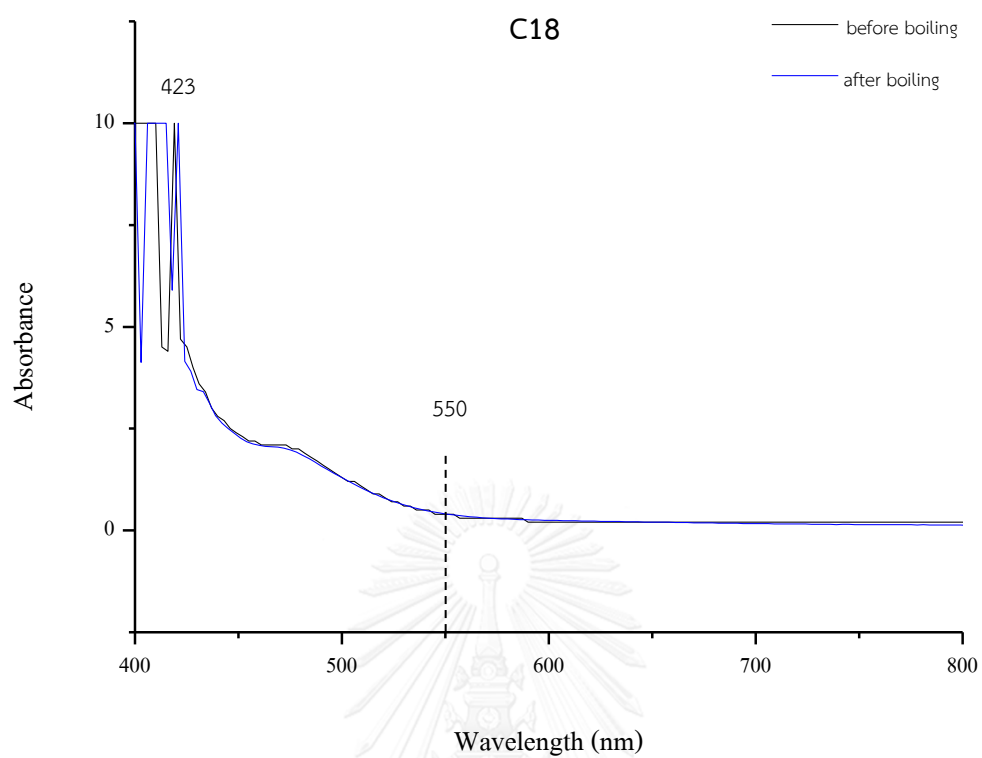




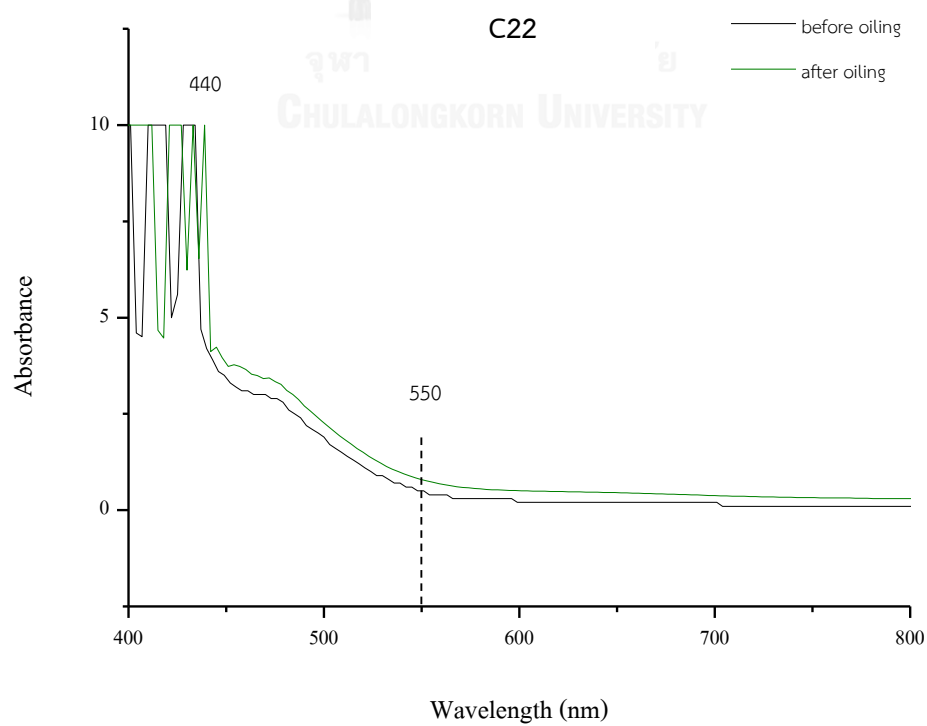
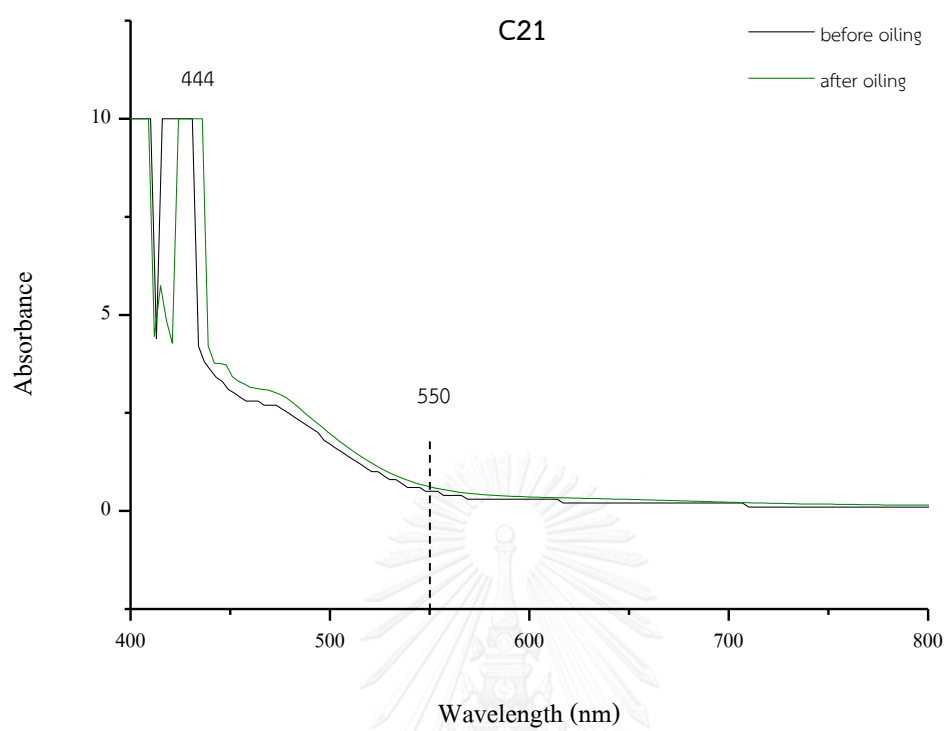


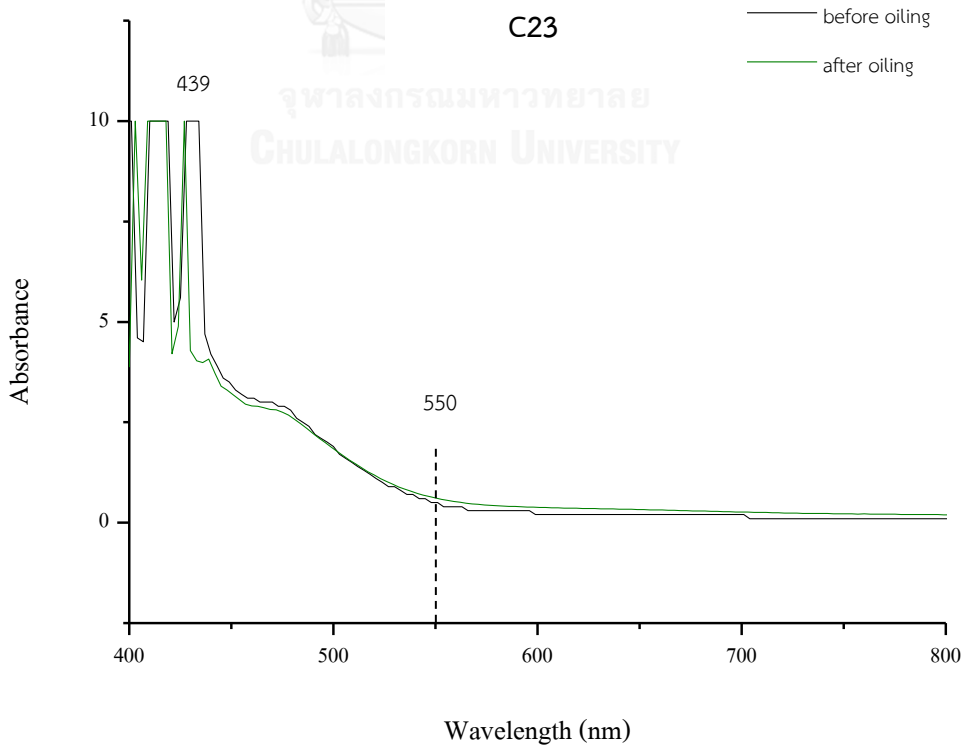
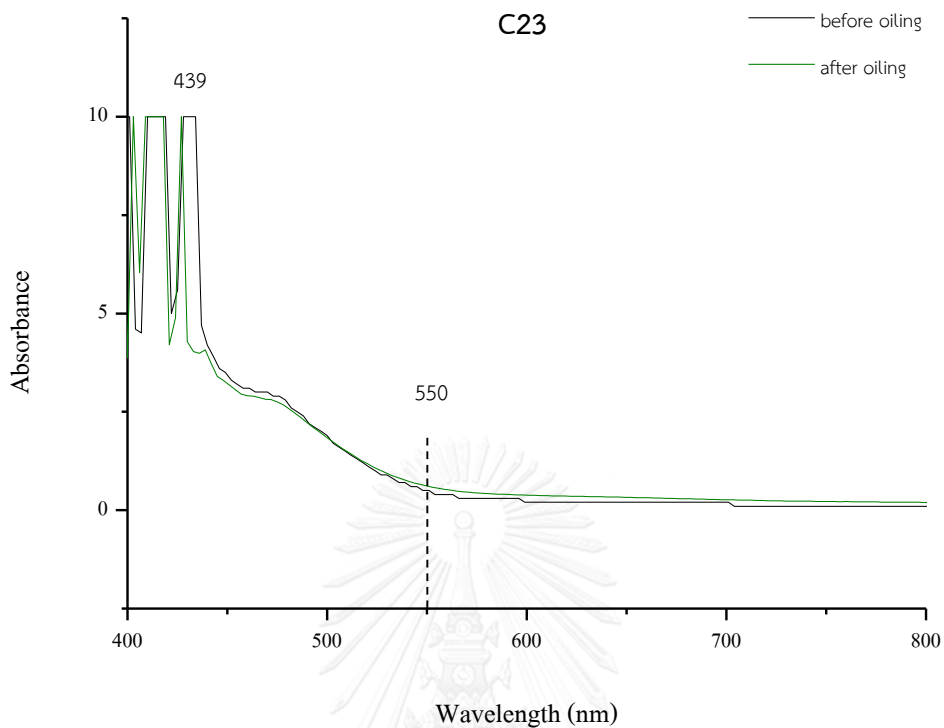










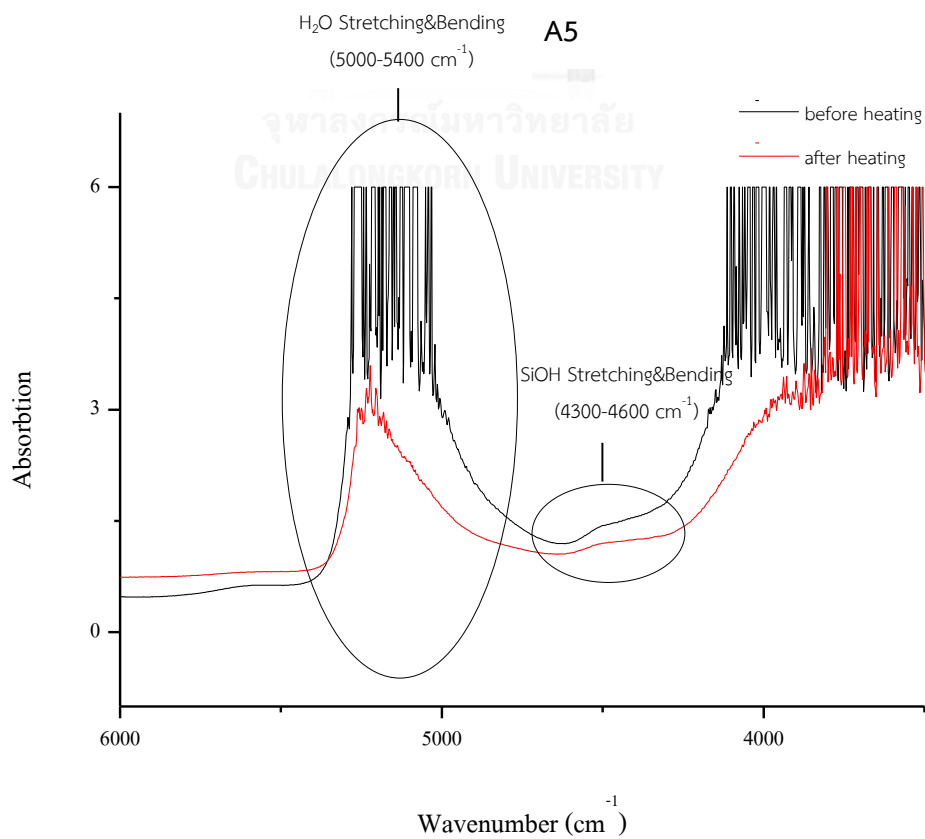
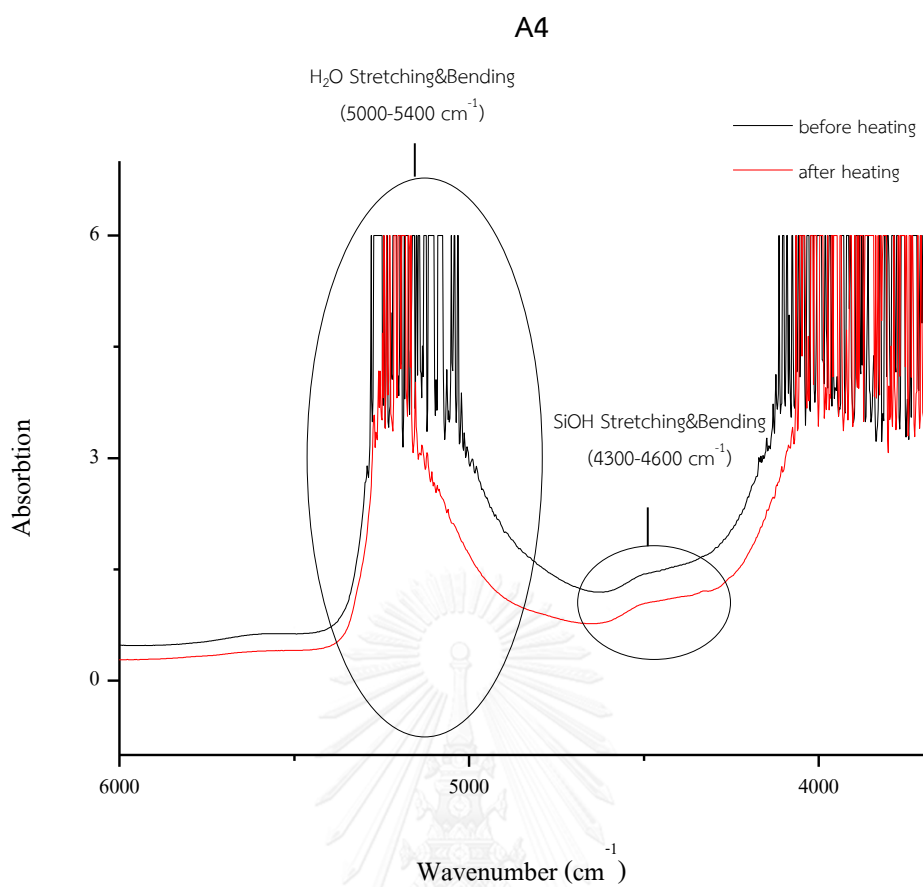


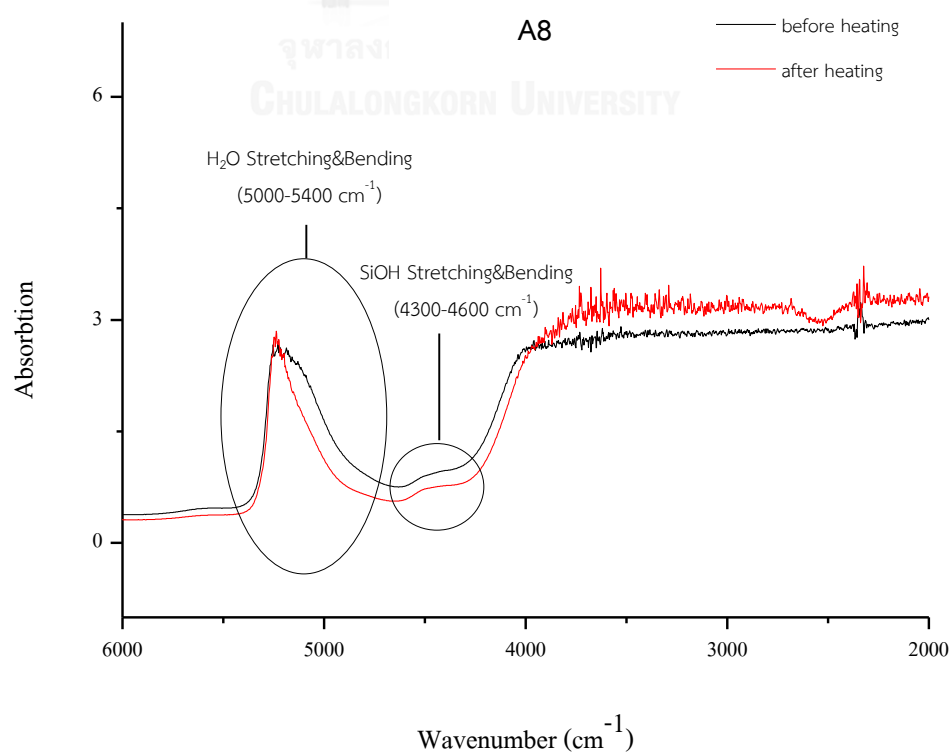
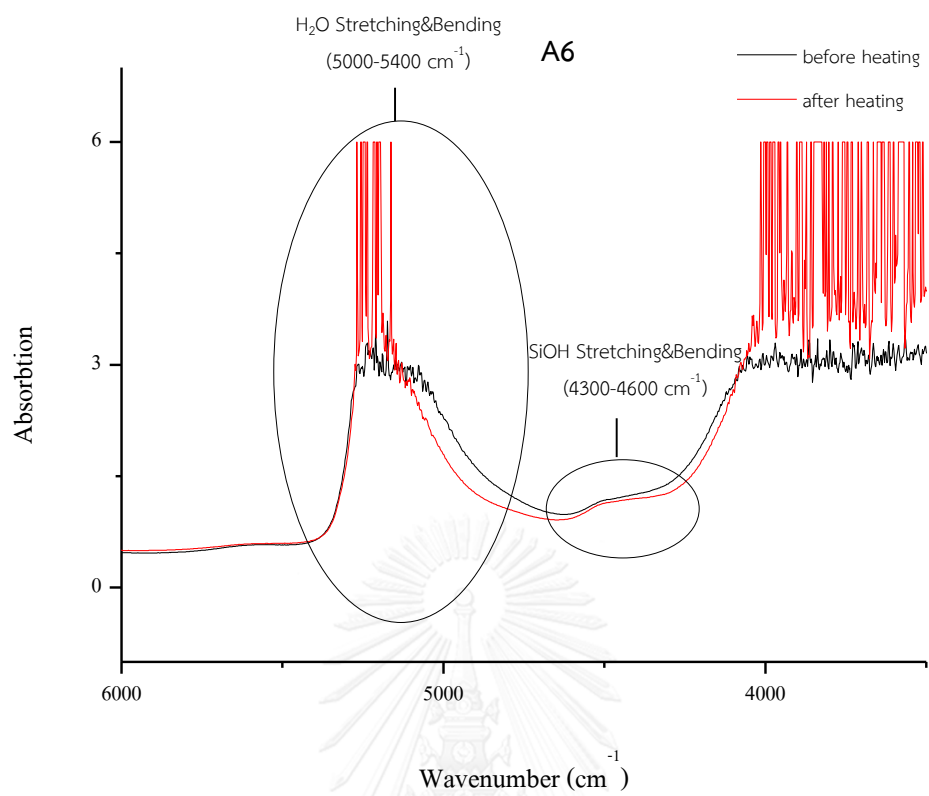


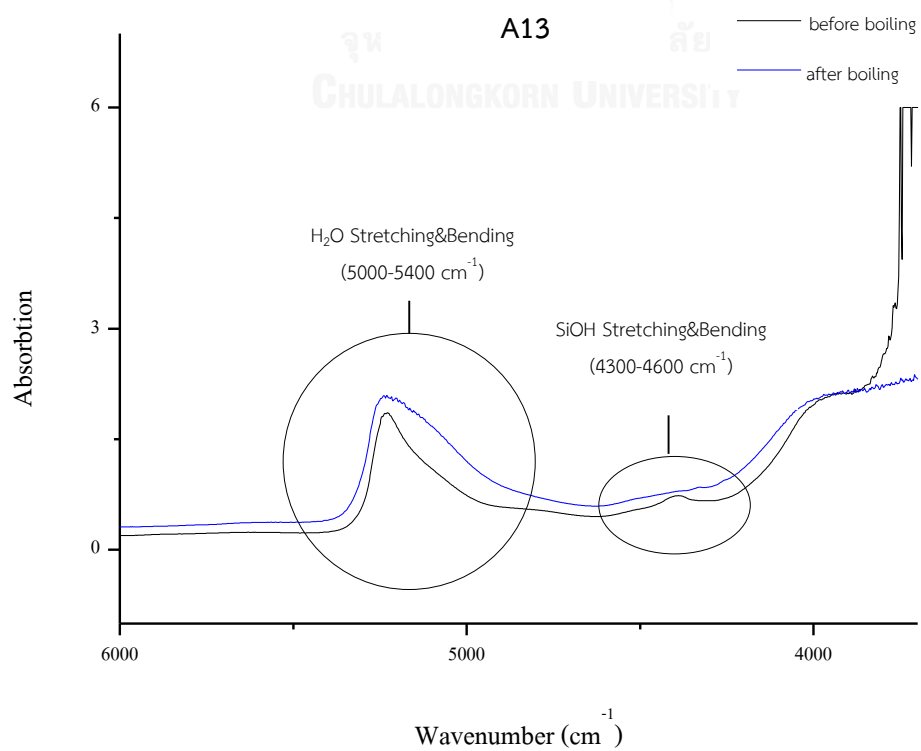
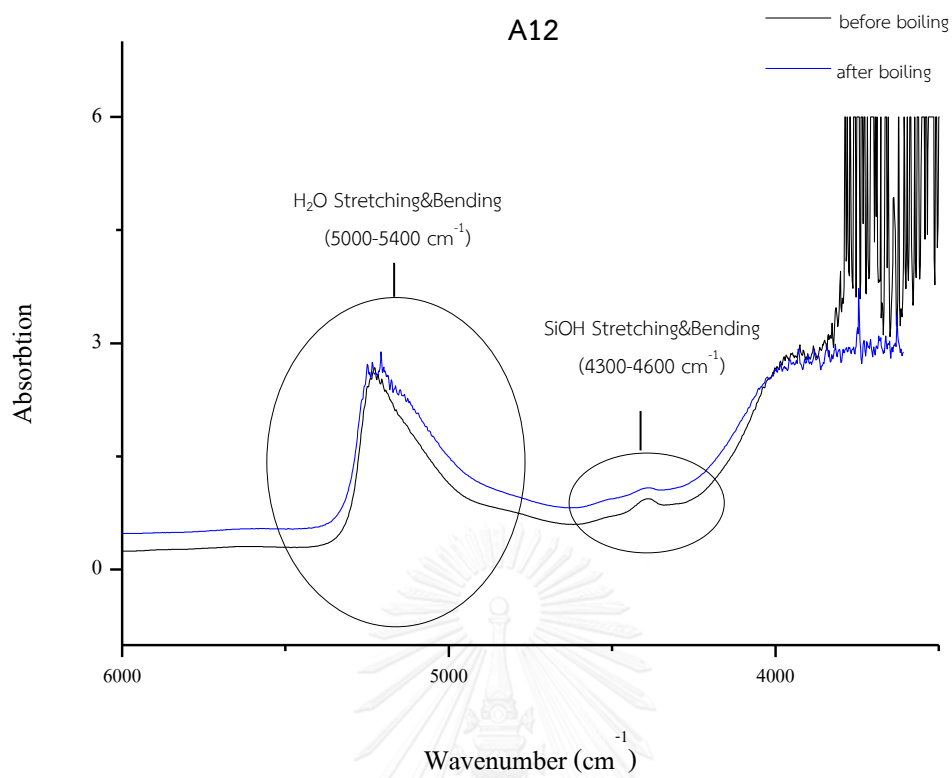
APPENDIX C

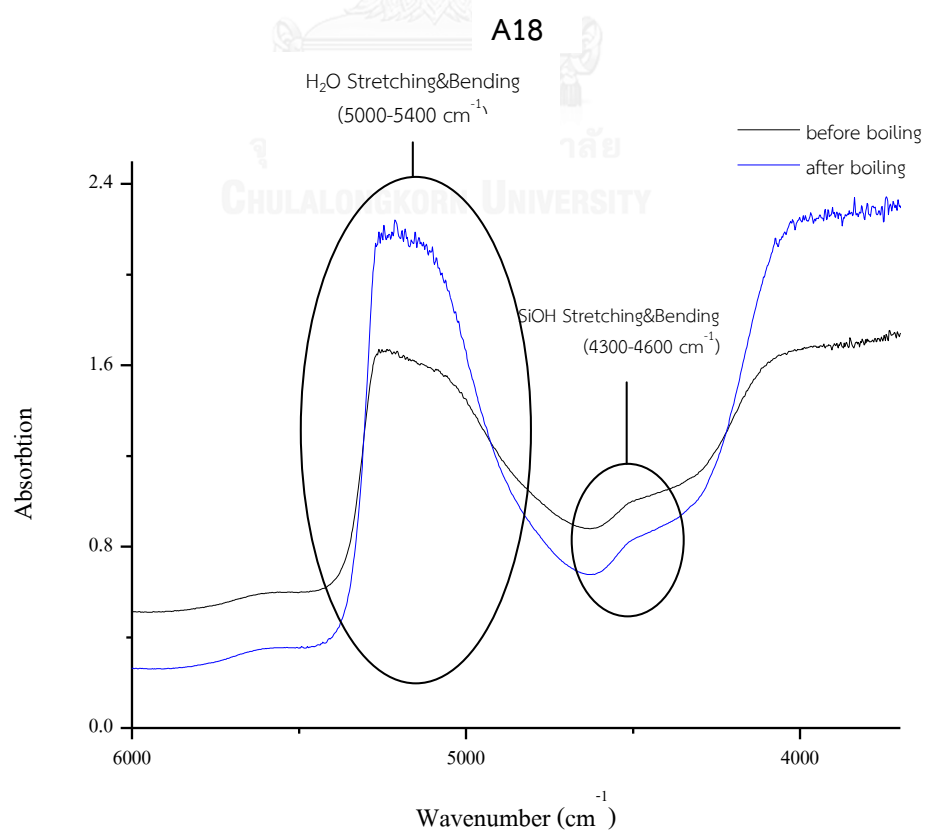
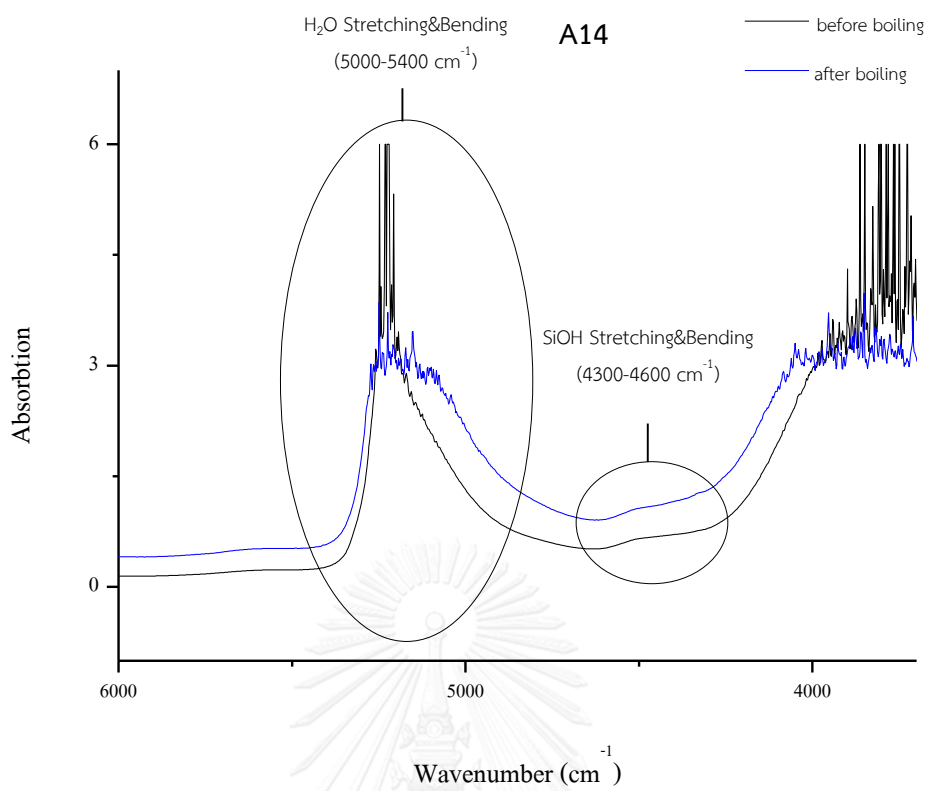
FTIR Spectra of opals before and after enhancement

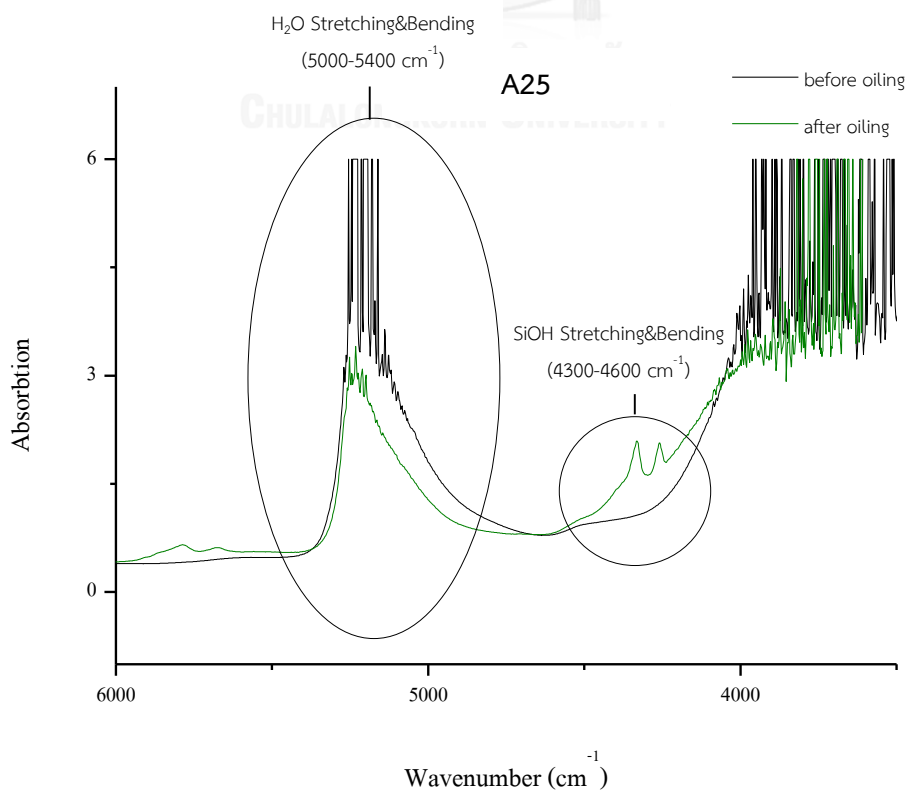
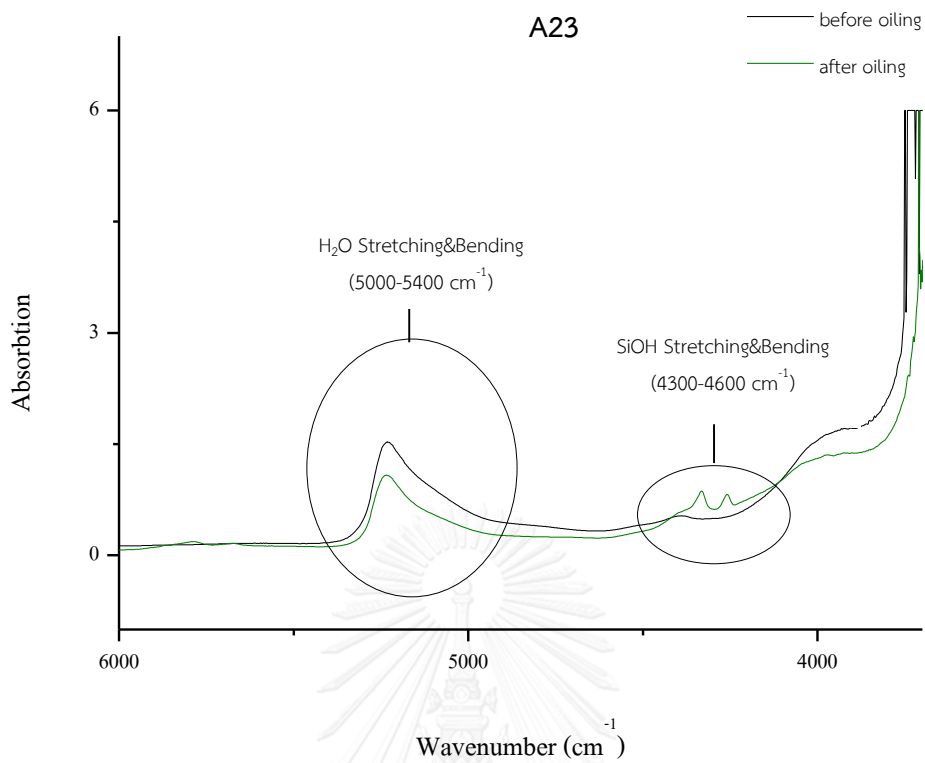
Ethiopian Precious opal (Heating)	: A4, A5, A6, A8
Ethiopian Precious opal (Boiling)	: A12, A13, A14, A18
Ethiopian Precious opal (Oiling)	: A23, A25, A26, A28
Malagasy White fire opal (Heating)	: B4, B5, B6, B7
Malagasy White fire opal (Boiling)	: B11, B16, B17, B18
Malagasy White fire opal (Oiling)	: B22, B23, B25, B30
Malagasy Orange fire opal (Heating)	: C2, C3, C4, C8
Malagasy Orange fire opal (Boiling)	: C12, C14, C19, C20
Malagasy Orange fire opal (Oiling)	: C21, C23, C25, C26



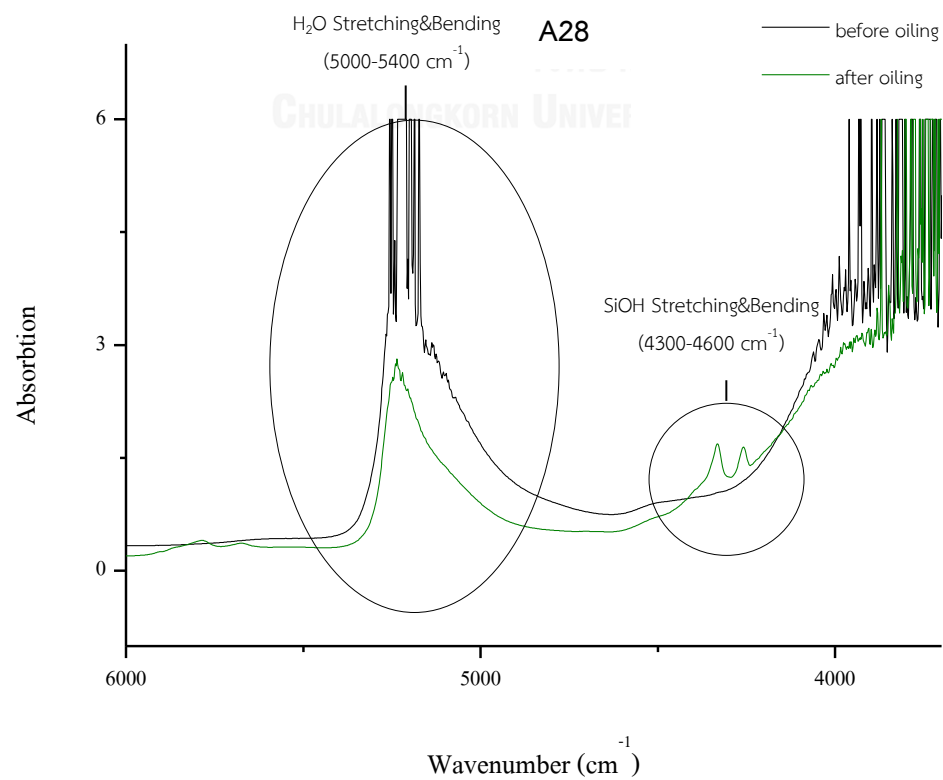
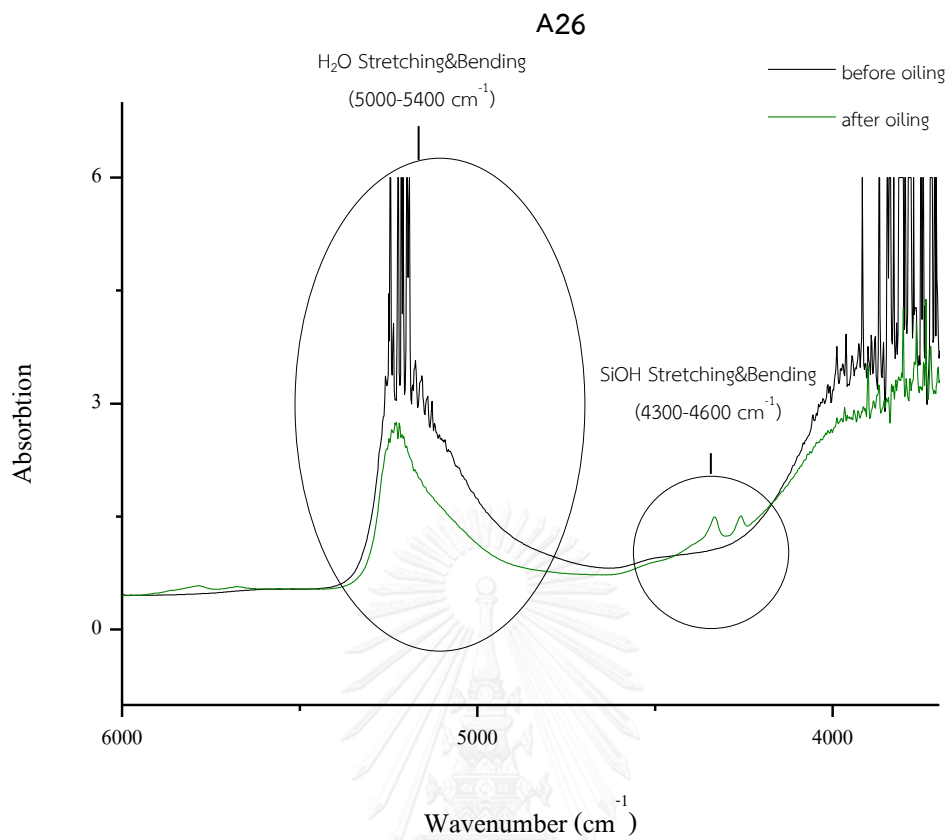


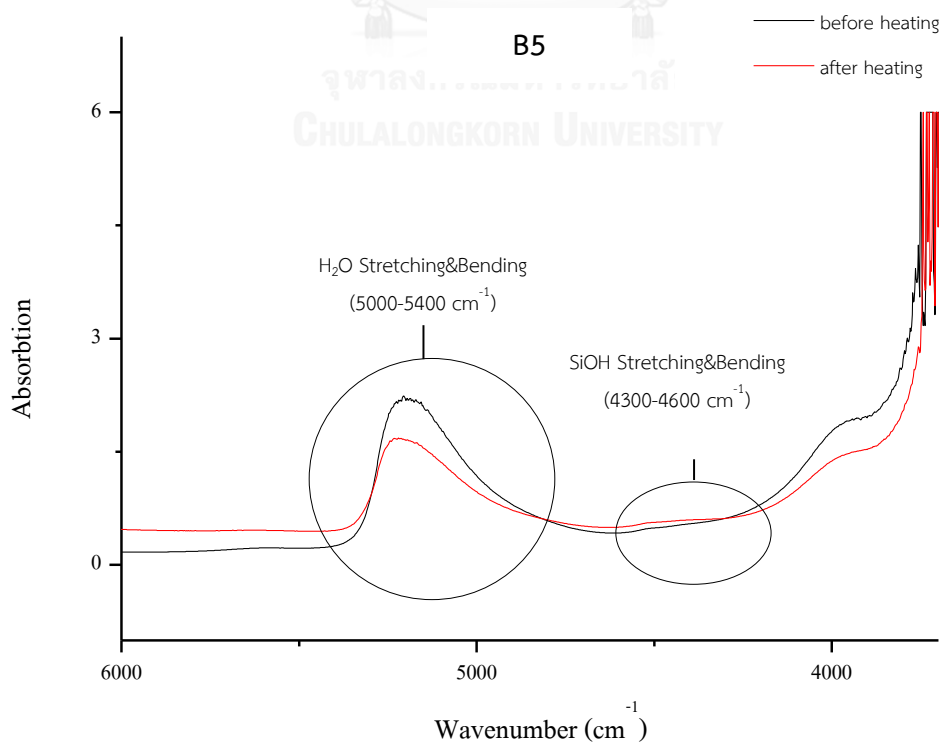
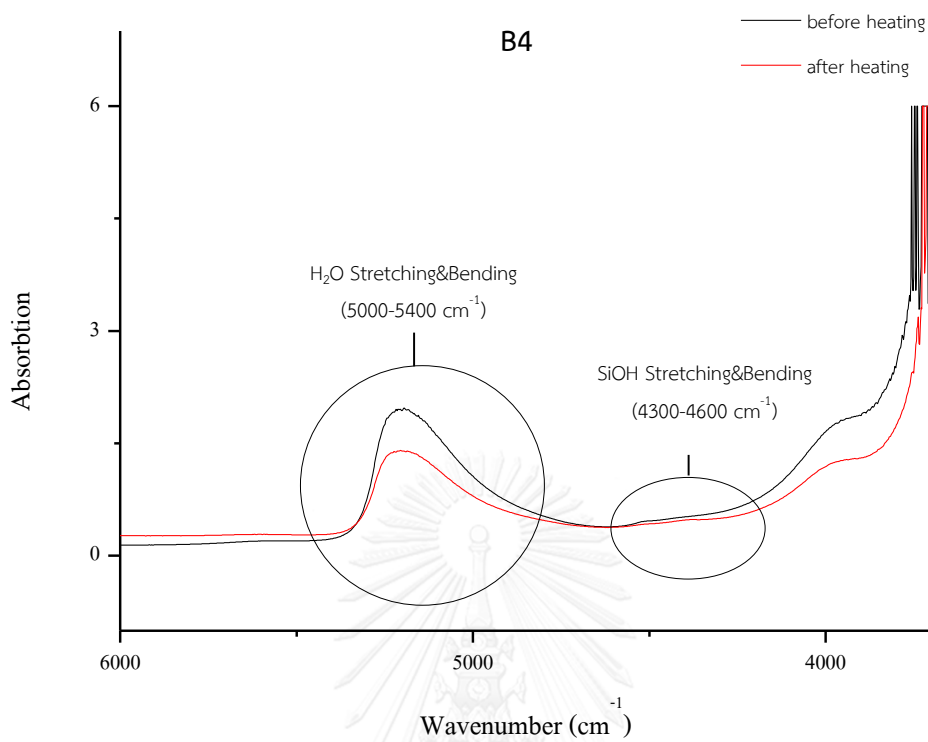


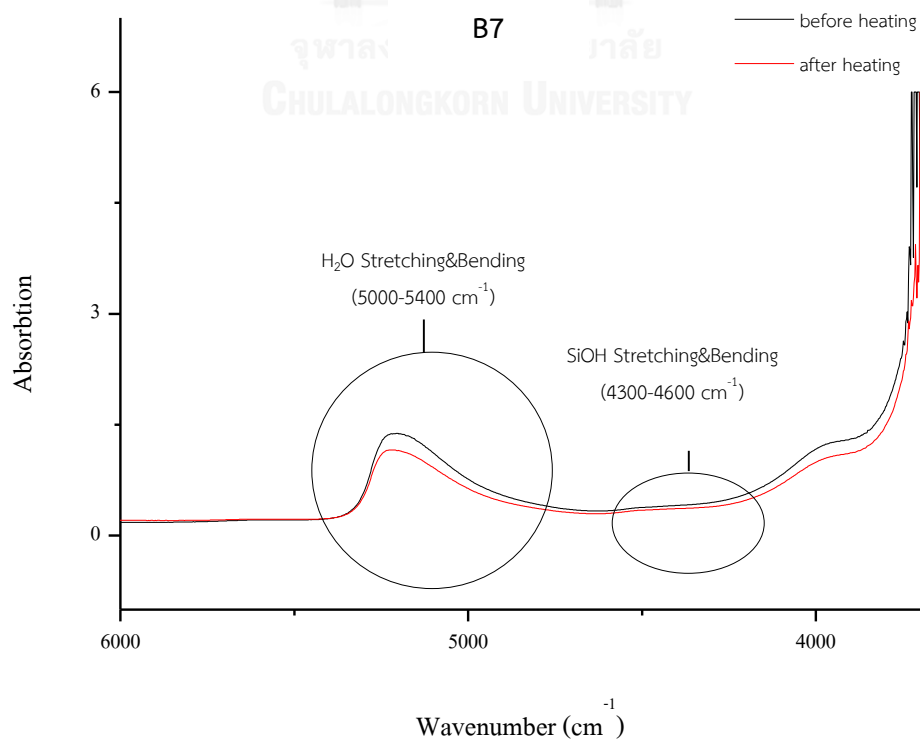
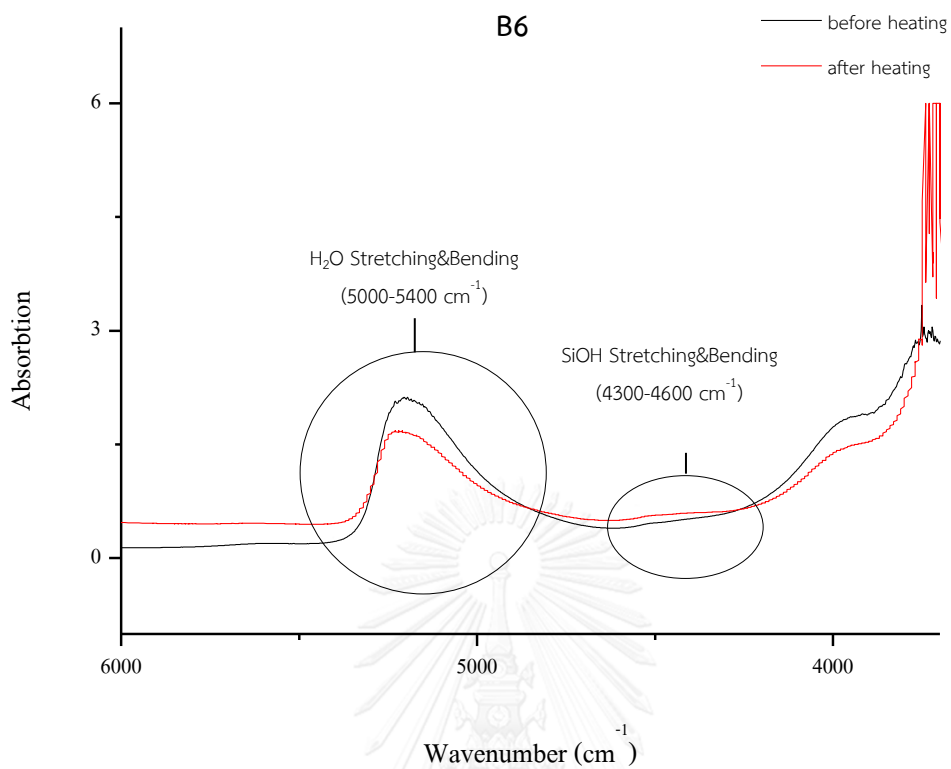


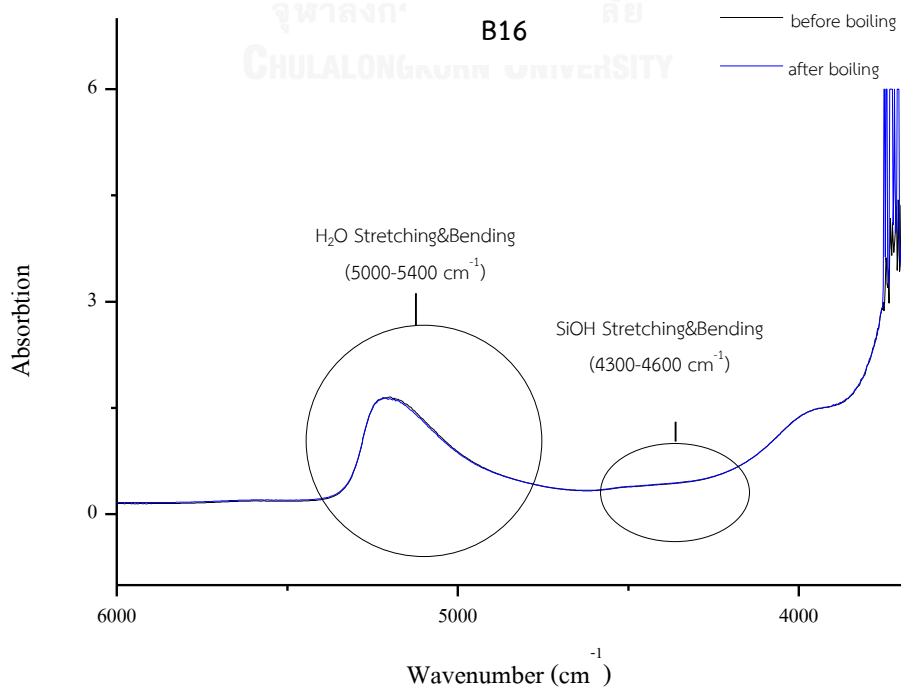
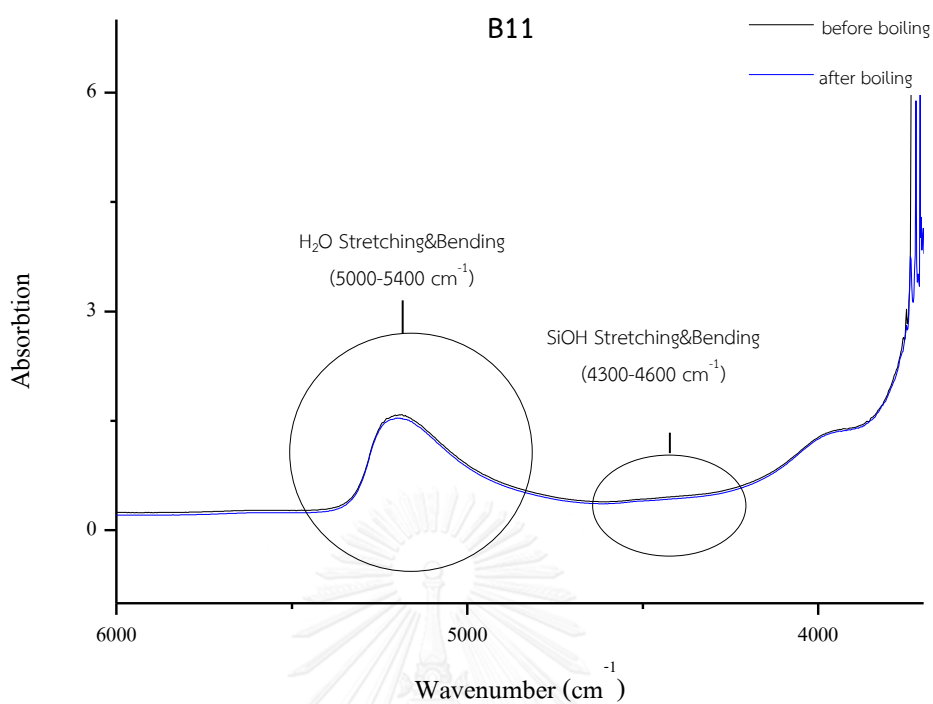


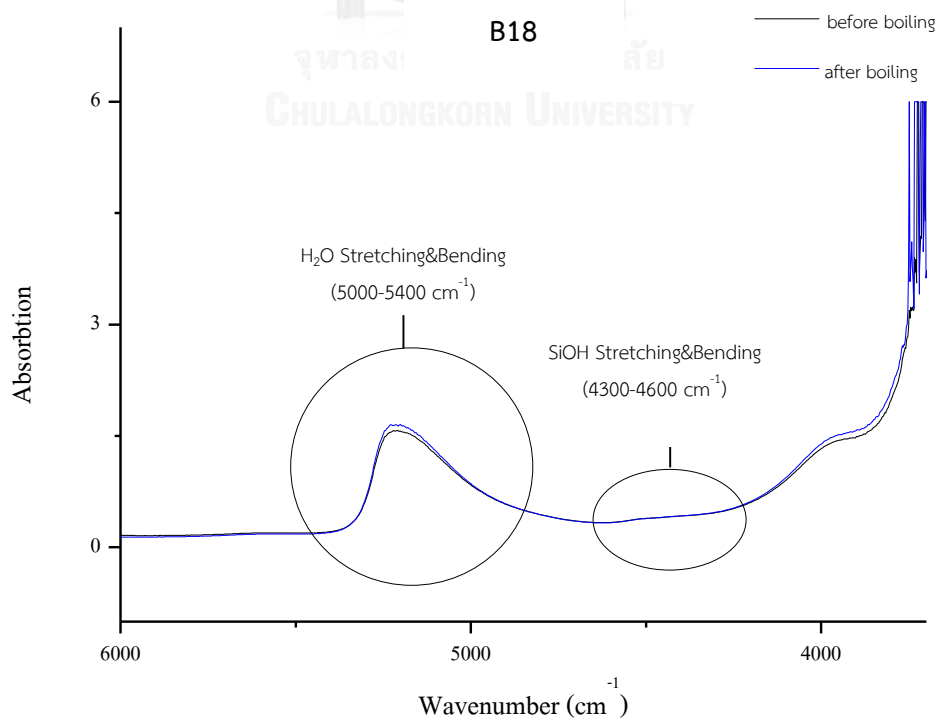
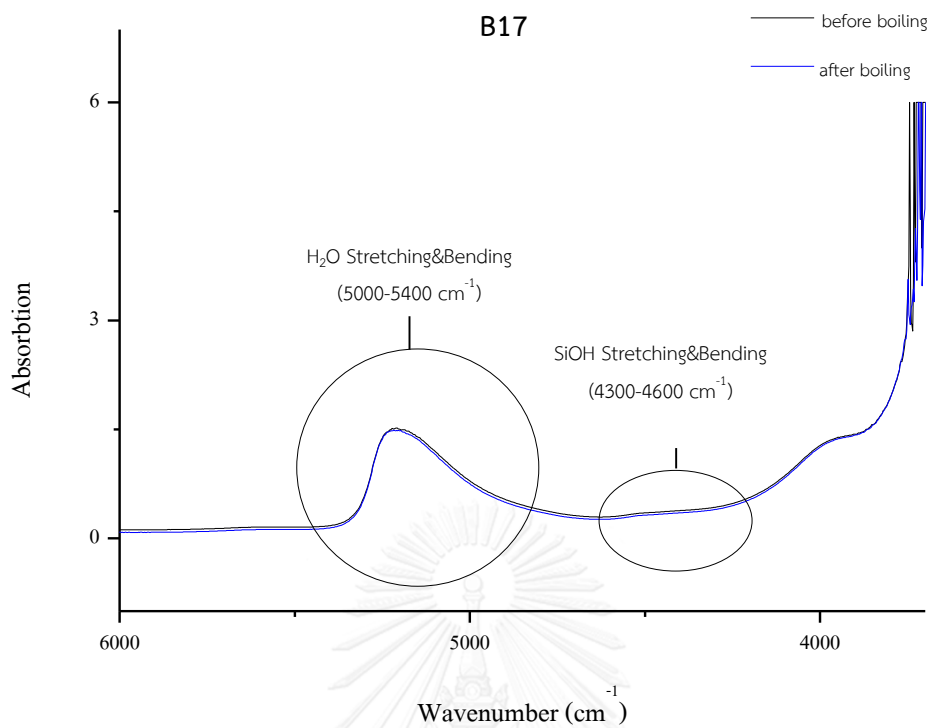


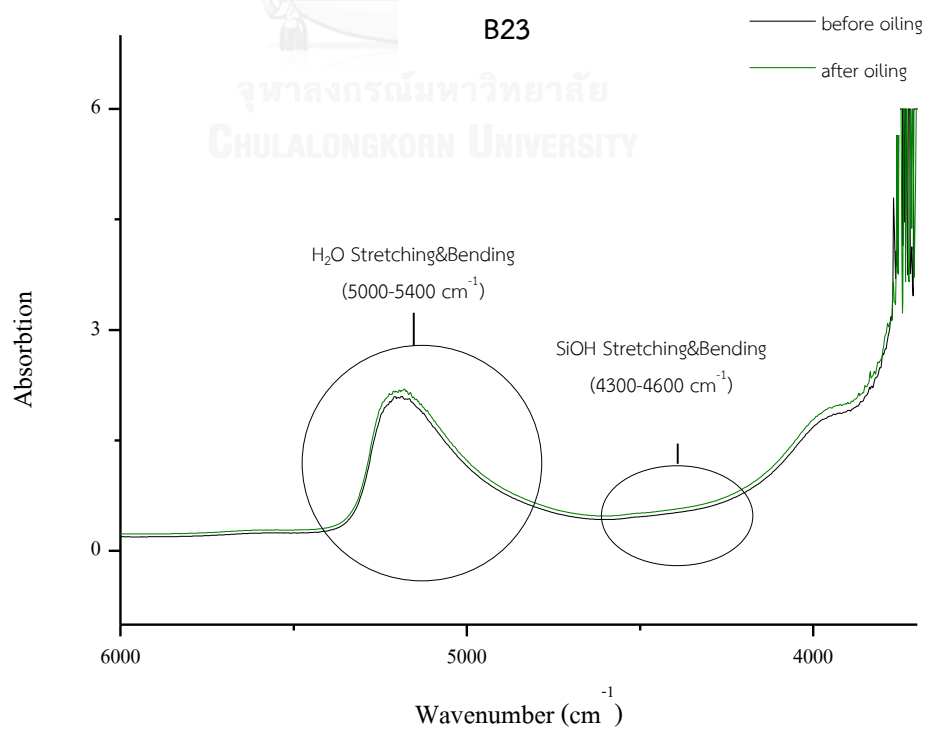
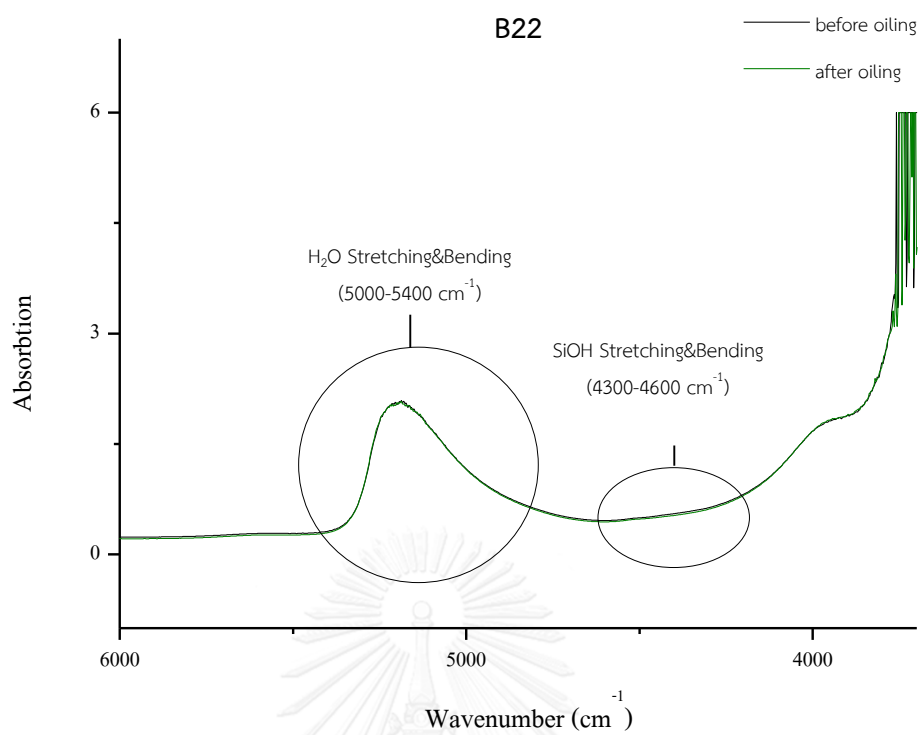


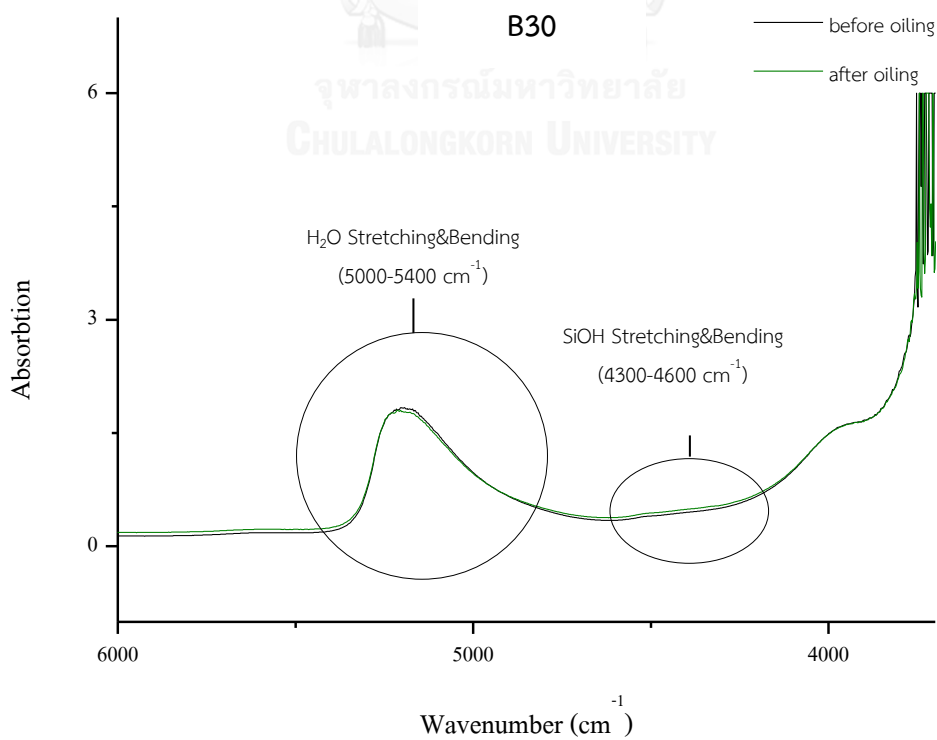
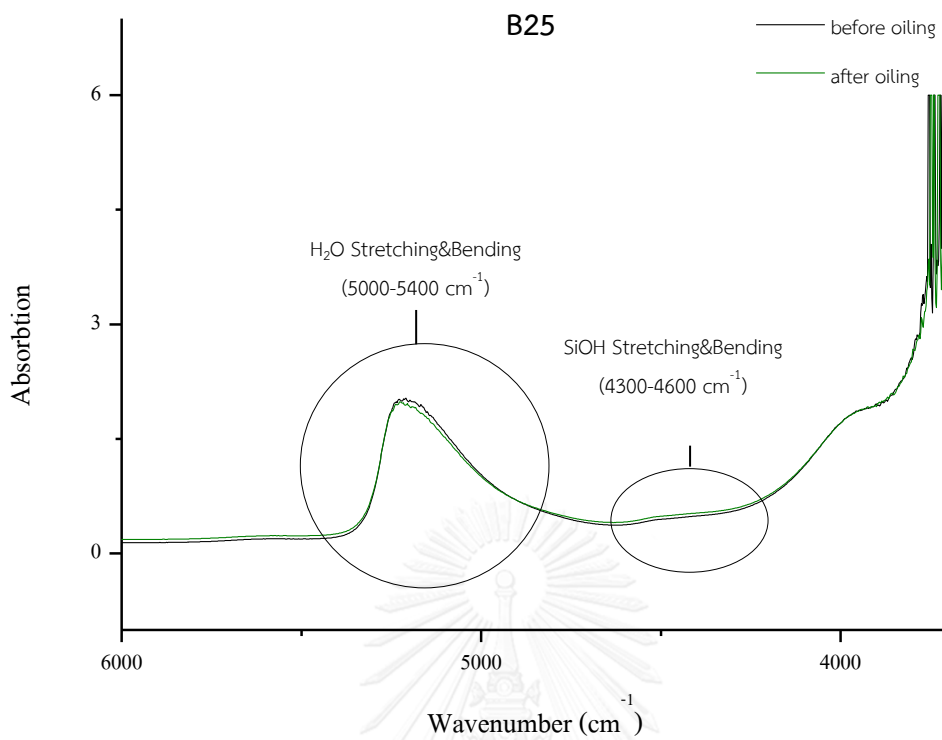


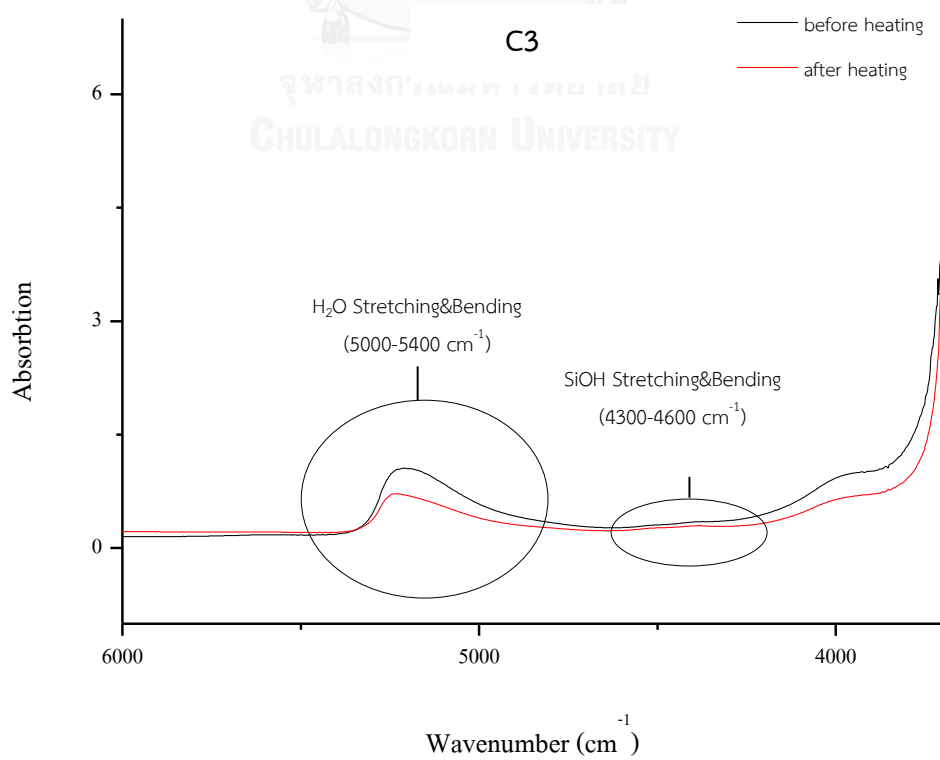
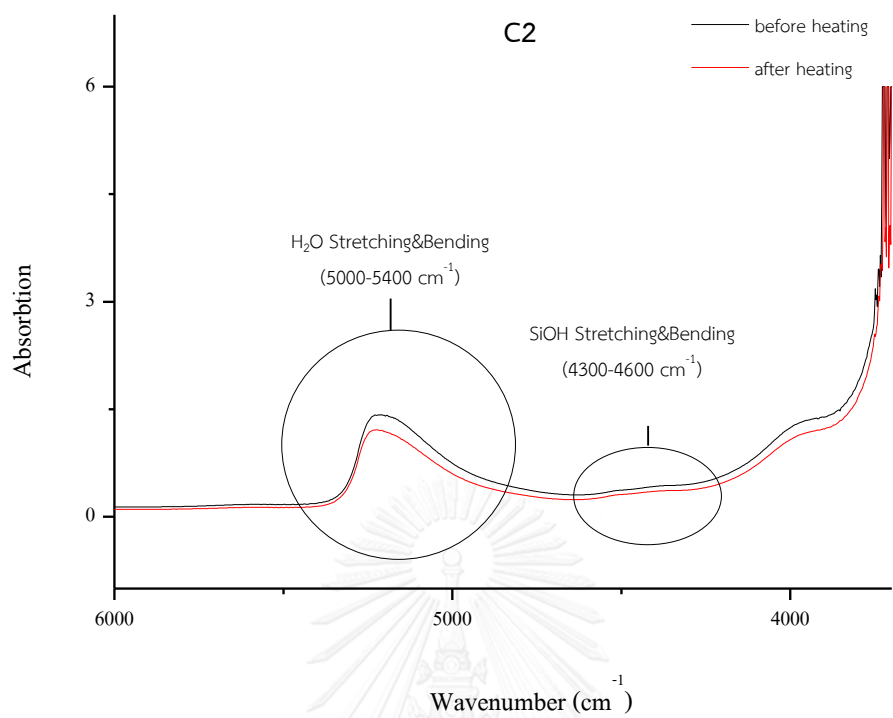




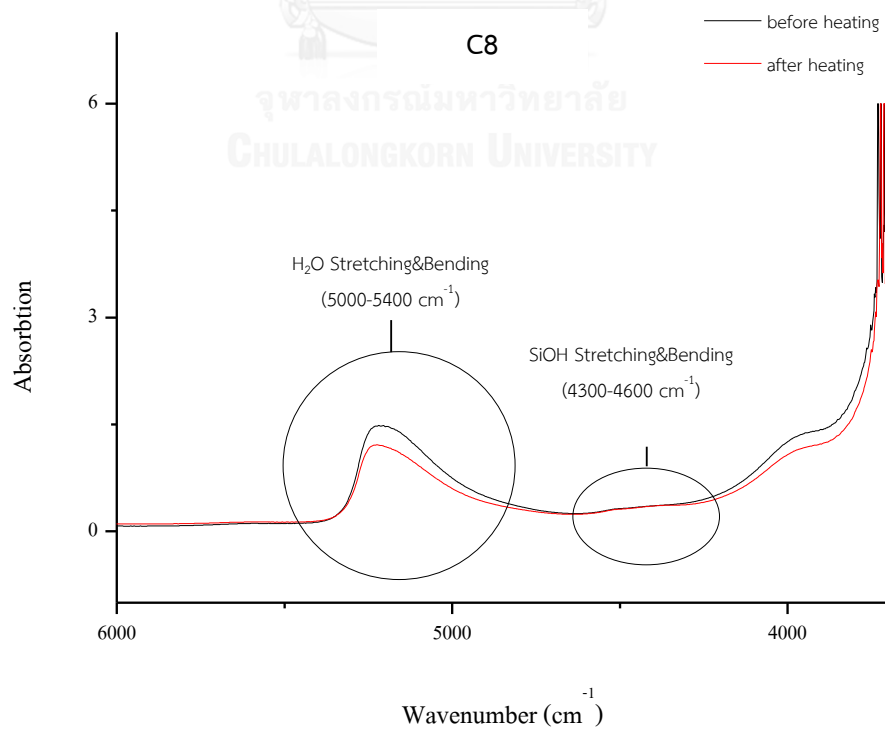
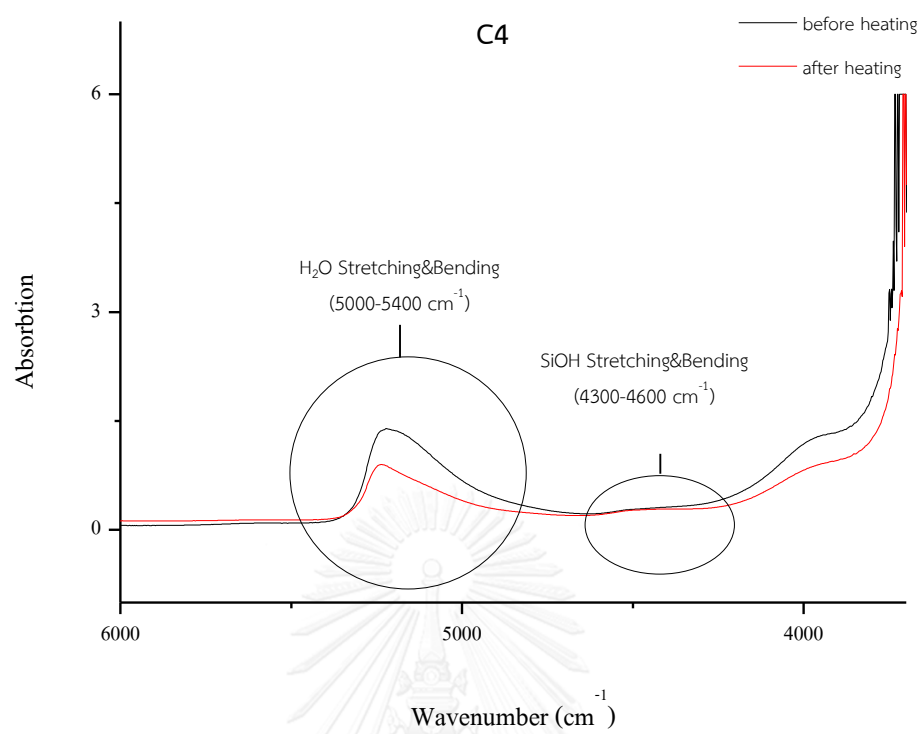


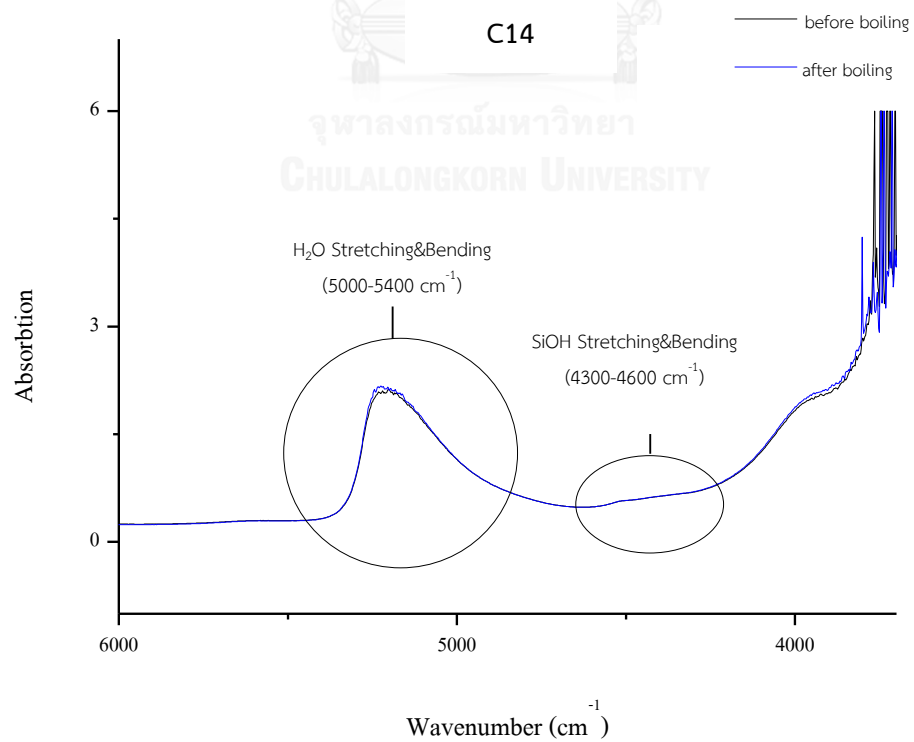
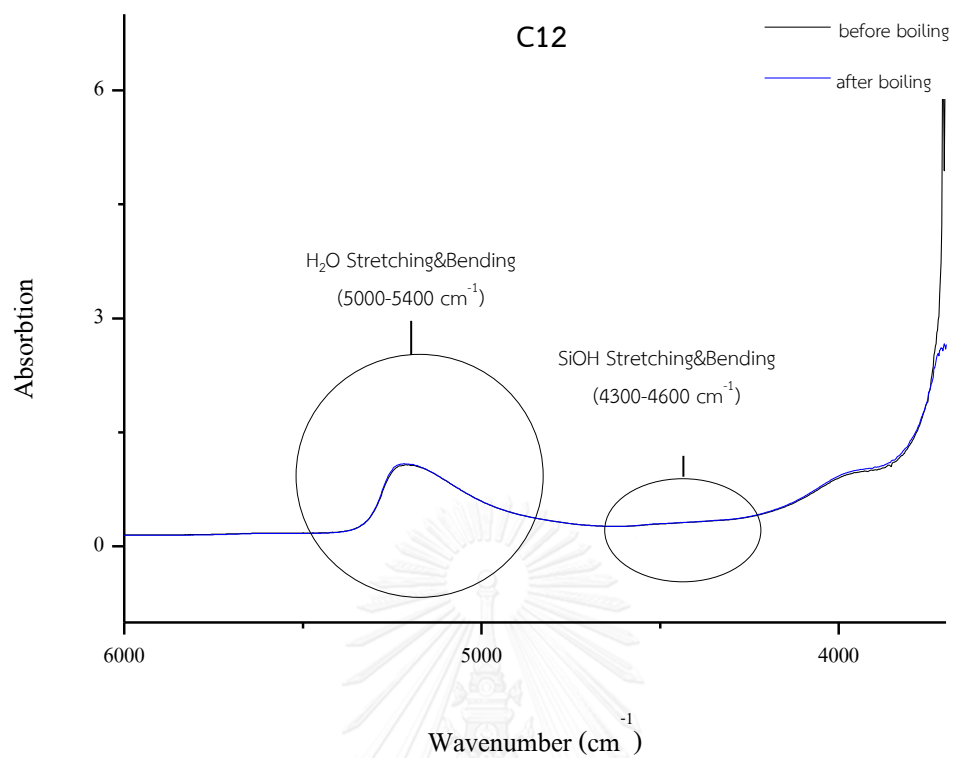


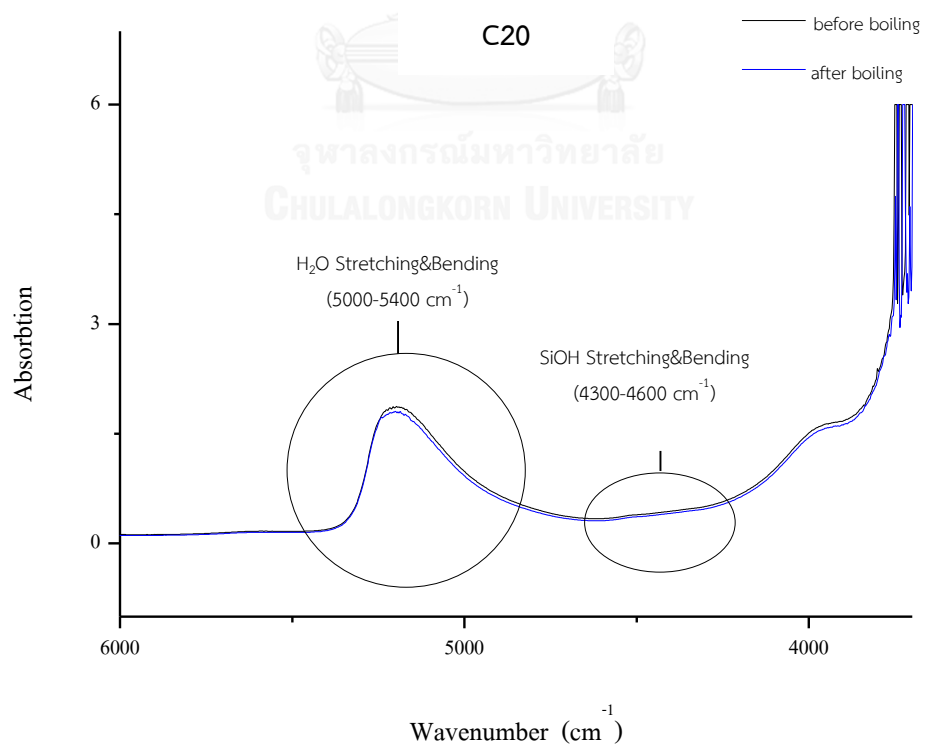
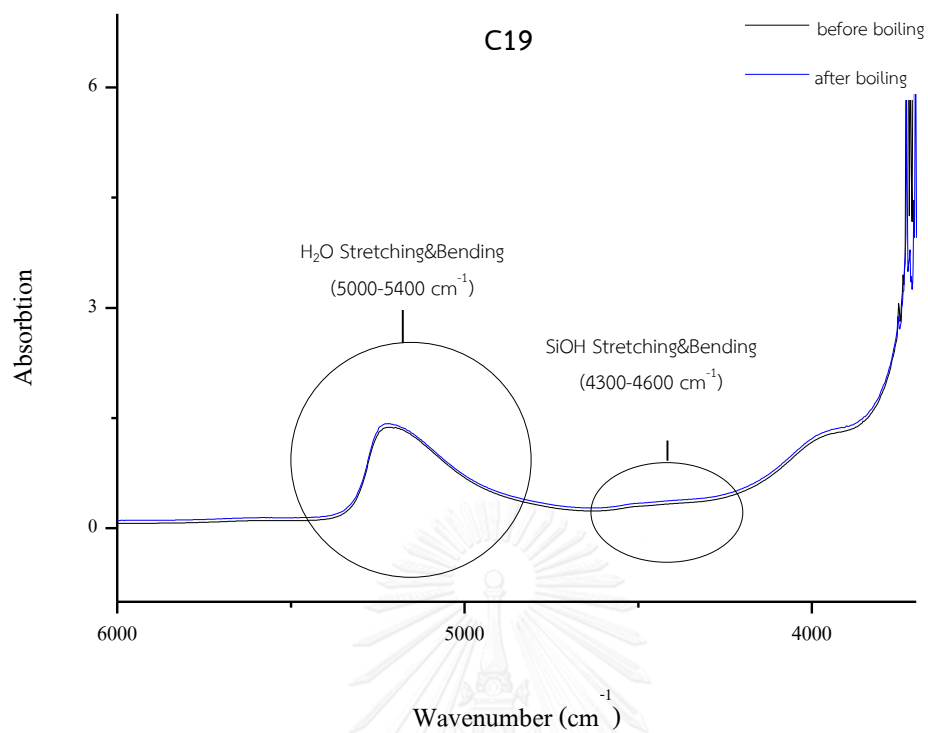


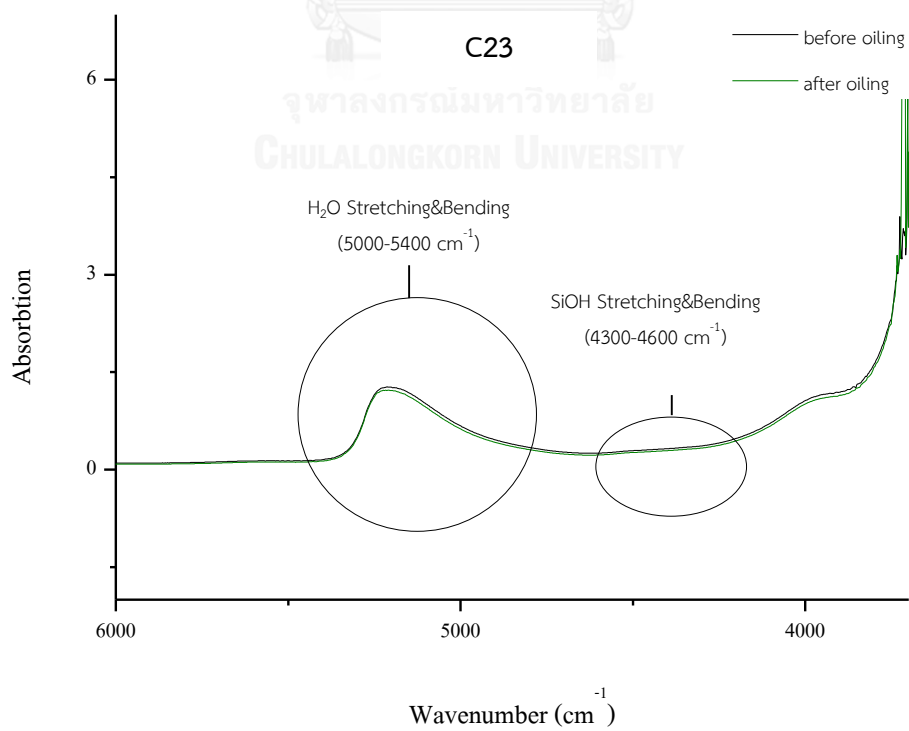
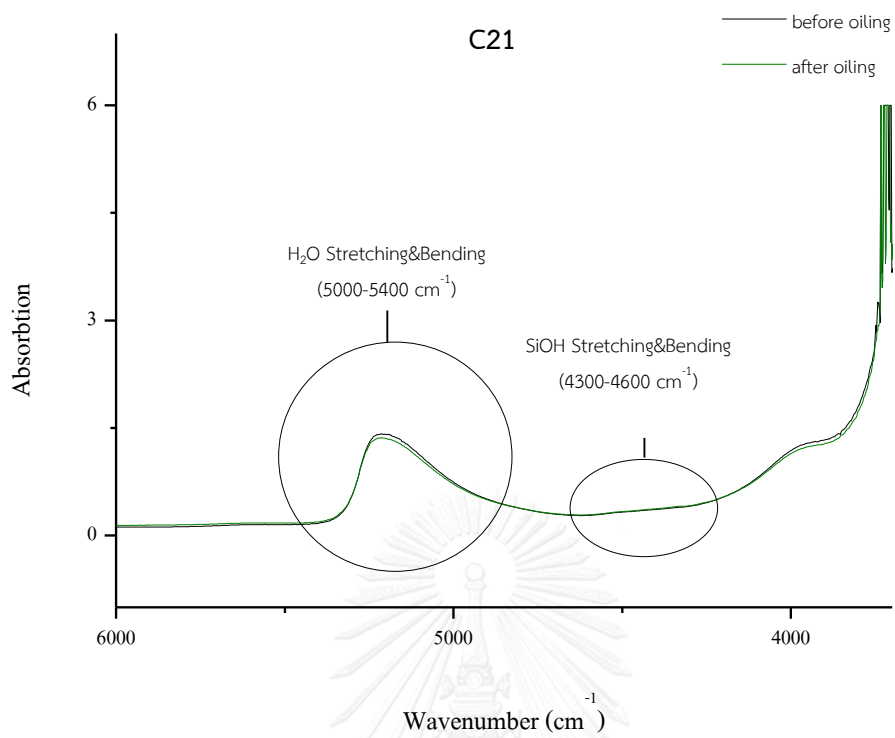


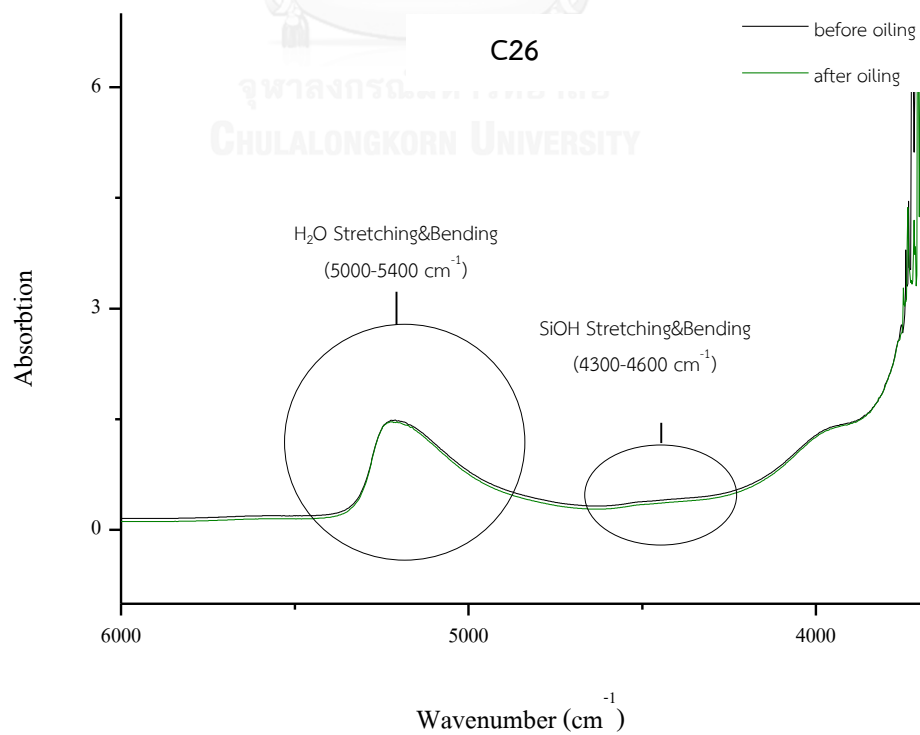
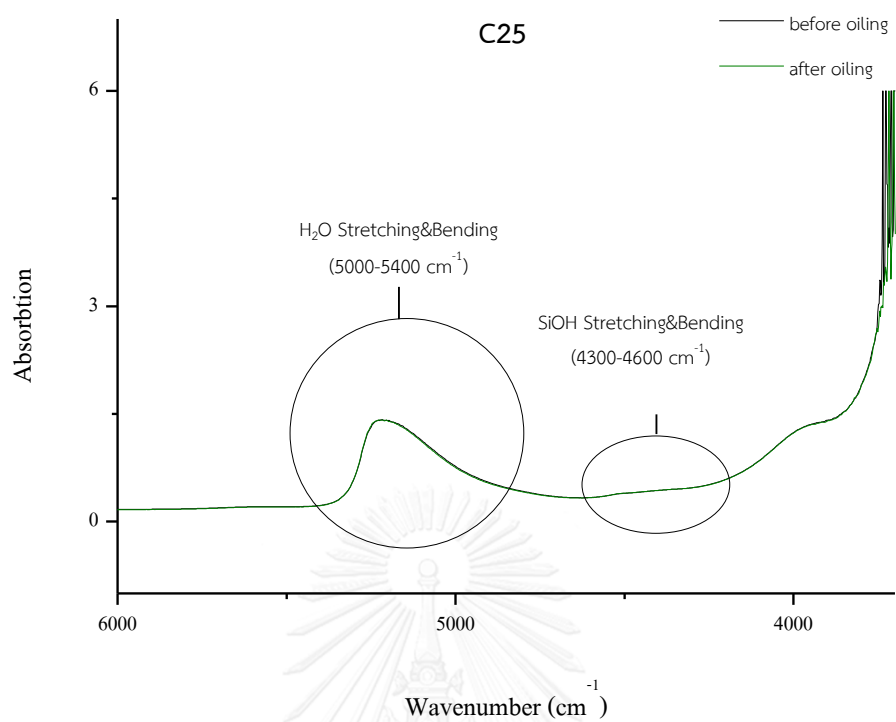






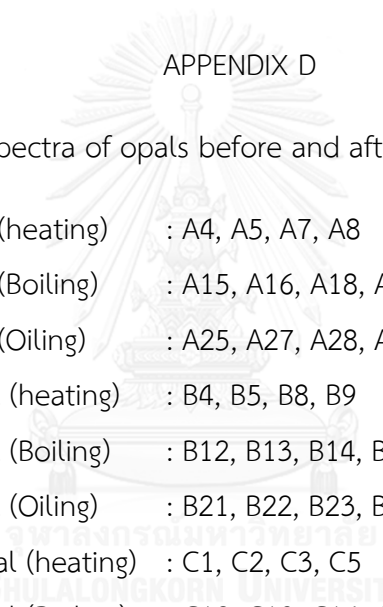




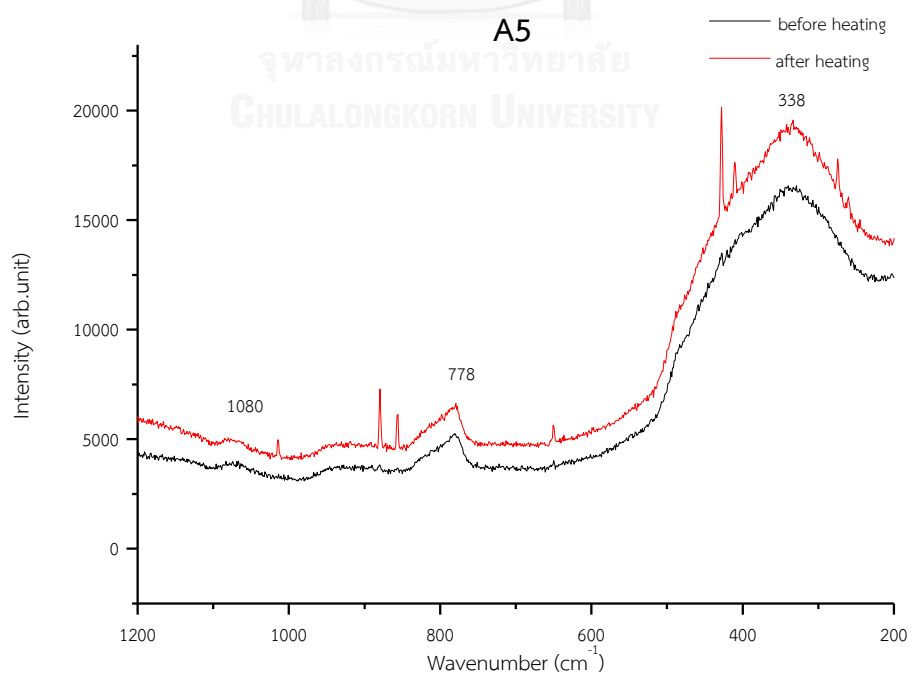
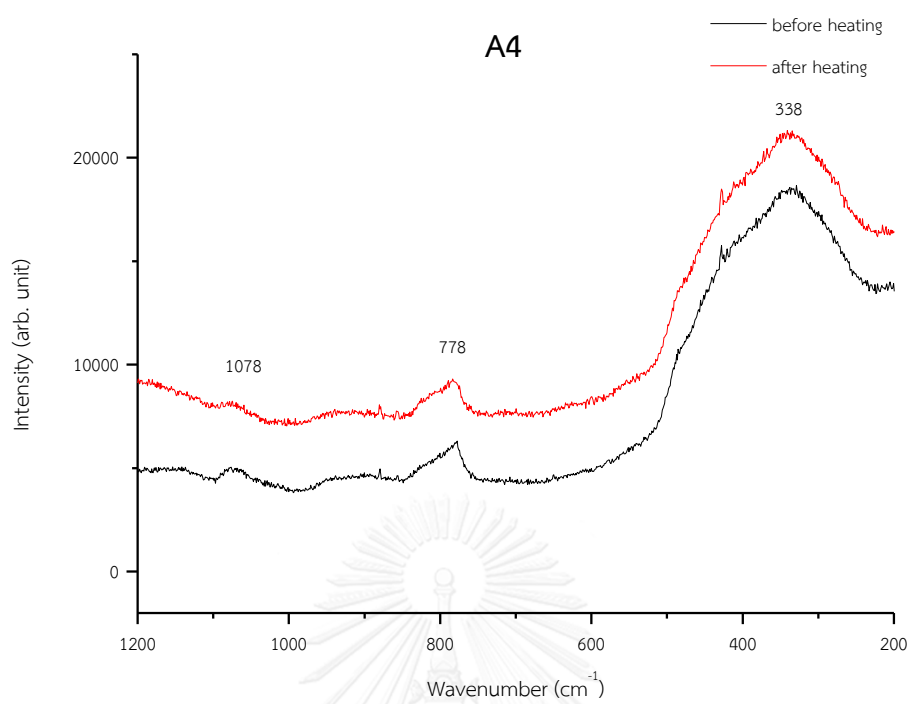


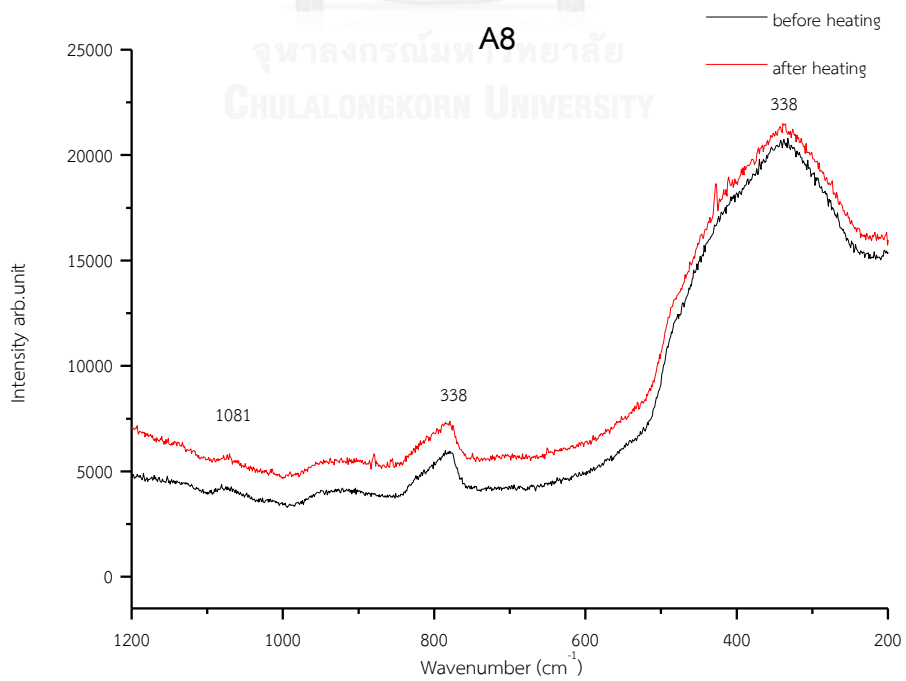
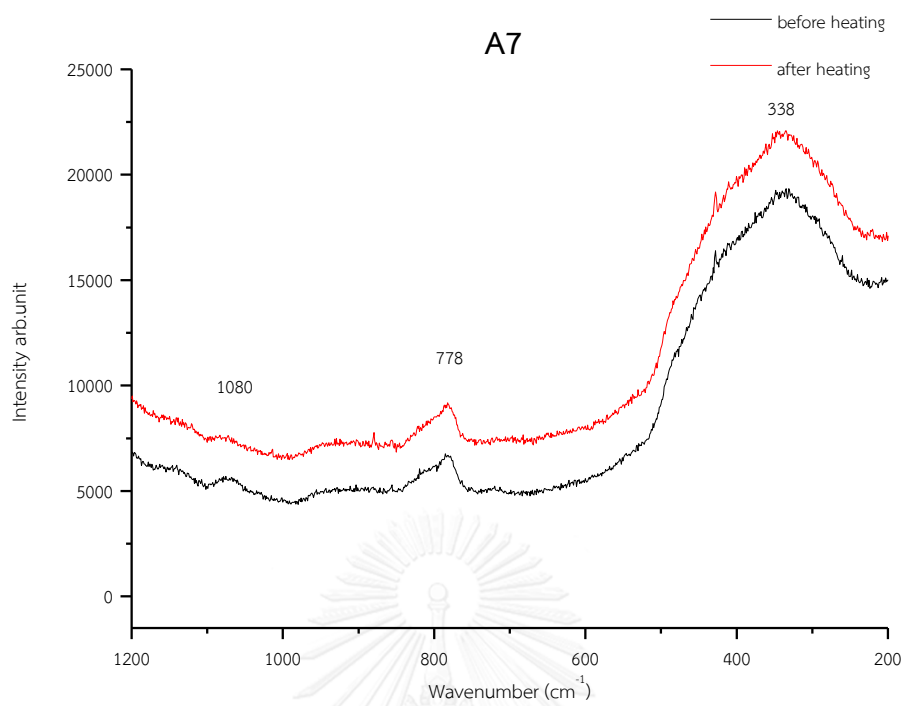
## APPENDIX D

## Raman Spectra of opals before and after enhancement

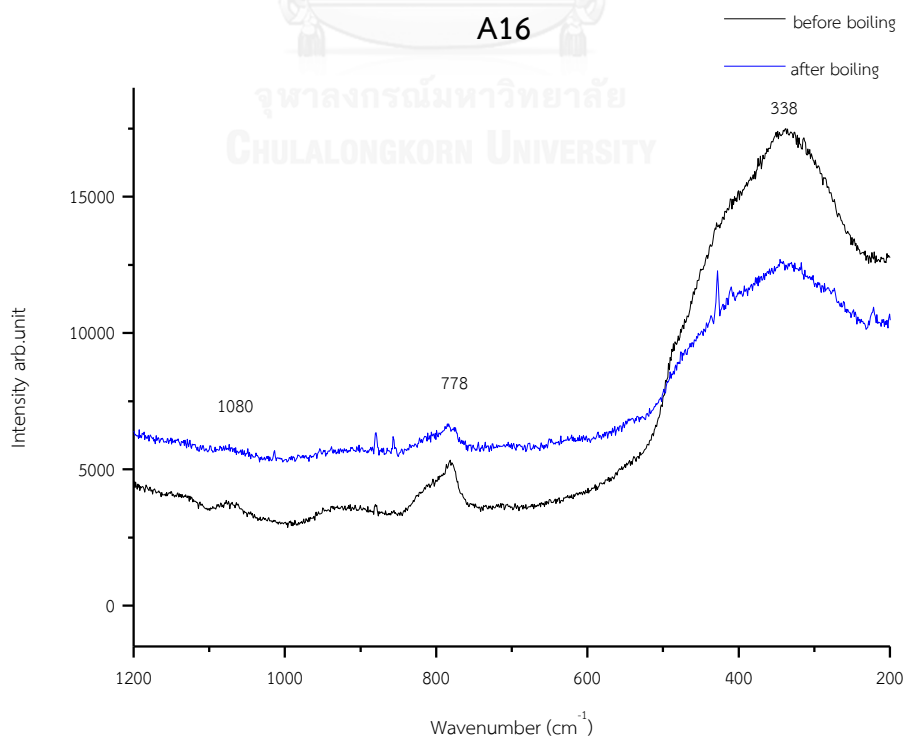
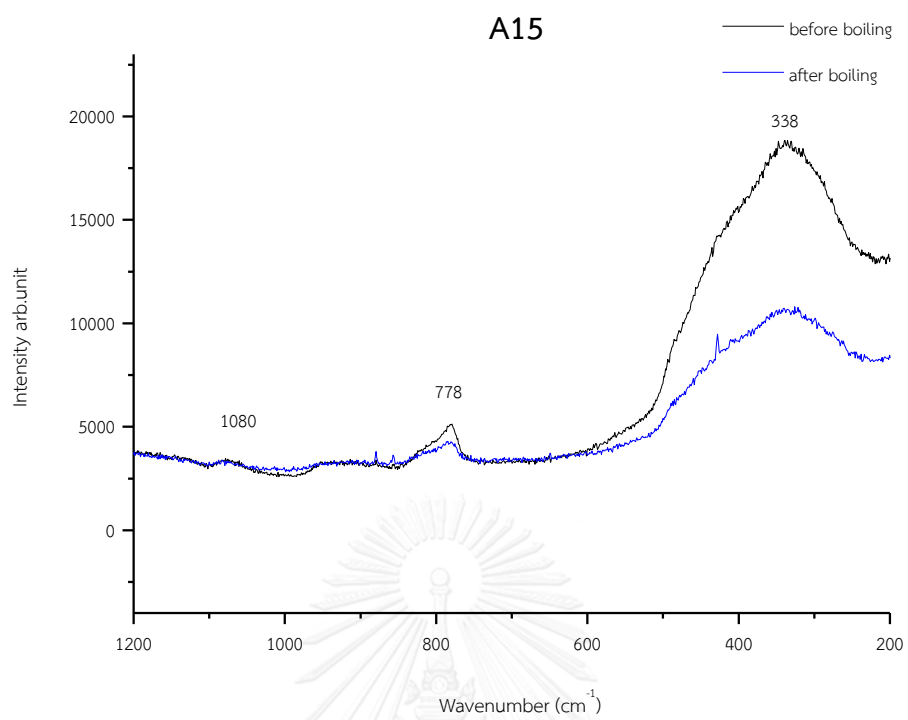


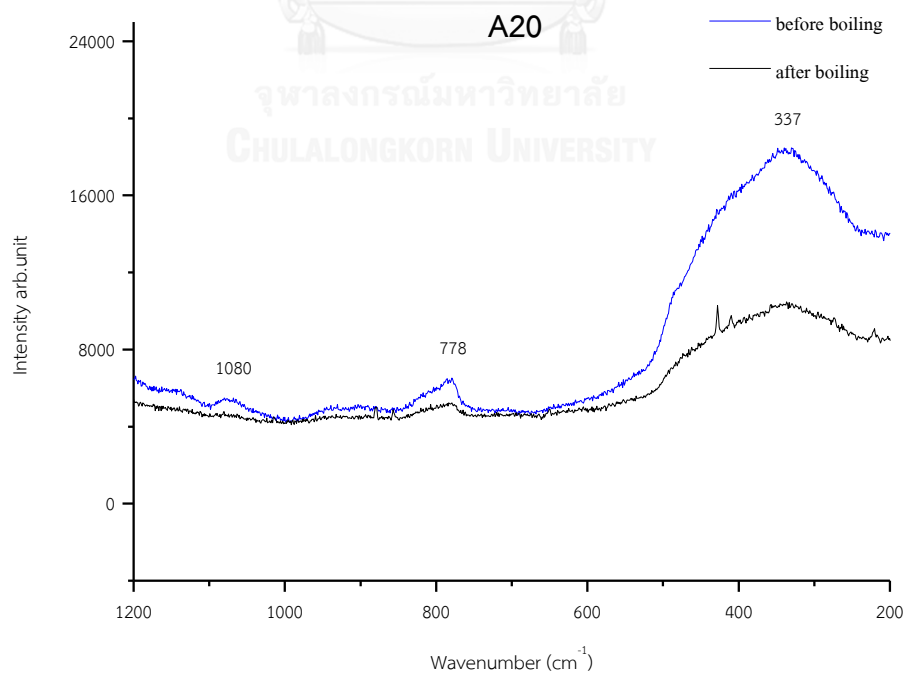
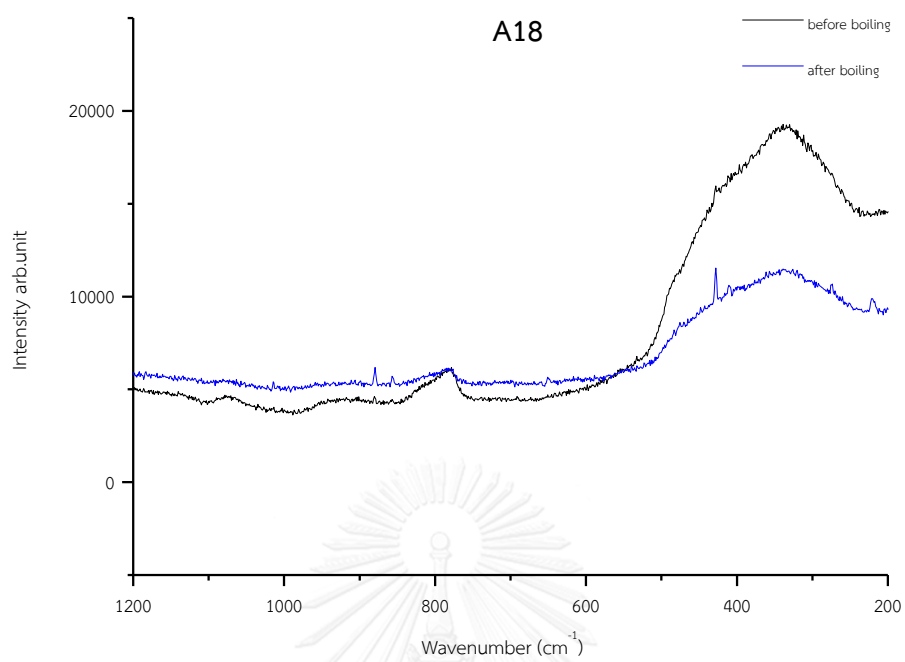
Ethiopian Precious opal (heating)	: A4, A5, A7, A8
Ethiopian Precious opal (Boiling)	: A15, A16, A18, A20
Ethiopian Precious opal (Oiling)	: A25, A27, A28, A29
Malagasy White fire opal (heating)	: B4, B5, B8, B9
Malagasy White fire opal (Boiling)	: B12, B13, B14, B15
Malagasy White fire opal (Oiling)	: B21, B22, B23, B25
Malagasy Orange fire opal (heating)	: C1, C2, C3, C5
Malagasy Orange fire opal (Boiling)	: C12, C13, C14, C15
Malagasy Orange fire opal (Oiling)	: C21, C22, C23, C24

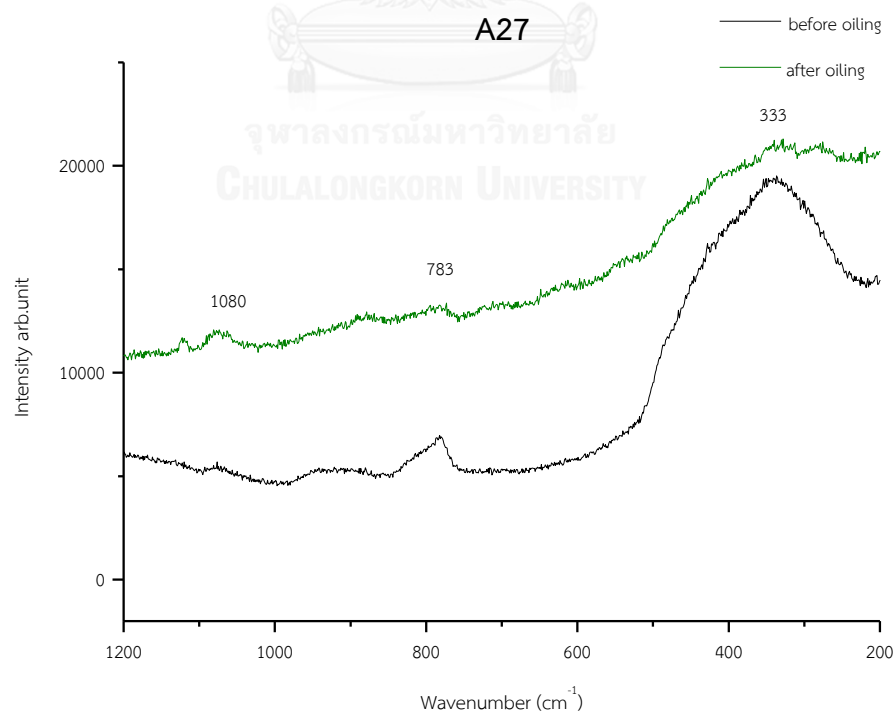
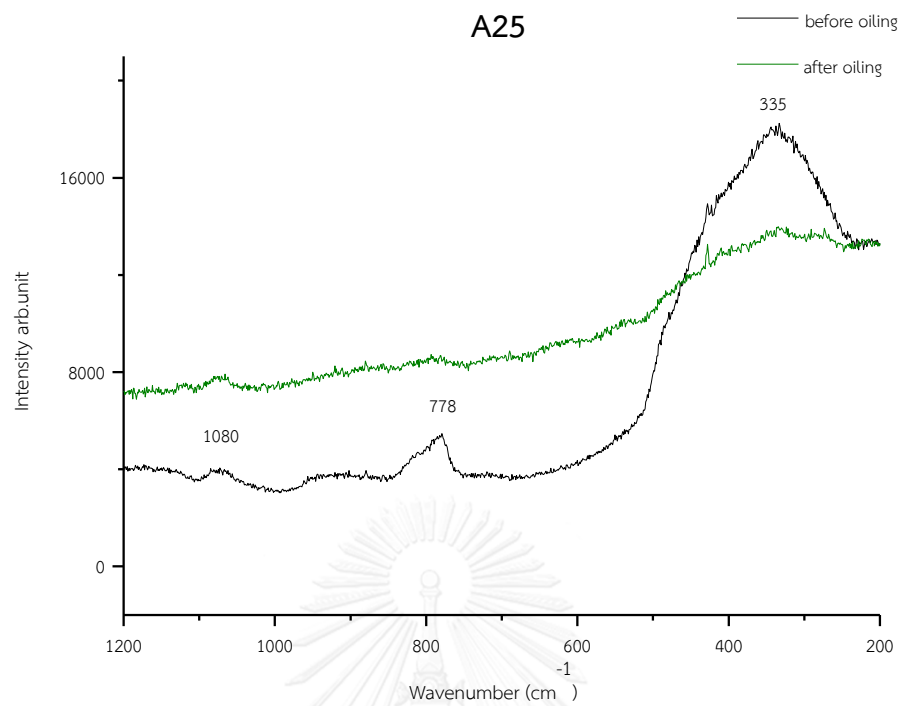


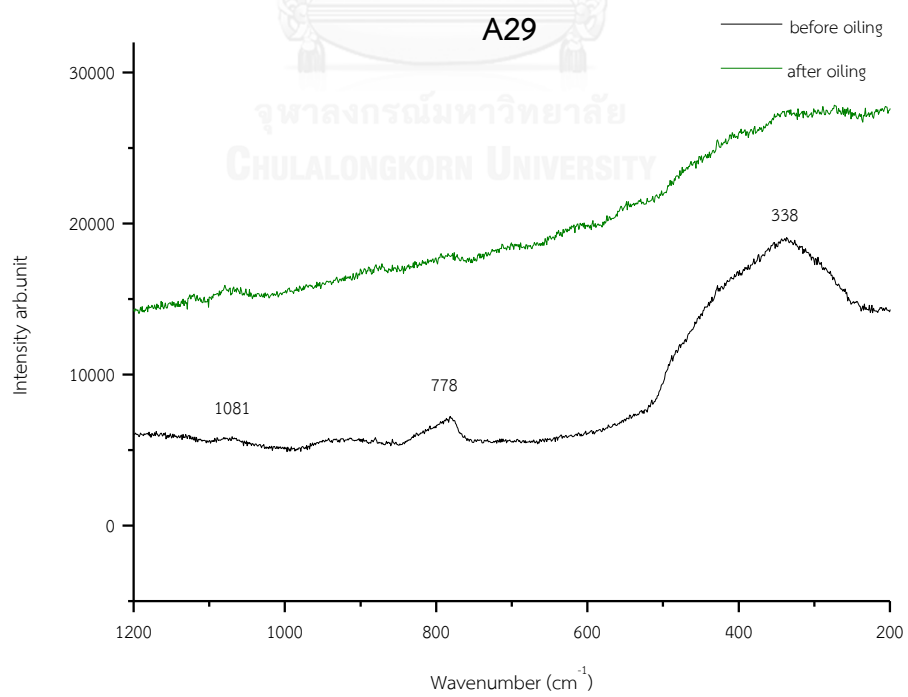
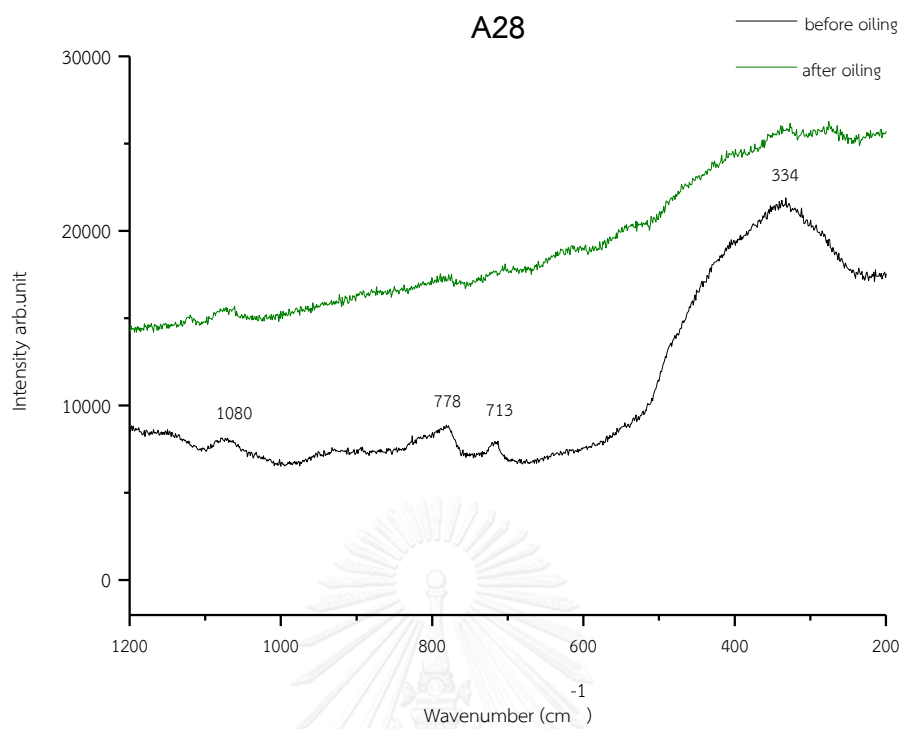


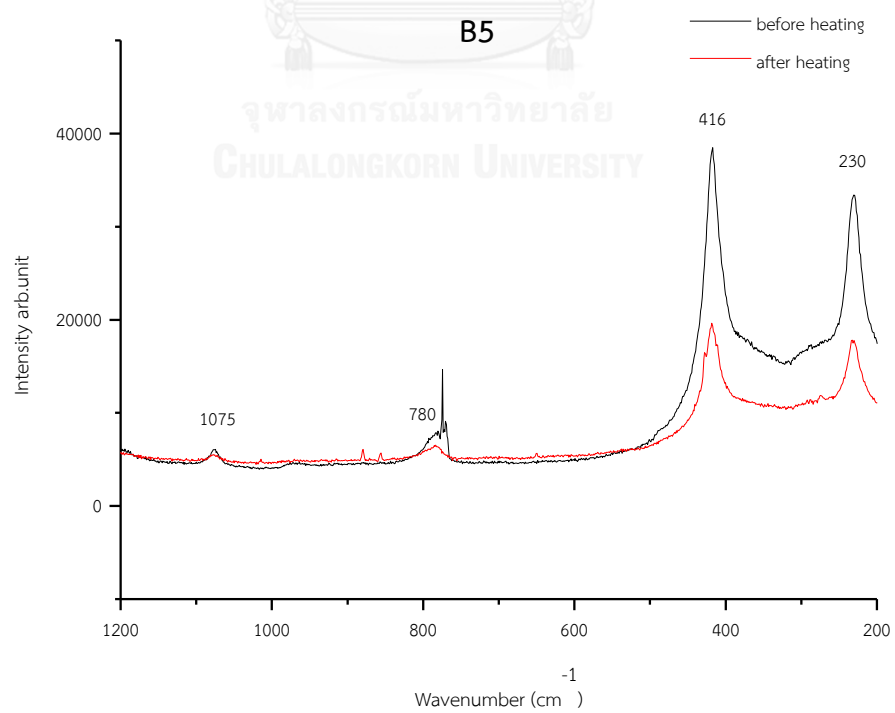
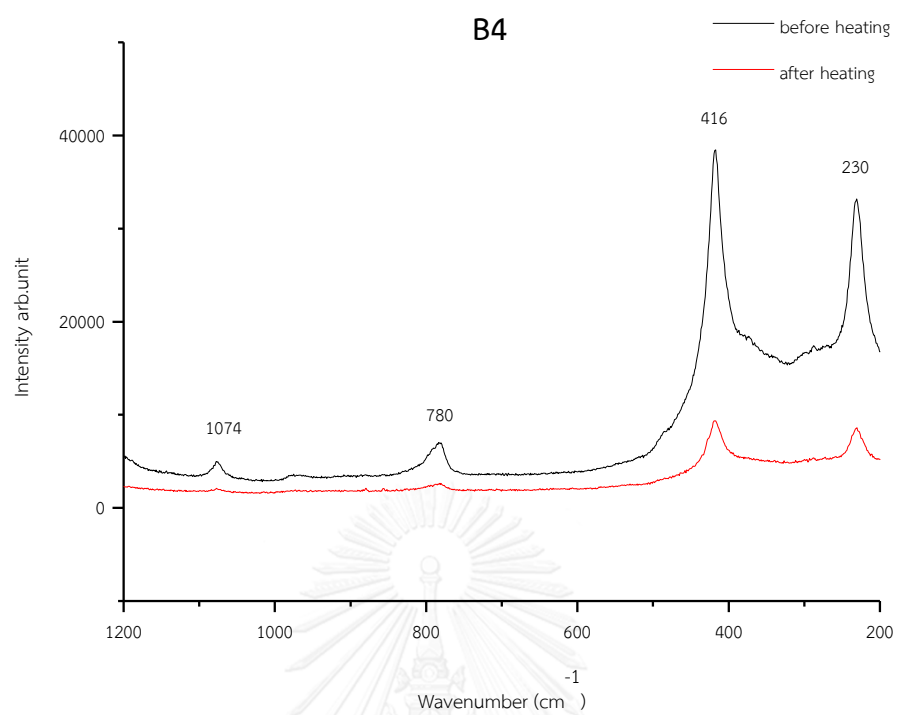


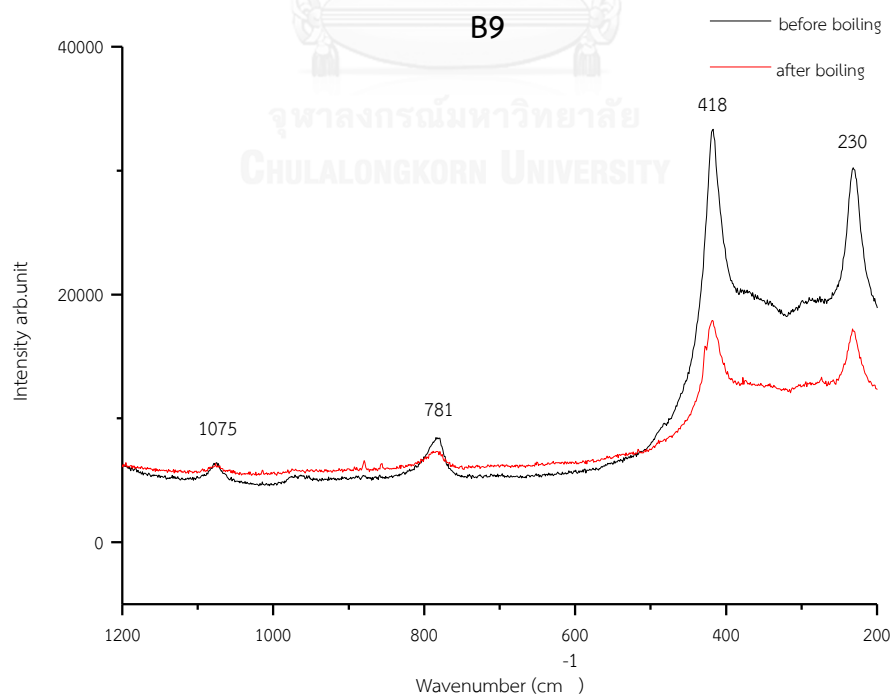
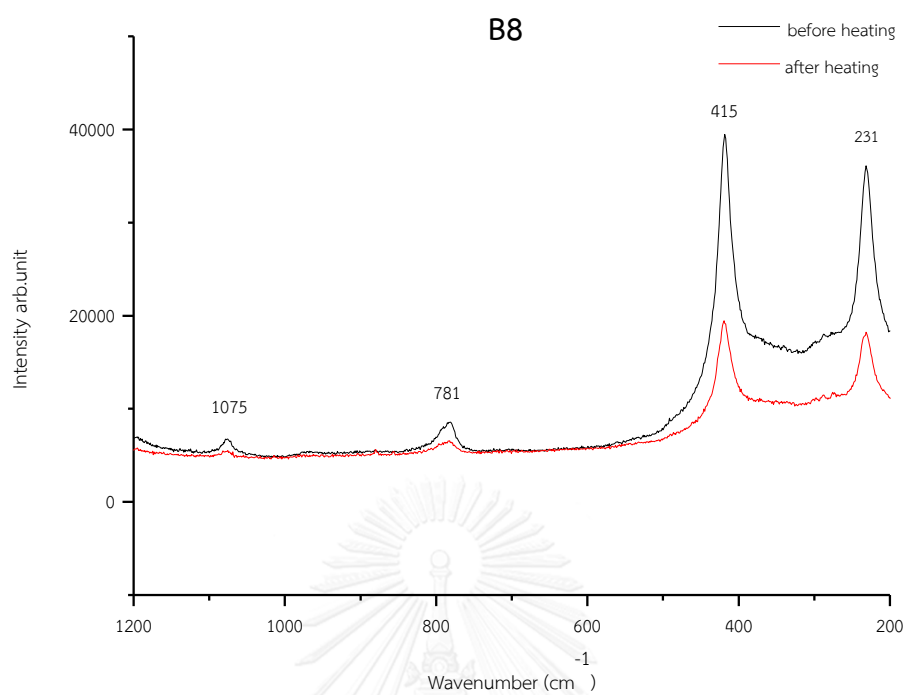


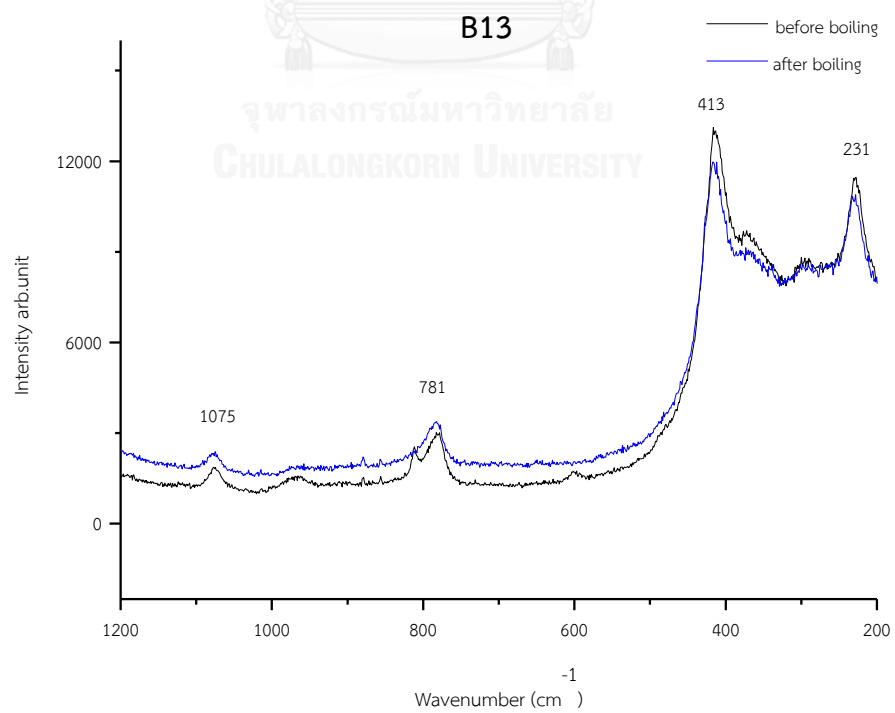
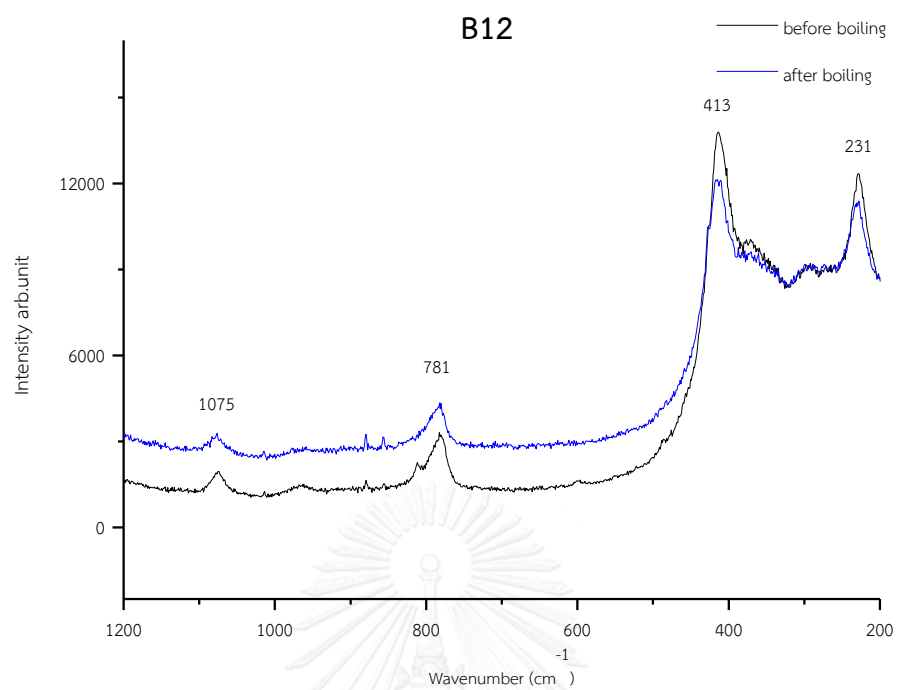


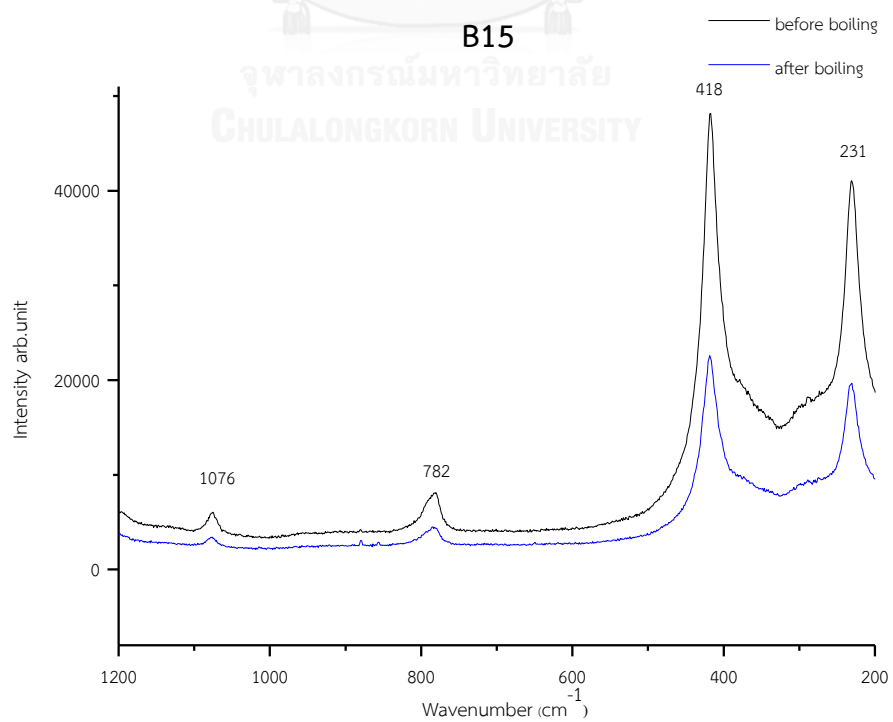
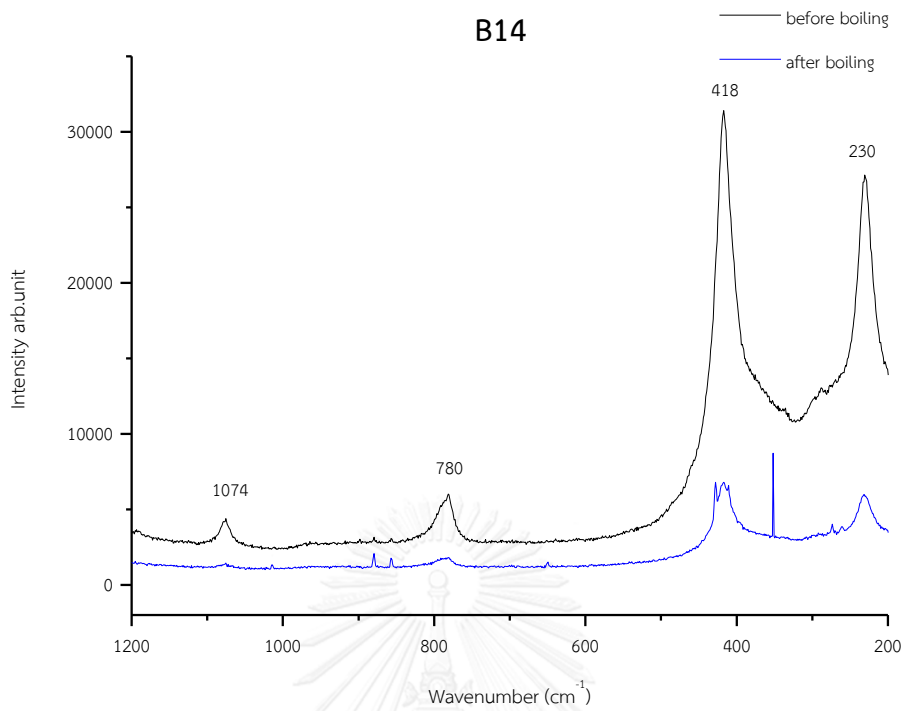




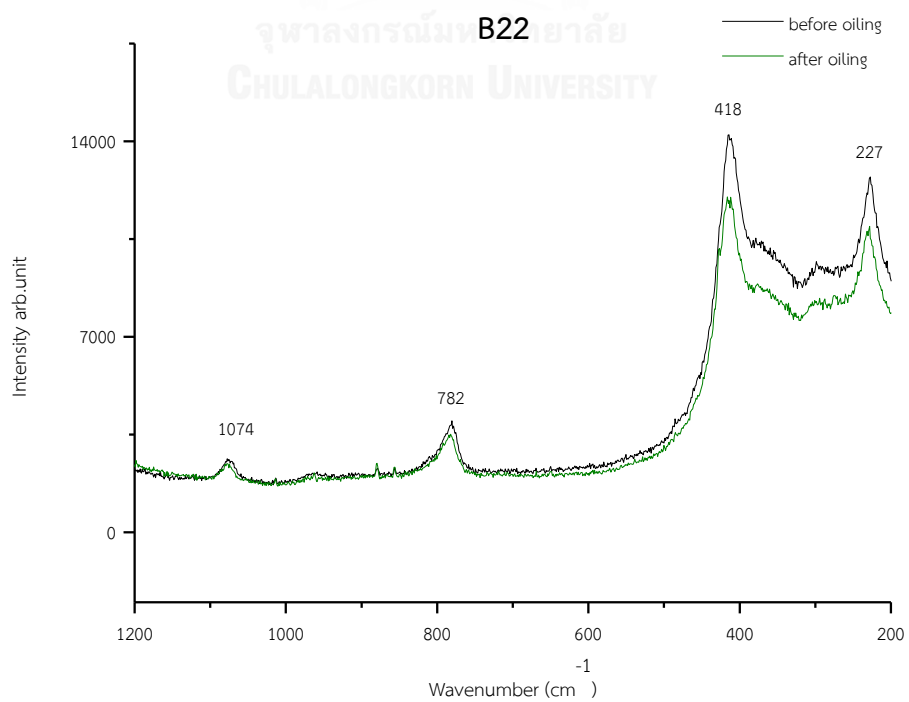
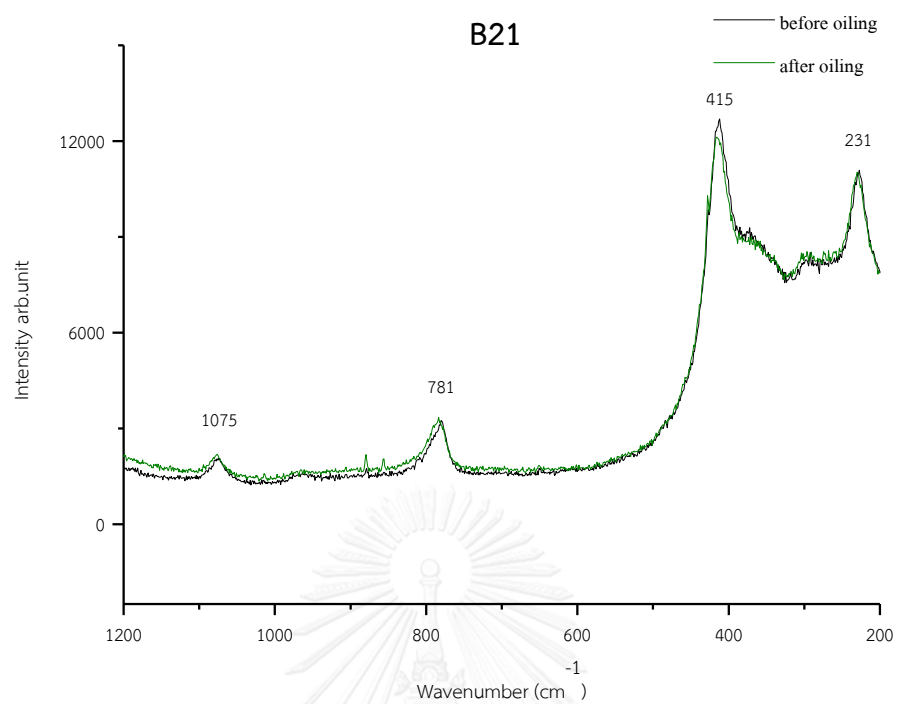


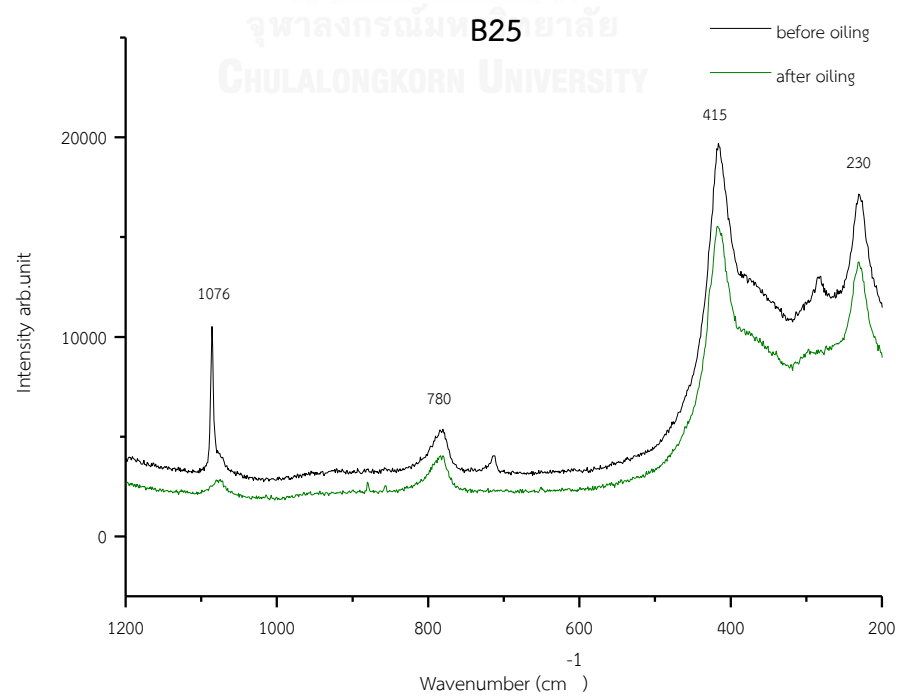
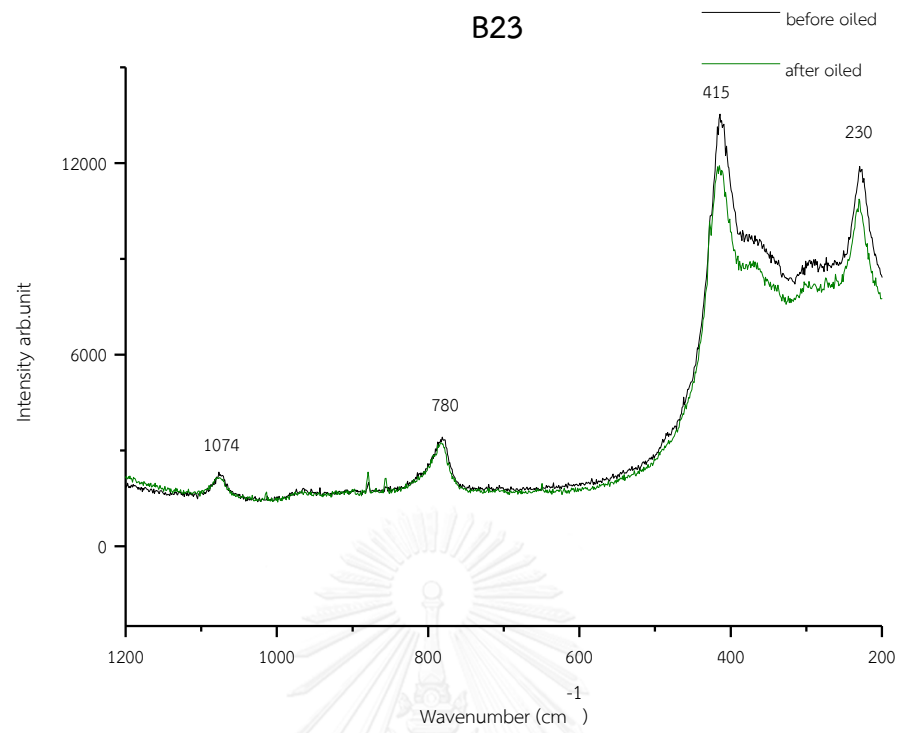


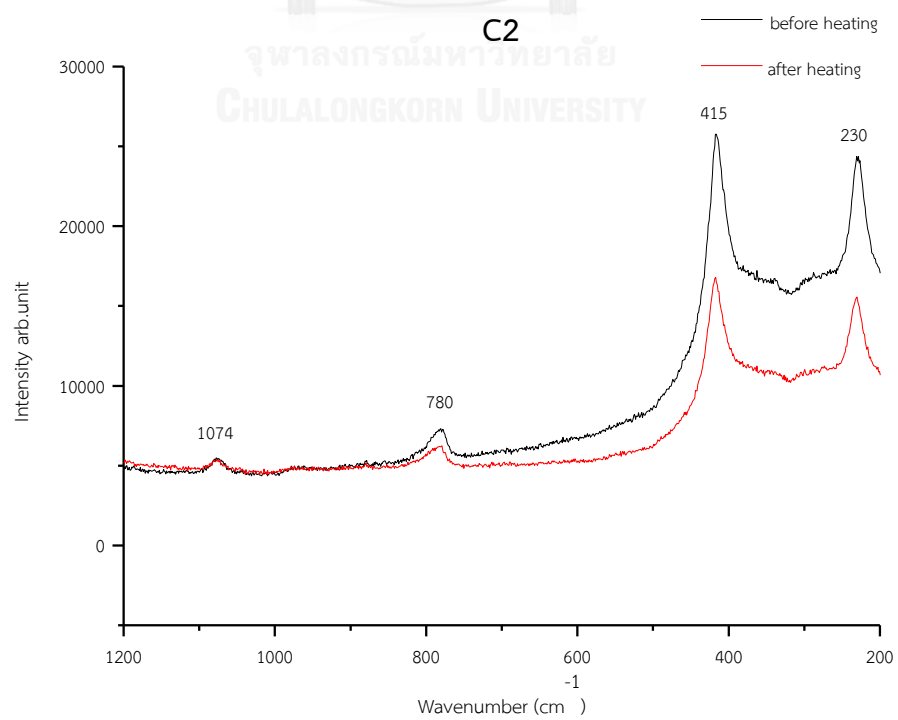
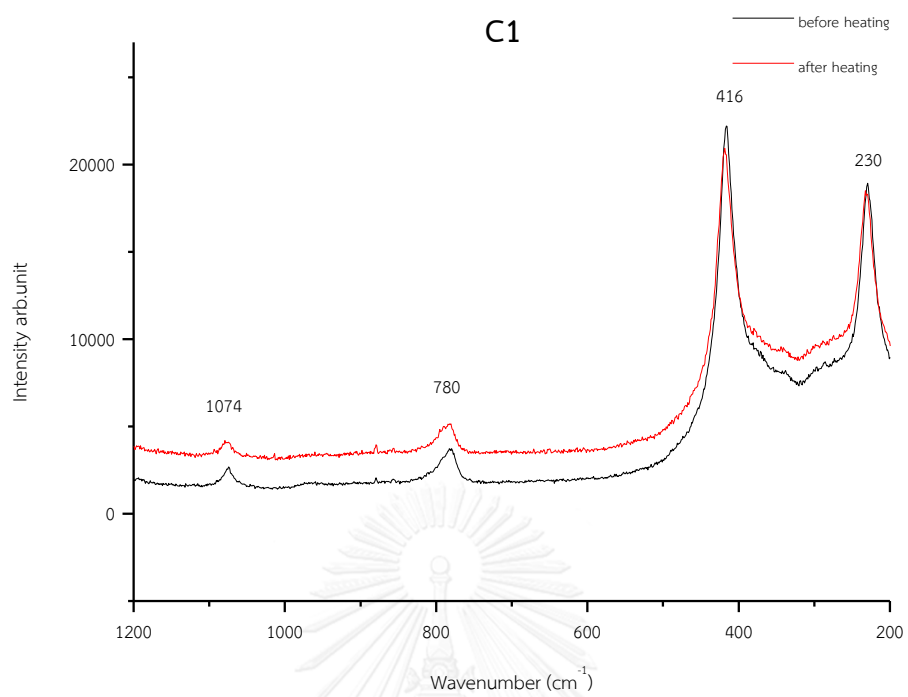


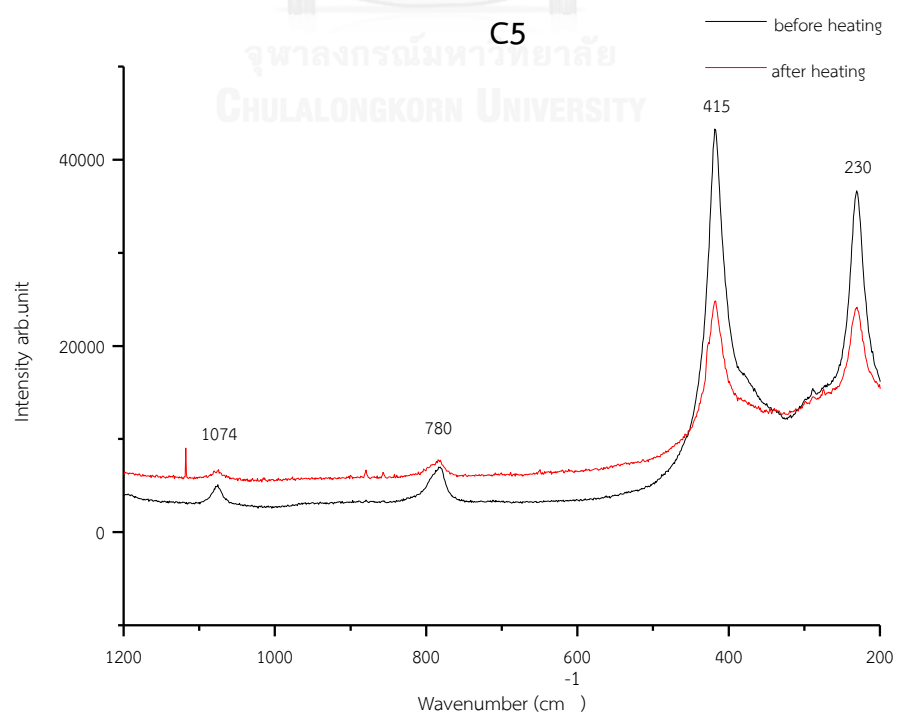
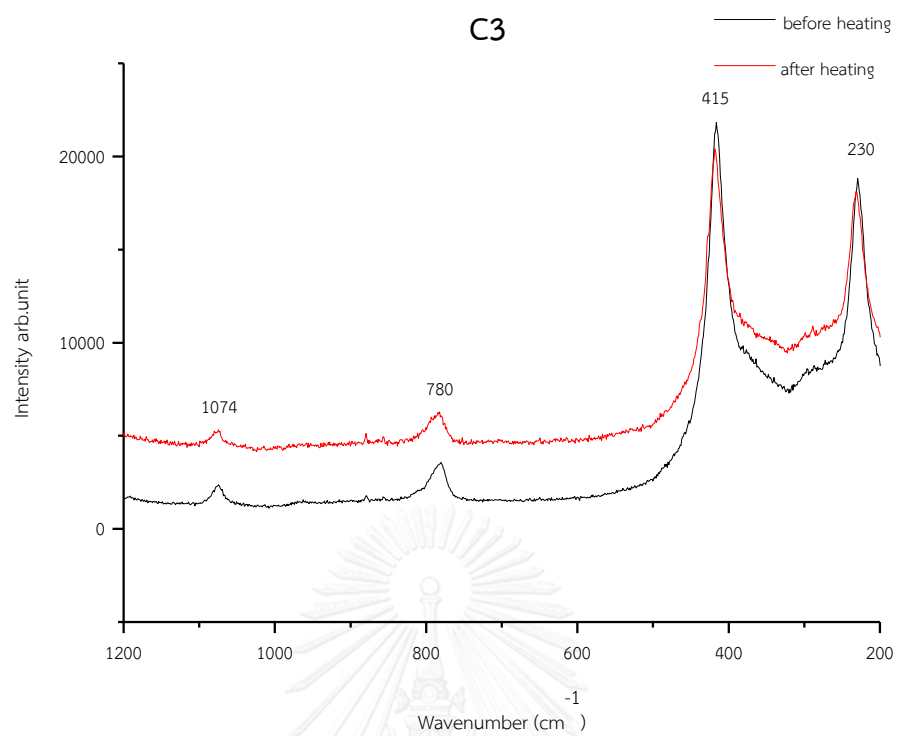


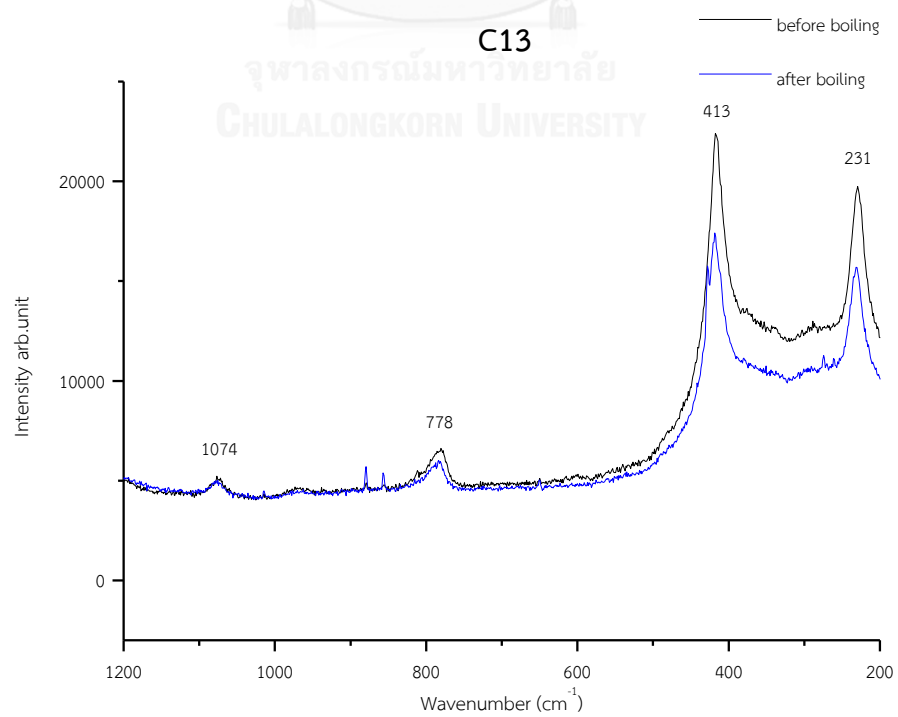
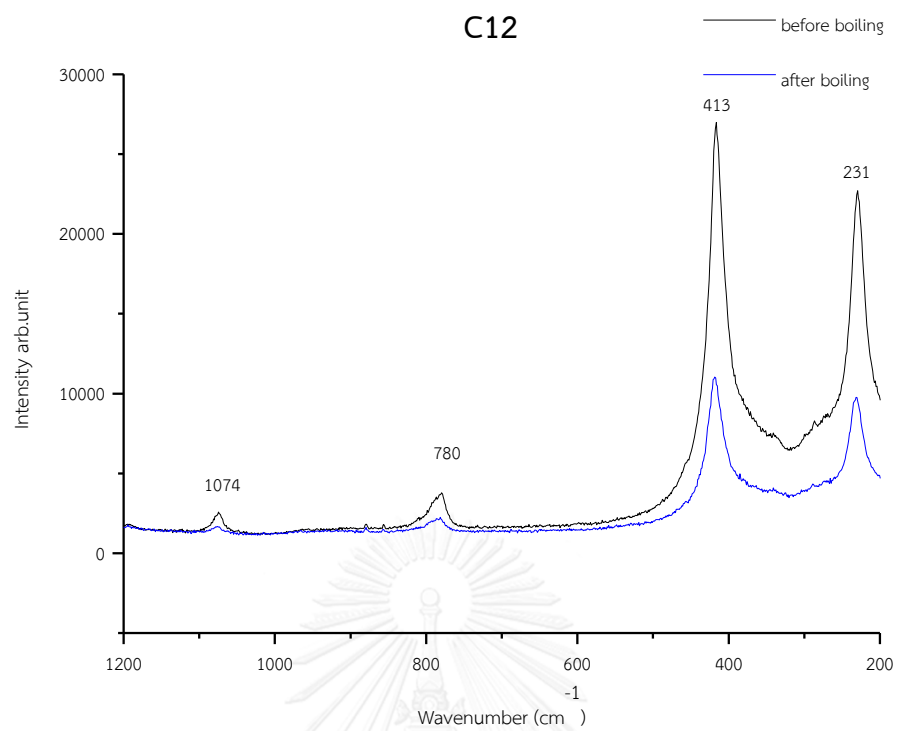


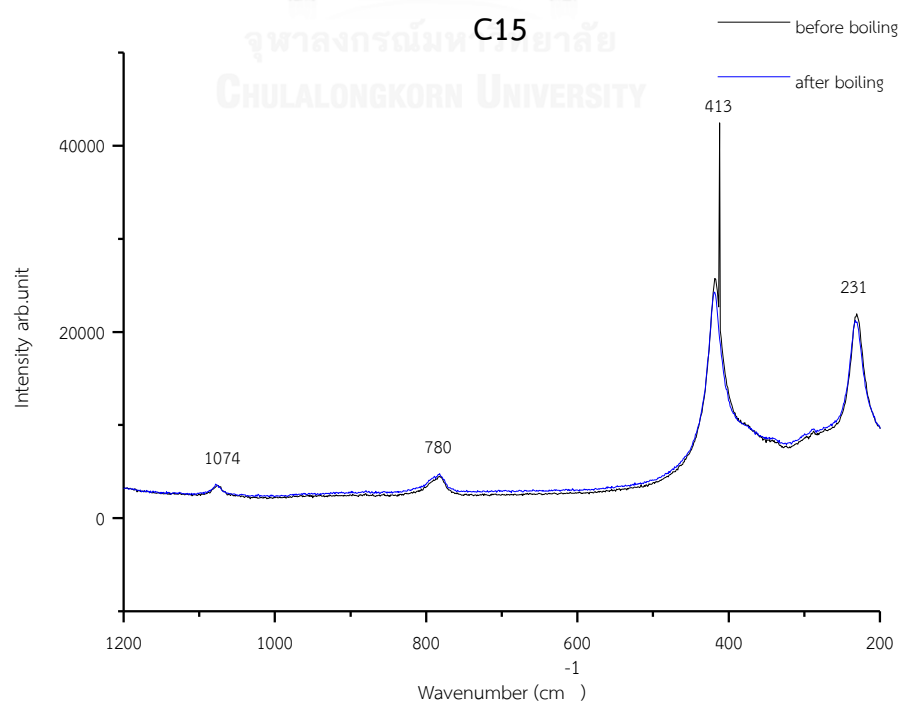
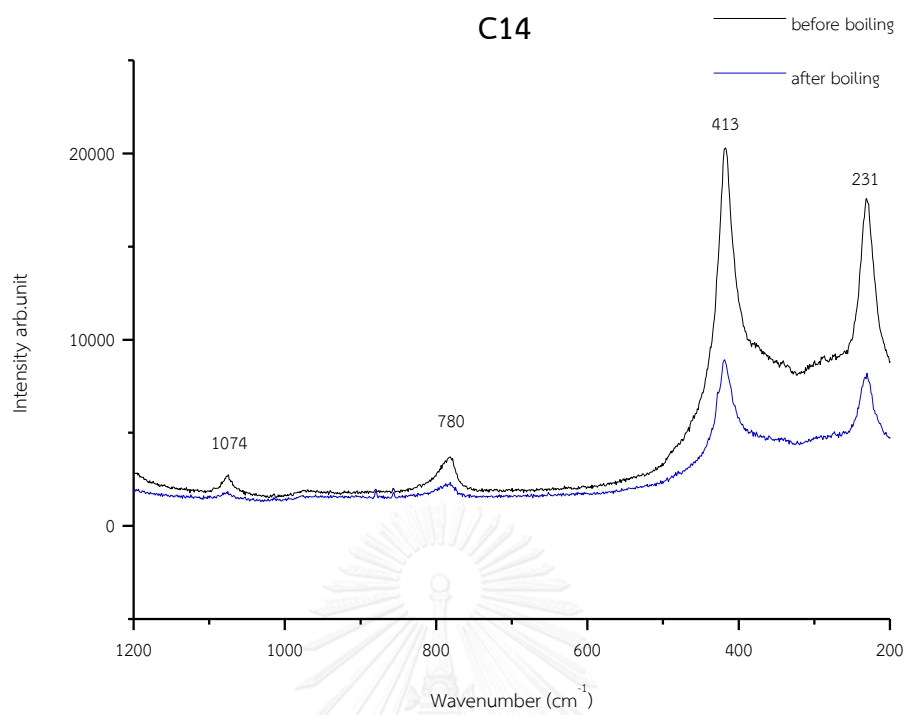


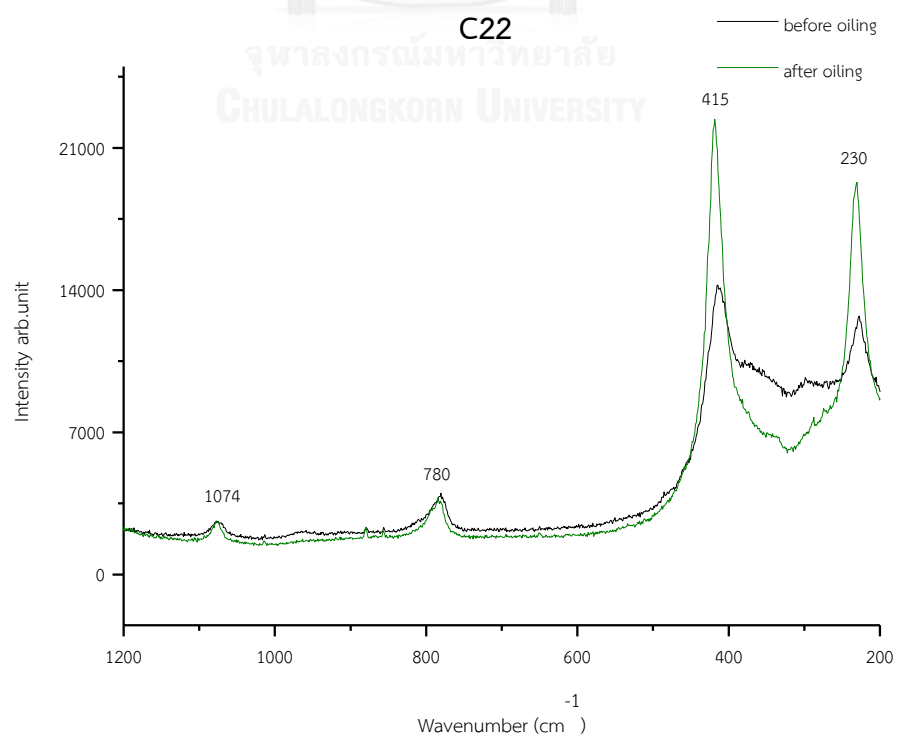
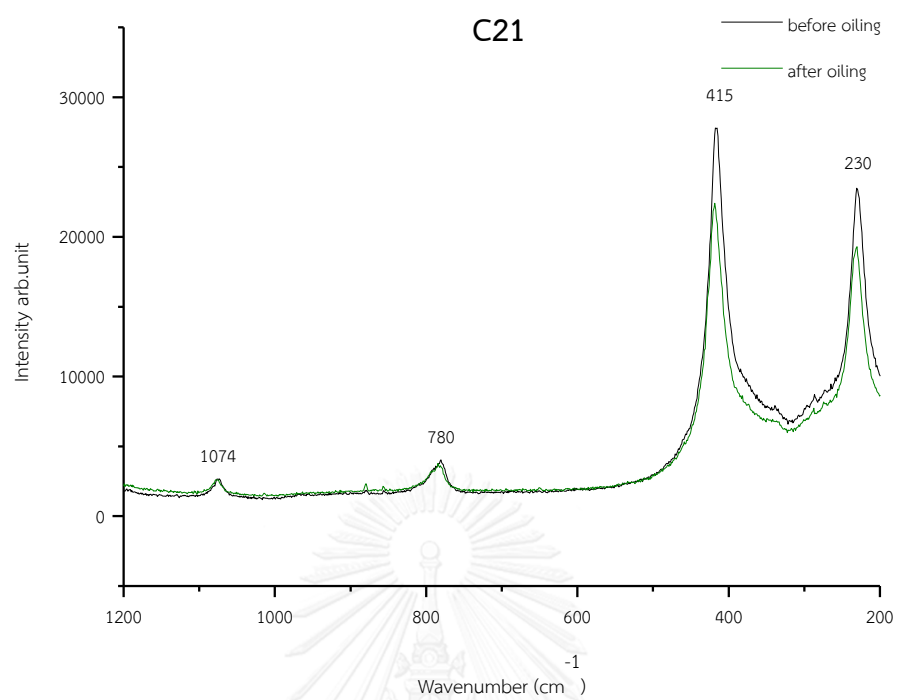


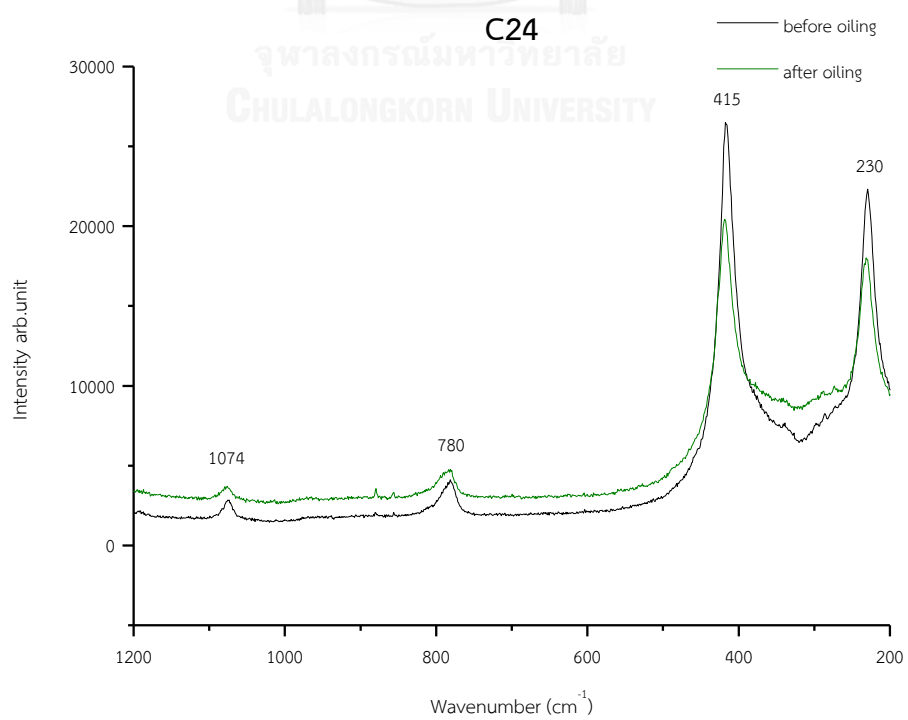
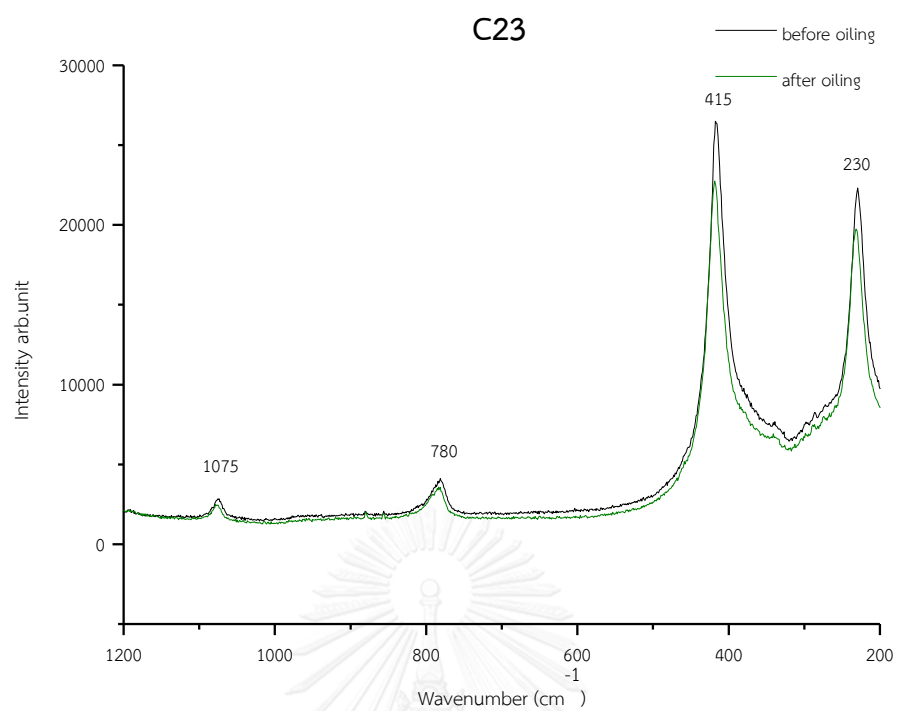














## VITA

Miss Supansa Toaree was born in July 7, 1990, at Bangkok. She graduated with bachelor degree in a major of gems and jewelry from Faculty of Gems, Burapha University in 2011. At the present, She studies in a Master program in Geology, Earth Sciences Program at Chulalongkorn University.

